



UNIVERSITY OF
LEICESTER

Nucleation and Growth Phenomena of Silver in Physical Developer for Latent Fingerprint Visualisation

Thesis submitted for the degree of

Doctor of Philosophy

at the University of Leicester

by

Jodie Louise Coulston MChem

Department of Chemistry

University of Leicester

2018

Nucleation and Growth Phenomena of Silver in Physical Developer for Latent Fingerprint Visualisation

Jodie Louise Coulston

Fingerprints are used to identify individuals in both criminal and civil cases based on their unique pattern of characteristic ridge details. Latent, i.e. non-visible, fingerprints are the most commonly exploited type of fingermark, since they are frequently left at a crime scene. However, they must be visualised via an enhancement method, the nature of which is dependent on the substrate. Physical developer (PD) is a widely used effective chemical enhancement method for the visualisation of fingerprints on porous surfaces, notably paper. The principle of the technique is based on a ferrous/ferric redox couple reducing silver ions to colloidal silver metal, which is stabilised by a surfactant formulation. Recent environmental legislation banning a crucial surfactant component – Synperonic N – motivates the design of a new formulation. This requires determination of the mechanism of the PD process and the roles of the components; previous work is macroscopic and empirical. This thesis describes solution and interfacial measurements and surface imaging that provide mechanistic insights and real-time dynamics of the process. Dynamic light scattering and microscopy reveal the particle size in solution. These particles deposit selectively on the fingermark, interacting with chemical constituents identified via spot tests, and grow to a size over an order of magnitude greater than in solution. Silver nucleation and growth on the surface are independent of the age of the mark. Neutron reflectivity measurements revealed that the cationic surfactant component, n-dodecylamine acetate, adsorbs more strongly to a silver surface in the presence of a non-ionic surfactant. Working solution stability variations with surfactant formulation are characterised, together with the effect on latent mark development times. The mechanistic and structural insights are used to design an alternative PD formulation with greater stability at no loss of the image quality.

Acknowledgements

The completion of this thesis would not have been possible without the huge support and encouragement I received from family, friends and colleagues. Though I cannot name you all personally here, I am truly grateful to every one of you.

I would like to thank my supervisors, Professor A. Robert Hillman and Vaughn Sears for the immense support and guidance throughout my PhD. Also, to Alex Goddard, for the continuous help with instrumentation and his understanding of the PhD process. I would also like to thank Rob Barker for the invaluable support and guidance regarding the neutron studies and most importantly, keeping me sane during the night shifts!

My friends and colleagues in the chemistry department have provided the utmost support and company, with special thanks to Jonathon Brooks. I am indebted to my family for always believing in me, especially my mum who was always at the end of the phone when I needed to vent! Finally, I cannot express how grateful I am to my partner, Charlie, for his unequivocal support and always being there to put a smile on my face.

Contents

Abstract	i
Acknowledgements	ii
Contents	iii
List of Tables	vii
List of Figures	viii
Abbreviations	xx

Chapter 1: Introduction	1
1.1 Introduction	2
1.2 Fingerprints	3
1.2.1 Individuality of Fingerprints	3
1.2.2 History of Fingerprint Identification	6
1.2.3 Current Identification Protocol	7
1.2.4 Types of Fingerprint	8
1.2.5 Composition of Fingerprint Residue	9
1.3 Development of Latent Fingerprints	12
1.3.1 Enhancement Methods for Non-Porous Surfaces	12
1.3.2 Enhancement Methods for Porous Surfaces	16
1.3.3 Fingerprint Development Sequence	18
1.3.4 Recent Developments	20
1.4 Physical Developer and Related Methods	21
1.4.1 History of Physical Developer	22
1.4.2 Current Theory of the PD Process	26
1.4.3 Metal Deposition Enhancement	32
1.5 Objectives	33
1.6 References	34

Chapter 2: Methodology	42
2.1 Introduction	43
2.2 Microscopy	43
2.2.1 Optical Profilometry	43
2.2.2 Atomic Force Microscopy	44
2.2.3 Scanning Electron Microscopy	46

2.3	Light Scattering	48
	2.3.1 Dynamic Light Scattering	48
2.4	Spectroscopy	50
	2.4.1 Raman Spectroscopy	50
2.5	Neutron Reflectivity	52
	2.5.1 Neutron-nuclei Interactions	52
	2.5.2 Reflectivity Theory	53
	2.5.3 Data Analysis	58
2.6	References	59
 Chapter 3: Experimental		 64
3.1	Introduction	65
3.2	Materials	65
	3.2.1 Fingerprint Deposition	65
	3.2.2 Substrates	66
	3.2.3 Reagents	67
3.3	Instrumentation	70
	3.3.1 Imaging	70
	3.3.2 Compositional Analysis	71
	3.3.3 Surface and Interfacial Analysis	71
	3.3.4 Spectroscopy	71
	3.3.5 Neutron Reflectivity	72
3.4	Procedures	73
	3.4.1 Environmental Conditions	73
	3.4.2 Growth and Dynamics of Silver for Fingerprint Visualisation	73
	3.4.3 Split Prints	75
	3.4.4 Spot Tests	76
	3.4.5 Physical Developer Procedure	77
	3.4.6 Superglue Fuming	79
	3.4.7 Preparation of Quartz Blocks for Neutron Reflectivity	80
	3.4.8 Fingerprint Grading	81
3.5	References	81

Chapter 4: Understanding the Fundamentals of the Physical Developer

Process	83
4.1 Introduction	84
4.2 Results	84
4.2.1 Development of Marks Derived from Different Sweat Types	84
4.2.2 Spot tests	91
4.2.3 Growth and Dynamics of Silver for Fingerprint Visualisation	102
4.2.4 Compositional Analysis of the Developed Fingerprints	124
4.3 Conclusions	127
4.4 References	128

Chapter 5: Evaluation of Tween 20 Using Microscopy and Neutron

Reflectivity	131
5.1 Introduction	132
5.2 Results	132
5.2.1 Role of the Non-Ionic Surfactant	132
5.2.2 Growth and Dynamics of Silver for Fingerprint Visualisation	135
5.2.3 Neutron Reflectivity Study of Surfactant Adsorption	151
5.3 Conclusions	168
5.4 References	169

Chapter 6: Reformulation and Optimisation of the Physical Developer

Process	171
6.1 Introduction	172
6.2 Results	172
6.2.1 Reformulation of the PD Working Solution with Alternative Non-Ionic Surfactants	172
6.2.2 Raman Spectroscopy of Surfactant Adsorption	204
6.2.3 Extension of PD to Alternative Porous Surfaces	211
6.3 Conclusions	218
6.4 References	219

Chapter 7: Conclusions and Future Work	221
7.1 Conclusions	222
7.2 Future Work	226
7.3 References	227
Appendix	229
A. Spot Tests	230
Bibliography	235

List of Tables

Table 1.1 - Eccrine components in fingerprint residue

Table 1.2 - Relative amount of sebaceous components in fingerprint residue

Table 1.3 - Philips FC1 Jonker PD formulation

Table 1.4 - Modified PD formulation by Morris (AWRE)

Table 1.5 - Current PD working solution formulation

Table 3.1 - Leather and suede swatches - Purple suede, Nubuck suede, brown suede, navy matte leather, embossed leather and patent leather were all bovine sources (University of Northampton). White and black faux leather were sourced from an external supplier

Table 3.2 - Chemicals for the redox solution

Table 3.3 - Detergent system formulations

Table 3.4 - Volumes for the working solution

Table 3.5 - Working solution formulations with various detergent systems

Table 3.6 - Eccrine and sebaceous components with their corresponding solvent and concentration

Table 3.7 - Bandey grading system

Table 4.1 - Eccrine and sebaceous components with their corresponding solvent and concentration

Table 5.1 - Fit parameters for the reflectivity profiles in figure 5.20

Table 5.2 Fit parameters for the reflectivity profiles in figure 5.26

Table 5.3 - Fit parameters for the reflectivity profiles in figure 5.28

Table 5.4 - Fit parameters for the reflectivity profiles in figure 5.26. The values for the Ag roughness in black correspond to 3.5 mM h-DDAA, red to 5 mM h-DDAA, blue to 6 mM h-DDAA and green to 8 mM h-DDAA

Table 6.1 - DLS results of surfactant particle sizes

Table 6.2 - DLS results of particle sizes in the detergent systems

Table 6.3 - DLS results of particle sizes in the PD working solutions

List of Figures

- Figure 1.1 - Primary fingerprint patterns - loop, arch and whorl
- Figure 1.2 - Minimum features required for a loop pattern
- Figure 1.3 - Examples of common minutiae features
- Figure 1.4 - Fingerprint developed with carbon black powder
- Figure 1.5 - Fingerprint developed with superglue fuming
- Figure 1.6 - Proposed nucleophilic mechanism for superglue polymerisation
- Figure 1.7 - Fingerprint development using iron oxide powder suspension
- Figure 1.8 - Formation of Ruhemann's Purple
- Figure 1.9 - Fingerprint developed with Ninhydrin
- Figure 1.10 - DFO and Indanedione
- Figure 1.11 - Fingerprint developed using DFO
- Figure 1.12 - Fingerprint development sequence non-porous (above) and for porous surfaces (below)
- Figure 1.13 – Schematic of the proposed staggered conformation of the cationic surfactant around the silver particles (not to scale)
- Figure 1.14 - Timeline of PD
- Figure 1.15 – Synperonic N
- Figure 1.16 - Tween 20
- Figure 1.17 - Oil Red O (ORO)
- Figure 1.18 - Nile Red
- Figure 2.1 - Diagram showing stabilised silver particles in solution and deposited silver particles of developed fingerprint image using PD
- Figure 2.2 - Schematic of an optical profiler
- Figure 2.3 - Schematic diagram of AFM components
- Figure 2.4 - Schematic of SEM components
- Figure 2.5 - (a) Small particles showing rapid fluctuations in intensity of scattered light with time (b) Correlation graph generated from DLS software
- Figure 2.6 - Rayleigh, Stokes and Anti-Stokes scattering

Figure 2.7 - Schematic of an incident wave vector hitting a sample point producing a reflected wave vector

Figure 2.8 - Elastic scattering

Figure 2.9 - Total reflection where θ_1 is the angle of refraction

Figure 2.10 - Specular reflection at the surface and interface

Figure 2.11 - Off-specular reflection from rougher surfaces

Figure 2.12 - An example of a simple reflectivity profile

Figure 2.13 - Neutron cell configuration

Figure 3.1 - (a) Preliminary design for recording the continuous development via PD (b) custom stage design

Figure 3.2 - Grids used for testing individual sebaceous (top) and eccrine (bottom) components with PD

Figure 3.3 - Physical developer procedure

Figure 3.4 - Chemical structures of ethyl-2-cyanoacrylate and dimethylamino benzaldehyde (DMAB)

Figure 3.5 - Silanisation of quartz blocks

Figure 4.1 - Natural, eccrine and sebaceous fingerprints deposited on white copy paper and aged under ambient conditions for 1 day and then developed using PDF1S. The columns represent replicates for each type of mark

Figure 4.2 - Natural, eccrine and sebaceous fingerprints deposited on white copy paper and aged under ambient conditions for 14 days and then developed via PDF1S. The columns represent replicates for each type of mark

Figure 4.3 - Natural, eccrine and sebaceous fingerprints deposited on white copy paper and aged under ambient conditions for 28 days then developed via PDF1S. The columns represent replicates for each type of mark

Figure 4.4 - Split prints of natural, eccrine and sebaceous fingerprints deposited on white copy paper and aged for 1 (a-c), 14 (d-f) and 28 (g-i) days under ambient conditions and then developed via PDF1S. The left side of the prints were aged under ambient conditions and the right side of the prints were heated to 100 °C for 20 minutes prior to development

Figure 4.5 - Natural, eccrine and sebaceous split prints deposited on white copy paper and aged for 1 day under ambient (left) and wetted (right) conditions and then developed via PDF1S with the corresponding 3D microscopy image (5x). Tick marks every 200 μm

Figure 4.6 – PDF1S treatment applied to individual eccrine components spot test, which were deposited on white copy paper and aged for 1 day under ambient conditions - Set 1. The left hand column shows the type of eccrine component and the rows show variations in the concentration

Figure 4.7 – PDF1S treatment applied to individual sebaceous components spot test, which were deposited on white copy paper and aged for 1 day under ambient conditions - Set 1. The left hand column shows the type of sebaceous component and the rows show the variation in concentration

Figure 4.8 – PDF1S treatment applied to individual sebaceous components spot test, which were deposited on white copy paper and aged for 1 day under ambient conditions - Set 2. The left column shows the type of sebaceous components and the rows show the variation in concentration

Figure 4.9 – PDF1S treatment applied to individual sebaceous components spot test, which were deposited on white copy paper and aged for 1 day under ambient conditions - Set 3. The left column shows the type of sebaceous component and the rows show the variation in concentration

Figure 4.10 – 3D microscopy image (50x) of squalene 50 mM (left) and serine 100 mM (right) – Tick marks every 20 μm

Figure 4.11 – PDF1S treatment applied to (a) individual eccrine component (set 1) and (b) sebaceous component (set 2) samples deposited on white copy paper and aged for 1 day under wetted conditions. The left hand columns of both images show the type of component and the rows show the variation in concentration

Figure 4.12 – PDF1S treatment applied to mixture of sebaceous and eccrine component deposited on white copy paper and aged for 1 day under ambient conditions: (a) sebaceous component deposited first, followed by eccrine component (set 2) and (b) eccrine component deposited first, followed by sebaceous component (set 2)

Figure 4.13 – PDF1S treatment applied to emulsion spot test deposited on white copy paper and aged for 1 day under ambient conditions with 5x 3D microscopy image of palmitic acid/lactic acid (Tick marks every 200 μm)

Figure 4.14 – PDF1S treatment applied to emulsion spot tests deposited on white copy paper and aged for 7, 14 and 28 days

Figure 4.15 – PDF1S treatment applied to emulsion spot tests with 10 mM of sebaceous content deposited on white copy paper and aged for 1, 7, 14 and 28 days

Figure 4.16 - 1 day old fingerprints deposited on white copy paper and aged under ambient conditions then developed with PDF1S with the associated Bandey grades

Figure 4.17 - Macroscopic to microscopic view of a fingerprint developed via PDF1S. 5x image (Tick marks every 200 μm), 50x image (Tick marks every 20 μm)

Figure 4.18 - DLS graph for particle size in the PDF1S working solution

Figure 4.19 – The growth development of silver from 30 seconds to 15 minutes for fingerprints deposited on white copy paper and aged for 1 day under ambient conditions then developed via PDF1S

Figure 4.20 – 3D microscopy images (50x) for the growth development of 1 day old marks processed for 30 seconds to 15 minutes for the samples in figure 4.19. Tick marks every 20 μm

Figure 4.21 - Graph of silver particle diameter vs time of development for 3 sets of 1 day old marks aged under ambient conditions developed via PDF1S. Data from figure 4.19 and two replicates

Figure 4.22 - Graph of the number of particles within 140 μm^2 area vs. time of development for 1 day old marks analysed in figure 4.19

Figure 4.23 - The growth development of silver from 30 seconds to 15 minutes for fingerprints deposited on white copy paper and aged for 14 days under ambient conditions then developed via PDF1S

Figure 4.24 – 3D microscopy images (50x) for the growth development of 14 day old marks processed for 30 seconds to 15 minutes for the samples in figure 4.23. Tick marks every 20 μm

Figure 4.25 - Graph of silver particle diameter vs time of development for 3 sets of 14 day old marks aged under ambient conditions developed via PDF1S. Data from figure 4.23 and two replicates

Figure 4.26 - Graph of the number of particles within 140 μm^2 area vs. time of development for 14 day old marks analysed in figure 4.23

Figure 4.27 - The growth development of silver from 30 seconds to 15 minutes for fingerprints deposited on white copy paper and aged for 28 days under ambient conditions then developed via PDF1S

Figure 4.28 – 3D microscopy images (50x) for the growth development of 28 day old marks processed for 30 seconds to 15 minutes in figure 4.27. Tick marks every 20 μm

Figure 4.29 - Graph of silver particle diameter vs time of development for 3 sets of 28 day old marks aged under ambient conditions developed via PDF1S. Data from samples in figure 4.27 and two replicates

Figure 4.30 - Graph of the number of particles within 140 μm^2 area vs. time of development for 28 day old marks analysed in figure 4.27

Figure 4.31 - Split prints deposited on white copy paper and aged for 1, 14 and 28 days under ambient conditions then developed via PDF1S (3 replicates for each age of mark)

Figure 4.32 – 3D microscopy images (50x) for a sample of the growth development of a 1 day old mark processed for 1-15 minutes in figure 4.31. Tick marks every 20 μm

Figure 4.33 – 3D microscopy images (50x) for a sample of the growth development of a 14 day old mark processed for 1-15 minutes. Tick marks every 20 μm

Figure 4.34 – 3D microscopy images (50x) for a sample of the growth development of a 28 day old mark processed for 1-15 minutes. Tick marks every 20 μm

Figure 4.35 - Graph of silver particle diameter vs time of development for average of 5 sets of 1, 14 and 28 day old marks aged under ambient conditions developed via PDF1S

Figure 4.36 - Still images taken from the live video of the PD development process

Figure 4.37 – (a) SEM image of a 1 day old fingerprint on white copy paper (figure 4.16b) aged under ambient conditions developed via PDF1S with (b) and (c) the corresponding EDX analyses in the indicated area

Figure 4.38 - SEM image of deposited silver particles on a 1 day old fingerprint (figure 4.16e) aged under wetted conditions developed with PDF1S

Figure 4.39 - SEM images of developed fingerprints at 1, 5 and 15 minutes for 1 day old fingerprints aged under ambient conditions developed with PDF1S

Figure 4.40 - Schematic of the size of the silver particles in solution with progressive growth of silver observed on the surface (not to scale)

Figure 5.1 - 1 day old fingerprints deposited on white copy paper and aged under ambient conditions then developed with PD working solutions with only DDAA as the surfactant system (The rows are replicates)

Figure 5.2 - The growth development of silver from 1 to 60 minutes for fingerprints deposited on white copy paper and aged for 1 day under ambient conditions then developed via PDF2T (2 day old solution)

Figure 5.3 - 3D microscopy images (50x) for the growth development of 1 day old marks processed for 30 seconds to 15 minutes for the samples in figure 5.2. Tick marks every 20 μm

Figure 5.4 - 3D microscopy images (50x) for the growth development of 1 day old marks processed for 45 to 60 minutes for the samples in figure 5.2. Tick marks every 20 μm

Figure 5.5 - Graph of silver particle diameter vs time of development for 3 sets of 1 day old marks aged under ambient conditions developed via PDF2T (2 day old solution). Data from figure 5.2 and two replicates

Figure 5.6 - The growth development (1-15 mins) of silver for fingerprints deposited on white copy paper and aged for 1 day under ambient conditions then developed via PDF2T (2 day old solution)

Figure 5.7 - 3D microscopy images (50x) for the growth development of 1 day old marks processed for 1 to 15 minutes for the samples in figure 5.6. Tick marks every 20 μm

Figure 5.8 - Graph of silver particle diameter vs time of development (1-15 mins) for 3 sets of 1 day old marks aged under ambient conditions developed via PDF2T (2 day old solution). Data from figure 5.6 and two replicates

Figure 5.9 – Split prints deposited on white copy paper and aged for 1 day under ambient conditions then developed via PDF2T (2 day old solution) 3 replicates for each age of mark

Figure 5.10 - 3D microscopy images (50x) for a sample of the growth development of a 1 day old mark processed for 1-30 minutes in figure 5.9. Tick marks every 20 μm

Figure 5.11 - 3D microscopy images (50x) for a sample of the growth development of 1 day old mark processed for 1-15 minutes in figure 5.9. Tick marks every 20 μm

Figure 5.12 - Graph of silver particle diameter vs time of development (1-30 minutes) for the average of 5 sets of 1 day old marks aged under ambient conditions developed via PDF2T (2 day old solution)

Figure 5.13 – Split prints deposited on white copy paper and aged for 14 and 28 days under ambient conditions then developed via PDF2T (3 replicates for each age of mark)

Figure 5.14 - 3D microscopy images (50x) for a sample of the growth development of 14 day old mark processed for 1-15 minutes in figure 5.13. Tick marks every 20 μm

Figure 5.15 - 3D microscopy images (50x) for a sample of the growth development of a 28 day old mark processed for 1-15 minutes in figure 5.13. Tick marks every 20 μm

Figure 5.16 - Graph of silver particle diameter vs time of development for the average of 5 sets of 1, 14 and 28 day old marks aged under ambient conditions developed via PDF2T (Working solution age varied)

Figure 5.17 - The growth development of silver from 30 seconds to 15 minutes for fingerprints deposited on white copy paper and aged for 1 day under ambient conditions then developed via PDF2T (2 week old solution)

Figure 5.18 - 3D microscopy images (50x) for the growth development of 1 day marks processed for 30 seconds to 15 minutes for the samples in figure 5.17. Tick marks every 20 μm

Figure 5.19 - Graph of silver particle diameter vs time of development (30 seconds-15 minutes) for 3 sets of 1 day old marks aged under ambient conditions developed via PDF2T (2 week old solution). Data from figure 5.17 and two replicates

Figure 5.20 - Neutron reflectivity profiles for the adsorption of h-DDAA in D_2O with the bare silver surface in D_2O . The circles represent the measured data and the lines are the respective fits of that data, fitted using RasCal ($\chi^2 = 81.9$ for whole data set)

Figure 5.21 - SLD profiles for the adsorption of h-DDAA in D_2O . Data from figure 5.20 and fitted using RasCal

Figure 5.22 - Thickness of h-DDAA layer with increasing concentration of h-DDAA

Figure 5.23 - Proposed structure of h-DDAA on the planar silver surface

Figure 5.24 - AFM images of the Ag coating

Figure 5.25 - Tween 20 (13) used in the neutron experiments

Figure 5.26 - Neutron reflectivity profiles for the adsorption of d-Tween in H₂O with the bare silver surface in H₂O. The circles represent the measured data and the lines are the respective fits of that data, fitted using RasCal ($\chi^2 = 107.3$ for whole data set)

Figure 5.27 SLD profile for the adsorption of d-Tween in H₂O. Data from figure 5.26, fitted using RasCal

Figure 5.28 - Neutron reflectivity profiles for the adsorption of h-Tween in D₂O with the bare silver surface in D₂O. The circles represent the measured data and the lines are the respective fits of that data, fitted using RasCal ($\chi^2 = 86.4$ for whole data set)

Figure 5.29 - SLD profile for the adsorption of h-Tween in D₂O. Data from figure 5.26 and fitted using RasCal

Figure 5.30 - Neutron reflectivity profiles for the adsorption of h-DDAA and d-Tween in D₂O. The circles represent the measured data and the lines are the respective fits of that data ($\chi^2 = 82.5$ for whole data set)

Figure 5.31 - SLD profile for the adsorption of h-DDAA and d-Tween in D₂O. Data from figure 5.30, fitted using RasCal

Figure 5.32 - Proposed structure of h-DDAA and d-Tween on the planar silver surface

Figure 6.1 - Structure of Brij C10 (above) and DGME (below)

Figure 6.2 - The growth development of silver from 30 seconds to 15 minutes for fingerprints deposited on white copy paper and aged for 1 day under ambient conditions then developed via PDF3B1

Figure 6.3 - Difference between a clear and cloudy PD working solution (0-2 days) and evidence of silver precipitation (0-2 days)

Figure 6.4 - 3D microscopy images (50x) for the growth development of 1 day old marks processed for 30 seconds to 15 minutes for the samples in figure 6.2. Tick marks every 20 μm

Figure 6.5 - Graph of silver particle diameter vs time of development for 3 sets of 1 day old marks aged under ambient conditions developed via PDF3B1. Data from figure 6.2 and two replicates

Figure 6.6 - Growth development from 30 seconds to 15 minutes for 1 day old marks deposited on white copy paper and aged for 1 day under ambient conditions then developed via PDF4B2

Figure 6.7 - 3D microscopy images (50x) for the growth development of 1 day old marks processed for 30 seconds to 15 minutes for the samples in figure 6.6. Tick marks every 20 μm

Figure 6.8 - Graph of silver particle diameter vs time of development for 3 sets of 1 day old marks aged under ambient conditions developed via PDF4B2. Data from figure 6.6 and two replicates

Figure 6.9 - 1 day old fingerprints deposited on white copy paper and aged under ambient conditions then developed after 20 minutes using PDF4B2 with corresponding microscopy data. Tick marks every 20 μm

Figure 6.10 - Split prints deposited on white copy paper and aged for 1, 14 and 28 days under ambient conditions then developed via PDF4B2. 'm' refers to minutes. (3 replicates for each age of mark)

Figure 6.11 – 3D microscopy images (50x) for the growth development of a 1 day old mark processed for 1-15 minutes using PDF4B2. Tick marks every 20 μm

Figure 6.12 – 3D microscopic images (50x) for the growth development of a 14 day old mark processed for 1-15 minutes using PDF4B2. Tick marks every 20 μm

Figure 6.13 – 3D microscopy images (50x) for the growth development of a 28 day old mark processed for 1-15 minutes using PDF4B2. Tick marks every 20 μm

Figure 6.14 - Graph of silver particle diameter vs time of development for average of 5 sets of 1, 14 and 28 day old marks aged under ambient conditions developed via PDF4B2

Figure 6.15 - The growth development of silver from 30 seconds to 15 minutes for fingerprints deposited on white copy paper and aged for 1 day under ambient conditions then developed via PDF5D1

Figure 6.16 - 3D microscopy images (50x) for the growth development of 1 day old marks processed for 30 seconds to 15 minutes for the samples in figure 6.15. Tick marks every 20 μm

Figure 6.17 - Graph of silver particle diameter vs time of development for 3 sets of 1 day old marks aged under ambient conditions developed via PDF5D1

Figure 6.18 – Fingerprints deposited on white copy paper and aged for 1 day under ambient conditions then developed after 20 minutes using PDF5D1 with corresponding microscopy images 5x (left) and 50x (right) for the second fingerprint

Figure 6.19 - Split prints deposited on white copy paper and aged for 1, 14 and 28 days under ambient conditions then developed via PDF5D1 (3 replicates for each age of mark)

Figure 6.20 – 3D microscopy images (50x) for the growth development of a 1 day old mark processed for 1-15 minutes. Tick marks every 20 μm ('m' refers to minutes)

Figure 6.21 – 3D microscopy images (50x) for the growth development of a 28 day old mark processed for 1-15 minutes. Tick marks every 20 μm

Figure 6.22 – 3D microscopy images (50x) for the growth development of a 28 day old mark processed for 1-15 minutes. Tick marks every 20 μm ('m' refers to minutes)

Figure 6.23 - Graph of silver particle diameter vs time of development for average of 5 sets of marks aged under ambient conditions for 1, 14 and 28 days then developed via PDF5D1

Figure 6.24 - The growth development of silver from 30 seconds to 15 minutes for fingerprints deposited on white copy paper and aged for 1 day under ambient conditions then developed via PDF6D2

Figure 6.25 - 3D microscopy images (50x) for the growth development of 1 day old marks processed for 30 seconds to 15 minutes for the samples in figure 6.24. Tick marks every 20 μm

Figure 6.26 - Graph of silver particle diameter vs time of development for 3 sets of 1 day old marks aged under ambient conditions developed via PDF6D2. Data from figure 6.24 and two replicates

Figure 6.27 – Fingerprints deposited on white copy paper and aged for 1 day under ambient conditions then developed after 20 minutes via PDF6D2 with corresponding microscopy images (50x – Tick marks every 20 μm)

Figure 6.28 - Split prints deposited on white copy paper and aged for 1, 14 and 28 days under ambient conditions then developed via PDF6D2 (3 replicates for each age of mark)

Figure 6.29 – 3D microscopy images (50x) for the growth development of a 1 day old mark processed for 1-15 minutes. Tick marks every 20 μm ('m' refers to minutes)

Figure 6.30 – 3D microscopy images (50x) for the growth development of a 14 day old mark processed for 1-15 minutes. Tick marks every 20 μm

Figure 6.31 – 3D microscopy images (50x) for the growth development of a 28 day old mark processed for 1-15 minutes. Tick marks every 20 μm

Figure 6.32 - Graph of silver particle diameter vs time of development for average of 5 sets of 1, 14 and 28 day old marks aged under ambient conditions developed via PDF6D2

Figure 6.33 - Graph of the silver particle diameter vs time of development for the average of 3 sets for 1 day old fingerprints aged under ambient conditions and then developed with varying detergent systems of PD shown in the graph legend

Figure 6.34 - Raman spectra of the silver surface, surfactant component and silver-surfactant interaction for (a) DDAA (b) Synperonic-N (c) Tween 20 (d) DGME and (e) Brij C10

Figure 6.35 - Raman spectra of the silver surface, detergent system and silver-detergent interaction for (a) DDAA-Synperonic-N (b) DDAA-Tween 20 (c) DDAA-DGME and (d) DDAA-Brij C10

Figure 6.36 – Schematic of the structural conformation of DDAA and the silver particulate (not to scale)

Figure 6.37 – Schematic of the structural conformation of DGME and the silver particulate (not to scale)

Figure 6.38 – Schematic of the structural conformation of Brij C10 and the silver particulate (not to scale)

Figure 6.39 - Leather and suede (bovine sources) surfaces that showed no fingerprint development with PDF1S or superglue fuming

Figure 6.40 – Fingerprints deposited on patent leather and aged for 1 day under ambient conditions then developed using PDF1S

Figure 6.41 – Fingerprints deposited on patent leather and aged for 1 day under ambient conditions then developed on patent leather using superglue fuming (chapter 3, section 3.4.6) – 3 replicates

Figure 6.42 – Fingerprints deposited on patent leather and aged for 7 days under ambient conditions then developed using PDF1S

Figure 6.43 – Fingerprints deposited on patent leather and aged for 7 days under ambient conditions then developed using superglue fuming

Figure 6.44 – Microscopy analysis of fingerprint ridge detail for a 1 day old mark on patent leather developed using PDF1S – (a) 2D image and (b) 3D image (50x) - tick marks every 20 μm

Figure 6.45 – Fingerprints deposited on navy matte leather and aged for 1 and 7 days under ambient conditions on then developed using PDF1S

Figure 6.46 – Microscopy analysis of a fingerprint ridge for a 7 day old mark on navy matte leather developed using PDF1S – (a) 2D image (b) 3D image (50x) - tick marks every 20 μm

Figure 6.47 – (a) Fingerprint deposited on white faux leather and aged for 7 days under ambient conditions developed using PDF1S (b) 2D image (c) 3D image (50x) - tick marks every 20 μm

Abbreviations

AFIS	Automated Fingerprint Identification System
AFM	Atomic Force Microscopy
AFR	Automated Fingerprint Recognition
AWRE	Atomic Weapons Research Establishment
CAST	Centre for Applied Science and Technology
CMC	Critical Micelle Concentration
DDAA	n-dodecylamine acetate
DFO	1, 8-diazafluoren-9-one
DGME	Decaethylene glycol mono-dodecyl ether
DLS	Dynamic Light Scattering
ESEM	Environmental Scanning Electron Microscopy
FVM	Fingerprint Visualisation Manual
HPLC	High Performance Liquid Chromatography
IAFS	International Association of Forensic Sciences
IAFIS	Integrated Automated Fingerprint Identification System
IAI	International Association of Identification
IFRG	International Fingerprint Research Group
IND	1, 2-Indandione
IPA	Isopropyl alcohol
MALDI-MS	Matrix Assisted Laser Desorption Ionisation – Mass Spectroscopy
MMD	Multi Metal Deposition
MPTS	(3-mercaptopropyl)-trimethoxysilane
NAFIS	National Automated Fingerprint Identification System
NR	Neutron Reflectivity
ORO	Oil Red O
PD	Physical Developer
SANS	Small Angle Neutron Scattering
SEM	Scanning Electron Microscopy
SLD	Scattering Length Density
SMD	Single Metal Deposition
VMD	Vacuum Metal Deposition
WS	Working Solution

Chapter 1: Introduction

1.1	Introduction	2
1.2	Fingerprints	3
1.2.1	Individuality of Fingerprints	3
1.2.2	History of Fingerprint Identification	6
1.2.3	Current Identification Protocol	7
1.2.4	Types of Fingerprint	8
1.2.5	Composition of Fingerprint Residue	9
1.3	Development of Latent Fingerprints	12
1.3.1	Enhancement Methods for Non-Porous Surfaces	12
1.3.2	Enhancement Methods for Porous Surfaces	16
1.3.3	Fingerprint Development Sequence	18
1.3.4	Recent Developments	20
1.4	Physical Developer and Related Methods	21
1.4.1	History of Physical Developer	22
1.4.2	Current Theory of the PD Process	26
1.4.3	Metal Deposition Enhancement	32
1.5	Objectives	33
1.6	References	34

1.1 Introduction

Fingerprint evidence remains one of the most common evidence types retrieved and analysed from a crime scene.¹ The importance of fingerprint evidence is predominant in the identification of potential suspects but also to aid elimination of the innocent. Locard's principle, 'every contact leaves a trace', is influential in forensic science especially for fingerprint evidence. Fingerprints will almost definitely be left at a scene as they are deposited whenever an object is touched or grabbed (provided the perpetrator was not wearing gloves). Specific development methods are chosen, of which there is a vast list to choose from², to visualise any fingerprints which are chosen according to the surface of the evidential item. These fingerprints could be visible (visible to the naked eye), plastic (an impression left in a soft surface) or latent (non-visible).

Latent fingerprints are invisible to the naked eye due to the association with sweat and oils on the fingertips; therefore these must be visualised in order to produce an image that could be used in fingerprint identification. The current development methods used in the UK and internationally, are well established as effective techniques but in some cases the underlying chemistry is not understood or optimisation is required.

The principle of fingerprint development and identification is the same globally – a fingerprint must be enhanced and a match must be made to identify the perpetrator of a crime. The practical applications to both the development and the identification processes have slight variations in their approach. Collaborative conferences are held regularly allowing for both national and international research groups and law enforcement to discuss and evaluate their work. These include the International Association of Identification (IAI), the International Fingerprint Research Group (IFRG) and the International Association of Forensic Sciences (IAFS).

The work presented in this thesis focuses on latent fingerprint development for porous surfaces with physical developer (PD), a reagent which has to be reformulated but the chemistry must first be understood.

1.2 Fingerprints

Fingerprints are a powerful means of identification, based on the characteristic ridge details. These ridge details arise from the friction ridge skin which is located on the fingers, palms and soles of the feet. This skin in the epidermal layer is thicker, which is thought to allow gripping of objects.³ Fingerprint ridges are developed *in utero* during the eighth week of gestation and become permanent at approximately the seventeenth week of embryonic development.^{3,4} The unique nature of fingerprints is supported further by calculations completed by Sir Francis Galton who concluded in 1892 that there was a 1 in 64 billion chance two people would have identical fingerprints.⁵ No two fingerprints have been found to be the same, not even for identical twins.¹

In addition to the unique nature of fingerprints, they will remain unchanged throughout a lifetime, except in cases of deep scarring.¹ Although these scars could obscure ridge details, they act as further unique characteristics which could act as an identifying feature.⁶ In addition to this, it is also possible to take fingerprints from a body post-mortem for identification.⁷ This can be useful in several cases, such as if the body is dismembered or there are facial injuries and incidents of mass disasters.

1.2.1 Individuality of Fingerprints

The ridge details mentioned in section 1.2 are responsible for the individuality of fingerprints due to the unique patterns that are present. Since the publication of Galton's work, fingerprints have been classified into a primary pattern of either a loop, arch or whorl (figure 1.1) each of which has its own sub-categories.⁵



Figure 1.1 - Primary fingerprint patterns - loop, arch and whorl

The secondary level details, minutiae features, form the distinctive ridge characteristics within the primary pattern. It is also possible to observe tertiary level detail within fingerprints, including sweat pores and ridge sizes.

1.2.1.1 Loops

In order to be classified as a true loop (figure 1.2) the pattern must fulfil several criteria. There must be a minimum ridge count of one, a delta, core and a minimum of one recurving ridge (enters from one side of the finger and exits the same side).^{8,9} The delta is the point of a ridge where two parallel lines diverge.

Loops are the most commonly occurring fingerprint pattern, accounting for 60-65% of the fingerprint population.⁶ There are two main loop sub-types; the radial and ulnar loop which differ in the direction the loop opens (towards the thumb for radial or towards the little finger for ulnar).



Figure 1.2 - Minimum features required for a loop pattern

1.2.1.2 Arches

Arches fall into the lowest population category, contributing to only 5% of all fingerprints. There are two sub-types: the plain and tented arch. The plain arch pattern itself is the simplest of all three primary patterns, with no deltas or cores.⁶ The plain arch is observed when the ridges flow from one side to the other, whereas the tented arch ridges form a spike in the centre or two ridges meet at an angle less than 90°. ^{1, 6}

1.2.1.3 Whorls

Whorls make up the remaining 30-35% of all pattern types. There are four distinct categories for whorls: plain, central pocket loop, double loop and accidental whorls. Accidental whorls cannot be described by any other pattern but could be a combination of a loop and whorl as well as having more than two deltas.⁸

As figure 1.1 shows, whorl patterns have circular ridges and must have two deltas. The plain and central pocket loop whorl have at least one ridge which forms a complete circuit.⁶ A double loop whorl forms from two loops merged together.

1.2.1.4 Minutiae Features

The primary pattern is always determined first when analysing fingerprints to allow elimination, for example of whorls if the evidential fingerprint is a loop. The secondary level details, minutiae features, are the characteristic details upon which identification is based. Some of these characteristic ridge features are shown in figure 1.3.

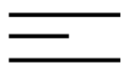
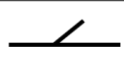
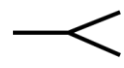
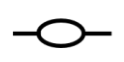
Ridge Ending	
Independent Ridge	
Spur	
Bifurcation	
Lake	
Crossover	
Island	

Figure 1.3 - Examples of common minutiae features

When a fingerprint examiner is attempting to match a suspected fingerprint to a fingerprint on file, it is solely down to the examiner to determine a match or not. If they can identify enough features in the same positions, then they can conclude a true positive match.¹ The fingerprint examiner must have their opinion validated by two other fingerprint officers but this change is only recent; prior to this it was required that there had to be at least 16 points matching features. This process of identification is the standard in the UK as well as in the US – there is no standard requirement for the number of matching characteristics. Other countries, such as Australia and Germany, adopt a minimum of 12 matching features, most likely based on Locard’s observation which stated 12 points result in a positive identification.

1.2.2 History of Fingerprint Identification

Fingerprints have been observed as early as 7000 BC in Jericho, where thumbprints were found in bricks, and have been used for identification in China (600-700 AD) to seal documents and contracts.⁹ In 1684, the first studies concerning fingerprint ridge patterns as well as sweat pores were documented, including accurate drawings by Nehemiah Grew.⁹⁻¹¹ Over 100 years later, Johannes Purkinje published a thesis in 1823 covering fingerprint ridges in which nine categories were classified with

four patterns identified: a loop, arch, tent and whorl.⁹ In 1858, Sir William Herschel was the first person to implement the official use of fingerprints for identification whilst serving the British Civil Service in Bengal, India.¹⁰

The work of Herschel inspired the first publication in a scientific journal, *Nature*, discussing fingerprint ridge details by Dr Henry Faulds in 1880, who also suggested fingerprints could be used in criminal investigations.^{9, 10} In 1892, *Finger Prints* was published by Sir Francis Galton detailing the classification of the three main pattern types (loop, arch and whorl) still in use today.

It was evident that fingerprints were of great interest but it was not until 1901 that Sir Edward Henry introduced the use of fingerprints as a means of criminal identification in Scotland Yard, UK and the first conviction from fingerprint evidence occurred in 1902.¹¹ This was the basis of the ten print system that is used in present UK law enforcement – all ten fingerprints are recorded upon an arrest.

1.2.3 Current Identification Protocol

It is conclusive that the unique nature of fingerprints makes them a powerful means of identification. However the determination of an identification in the UK, is an opinion. As mentioned in section 1.2.1.4, the fingerprint examiner will analyse a suspected fingerprint and only have the final decision validated by two other examiners. The three outcomes that come from an analysis will either be: an identification, exclusion or inconclusive.¹² These outcomes are a result of the ACE-V process commonly used by fingerprint examiners worldwide, which stands for a four stage process of analysis, comparison, evaluation and verification. Although this method is accepted for practical use and is logical, it has received several criticisms as there is no statistical standard and there are discrepancies or deliberate variations between countries.¹³ (See section 1.2.1.4).

Evidential fingerprints must be compared to fingerprints from a set of potential suspects on file. Until 1970, all fingerprint files were kept on fingerprint cards which

were stored and handled by hand. Undoubtedly this was a painstaking process which became more difficult with the sheer number of records to file. The automated fingerprint recognition technology (AFR) was developed to replace the need for paper records. AFR became the National Automated Fingerprint Identification System (NAFIS). In 2001, this technology was available to all police forces across England and Wales.

In 2005, IDENT1 replaced NAFIS in order to incorporate Scottish police forces and is the national database for fingerprints, palm prints and crime scene marks.¹ The AFIS technology (Automated Fingerprint Identification System) is used globally. INTERPOL, with 192 member countries, hold a fingerprint database which authorized members can access. In addition to this, the FBI maintain their own national fingerprint database, IAFIS – Integrated Automated Fingerprint Identification System.

1.2.4 Types of Fingerprint

There are three types of fingerprint which could be recovered from the scene of a crime: visible (or patent), plastic (or 3D) and latent. These three types arise due to the type of surface or material that is touched. Exemplar fingerprints form the fourth category but these are not detected. Exemplar fingerprints will be deposited by a suspect or as part of elimination prints to aid the identification of a perpetrator.

1.2.4.1 Visible Fingerprints

Visible fingerprints are quite simply, as the name suggests, marks which are visible to the naked eye. Further development is not required and the fingerprints are photographed or lifted depending on the deposited material. Fingerprint lifting is a process of preserving a developed fingerprint by removing it from the surface using a clear, adhesive acetate sheet. Visible fingerprints are formed when a coloured substance such as paint, blood (in violent crime) or soot (from an arson case) is transferred from the fingertip when in contact with a surface e.g. a wall or windowsill.

1.2.4.2 Plastic Fingerprints

Plastic fingerprints are also referred to as 3D fingerprints due to the nature of their appearance. When a finger comes into contact with a soft material such as clay, soil or wax, a 3D impression is formed. As with visible fingerprints, plastic impressions can be photographed for examination. It is important to note that plastic prints can often be overlooked due to lighting and the material upon which they are formed; therefore it is imperative to thoroughly examine a crime scene and potential pieces of evidence.

1.2.4.3 Latent Fingerprints

Latent fingerprints are the most common type of mark that will be recovered. Unlike the other two types, latent fingerprints are not visible to the naked eye. This is due to the association with sweat and oils transferred from the fingertip to any surface that is touched, hence the high probability of detecting latent marks at a scene or on pieces of evidence (provided gloves are not worn by the perpetrator). In addition to this, these marks will not be visible to the perpetrator, making it less likely they would be removed for example by wiping the surface. Due to the 'invisibility' of latent fingerprints, they must first be visualised using a range of chemical treatments or physical techniques. The development of this type of mark is dependent on the porosity of the surface or substrate and the composition of the fingerprint residue.

1.2.5 Composition of Fingerprint Residue

Human perspiration is necessary in the regulation of body temperature through the evaporation of sweat, which has a cooling effect. The composition of human sweat secretions has been extensively studied throughout medical literature.¹⁴⁻²¹

There are three major sweat glands that are responsible for the secretion of human 'sweat': eccrine, sebaceous and apocrine. (The term sweat has been used here as the exact composition varies with each gland so there is not one unified composition of human sweat).

As mentioned above, the composition of human sweat types has been studied extensively with respect to medical¹⁵, physiological²² and biological²³ areas. The composition of latent fingerprint residue, on the other hand, has not been researched in as much depth because of the complexity of the residue itself. It can be assumed that the fingers and hands will come into contact with other areas of the body, particularly the face and hair throughout the day. Therefore, fingerprint residue is not as straightforward as it will contain a mixture of components from the aforementioned eccrine and sebaceous glands. Apocrine glands are found in axillary areas of the body such as the underarm and genital region²⁴; therefore apocrine components rarely contribute to latent fingerprint residue. In addition to this, it is highly probable that fingerprint residue could contain contaminants. These contaminants could be cosmetic, food residues or other foreign materials that remain on the surface of the hands and fingers.

As well as these added complexities, it is very rare that a fingerprint will ever be recovered immediately after deposition. Therefore, the residue components will change in nature and distribution over time and research has been done to identify these changes.²⁵⁻²⁸ The initial composition of fingerprint residue consists of the immediate compounds that are transferred from the finger to the surface. The aged composition is the modifications of the components but also any products which arise from these modifications as a result of chemical, physical and biological processes. The following sections will describe the eccrine and sebaceous components that have been reported to be present in fingerprint residue.

1.2.5.1 Eccrine Sweat

Eccrine glands can be found all over the body with the highest densities reported in the palms and soles (ca. 600-700 cm⁻²).^{19, 24} Eccrine sweat can be regarded as a dilute electrolyte solution because it is predominantly water (in excess of 98%) and inorganic salts, though some organic material has also been reported. One major salt, sodium chloride (NaCl) varies in concentration in each individual because of

factors such as salt intake and levels of physical activity but average values of 5-100 mEq/l have been reported.¹⁴

Element or Compound	Concentration/per fingerprint
Amino acids	0.2-1 µg ²⁹⁻³³
Proteins	384 µg ^{31, 34}
Lactic acid	9-10 µg ^{31, 33, 35}
Sodium	0.2-6.9 µg ^{33, 35}
Chloride	1-15 µg ^{33, 35}
Urea	0.4-1.8 µg ^{33, 35}
Potassium	0.2-0.5 µg ^{33, 35}
Ammonia	0.2-0.3 µg ^{33, 35}
Magnesium, Zinc, Copper	Trace ^{31, 33}

Table 1.1 - Eccrine components in fingerprint residue

1.2.5.2 Sebaceous Sweat

The sebaceous glands are associated with areas of hair follicle growth and are located predominantly on the face and scalp. Sebaceous material is commonly found in fingerprint residue as our face and hair are areas of the body that the fingers will come into contact with regularly. Sebum is secreted from these glands which is a complex mixture of lipids and will vary depending on the individual.¹⁷

Class of Compound	Relative amount
Triglycerides	30-40 %
Fatty acids	15-25 %
Wax esters	20-25 %
Squalene	10-12 %
Cholesterol	1-3 %

Table 1.2 - Relative amount of sebaceous components in fingerprint residue^{17, 28, 31, 36-38}

1.3 Development of Latent Fingerprints

1.3.1 Enhancement Methods for Non-Porous Surfaces

Non-porous surfaces can vary in terms of surface roughness, density and composition. Dependent on these factors, specific fingerprint development techniques can be used, which will be discussed in the following sections.

1.3.1.1 Powders

Powdering is one of the most common development methods for relatively smooth, hard, non-porous surfaces such as glass, dense plastics and ceramic.^{1, 37} The cheap, fast and simple nature of powdering makes it a popular visualisation technique. It is a physical process in which the powder particles will adhere to the 'sticky' (grease and oil) components of fingerprint residue. It is applied with a soft-haired brush which is the only disadvantage as too much force could destroy the fingerprint ridge detail.³⁹



Figure 1.4 - Fingerprint developed with carbon black powder

Powdering will often be carried out at the scene where items cannot be taken to the laboratory (e.g. bathroom tiles, wall mirrors). Any developed marks will be photographed and lifted to be analysed for identification. Typically, black (carbon) or aluminium powders will be used but coloured powders are available. Coloured powders will only be used after processes such as superglue fuming as they can be fluorescent to enhance visualisation.

1.3.1.2 Superglue Fuming

Superglue fuming (ethylcyanoacrylate fuming) is a widely accepted, effective method for latent fingerprint development on non-porous surfaces. It is particularly effective for soft plastics (polyethylene and polypropylene – excluding cling film) of both high and low density.²

Superglue fuming is a chemical process in which an interaction between superglue vapours and components of the fingerprint residue result in the formation of a white polymer on the surface of the fingerprint. Due to the hazardous nature of the superglue fumes, the process should normally be carried out in the laboratory in a fuming cabinet to ensure suitable ventilation. Current superglue cabinets are automated and allow the humidity to be set between 75-90% and the superglue to be heated to 120 °C. Sufficient development and contrast can be achieved in 10-30 minutes.



Figure 1.5 - Fingerprint developed with superglue fuming²

Though the method is well established, the exact mechanism between the fingerprint components and the polymerisation of cyanoacrylate monomers is not fully understood. The polymerisation of ethylcyanoacrylate monomers is initiated by a nucleophile (Lewis base) and this mechanism has been studied previously.^{40, 41} However, it remains unclear as to which of the components of the fingerprint residue

initiate the polymerisation. The majority of fingerprint residue is water which could act as the nucleophilic initiator.⁴²⁻⁴⁴ Superglue fuming is known to be more effective for fresher marks compared to aged marks, which supports the theory that water activates the polymerisation as water is readily lost as the mark ages.

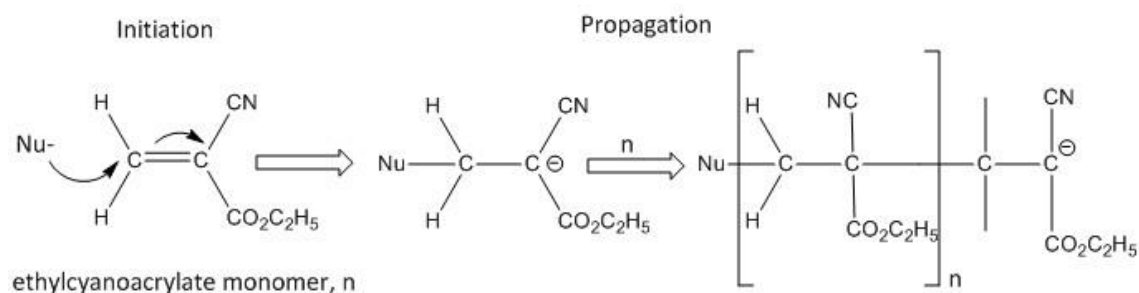


Figure 1.6 - Proposed nucleophilic mechanism for superglue polymerisation

As superglue fuming results in a white polymer, this can often be disadvantageous for light coloured backgrounds. Basic Yellow 40, a fluorescent dye, is often used for post-processing to aid visualisation.⁴⁵

Recently, a one-step fuming method using the reagent Lumicyano™ has been evaluated, which eliminates the second stage dyeing step as the glue is fluorescently active.⁴⁶⁻⁴⁸ In addition to this, another commercial one-step superglue reagent, PolyCyano (Foster and Freeman Ltd.) is also available.^{46, 49, 50} This glue is a solid powder that has to be heated to a higher temperature of 230 °C and although current fuming cabinets can be modified to reach this temperature, it introduces further hazards.

1.3.1.3 Powder Suspension

Powder suspensions work on the same principle as conventional dry powders with the exception that they can be used on non-porous surfaces that have previously been wetted.⁵¹ In addition to this, they are particularly effective for adhesive surfaces. The reagent consists of small powder particles suspended in a detergent and wetting agent solution. Iron oxide(II/III) and carbon based powders result in black fingerprints whereas titanium dioxide suspensions produce white fingerprints, thus making them a suitable reagent for lighter and dark backgrounds respectively.² The powder is applied

using a wet brush, allowed to process for 10-20 seconds and the excess suspension is rinsed with distilled water.



Figure 1.7 - Fingerprint development using iron oxide powder suspension

Although it is accepted that the powder particles adhere to components of the fingerprint residue, the exact mechanism is unknown.^{2, 52, 53} The sebaceous content of the fingerprint residue could effectively strip the surfactant molecules away from the powder particles exposing them for deposition. However, the complex nature of fingerprint residue means several components could be responsible.² It is known that particle size is important to generate the spatially selective deposition which has been studied microscopically.⁵⁴ Powder suspensions have recently been evaluated as potential method for development of latent marks on the new UK polymer banknotes with promising results.⁵⁵

1.3.1.4 Vacuum Metal Deposition (VMD)

Vacuum metal deposition (VMD) is a physical process that is carried out in the laboratory in a vacuum chamber. Metal wires or pellets are thermally evaporated and a thin metal film is deposited on the surface of the fingerprint ridges. The two most common VMD options are gold/zinc and silver deposition. VMD is very effective for a range of non-porous surfaces and some semi-porous surfaces such as fabric^{56, 57} and has been tested on the new UK polymer banknotes.^{55, 58}

Gold and silver initially deposit onto the greasy components of a fingerprint providing nucleation sites for further silver deposition or zinc for the gold/zinc system (as zinc will not deposit on the residue so improves the contrast observed after gold deposition).²

VMD is a very sensitive technique that is often used preferentially to superglue fuming as it is capable of developing marks on surfaces with contamination, exposure to harsh environmental conditions and aged marks.^{2, 59, 60}

1.3.2 Enhancement Methods for Porous Surfaces

Porous surfaces can also vary in surface roughness, density and composition but, unlike non-porous surfaces, they are capable of absorbing liquids, i.e. fingerprint residue and water. This means that the fingerprint development techniques required for porous surfaces often target the water-soluble components of fingerprint residue and are solutions themselves, as explained in the following sections.

1.3.2.1 Ninhydrin

Ninhydrin is an amino acid sensitive reagent which produces purple coloured fingermarks. This purple compound is known as Ruhemann's Purple, as shown in figure 1.8. It has been used for latent fingerprint development from porous surfaces since the 1950s and has been studied extensively.⁶¹⁻⁶⁷

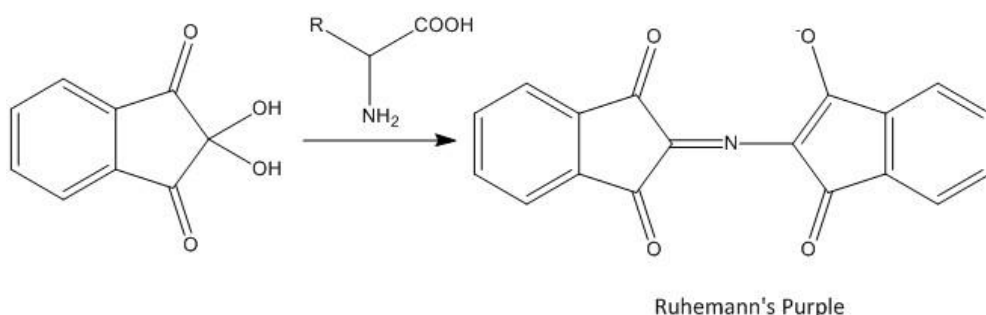


Figure 1.8 - Formation of Ruhemann's Purple



Figure 1.9 - Fingerprint developed with Ninhydrin

The solution is prepared by dissolving ninhydrin in HFE 7100 but a more concentrated solution can be prepared using acetic acid, ethanol and ethyl acetate.² The item in question is simply immersed in the ninhydrin solution and removed immediately after, effectively 'dipping' the item, and left to dry in an area with suitable ventilation. The solution can also be brushed on but this must be meticulously done to avoid obscuring potential marks. It is possible to spray ninhydrin solution however this is normally discouraged due to the risk of asphyxiation from solvent evaporation. If there are any developed fingerprints, these will usually appear after 24 hours but the process can be accelerated with the use of a ninhydrin oven.

1.3.2.2 DFO

DFO (1, 8-diazafluoren-9-one) is an analogue of ninhydrin which also reacts with the amino acid components of a fingerprint but produces a fluorescent product.

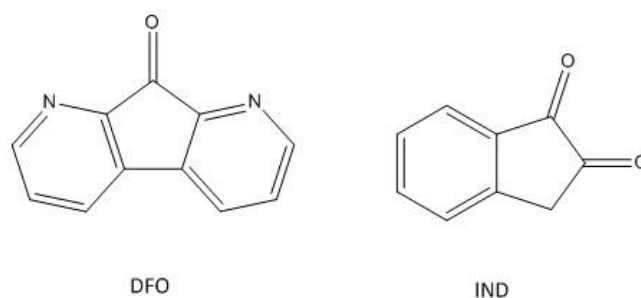


Figure 1.10 - DFO and Indanedione



Figure 1.11 - Fingerprint developed using DFO²

DFO was originally recommended for use to develop latent fingerprints after the discovery and introduction of ninhydrin.⁶⁸ However it is recommended to primarily use DFO, and ninhydrin is used as a secondary process to develop further marks.² Similarly to ninhydrin, the DFO working solution is prepared by dissolving DFO in a solvent mixture (methanol, acetic acid, HFE 71D and HFE 7100) and the processed marks must be heated to 100 °C for at least 20 minutes.² It is possible to heat to higher temperatures for shorter times but this introduces a risk of damaging the substrate. However, without heating acceleration the reaction will take many hours.⁶⁹ The samples are excited with green light (500-550 nm). The fluorescent product is proposed to be two DFO molecules linked with a nitrogen atom analogous to the Ruhemann's Purple product seen with ninhydrin.^{2, 68}

Another reagent and analogue to ninhydrin, 1, 2-Indandione (IND), is an alternative for detection of fingermarks on porous surfaces. Research has shown it to be effective, but not superior to DFO, which should still be considered first when developing marks on porous items.^{66, 70-73}

1.3.3 Fingerprint Development Sequence

As discussed in section 1.3.1 and 1.3.2, the degree of porosity of the surface upon which the fingerprint is deposited will determine the technique and sequence of development to follow. In addition to this, it is important to consider any detrimental

effects to the sample when choosing a technique to use as some methods are destructive. If the evidential item needs to be retained or further analysis is required, these factors will contribute to the development sequence.

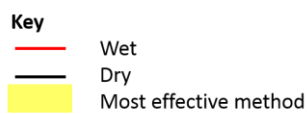
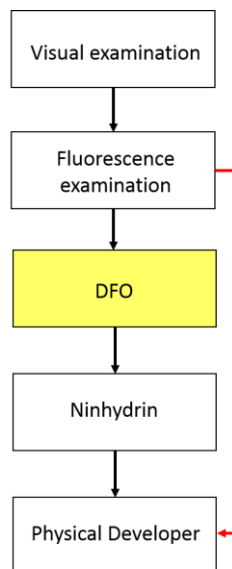
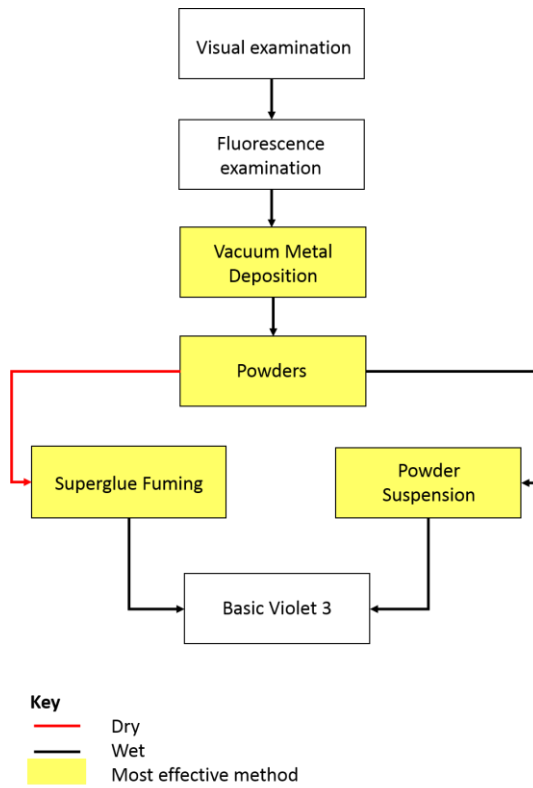


Figure 1.12 - Fingerprint development sequence non-porous (above) and for porous surfaces (below).²

Figure 1.12 shows the general fingerprint development sequence for non-porous and porous surfaces respectively. These sequences have been adapted according to the UK Centre for Applied Science and Technology (CAST) fingerprint visualization manual (FVM)² and only show the general techniques to consider as well as highlighting which method(s) would be the most effective. There are other fingerprint development techniques that have not been included as these are more specific to a particular surface, for example multi-metal deposition (MMD) is the most effective method for plastic cling film. The FVM contains all the current and novel fingerprint development methods which are graded from A-F where category A processes are routinely used and should be considered first. Category B and C processes are occasionally used operationally but usually only after all category A processes have been considered. The main difference between the two is that category B processes are established methods but have not been fully evaluated and validated, whereas category C methods are novel processes currently being researched and/or optimised. The final two categories are methods which have shown no operational benefit or should not be used due to health and safety reasons.

1.3.4 Recent Developments

There is a considerable amount of research evaluating both novel and optimised methods for latent fingerprint detection.⁷⁴⁻⁷⁶ Several of these studies have been discussed in sections 1.3.2 and 1.3.3 including those relating to LumicyanoTM and 1, 2-Indandione. Those methods are comparable in that they all rely on an interaction of the reagent with the fingerprint residue itself. In contrast, research on metal surfaces has been carried out to develop the substrate using the fingerprint residue as a barrier producing a negative image. These include the electrodeposition of polymers onto stainless steel^{77, 78} and the electroless deposition of silver onto copper-containing surfaces.⁷⁹

Due to an increase in wildlife related crime and riots that have happened in the last few years, it has become necessary to be able to develop fingerprints on more

challenging surfaces. There has been research conducted to address these difficult surfaces such as elephant ivory⁸⁰ as well as rocks and stones.^{81, 82}

In addition to recent innovations regarding the development of latent fingerprints, there have been ground-breaking developments concerning information the fingerprint deposit itself can provide. Researchers (Francese et al.) have been collaborating with law enforcement to identify components present in the fingerprint residue using MALDI-MS (Matrix Assisted Laser Desorption Ionisation-Mass Spectrometry). The technique has been shown to reveal crucial information from the fingerprint such as the sex of the offender, any drugs, food or drink consumed, whether blood has been touched and if there has been contact with condom lubricants, including identifying the brand.⁸³⁻⁸⁵

1.4 Physical developer and Related Methods

Physical developer (PD) is an immersion based technique for the development of latent fingerprints on porous surfaces. It is typically used at the end of the porous surface sequence after ninhydrin or DFO (section 1.3.2.1 and 1.3.2.2) unless the item in question has previously been wetted. In this case, PD is the only technique capable of developing fingermarks on wetted porous surfaces.

PD is listed in the UK Home Office fingermark visualisation manual as a Category A process. This means that PD is a standard process for routine operational use that has been fully evaluated by the Home Office according to ISO 17025 standards. Category A processes should always be used before trying a different, lower tier category process.

Three component solutions comprise the PD working solution: a redox, a detergent and a silver solution. A ferrous/ferric redox couple allows for the reduction of silver ions to silver atoms, which aggregate to form silver particles, (Equation 1.1) which are in turn stabilised by a cationic surfactant.



The energetics of the process are carefully balanced such that the silver particles remain stable in solution until a substrate is introduced. Spatially selective deposition occurs, resulting in silver deposition on only the fingerprint ridges producing a grey/black image. The exact mechanism as to how the silver is deposited onto the fingerprint ridges and the role of the surfactants in solution is poorly understood – this will be a major feature of the research described later in this thesis.

The general consensus on the use of PD in police forces and forensic laboratories is that it is time-consuming, labour intensive and generally only used as a last resort. As part of this research, police forces and forensic laboratories were surveyed for their opinion on the use of PD. Of the 18 police forces visited nationwide in 2016, the majority concluded they would only use PD if the evidential item in question required it or no other preferential method had worked. This is mainly due to the costs and time associated with using the method and many have reported PD does not appear to produce developed marks comparable to those reported by CAST. Other police forces are using PD more regularly and continuing to validate the method in their laboratories for accreditation.

It is unclear whether the issues with PD not working as effectively are a cause of incorrectly making up the working solution, understanding the protocol or simply the item was not suitable for fingerprint development. Nonetheless, PD is an effective development technique and currently the only method used for paper surfaces that have been wetted; therefore it is paramount that the chemistry is better understood and the process is optimised.

1.4.1 History of Physical Developer

Physical developer was not originally designed for the use of fingerprint detection but rather for photographic development. In silver photography, a film of silver halide crystals in a gelatin matrix is exposed to light generating silver metal particles. These silver particles act as nuclei for further enhancement of the photographic image when immersed in the developer solution. The developer solution

contains an electron donor that will specifically reduce the silver nuclei with a larger number of atoms than the critical value.^{86, 87}



The process is stopped with a fixing solution and contrast is achieved between the grey/black reduced silver metal and the transparent matrix.^{86, 88}

The nature of this development process is chemical as the source of silver ions is in the silver halide matrix compared to physical development in which the developer solution contains the source of silver ions.

In 1969-71, Jonker et al. introduced the use of a physical developer for the photo-fabrication of printed circuit boards at the Philips Research Laboratories.^{89, 90} It was this work that formulated a stabilised physical developer with the addition of a cationic surfactant to increase the half-life of the working solution. It was proposed that the cationic surfactant molecules surrounded the silver particles in a staggered conformation to prevent aggregation in the solution. However, there were still issues controlling the rate of development with the rate of spontaneous nucleation.

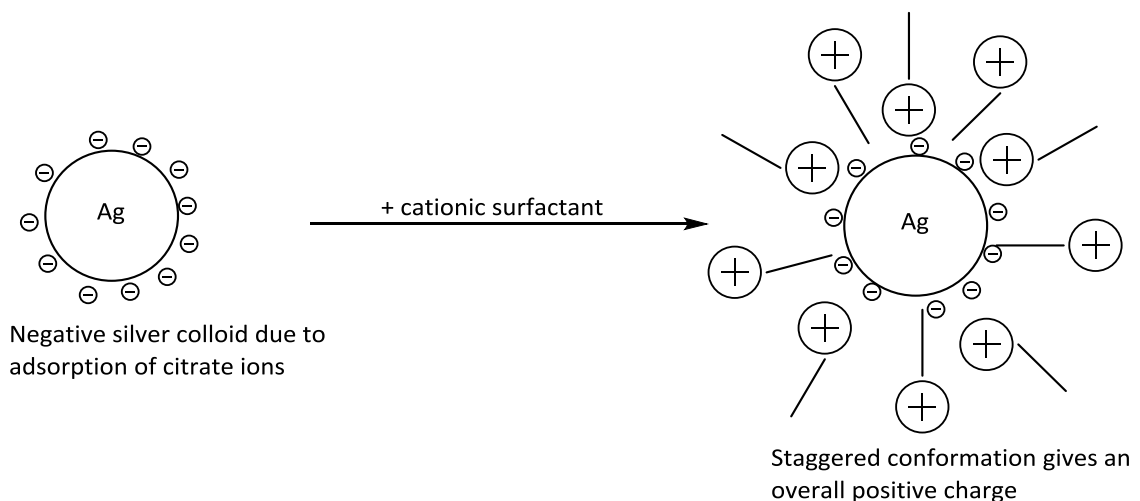


Figure 1.13 – Schematic of the proposed staggered conformation of the cationic surfactant around the silver particles (not to scale)

Jonker et al. determined that the rate of nucleation, J , (Equation 1.3) was highly dependent on the electrochemical potential, ΔE , which had to be finely balanced such that silver reduction was possible whilst maintaining stability.

$$J = C \exp[-B/(\Delta E)^2] \quad (1.3)$$

To control the energetics of the working solution, the ferrous/ferric redox couple was used to successfully reduce silver ions to silver particles (equation 1.1) whilst preventing the aggregation and subsequent precipitation of silver metal from the solution. The original formulation for PD from Jonker is detailed in table 1.3.

Component	Amount	Concentration
Ammonium ferrous sulfate hexahydrate	78.4 g	0.1999 M
Iron (III) nitrate nonahydrate	32.3 g	0.0780 M
Silver nitrate	8.49 g	0.0500 M
Citric acid	21 g	0.1093 M
Armac 12D (lauramine acetate)	0.2 g	815 μ M
Lissapol NDB	0.4 ml	699 μ M
Water	1 L	

Table 1.3 - Philips FC1 Jonker PD formulation⁹¹

The use of PD for latent fingerprint development was discovered accidentally. In the early 1970s, Morris, who was working for the Atomic Weapons Research Establishment (AWRE) discovered that a fingerprint developed when processing a photograph. In 1975, Morris began to research Jonker's PD formulation under contract for the Police Scientific Development Branch (now Home Office Centre for Applied Science and Technology, CAST). The work was motivated by the need to make the PD reagent more accessible to police forces in terms of reagent preparation and shelf life as well as effective fingerprint development.

Morris identified that the ratio of the ionic concentrations controlled the thermodynamics of the process but the rate of fingerprint development was dependent on the Fe^{2+} and Ag^+ concentrations only.⁹¹ The modified PD formulation is

listed in table 1.4 which is not dissimilar to the current formulation used today as recommended by CAST.²

Component	Amount	Concentration
Ammonium ferrous sulfate hexahydrate	80 g	0.2040 M
Iron (III) nitrate nonahydrate	30 g	0.0743 M
Silver nitrate	10 g	0.0589 M
Citric acid	20 g	0.1041 M
Armac 12D (dodecylamine acetate)	0.2 g	815 μ M
Lissapol NDB (Synperonic N)	0.4 ml	699 μ M
Water	1 L	

Table 1.4 - Modified PD formulation by Morris (AWRE)⁹¹

Along with Goode and Wells, Morris observed variations in the effectiveness of the cationic surfactant from different suppliers and batches.⁹² The work determined that the surfactant concentration was not the critical factor but that the optimum carbon length chain should be between 12-17 and the surfactant concentration should be below the critical micelle concentration (CMC).⁹²

In addition to the thermodynamics of the PD process, Morris investigated potential trigger materials for silver deposition on the fingerprint residue. The first theory proposed that chloride ions present in the fingerprint residue could react with silver producing silver chloride which would degrade to silver metal when exposed to light, providing a nucleation site for further silver deposition.⁹³ This theory was only applicable to items which had not been wetted. In 1996, it was reported that salts or chloride are not required for PD silver deposition but lipids and proteins are.⁹⁴

The second theory involved 'surfactant stripping' which was promoted by a hydrocarbon component of the paper surface. The cationic surfactant would be stripped from the silver particle exposing the silver surface to deposit onto the paper.⁹³ Morris also tested several lipid components of fingerprint residue but only observed a positive reaction from cholesterol stearate and squalene.⁹⁵ The exact trigger materials were not established during the AWRE work but Goode and Morris later published a

comprehensive review of latent fingerprint development which included the PD method.⁹⁶ Prior to this, in 1981, PD was first used in casework by Hardwick.⁹⁷

It became commonly accepted that the water-insoluble components of fingerprint residue were responsible for the deposition of silver in PD; the exact mechanism is still unknown.⁹⁸⁻¹⁰⁹ This theory was not unreasonable given that PD is very effective for porous items which have previously been wetted and it can be assumed that the water-soluble eccrine material is dissolved. However, it has been proposed that the sebaceous lipid material hardens with age, trapping the eccrine material.² The targets for PD have been recently explored by de la Hunty et al. who have confirmed that the lipid material is not solely responsible and that eccrine components must be present for effective PD development.^{110, 111} An outline of the history of PD can be seen in figure 1.14 with some features further explored in section 1.4.2.

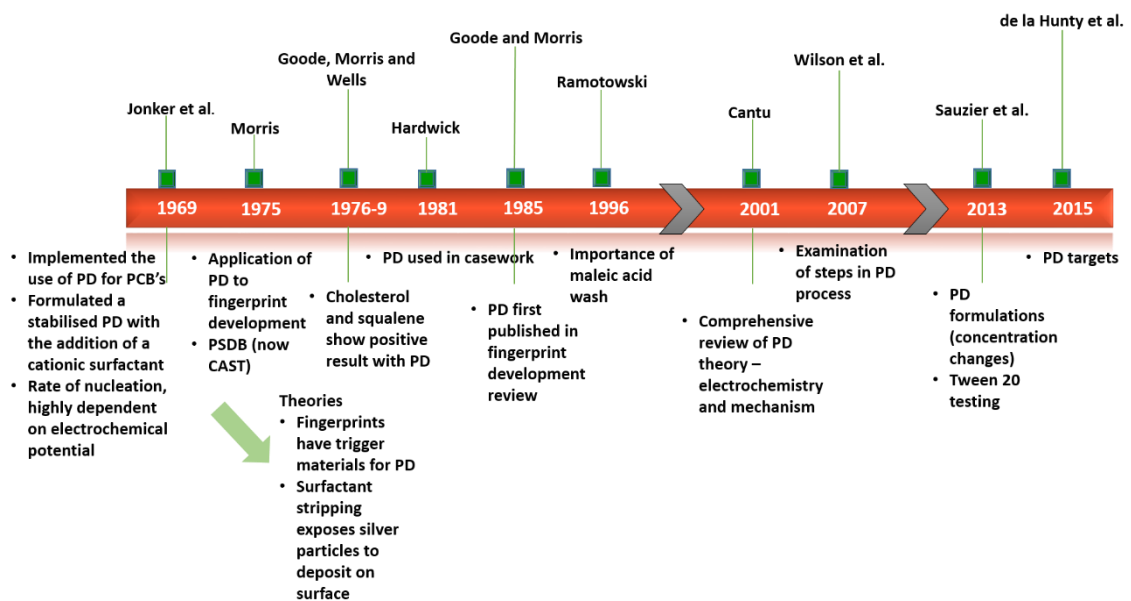


Figure 1.14 - Timeline of PD

1.4.2 Current Theory of the PD Process

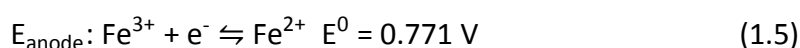
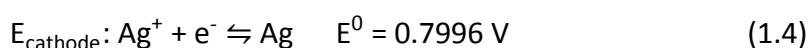
The current formulation for PD, as listed in the Fingerprint Visualisation Manual, is based on the work conducted by Morris and is shown in table 1.5. This is

the formulation recommended by CAST, although there are commercial kits available. It is not recommended to use these commercial kits as one of the limitations of PD is the sensitivity of silver to deposit randomly if not carefully controlled. Ramotowski did compare some of these kits and results were comparable to a prepared PD solution.⁹⁸ The shelf life can be lower with the commercial kits which is not cost effective compared to preparing a PD solution which will then have a longer shelf life if stored correctly.

Redox Solution		Detergent Solution		Silver Solution	
Iron (III) nitrate nonahydrate	30 g	n-dodecylamine acetate	2.8 g	Silver nitrate	10 g
Ammonium ferrous sulfate hexahydrate	80g	Synperonic N	2.8 g	Deionised water	50 mL
Citric acid, anhydrous	20 g	Deionised water	1 L		
Deionised water	900 mL				
PD Working Solution					
900 mL		40 mL		50 mL	

Table 1.5 - Current PD working solution formulation²

It is important that each chemical is added to the solvent and each solution is added in the order listed in Table 1.5. This is because of the finely controlled energetics of the PD solution.



$$\Delta E^0 = E_{\text{cathode}} - E_{\text{anode}} = 0.7996 - 0.771 = 0.0286 \text{ V} = \mathbf{28.6 \text{ mV}} \quad (1.6)$$

Cantu explained in his comprehensive review of the electrochemistry of the PD process, that the working solution behaves like an electrochemical cell.¹⁰³ (See

equations 1.4-1.6). In order for the reaction to be thermodynamically feasible, ΔE must be positive according to $\Delta G = -nFE^\circ$. However, the spontaneous formation of silver metal in solution must be suppressed.⁹⁰ Thus ΔE is as close to zero as possible to allow a thermodynamically feasible reaction as well as a kinetically stable solution that does not hinder the physical development process.

Citric acid is added to the redox solution to control the amount of ferric ions produced through complexation. In addition to this, it maintains a low pH (ca. 1.3) which is essential for the PD process. It has been proposed that a low pH could protonate components of the fingerprint residue (proteins, amines) providing nucleation sites for the silver to deposit.¹⁰³

As discussed in section 1.4.1, the addition of a cationic surfactant improved the solution stability but the role of the non-ionic surfactant component is not completely understood. It has been proposed that the non-ionic surfactant was added to aid dissolution of the cationic surfactant and to prevent the subsequent precipitation.⁸⁹ The current non-ionic surfactant, Synperonic N (figure 1.15), has been banned due to environmental issues and without it, PD does not work efficiently.¹¹² Several research groups worldwide are already using Tween 20 (figure 1.16) as a replacement for PD but there is little agreement on how much should be used and the appearance of the working solutions.^{113, 114} Tween 20 does appear to improve the stability of the working solution indicating that the non-ionic surfactant has more of a fundamental role but testing in the UK is still ongoing.^{37, 115}

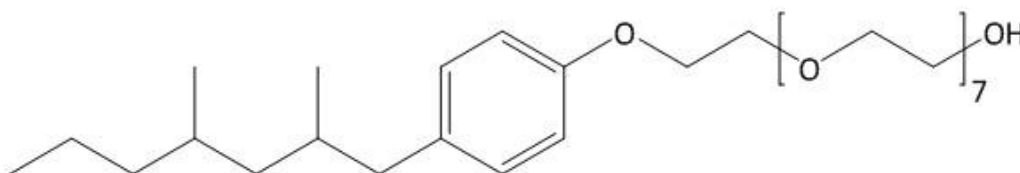


Figure 1.15 – Synperonic N

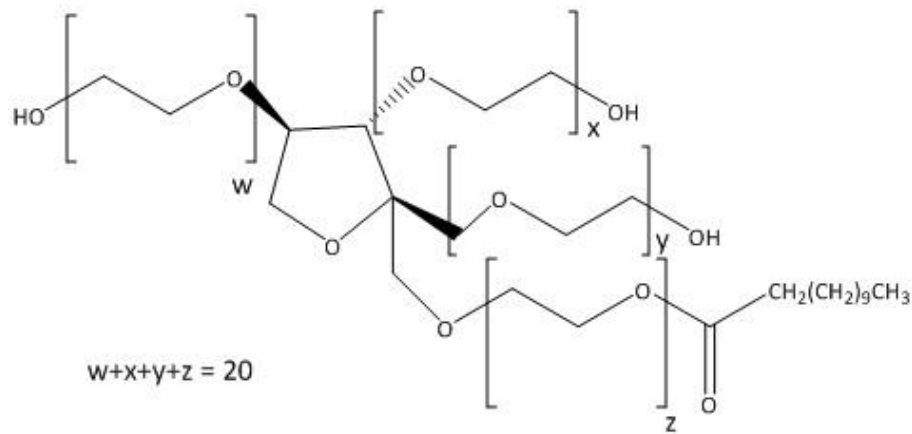


Figure 1.16 - Tween 20

Prior to the development stage of the PD process, a maleic acid pre-wash is required; this was first reported in 1981.⁹⁷ The importance of the acid pre-wash was reiterated by Ramotowski in 1996 and several other acids have since been investigated including malic and nitric acid.^{100, 107, 115, 116} Many papers currently contain ‘fillers’ such as calcium carbonate which will react with the silver particles to produce silver oxide. This effectively results in the whole paper surface turning black, obscuring any potential fingerprints.

There has been work published concerning the PD formulation concentrations, however this has not changed the standard procedure recommended by CAST in the UK. The research studying the effect of changing the concentrations of the working solution components has not resulted in an optimised PD method that produces higher quality fingerprints compared to the current formulation.^{99, 100, 103, 107} Instead of researching the foundations of PD further, some research has been published suggesting replacement of PD with alternative techniques.

Oil Red O (ORO) represented in figure 1.17 was introduced as an alternative because it is a lipid stain;¹¹⁷ this is expected to target similar components of the fingerprint residue, as PD is reported to react with water-insoluble components.

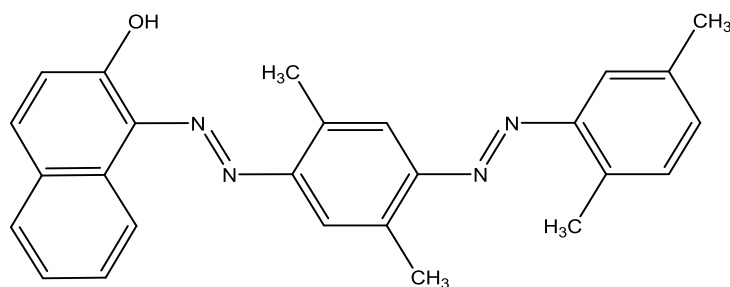


Figure 1.17 - Oil Red O (ORO)

The procedure for use of ORO is similar to PD: the sample is immersed in the staining solution followed by a buffer solution and final water rinse to remove the excess. The resulting fingerprint is red in colour against a light pink background. Wood and James carried out a study to directly compare ORO against PD using different types of paper, different liquids for immersion of the samples for 1 hour, 24 hours and 1 week as well as using loaded fingerprints and natural marks.¹⁰⁴ The main conclusions drawn from the paper indicated that ORO was much more effective when the prints were purposely loaded with sebaceous sweat, which is not useful in a criminal context. PD was not outperformed by ORO for the natural marks in terms of the ridge detail achieved under all the conditions tested. It is also worth noting that some fingerprints can take up to 90 minutes to develop using ORO, which is considerably longer than 15 minutes for PD.

Another comparison study published recently reports similar results to Wood and James for the testing of natural marks.¹⁰⁶ ORO was not superior to PD in terms of developing more fingerprints or the resulting quality of those fingerprints. Similar results were confirmed, for example neither PD nor ORO are effective for cardboard substrates. Furthermore, PD proved its efficiency for development of aged fingerprints with reduced levels of sweat. ORO, on the other hand, produced no fingerprints with any identifiable ridge features. ORO was effective for fingerprints which were not aged for as long and the paper by Simmons suggests this is because ORO targets the labile fraction of the fingerprint residue.¹⁰⁶ This fraction contains components such as triglycerides which are likely to be lost quicker than other components of the fingerprint such as proteins. However, fingerprints are not always recovered from a

crime scene when they have just been deposited. Rather they are likely to have been aged for some time, suggesting that PD would be more effective for those porous surfaces.

Another lipophilic stain has been investigated as an alternative to PD, Nile red. (See figure 1.18). One of the attractive properties of Nile red is the luminescent ability which offers enhanced contrast between the fingerprint and the background substrate.

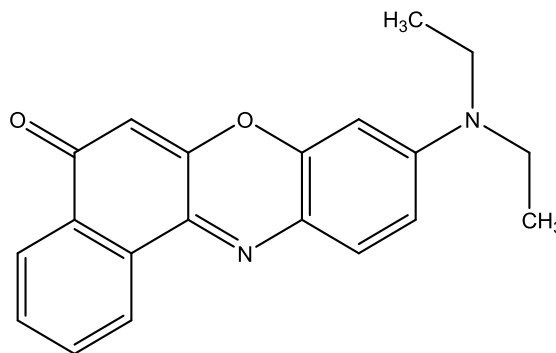


Figure 1.18 - Nile Red

Recent literature has compared Nile red with PD and similar results were observed to those of the ORO comparisons.¹⁰¹ Nile red was most effective on fresher fingerprints and did not outperform PD, but it was reported that Nile red could be used in sequence with PD to further improve weakly developed marks. A pseudo-operational trial carried out resulted in the development of three times as many fingerprints with PD rather than with Nile red.¹⁰¹ This highlights the fact that PD is extremely sensitive and the preferred choice of technique for paper substrates. Procedurally, Nile red treatment consists of a water rinse, immersion in the working solution, followed by a water rinse; development can take up to one hour. This is less labour intensive but Nile red seems more applicable for use after PD, rather than as an alternative, because the fingerprints are not of better quality.

1.4.3 Metal Deposition Enhancement

Multimetal deposition (MMD) was first introduced as a method for the visualisation of latent fingerprints in the late 1980s by Saunders.³⁷ The process incorporates two stages: the first is an immersion of the sample in a colloidal gold solution followed by the second stage which is an immersion in a modified physical developer solution. Unlike PD, MMD can be used on both porous and non-porous surfaces and is particularly effective on cling film.² Colloidal gold is deposited onto the fingerprint residue which then acts as a nucleation site for silver deposition.

The physical developer stage is modified such that it is considerably less stable with the addition of only Tween 20 as the surfactant stabiliser. The silver solution will only last ca. 15 minutes, contributing to one of the major limitations of the MMD process. Other weaknesses of MMD include: the need for scrupulously clean glassware both in preparation and application, it is time-consuming, achieving good contrast on darker backgrounds is difficult and it is only effective in a narrow pH range.¹¹⁸

In 2001, Schnetz and Margot published their optimised method named MMD-II.¹¹⁹ (Saunders' method being MMD-I). The reduction in the diameter of the colloidal gold particles was perhaps the most important refinement achieved. In MMD-I, the gold particles had an average diameter of 30 nm. Schnetz followed a method for colloidal gold formation which produced smaller particles with a diameter range of 3-17 nm.¹²⁰ This refinement meant that more gold was deposited in the first stage, which enhanced the silver stage, thus greatly improving the sensitivity of the technique. MMD-I and MMD-II were directly compared by Fairley et al. which concluded that practically, MMD-I was better but, in terms of efficiency, MMD-II was the better option.¹²¹

In 2009, Stauffer et al. proposed an alternative to MMD which he termed single metal deposition (SMD).¹²² The silver stage was removed and replaced with a hydroxylamine and gold chloride solution to further deposit gold onto gold particles. SMD was compared with MMD and results confirmed that SMD offered almost

identical advantages, such as sensitivity and selectivity but was more cost effective and less technically demanding. SMD was intended for practitioner use in favour of MMD but research has not indicated the regular use and SMD is currently regarded as a category C process in the Fingerprint Visualisation Manual. Category C processes are optional processes for occasional use when all other options have been exhausted.²

1.5 Objectives

As discussed in section 1.4, physical developer is a widely used (in the UK and globally), effective method for the development of latent fingerprints on porous surfaces but research regarding the mechanism and underlying chemistry of the technique is limited. The latter is particularly important for the pressing need of reformulation due to the banned surfactant component, Synperonic N. The work presented in this thesis aims to gain a further understanding of the fundamentals of the PD process with the goal of an optimised technique, which has not yet been achieved.

The first objective addresses the underlying chemistry of the technique. The mechanism will be explored through the use of split prints and spot tests (see chapter 3, section 3.4.3 and 3.4.4) to identify the targets for PD. The growth and dynamics of the silver colloidal particulates in solution to silver particulates on the surface will be examined microscopically and spectroscopically to further understand the behaviour and mechanism of PD.

The second objective for this thesis is to understand the role of the surfactants in the PD working solution. This will be studied through the technique of neutron reflectivity to observe and characterise surfactant adsorption on a planar silver surface. It is currently theorised that only the cationic surfactant component adsorbs onto the silver colloidal particles and the non-ionic component simply aids the dissolution of the cationic surfactant. In addition to this, different formulations for the detergent system in the working solution will be tested to determine whether effective fingerprint development is still possible.

The final aim of this work addresses the need to find an alternative non-ionic surfactant for the working solution that not only results in high quality fingerprints but that is environmentally benign. The growth and dynamics of the PD process with alternative surfactants will be studied as well as using Raman spectroscopy to observe any silver adsorption and to identify similarities with the current non-ionic surfactant Synperonic N. The alternative formulations will be tested under various conditions to identify if fingerprints are effectively developed. Lastly, alternative surfaces will also be tested to potentially extend the capability of the PD process.

1.6 References

1. A. R. W. Jackson and J. M. Jackson, *Forensic Science*, Pearson Prentice Hall, Harlow, 2004.
2. CAST, *Home Office Centre of Applied Science and Technology Fingerprint Visualisation Manual* 1st edn., 2014.
3. C. Champod, C. Lennard, P. Margot and M. Stoilovic, *Fingerprints and other ridge skin impressions*, CRC Press, Boca Raton, 2004.
4. J. Siegel, *Forensic Science*, Oneworld Publications, New York, NY, United States, 2016.
5. F. Galton, *Finger Prints*, Macmillan and Co., London 1892.
6. R. Saferstein, *Criminalistics: an introduction to forensic science*, Pearson Education, Upper Saddle River, N.J; Harlow, 2010.
7. B. T. Cutro and J. National Institute of, *The fingerprint sourcebook - chapter 4* U.S. Department. of Justice, Office of Justice Programs, National Institute of Justice, Washington, DC, 2011.
8. H. Moses Daluz, *Fundamentals of Fingerprint Analysis*, CRC Press, Bosa Roca, United States, 2014.
9. M. R. Hawthorne, *Fingerprints: analysis and understanding*, CRC Press, Boca Raton, 2009.
10. M. M. Houck, *Forensic Fingerprints*, Elsevier Science, San Diego, United States, 2016.
11. G. T. C. Lambourne, *Journal of the Forensic Science Society*, 1977, **17**, 95-98.

12. C. Lennard, *Australian Journal of Forensic Sciences*, 2013, **45**, 356-367.
13. S. V. Stevenage and C. Pitfield, *Forensic Science International*, 2016, **267**, 145-156.
14. S. Robinson and A. H. Robinson, *Physiological reviews*, 1954, **34**, 202-220.
15. M. Harker, H. Coulson, I. Fairweather, D. Taylor and C. A. Daykin, *Metabolomics*, 2006, **2**, 105-112.
16. S. S. Shetage, M. J. Traynor, M. B. Brown, M. Raji, D. Graham-Kalio and R. P. Chilcott, *Skin research and technology : official journal of International Society for Bioengineering and the Skin*, 2014, **20**, 97-107.
17. M. Picardo, M. Ottaviani, E. Camera and A. Mastrofrancesco, *Dermato-Endocrinology*, 2009, **1**, 68-71.
18. N. A. Taylor and C. A. Machado-Moreira, *Extreme physiology & medicine*, 2013, **2**, 4.
19. K. Sato, W. H. Kang, K. Saga and T. Sato, *J. American Academy of Dermatology*, 1989, **20**, 537-563.
20. T. Nikkari, *Journal of Investigative Dermatology*, 1974, **62**, 257-267.
21. B. A. McSwiney, *Proceedings of the Royal Society of Medicine*, 1934, **27**, 839-848.
22. R. S. Greene, D. T. Downing, P. E. Pochi and J. S. Strauss, *Journal of Investigative Dermatology*, 1970, **54**, 240-247.
23. D. T. Downing and J. S. Strauss, *Journal of Investigative Dermatology*, 1974, **62**, 228-244.
24. K. Wilke, A. Martin, L. Terstegen and S. S. Biel, *International Journal of Cosmetic Science*, 2007, **29**, 169-179.
25. A. Girod, L. Xiao, B. Reedy, C. Roux and C. Weyermann, *Forensic Science International*, 2015, **254**, 185-196.
26. C. Weyermann, C. Roux and C. Champod, *Journal of Forensic Sciences*, 2011, **56**, 102-108.
27. N. E. Archer, Y. Charles, J. A. Elliott and S. Jickells, *Forensic Science International*, 2005, **154**, 224-239.

28. S. Cadd, M. Islam, P. Manson and S. Bleay, *Science & Justice*, 2015, **55**, 219-238.
29. R. S. Croxton, M. G. Baron, D. Butler, T. Kent and V. G. Sears, *Forensic Science International*, 2010, **199**, 93-102.
30. S. K. Bramble, *Journal of Forensic Sciences*, 1995, **40**, 969-975.
31. A. Girod, R. Ramotowski and C. Weyermann, *Forensic Science International*, 2012, **223**, 10-24.
32. A. Richmond-Aylor, S. Bell, P. Callery and K. Morris, *Journal of Forensic Sciences*, 2007, **52**, 380-382.
33. H. C. Lee and R. E. Gaensslen, *Advances in fingerprint technology*, 2nd edn., CRC Press, Boca Raton, 2001.
34. V. Drapel, A. Becue, C. Champod and P. Margot, *Forensic Science International*, 2009, **184**, 47-53.
35. F. Cuthbertson, *The chemistry of fingerprints* AWRE Report No. 013/69, 1965.
36. A. Girod and C. Weyermann, *Forensic Science International*, 2014, **238**, 68-82.
37. R. Ramotowski, *Lee and Gaensslen's Advances in Fingerprint Technology, Third Edition*, CRC Press Inc, GB, 2013.
38. S. J. Cadd, L. Mota, D. Werkman, M. Islam, M. Zuidberg and M. de Puit, *Anal. Methods*, 2015, **7**, 1123-1132.
39. G. S. Sodhi and J. Kaur, *Forensic Science International*, 2001, **120**, 172-176.
40. P. J. Mankidy, R. Rajagopalan and H. C. Foley, *Polymer*, 2008, **49**, 2235-2242.
41. P. Klemarczyk, *Polymer* 2001, **42**, 2837-2848.
42. S. P. Wargacki, L. A. Lewis and M. D. Dadmun, *Journal of Forensic Sciences*, 2007, **52**, 1057-1062.
43. P. Czekanski, M. Fasola and J. Allison, *Journal of Forensic Sciences*, 2006, **51**, 1323-1328.
44. S. P. Wargacki, L. A. Lewis and M. D. Dadmun, *Journal of Forensic Sciences*, 2008, **53**, 1138-1144.
45. A. Bentolila, J. Totre, I. Zozulia, M. Levin-Elad and A. J. Domb, *Macromolecules*, 2013, **46**, 4822-4828.

46. K. J. Farrugia, P. Deacon and J. Fraser, *Science & Justice*, 2014, **54**, 126-132.
47. A. Khuu, S. Chadwick, X. Spindler, R. Lam, S. Moret and C. Roux, *Forensic Science International*, 2016, **263**, 126-131.
48. C. Prete, L. Galmiche, F. G. Quenum-Possy-Berry, C. Allain, N. Thiburce and T. Colard, *Forensic Science International*, 2013, **233**, 104-112.
49. S. Chadwick, L. Xiao, P. Maynard, C. Lennard, X. Spindler and C. Roux, *Australian Journal of Forensic Sciences*, 2014, **46**, 471-484.
50. G. Groeneveld, S. Kuijer and M. de Puit, *Science & Justice*, 2014, **54**, 42-48.
51. G. S. Bumbrah, *Egyptian Journal of Forensic Sciences*, 2016, **6**, 328-332.
52. F. Haque, A. D. Westland, J. Milligan and F. M. Kerr, *Forensic Science International*, 1989, **41**, 73.
53. C. Au, H. Jackson-Smith, I. Quinones, B. J. Jones and B. Daniel, *Forensic Science International*, 2011, **204**, 13-18.
54. B. J. Jones, R. Downham and V. G. Sears, *Surface and Interface Analysis*, 2010, **42**, 438-442.
55. R. P. Downham, E. R. Brewer, R. S. P. King, A. M. Luscombe and V. G. Sears, *Forensic Science International*, 2017, **275**, 30-43.
56. J. Fraser, P. Deacon, S. Bleay and D. H. Bremner, *Science & Justice*, 2014, **54**, 133-140.
57. S. Knighting, J. Fraser, K. Sturrock, P. Deacon, S. Bleay and D. H. Bremner, *Science & Justice*, 2013, **53**, 309-314.
58. L. W. Davis, P. F. Kelly, R. S. King and S. M. Bleay, *Forensic Science International*, 2016, **266**, e86-92.
59. N. Jones, D. Mansour, M. Stoilovic, C. Lennard and C. Roux, *Forensic Science International*, 2001, **124**, 167-177.
60. N. Jones, M. Stoilovic, C. Lennard and C. Roux, *Forensic Science International*, 2001, **115**, 73-88.
61. R. Jelly, E. L. Patton, C. Lennard, S. W. Lewis and K. F. Lim, *Analytica chimica acta*, 2009, **652**, 128-142.

62. N. Porpiglia, S. Bleay, L. Fitzgerald and L. Barron, *Science & Justice*, 2012, **52**, 42-48.
63. S. Berdejo, M. Rowe and J. W. Bond, *Journal of Forensic Sciences*, 2012, **57**, 509-514.
64. M. M. Joullie and T. R. Thompson, *Tetrahedron*, 1991, **47**, 8791-8830.
65. R. Yang and J. Lian, *Forensic Science International*, 2014, **242**, 123-126.
66. C. Marriott, R. Lee, Z. Wilkes, B. Comber, X. Spindler, C. Roux and C. Lennard, *Forensic Science International*, 2014, **236**, 30-37.
67. C. C. Chen, C. K. Yang, J. S. Liao and S. M. Wang, *Forensic Science International*, 2015, **257**, 314-319.
68. D. Wilkinson, *Forensic Science International*, 2000, **109**, 87-103.
69. M. Stoilovic, *Forensic Science International*, 1993, **60**, 141-153.
70. V. D'Elia, S. Materazzi, G. Iuliano and L. Niola, *Forensic Science International*, 2015, **254**, 205-214.
71. C. Wallace-Kunkel, C. Lennard, M. Stoilovic and C. Roux, *Forensic Science International*, 2007, **168**, 14-26.
72. D. E. Bicknell and R. S. Ramotowski, *Journal of Forensic Sciences*, 2008, **53**, 1108-1116.
73. M. F. Mangle, X. Xu and M. de Puit, *Science & Justice*, 2015, **55**, 343-346.
74. P. Hazarika and D. A. Russell, *Angewandte Chemie*, 2012, **51**, 3524-3531.
75. L. Xu, C. Zhang, Y. He and B. Su, *Science China Chemistry*, 2015, **58**, 1090-1096.
76. C. Lennard, *Australian Journal of Forensic Sciences*, 2013, **46**, 293-303.
77. A. L. Beresford and A. R. Hillman, *Anal Chem*, 2010, **82**, 483-486.
78. R. M. Brown and A. R. Hillman, *Physical Chemistry Chemical Physics : PCCP*, 2012, **14**, 8653-8661.
79. A. P. Abbott, J. Griffith, S. Nandhra, C. O'Connor, S. Postlethwaite, K. S. Ryder and E. L. Smith, *Surf. Coat. Technol.*, 2008, **202**, 2033-2039.
80. K. A. Weston-Ford, M. L. Moseley, L. J. Hall, N. P. Marsh, R. M. Morgan and L. P. Barron, *Science & Justice*, 2016, **56**, 1-8.

81. I. Hefetz, A. Cohen, Y. Cohen and A. Chaikovsky, *Journal of Forensic Sciences*, 2014, **59**, 1226-1230.
82. L. Davis and R. Fisher, *Science & Justice*, 2015, **55**, 97-102.
83. R. Bradshaw, R. Wolstenholme, L. S. Ferguson, C. Sammon, K. Mader, E. Claude, R. D. Blackledge, M. R. Clench and S. Francese, *The Analyst*, 2013, **138**, 2546-2557.
84. S. Francese, R. Bradshaw and N. Denison, *The Analyst*, 2017, **142**, 2518-2546.
85. M. J. Bailey, R. Bradshaw, S. Francese, T. L. Salter, C. Costa, M. Ismail, R. P. Webb, I. Bosman, K. Wolff and M. de Puit, *The Analyst*, 2015, **140**, 6254-6259.
86. J. Belloni, *Radiation Physics and Chemistry*, 2003, **67**, 291-296.
87. T. Tani, *Photographic Sensitivity : Theory and Mechanisms*, Oxford University Press, Cary, United States, 1995.
88. J. Belloni, *C. R. Physique 3*, 2002, 381-390.
89. H. Jonker, A. Molenaar and C. J. Dippel, *Photographic Science and Engineering*, 1969, **13**, 38-43.
90. H. Jonker, L. K. H. van Beek, C. J. Dippel, C. J. G. F. Janssen, A. Molenaar and E. J. Spiertz, *Journal of Photographic Science*, 1971, **19**, 96-105.
91. J. R. Morris, *Progress Sheet 1 AWRE Report* 1979.
92. G. C. Goode, J. R. Morris and J. M. Wells, *Chemical Aspects of Fingerprint Technology* SSCD Memo. No. 510, 1976-1977.
93. J. R. Morris, *The Detection of Latent Fingerprints on Wet Paper Samples* SSCD Memo. No. 367, 1975.
94. A. A. Cantu, *Notes on some latent fingerprint visualization techniques developed by Dr. George Saunders* U.S. Secret Service, Washington DC, 1996.
95. J. R. Morris, *Progress Sheet 8 AWRE Report*, 1977-1978.
96. G. C. Goode and J. R. Morris, *Latent Fingerprints: A Review of their Origin, Composition and Methods of Detection* AWRE Report no. 022/83, 1985.
97. S. A. Hardwick, *User Guide to Physical Developer - A reagent for detecting latent fingerprints*, Home Office Scientific Research and Development Branch, 1981.

98. R. Ramotowski, *Journal of Forensic Identification*, 2000, **50**, 363-384.
99. J. D. Wilson, A. A. Cantu, G. Antonopoulos and M. J. Surrency, *Journal of Forensic Sciences*, 2007, **52**, 320-329.
100. D. Burow, D. Seifert and A. A. Cantu, *Journal of Forensic Sciences*, 2003, **48**, 1-7.
101. K. Braasch, M. de la Hunty, J. Deppe, X. Spindler, A. A. Cantu, P. Maynard, C. Lennard and C. Roux, *Forensic Science International*, 2013, **230**, 74-80.
102. R. Ramotowski and A. A. Cantu, *Fingerprint Whorld*, 2001, **27**, 59-65.
103. A. A. Cantu, *Forensic Science Review*, 2001, **13**, 29-64.
104. M. A. Wood and T. James, *Science & Justice*, 2009, **49**, 272-276.
105. C. E. Phillips, D. O. Cole and G. W. Jones, *Journal of Forensic Identification*, 1990, **40**, 135-147.
106. R. K. Simmons, P. Deacon and K. J. Farrugia, *Journal of Forensic Identification*, 2014, **64**, 157-173.
107. D. Burow, *Journal of Forensic Identification*, 2003, **53**, 304-314.
108. G. S. Sodhi and J. Kaur, *Egyptian Journal of Forensic Sciences*, 2015, **6**, 44-47.
109. A. A. Cantu, D. A. Leben and K. Wilson, *Proc. SPIE 5071, Sensors and Command, Control, Communications and Intelligence (C3I) Technologies for Homeland Defense and Law Enforcement II*, 2003, **5071**, 164-167.
110. M. de la Hunty, S. Moret, S. Chadwick, C. Lennard, X. Spindler and C. Roux, *Forensic Science International*, 2015, **257**, 481-487.
111. M. de la Hunty, S. Moret, S. Chadwick, C. Lennard, X. Spindler and C. Roux, *Forensic Science International*, 2015, **257**, 488-495.
112. *Directive 2003/53/EC of the European Parliament and of the Council, Council Directive 76/769/EEC*, 2003.
113. M. de la Hunty, *Personal Communication* 2016.
114. V. G. Sears, *Personal Communication* 2014.
115. G. Sauzier, A. A. Frick and S. W. Lewis, *Journal of Forensic Identification*, 2013, **63**, 70-88.
116. R. Ramotowski, *Journal of Forensic Identification*, 1996, **46**, 673-677.

117. A. Beaudoin, *Journal of Forensic Identification*, 2004, **54**, 413-421.
118. A. Becue, A. Scoundrianos and S. Moret, *Forensic Science International*, 2012, **219**, 39-49.
119. B. Schnetz and P. Margot, *Forensic Science International*, 2001, **118**, 21-28.
120. J. W. Slot and H. J. Geuze, *European Journal of Cell Biology*, 1985, **38**, 87-93.
121. C. Fairley, S. M. Bleay, V. G. Sears and N. NicDaeid, *Forensic Science International*, 2012, **217**, 5-18.
122. E. Stauffer, A. Becue, K. V. Singh, K. R. Thampi, C. Champod and P. Margot, *Forensic Science International*, 2007, **168**, e5-9.

Chapter 2: Methodology

2.1	Introduction	43
2.2	Microscopy	43
	2.2.1 Optical Profilometry	43
	2.2.2 Atomic Force Microscopy	44
	2.2.3 Scanning Electron Microscopy	46
2.3	Light Scattering	48
	2.3.1 Dynamic Light Scattering	48
2.4	Spectroscopy	50
	2.4.1 Raman Spectroscopy	50
2.5	Neutron Reflectivity	52
	2.5.1 Neutron-nuclei Interactions	52
	2.5.2 Reflectivity Theory	53
	2.5.3 Data Analysis	58
2.6	References	59

2.1 Introduction

The aim of this chapter is to outline the underlying principles of the main techniques and instrumentation used throughout this thesis. These consist of techniques for topographical analysis and the determination of chemical and physical properties. The details of the specific instrumentation used are given in chapter 3.

The techniques chosen in this thesis reflect the ability to characterise and analyse both the PD solution and the developed fingerprint images. This will cover the microscopic to macroscopic scale, exploring the interfacial and surface chemistry of both suspended and deposited silver particles.

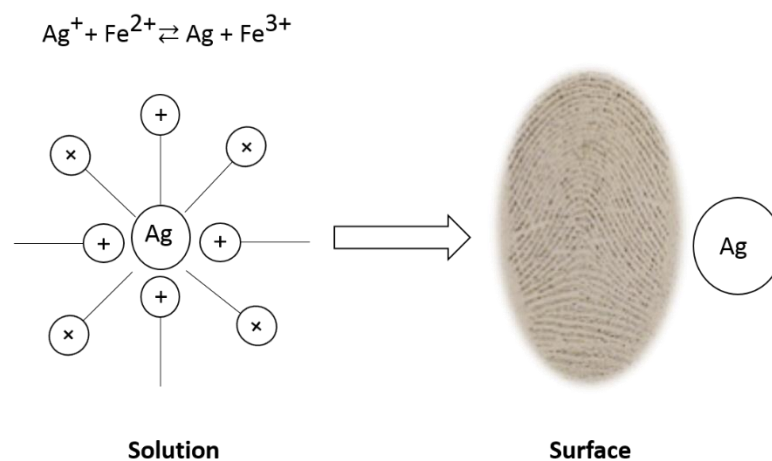


Figure 2.1 - Diagram showing stabilised silver particles in solution and deposited silver particles of developed fingerprint image using PD

2.2 Microscopy

2.2.1 Optical Profilometry

The main difference between an optical profiler and the more common optical microscope is the production of a 3D image. This in turn allows for a surface to be analysed with respect to surface roughness or specific feature dimensions.

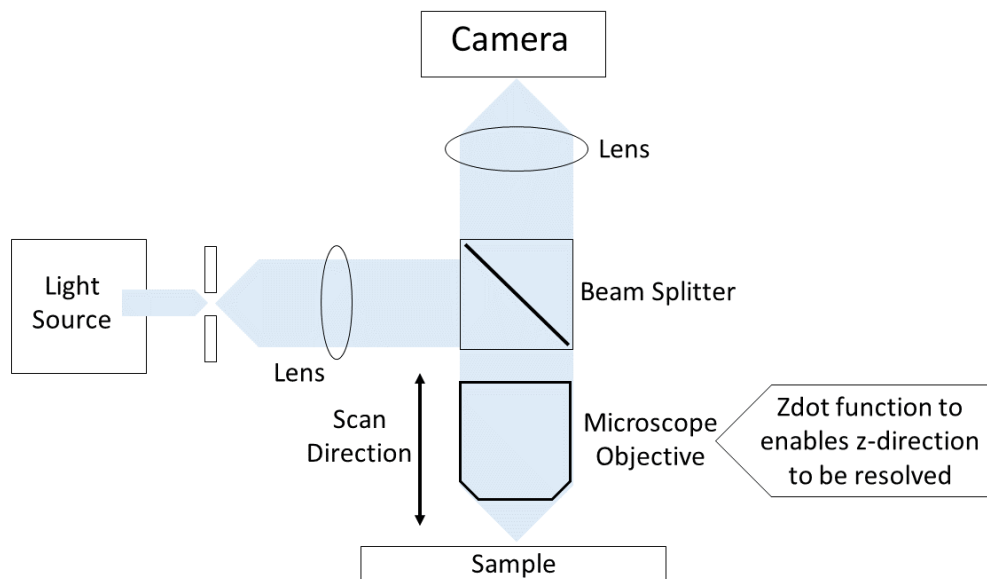


Figure 2.2 - Schematic of an optical microscope

The microscope is a laser-scanning system inducing confocal detection of elastic-scattered light. To generate this 3D image, the height (z-axis), is measured across the lateral x and y-axes over a series of changing step heights and the resulting 2D microscopic images are combined. The final image is coloured to represent the intensity of light scattered at the interface. The vertical resolution capability is ca. 0.1-4 μm with minute scale acquisition times. The non-contact nature of this technique means that surface analysis can be determined quickly without being destructive to the sample.

2.2.2 Atomic Force Microscopy

Atomic force microscopy (AFM) is a type of scanning probe microscopy technique which analyses the topography of a surface and is capable of nanometre resolution. AFM can analyse many solid surface types irrespective of conductivity as well as some liquid and biological samples.¹

The AFM probe is a sharp tip (usually silicon) on the end of a cantilever which is scanned laterally across the surface via a piezoelectric scanner.² The tip is scanned across the whole surface and variations in height and the forces between the tip and

surface cause the cantilever to deflect vertically. A laser is reflected by the cantilever deflections towards a four quadrant photodiode detector.³ A schematic diagram of these AFM components is shown in figure 2.3.

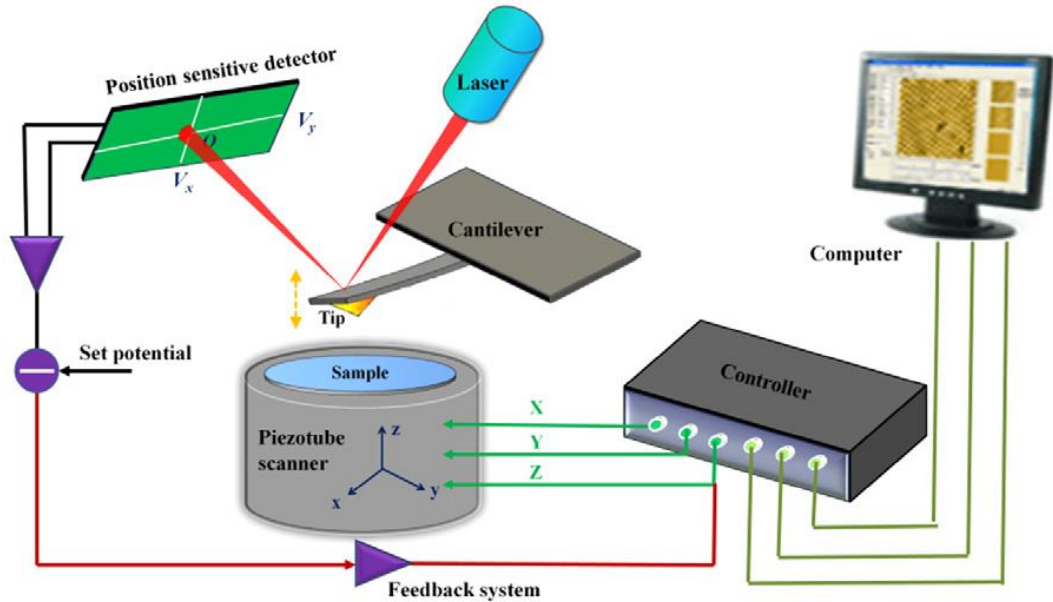


Figure 2.3 - Schematic diagram of AFM components³

Imaging via AFM can be static or dynamic. There are three modes of operation: contact, non-contact and tapping mode. As the name suggests, in contact mode, the tip is in constant contact with the surface measuring the repulsive forces. The disadvantage of the contact mode is that it is destructive to both the sample and the tip as it is effectively dragged across the surface. This mode would not be suitable for very rough surfaces.

In non-contact mode, the tip is held a small distance above the surface with the cantilever oscillating to measure the attractive Van der Waals forces. As the tip does not come into contact with the surface, it is less destructive to both the sample and the tip but sharp differences in the height of the sample could damage the probe. In addition to this, this mode is less effective for analysing specific surface features as only the forces are detected compared to height variations.

Tapping mode is considered an intermediate between contact and non-contact mode. In contact mode, the force is kept constant and in non-contact mode, the height is kept constant. During tapping mode, the cantilever is made to oscillate such that when it is rastered across the surface, the probe taps the surface a minimal number of times. Tapping mode offers the advantage of measuring both the variations in force between the probe and the surface as well as the physical surface features. The tip does still come into contact with the surface which means it will degrade over time but this is not as destructive as the constant force contact mode.

2.2.3 Scanning Electron Microscopy

A scanning electron microscope (SEM) focuses an electron beam on a sample and the signals from the sample interactions with the electrons provide information about the topography of the surface. The use of an electron source improves the resolution capability of the instrument, achieving nanometre resolution compared to a traditional light microscope with micrometre resolution.

The main components of the SEM system consist of: an electron source, condensers and objective lenses to focus the electron beam and the detectors (figure 2.4).

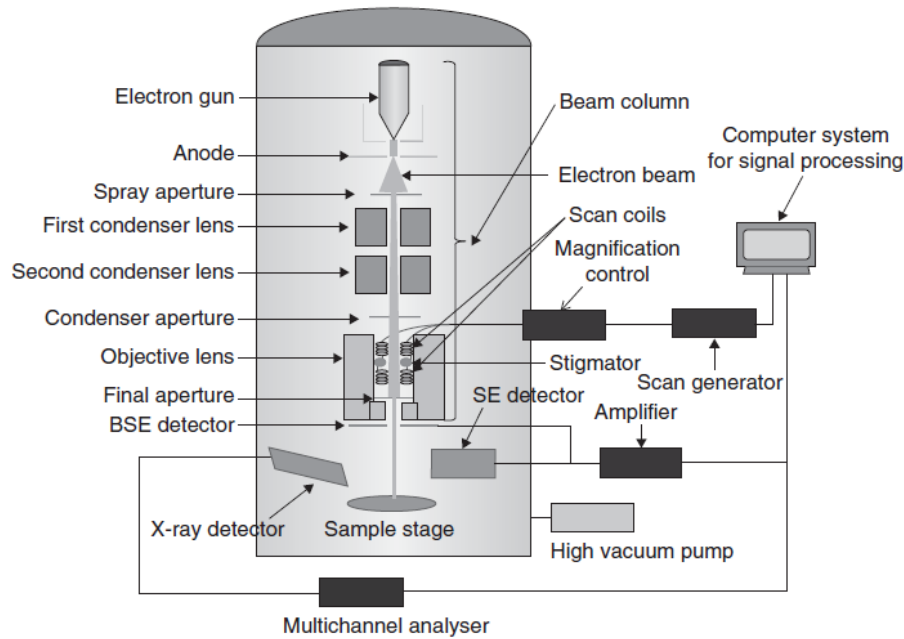


Figure 2.4 - Schematic of SEM components⁴

The condenser lens will firstly demagnify the crossover diameter of the electron beam such that it can be finely focused towards the objective lens.^{4, 5} The objective lens can then focus this probe across the sample surface in a raster pattern by directing the crossover along the optical axis.⁶ The electron interactions with the sample surface can produce several signals which include: secondary, backscattered and Auger electrons as well as characteristic X-rays.

Secondary electrons are the most commonly detected signal because they are low energy with a low depth production meaning highly resolved topographic contrast can be achieved. Backscattered electrons are higher in energy than secondary electrons but lower in quantity than the secondary electrons which have been generated from the sample to a nanometre depth. The resolution is therefore lower but they primarily give compositional information. When the incident electron beam forces an electron out of an inner shell, a higher energy electron from the outer shell fills this hole, releasing an X-ray photon whose energy is characteristic to a particular element. These emitted X-rays are detected by an energy dispersive spectrometer providing elemental analysis and thus compositional mapping of the sample.

2.3 Light Scattering

2.3.1 Dynamic Light Scattering

Dynamic light scattering (DLS), or quasi-elastic light scattering and photo correlation spectroscopy as it is also known, is a technique used to measure the size of particles either in a solution or suspension.⁷⁻¹² In addition to this, some DLS instrumentation has the capability to measure the zeta potential.¹³

DLS monitors the Brownian motion of the particles with light scattering. The larger the particle, the slower the Brownian motion will be. Incident light can be scattered elastically or inelastically. The intensity of the scattered light is proportional to the particle diameter. If the size of the particles are less than $1/10^{\text{th}}$ of the wavelength of the incident light, the scattered light will be equal in energy to the incident light and scattered elastically; this is termed, Rayleigh scattering. The opposite is true for Mie scattering, in which the size of the particles exceed $\lambda/10$ and the scattered light is not equal in energy to the incident light.¹³

DLS measures the hydrodynamic radius, R_H , which is the radius of a hard sphere that diffuses at the same speed as the particle being measured. This is a hypothetical parameter as most colloidal systems are not 'hard' and quite often solvated as well as non-spherical.¹³ The R_H will be dependent on the surface structure, nature of the solvent and the ionic strength. The hydrodynamic radius is connected the diffusion coefficient of the particles in suspension by Stokes-Einstein equation (see equation 2.1 where D_H is the hydrodynamic diameter, D_t is the diffusion coefficient, k_B is Boltzmann's constant, T is temperature and η is viscosity).

$$D_H = \frac{k_B T}{3\pi\eta D_t} \quad (2.1)$$

The three main components that make up a DLS system are: the laser, sample and detector. Typically a He-Ne laser (633 nm) will be used but the wavelength can vary depending on which light source is used. The sample is placed into a cuvette,

which can be disposable plastic or glass, via a syringe to prevent any dust getting into the sample which will scatter light. A photon detector will detect the scattered light at a small deflection angle but some instruments also contain a backscatter detector to minimise the signal to noise ratio.

A correlation function will be plotted during a DLS measurement and the appearance of this function depends on the size of the particles. The correlation function shows the scattering intensity vs time, where the intensity is compared to the intensity at some time after as the particles are constantly moving. The scattering signal, at a fixed small angle, which is revealed by the correlation function, enables the hydrodynamic radius to be determined. (See figure 2.5(a) and (b)).

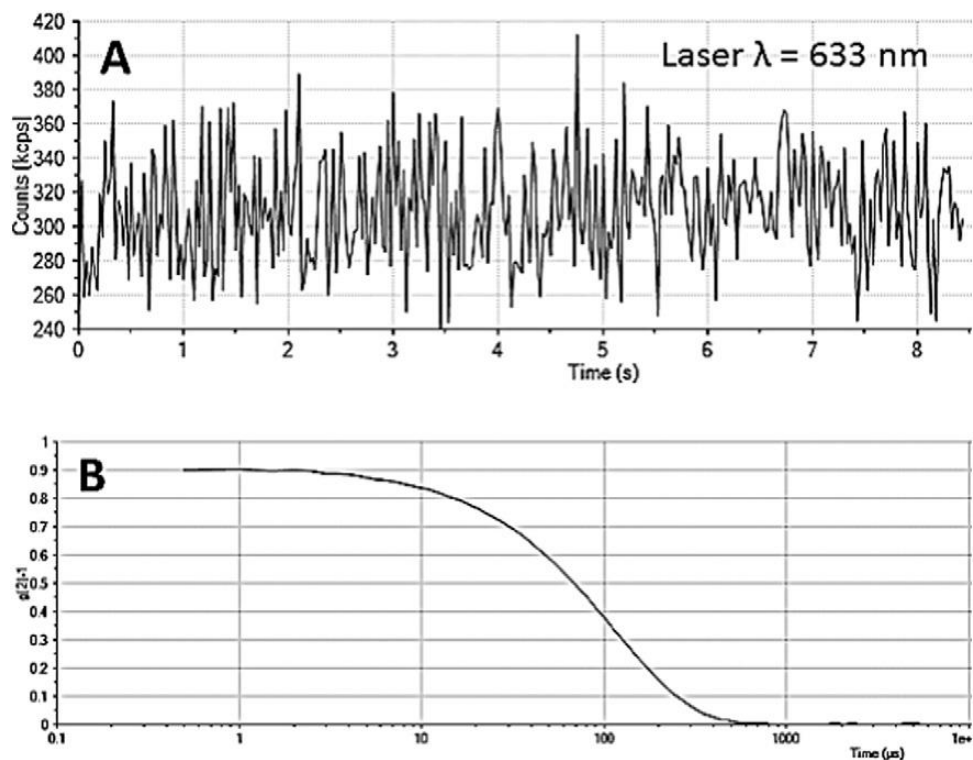


Figure 2.5 - (a) Small particles showing rapid fluctuations in intensity of scattered light with time (b) Correlation graph generated from DLS software¹³

Cumulative analysis of DLS data will provide the z-average mean particle size and the polydispersity index, which is also indicated by the gradient of the correlation function. The polydispersity index is a measure of the broadness of size distribution in a sample and ideally should be between 0-1. A polydispersity index greater than 1

indicates the sample has a broad range of particles sizes and may not be suitable for DLS measurements.

There are several characteristics of the sample that must be fulfilled for successful DLS measurements. The dispersant must be: transparent, the refractive index should be different to the particles of interest, clean, refractive index and viscosity should be known accurately and it must be compatible with the particles. These criteria are in accordance with the standards - ISO 13321, 1996. The concentration of the sample cannot be too high as this will cause multiple scattering but if the concentration is too low, there may not be enough scattered light produced. In order to determine a suitable concentration, repeated measurements can be performed at several dilutions as the concentration range suitable for detection will depend on the specific sample.

DLS software will produce an intensity, volume and number distribution curve each of which will present a slightly different R_H value. The particle diameter should be reported using the intensity distribution curve as the DLS relies on measuring the intensity of scattered light. Volume and number distributions can be used to report relative amounts from each peak.

2.4 Spectroscopy

2.4.1 Raman Spectroscopy

In Raman spectroscopy, the sample is illuminated with a monochromatic radiation source and the scattering from the sample is observed. The majority of the radiation will be scattered elastically such that the energy of the incident and scattering radiation is equal – Rayleigh scattering. A small proportion of the scattered radiation will be scattered at a higher or lower energy (inelastic scattering) which is known as Raman scattering of which there are two types: Stokes and Anti-Stokes. (See figure 2.6). Stokes shifts arise from a transition from a lower to higher energy level and therefore are most commonly measured in Raman spectroscopy.¹⁴ The Raman

spectrum presents the intensity of Raman shifts in wavenumbers relative to the laser frequency thus aiding the chemical identification of a molecule.

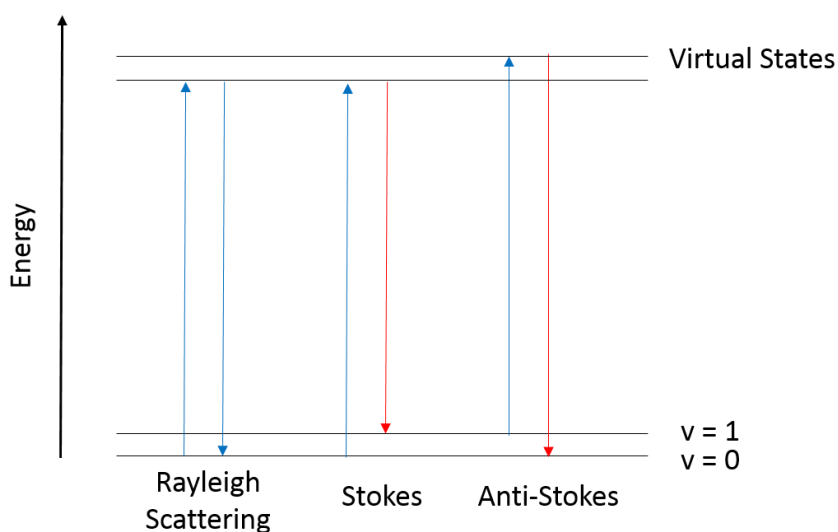


Figure 2.6 - Rayleigh, Stokes and Anti-Stokes scattering

A Raman instrument will consist of: a laser source, sample illumination system and a spectrometer. Typically the laser source will be either Argon ion (351-515 nm), Krypton ion (337-676 nm) or Helium-Neon (632 nm).¹⁵ The sample illumination system includes focusing and collecting lenses to ensure the sample is radiated and the scattering is detected as Raman scattering is weak.

In order to be Raman active, the sample must fulfil a selection rule such that the polarizability much change during the molecular vibration. The polarizability is a measure of how easily the electron cloud surrounding an atom can be distorted. This rule is different for IR spectroscopy in which the vibration must give rise to a change in the dipole moment; therefore Raman spectroscopy has the capability to observe different modes compared to IR spectroscopy.

2.5 Neutron Reflectivity

2.5.1 Neutron-nuclei Interactions

Interfaces exist within many materials of various length scales. To be able to analyse these interfaces, a technique capable of both vertical depth profiling and very high spatial resolution must be utilised whilst remaining non-destructive.

Neutrons do not possess a charge, meaning they are able to penetrate further into a system without being destructive to the sample. This means neutrons can be used to analyse structures with length scales varying from micrometre (μm) to Angstrom (\AA) scales.¹⁶⁻¹⁸ Neutrons will interact with the nuclei of atoms such that the scattering will be dependent on the atomic number. This means that neutrons are much more sensitive to the detection of lighter atoms even in the presence of heavier atoms. In addition to this, neutrons are able to distinguish between different isotopes. The scattering lengths (b) differ significantly between hydrogen (-3.74 fm^{19}) and deuterium (6.67 fm^{19}). This allows the option of isotopic substitution within the sample where H atoms are substituted for D atoms, which is known as contrast variation.^{20, 21}

Neutrons exhibit both wave and particle properties. The neutron-nuclei interaction results in a scattered wave which is dependent on the wavelength and angle. Upon the interaction of the neutron with the atom, the probability of the resultant scattering is related to the scattering length (b). This scattering will either be coherent or incoherent. The scattering occurs in a given area which is known as the cross section (Φ). This is related to the scattering length via equation 2.2.

$$\Phi = 4\pi|b^2| \quad (2.2)$$

From the bound coherent scattering lengths, the scattering length density (SLD, N_b) can be determined. This is the sum of the bound coherent scattering lengths (b_c) multiplied by Avogadro's constant and the density, divided by the molar mass (equation 2.3).

$$N_b = \frac{\sum b_c \cdot N_A \cdot \rho}{M} \quad (2.3)$$

2.5.2 Reflectivity Theory

Neutron reflectivity (NR) is a technique that can be used to analyse the thickness and composition of various layers within air/liquid²²⁻²⁵ (or solid) and solid/liquid interfaces.²⁶⁻²⁹ Neutron reflectivity has been extensively utilised to study surfactant films^{22, 30-58} as well as other applications including conducting polymer films⁵⁹⁻⁶² and proteins.^{29, 63-66}

When an incident neutron beam hits a sample point within a layered system, the reflected wave will then be scattered. The layers are separated according to their distance, d . Figure 2.7 explains the effect of constructive interference with respect to Bragg's law (equation 2.4).

$$n\lambda = 2d \sin\theta \quad (2.4)$$

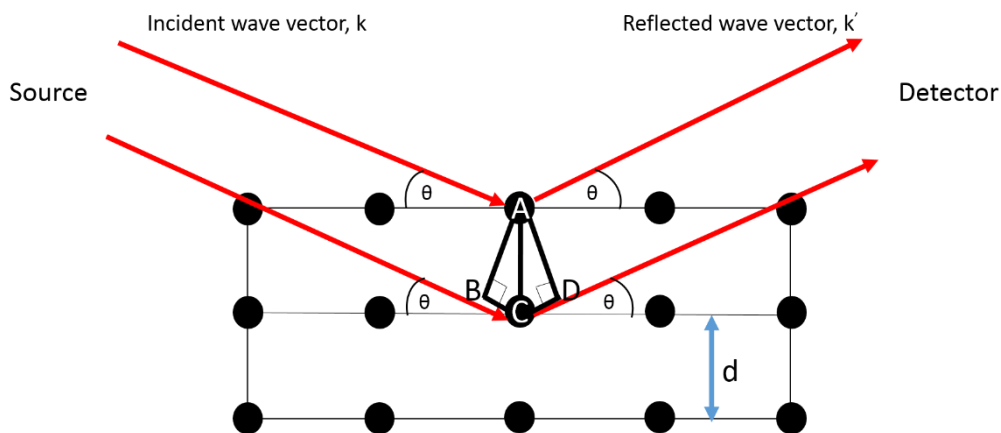


Figure 2.7 - Schematic of an incident wave vector hitting a sample point producing a reflected wave vector

Constructive interference is observed when two waves are in phase, which can only be achieved if the distance between the two reflected waves is equal to a multiple of the wavelength.

In neutron reflectivity, reflectivity (R) is the measured parameter which is a ratio of the reflected neutrons compared to the incident neutrons. This is plotted according to the scattering wave vector or momentum transfer (Q) which is perpendicular to the surface. Figure 2.8 and equations 2.5 and 2.6 illustrate this, where equation 2.5 represents Q which is the difference between the incident and reflected wave vectors. Equation 2.6 represents k, which is the magnitude of the wave vector.

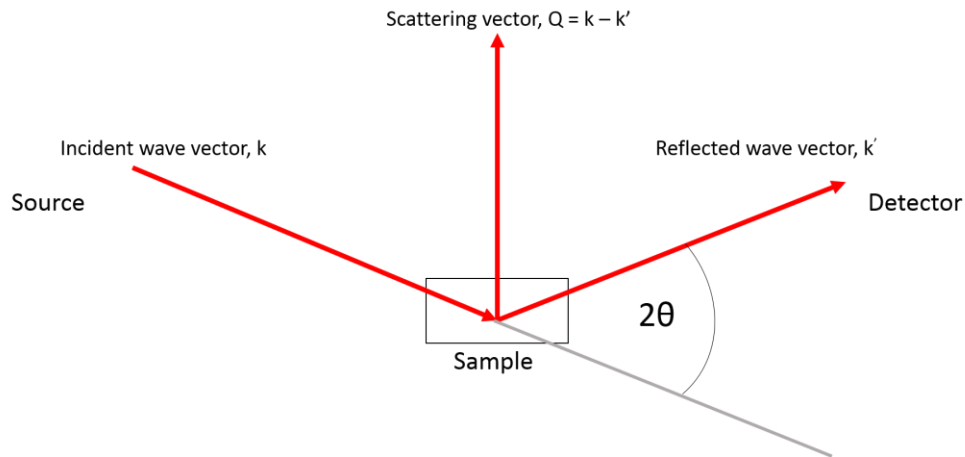


Figure 2.8 - Elastic scattering

$$Q = k - k' \quad (2.5)$$

$$k = \frac{2\pi}{\lambda} \quad (2.6)$$

From figure 2.8 and equations 2.5 and 2.6, Q can be derived according to wavelength and the angle of incidence (θ) as shown in equation 2.7.

$$Q = 2k \sin\theta = \frac{4\pi}{\lambda} \sin\theta \quad (2.7)$$

Depending on the roughness of the surface in question from which the neutron beam is scattered, different types of reflectivity will occur. If the surface is considered to be atomically flat then specular reflection is observed. When $R=1$, the incident intensity will be equal to the reflected intensity such that the angle of incidence (θ) will be equal to the reflected angle. Under these conditions, total reflection is observed, which is illustrated in figure 2.9.

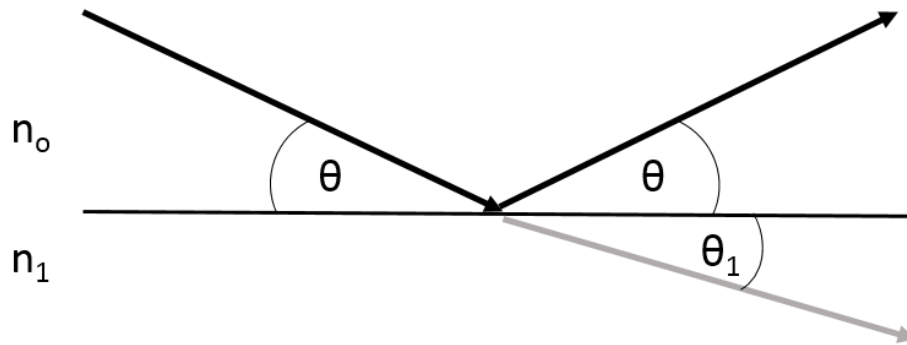


Figure 2.9 - Total reflection where θ_1 is the angle of refraction

Neutron reflectivity relies on the concepts of refractivity but rather than detecting changes in the refractive index, the changes in the scattering length densities are measured. The introduction of layers on the surface means that specular reflection is not only observed at the external surface but also at other interfaces. This is where the many advantages of neutron reflectivity are apparent as depth profiling is achieved. Figure 2.10 shows specular reflection from a surface with an additional layer.

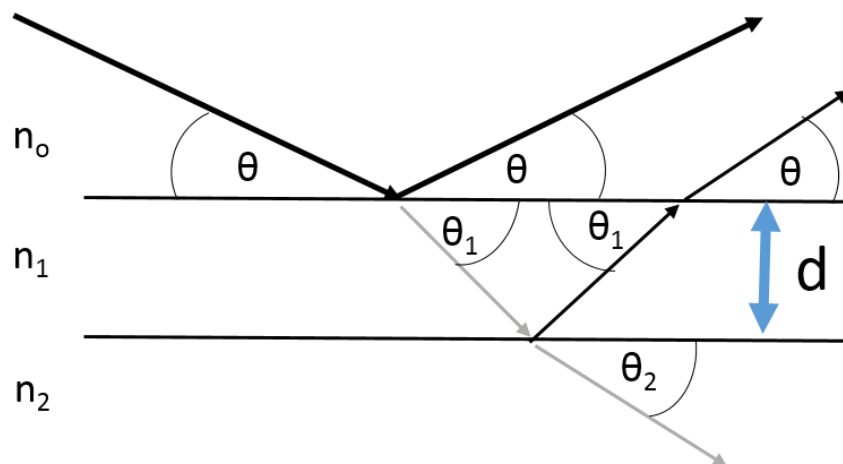


Figure 2.10 - Specular reflection at the surface and interface

Specular reflection assumes that the surface and interface are relatively smooth surfaces but some interfaces will be considerably rougher. Due to the variation in roughness, off-specular reflection is also observed as shown in figure 2.11.

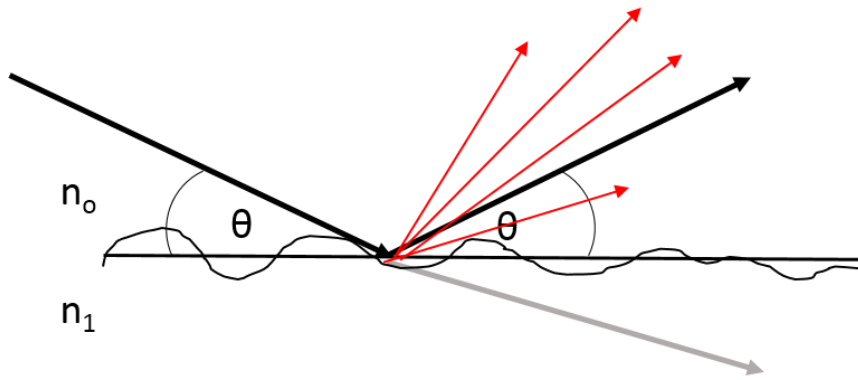


Figure 2.11 - Off-specular reflection from rougher surfaces

As previously mentioned, a reflectivity profile is a plot of R vs Q and this relationship is explained according to Fresnel's law, where k is the incident wave vector and k_t is the transmitted wave vector (equation 2.8).

$$r = \frac{k - k_t}{k + k_t} \quad (2.8)$$

The probability amplitude, r , describes the probability of finding a particle at some position and time. The intensity is measured in neutron reflectivity (R), which is related to Q according to Fresnel's reflectivity shown in equation 2.9.

$$R = r^2 = \left[\frac{Q - (Q^2 - Q_c^2)^{1/2}}{Q + (Q^2 - Q_c^2)^{1/2}} \right]^2 \quad (2.9)$$

Q_c (or Q_{crit}) is the critical edge and when $Q < Q_c$, total internal reflection occurs. The value for the critical edge can be determined from the SLDs (N_b) of the two bulk materials according to equation 2.10.

$$Q_c = (16\pi\Delta N_b)^{1/2} \quad (2.10)$$

The position of the critical edge will be indicated on the reflectivity plot.

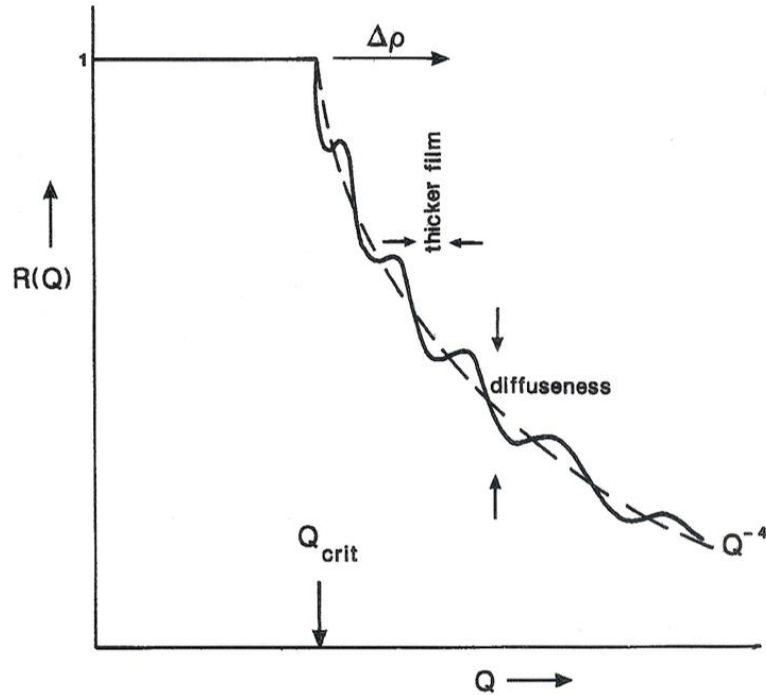


Figure 2.12 - An example of a simple reflectivity profile⁶⁷

Figure 2.12 represents a typical reflectivity profile and the fringe spacing is related to the thickness of the layers according to equation 2.11.

$$\Delta Q = \frac{2\pi}{d} \quad (2.11)$$

One of the practical issues in neutron reflectivity experiments is the rapid decrease in reflectivity with the increase in Q. This means that at higher Q the signal can be lost in the background signal. Therefore to be able to observe the fringes at higher Q values a sufficient resolution must be used; this is dependent on the specific instrument.

The fringes also give an indication of the roughness of the surface/interface. This is observed in the reflectivity plot by a rapid decay in the profile and smoothing of the fringes. Rougher surfaces will show a more rapid decrease in the reflectivity profile.

The neutron experiments in this thesis were performed on INTER⁶⁸ and SURF at the ISIS facility, Oxford, UK. Measurements were performed *in situ* using multiple reflection angles to maximise the Q range. Each experiment was performed in the respective solvents.

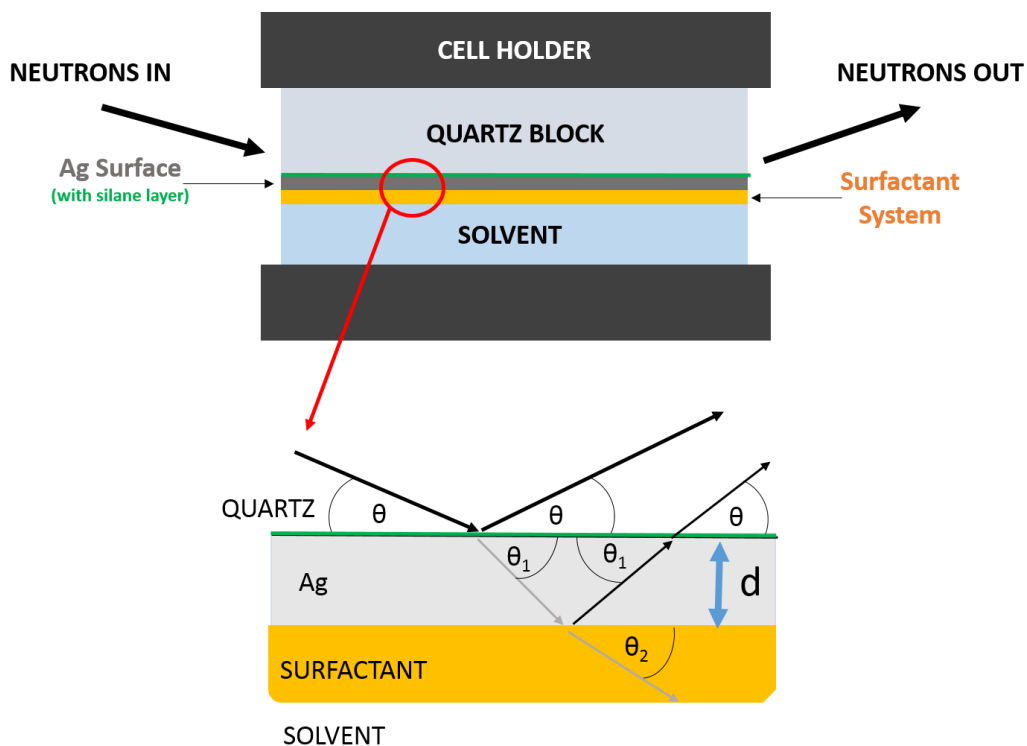


Figure 2.13 - Neutron cell configuration

Laser alignment is performed when placing the cell in the sample holder of the instrument with respect to the height and angle of the neutron beam. The instrument consists of: a neutron source, choppers (for wavelength selection), collimation slits, sample holder and the detector.

2.5.3 Data Analysis

From the reflectivity profile, estimations for the thickness can be determined but in order to obtain greater and more accurate information, the data must be fitted. The raw data was reduced on site using Open Genie or Mantid software. The RasCal fitting program was used to fit all reduced data.⁶⁹ Within the software, a model of the system can be generated allowing for fixed parameters to be inputted. The four

parameters that are fitted are: the thickness ($d/\text{\AA}$), the SLD ($N_b/\text{\AA}^{-2} \times 10^{-6}$), roughness ($\sigma/\text{\AA}$) and hydration (% v/v). RasCal defines the SLD of a layer as follows in equation 2.12.

$$\text{Layer SLD}_{\text{Actual}} = \text{Layer SLD}_{\text{Ideal}} \times (1 - \text{Hydration}) + (\text{Bulk}_{\text{SLD}} \times \text{Hydration}) \quad (2.12)$$

The quality of the fit is represented by the χ^2 value and generally speaking the lower this value is, the better the model is fitted to the data. However, a lower value does not always mean that the data is suitably fitted. It is important to take into account how well the fitted plot matches to the raw data visually. This is because the χ^2 value will be calculated for the whole data set across the whole Q range. At higher values of Q, there will be fewer data points which will have larger error bars. Therefore the best value of χ^2 may not consider the fitted data at high Q.

2.6 References

1. G. Haugstad, *Atomic Force Microscopy : Understanding Basic Modes and Advanced Applications*, Wiley, United States, 2012.
2. H. Wolfschmidt, C. Baier, S. Gsell, M. Fischer, M. Schreck and U. Stimming, *Materials*, 2010, **3**, 4196-4213.
3. G. Dan, X. Guoxin and L. Jianbin, *Journal of Physics D: Applied Physics*, 2014, **47**, 013001.
4. G. W. Padua and Q. Wang, *Nanotechnology Research Methods for Food and Bioproducts*, Wiley, Hoboken, United States 2012.
5. Y. Leng, *Materials Characterization : Introduction to Microscopic and Spectroscopic Methods*, John Wiley & Sons, Incorporated, Weinheim, Germany 2013.
6. W. J. Croft, *Under the Microscope : A Brief History of Microscopy*, World Scientific Publishing Co Pte Ltd, Singapore, 2006.
7. K. Morishima and T. Sato, *Langmuir*, 2014, **30**, 11513-11519.
8. P. Chatterjee and S. Hazra, *RSC Adv.*, 2015, **5**, 69765-69775.

9. F. Sun, T. C. Jaspers, P. M. van Hasselt, W. E. Hennink and C. F. van Nostrum, *Pharm Res*, 2016, **33**, 2168-2179.
10. B. Richard, J. L. Lemyre and A. M. Ritcey, *Langmuir*, 2017, **33**, 4748-4757.
11. S. Krickl, D. Touraud and W. Kunz, *Industrial Crops and Products*, 2017, **103**, 169-174.
12. S. Vargas, B. E. Millan-Chiu, S. M. Arvizu-Medrano, A. M. Loske and R. Rodriguez, *J Microbiol Methods*, 2017, **137**, 34-39.
13. S. Bhattacharjee, *J Control Release*, 2016, **235**, 337-351.
14. G. S. Bumbrah and R. M. Sharma, *Egyptian Journal of Forensic Sciences*, 2016, **6**, 209-215.
15. J. R. Ferraro, K. Nakamoto and C. W. Brown, *Introductory Raman Spectroscopy*, Elsevier Science, San Diego, United States 2002.
16. G. L. Squires, *Introduction to the Theory of Thermal Neutron Scattering*, Dover Publications, New York, USA, 1997.
17. A. Furrer, J. Mesot and T. Strassle, *Neutron Scattering in Condensed Matter Physics*, World Scientific Publishing Co. Ltd, Singapore, 2009.
18. B. T. M. Willis and C. J. Carlile, *Experimental Neutron Scattering*, Oxford Univeristy Press 2009.
19. *Neutron News*, 1992, **3**, 29-37.
20. R. M. Richardson, M. J. Swann, A. R. Hillman and S. J. Roser, *Faraday Discussions*, 1992, **94**, 295-306.
21. J. Penfold and R. K. Thomas, *J. Phys. Condens. Matter* 1990, **2**, 1369-1412.
22. E. M. Lee, R. K. Thomas, P. G. Cummins, E. Staples, J. Penfold and A. Rennie, *Chemical Physics Letters*, 1989, **162**, 196-202.
23. R. Shahlori, G. I. N. Waterhouse, T. A. Darwish, A. R. J. Nelson and D. J. McGillivray, *CrystEngComm*, 2017, **19**, 5716-5720.
24. J.-C. Wu, T.-L. Lin, U. S. Jeng and N. Torikai, *Physica B: Condensed Matter*, 2006, **385-386**, 838-840.
25. T. L. Crowley, E. M. Lee, E. A. Simister, R. K. Thomas, J. Penfold and A. R. Rennie, *Colloids and Surfaces*, 1991, **52**, 85-106.

26. M. Kreuzer, T. Kaltofen, R. Steitz, B. H. Zehnder and R. Dahint, *Review of Scientific Instruments*, 2011, **82**, 023902.
27. G. Fragneto-Cusani, *Journal of Physics: Condensed Matter*, 2001, **13**, 4973-4989.
28. S. A. Holt, P. A. Reynolds and J. W. White, *Physical Chemistry Chemical Physics*, 2000, **2**, 5667-5671.
29. T. Perevozchikova, H. Nanda, D. P. Nesta and C. J. Roberts, *J. Pharm. Sci.*, 2015, **104**, 1946-1959.
30. J. C. Schulz, G. G. Warr, P. D. Butler and W. A. Hamilton, *Physical Review E*, 2001, **63**, 041604.
31. J. R. Howse, R. Steitz, M. Pannek, P. Simon, D. W. Schubert and G. H. Findenegg, *Physical Chemistry Chemical Physics*, 2001, **3**, 4044-4051.
32. J. Penfold, R. K. Thomas, P. X. Li, J. T. Petkov, I. Tucker, J. R. Webster and A. E. Terry, *Langmuir*, 2015, **31**, 3003-3011.
33. P. X. Li, C. C. Dong and R. K. Thomas, *Langmuir*, 2011, **27**, 1844-1852.
34. J. Penfold, E. J. Staples, I. Tucker, L. J. Thompson and R. K. Thomas, *International Journal of Thermophysics*, 1999, **20**, 19-34.
35. R. Zhang and P. Somasundaran, *Advances in Colloid and Interface Science*, 2006, **123-126**, 213-229.
36. P. X. Li, Z. X. Li, H. H. Shen, R. K. Thomas, J. Penfold and J. R. Lu, *Langmuir*, 2013, **29**, 9324-9334.
37. J. Penfold, E. Staples, L. Thompson and I. Tucker, *Colloids and Surfaces A: Physicochem. Eng. Aspects*, 1995, **102**, 127-132.
38. J. R. Lu, E. Simister, E. Lee, R. K. Thomas, A. Rennie and J. Penfold, *Langmuir*, 1992, **8**, 1837-1844.
39. J. Eastoe and J. S. Dalton, *Advances in Colloid and Interface Science*, 2000, **85**, 103-144.
40. E. Staples, L. Thompson and I. Tucker, *Langmuir*, 1994, **10**, 4136-4141.
41. J. Penfold, R. K. Thomas, P. Li, J. T. Petkov, I. Tucker, A. R. Cox, N. Hedges, J. R. Webster and M. W. Skoda, *Langmuir*, 2014, **30**, 9741-9751.

42. C. E. Morgan, C. J. Breward, I. M. Griffiths, P. D. Howell, J. Penfold, R. K. Thomas, I. Tucker, J. T. Petkov and J. R. Webster, *Langmuir*, 2012, **28**, 17339-17348.
43. R. Steitz, P. Müller-Buschbaum, S. Schemmel, R. Cubitt and G. H. Findenegg, *Europhysics Letters (EPL)*, 2004, **67**, 962-968.
44. R. Atkin, *Advances in Colloid and Interface Science*, 2003, **103**, 219-304.
45. R. K. Thomas, *Annual Review of Physical Chemistry*, 2004, **55**, 391-426.
46. D. J. Cooke, J. R. Lu, E. Lee and R. K. Thomas, *J. Phys. Chem.* , 1996, **100**, 10298-10303.
47. S. Kundu, D. Langevin and L. T. Lee, *Langmuir*, 2008, **24**, 12347-12353.
48. J. Penfold, E. Staples and I. Tucker, *Langmuir*, 2002, **18**, 2967-2970.
49. D. J. Taylor, R. K. Thomas and J. Penfold, *Advances in Colloid and Interface Science*, 2007, **132**, 69-110.
50. L. T. Lee, E. K. Mann, O. Guiselin, D. Langevin, F. B. and J. Penfold, *Macromolecules*, 1993, **26**, 7046-7052.
51. L. T. Lee, *Current Opinion in Colloid & Interface Science*, 1999, **4**, 205-213.
52. E. Staples, L. Thompson, I. Tucker, J. Hines, R. K. Thomas and J. R. Lu, *Langmuir*, 1995, **11**, 2496-2503.
53. J. Penfold, E. J. Staples, I. Tucker, L. Thompson and R. K. Thomas, *Physica B*, 1998, **248**, 223-228.
54. J. Penfold, R. K. Thomas, E. Simister, E. Lee and A. Rennie, *J. Phys. Condens. Matter*, 1990, **2**, SA411-SA416.
55. P. G. Cummins, J. Penfold, R. K. Thomas, E. Simister and E. Staples, *Physica B*, 1992, **180 & 181**, 483-484.
56. J. Penfold, I. Tucker, J. Petkov and R. K. Thomas, *Langmuir*, 2007, **23**, 8357-8364.
57. J. R. Lu, R. K. Thomas and J. Penfold, *Advances in Colloid and Interface Science*, 2000, **84**, 143-304.
58. P. A. Ash, C. D. Bain and H. Matsubara, *Current Opinion in Colloid & Interface Science*, 2012, **17**, 196-204.

59. A. Glidle, C. S. Hadyoon, N. Gadegaard, J. M. Cooper, A. R. Hillman, A. R. Wilson, K. S. Ryder, J. R. P. Webster and R. Cubitt, *Journal of Physical Chemistry B*, 2005, **109**, 14335-14343.
60. A. Glidle, A. R. Hillman, K. S. Ryder, E. L. Smith, J. M. Cooper, R. Dalgliesh, R. Cubitt and T. Geue, *Electrochimica Acta*, 2009, **55**, 439-450.
61. A. Glidle, J. Cooper, A. R. Hillman, L. Bailey, A. Jackson and J. R. P. Webster, *Langmuir*, 2003, **19**, 7746-7753.
62. A. Glidle, A. R. Hillman, K. S. Ryder, E. L. Smith, J. Cooper, N. Gadegaard, J. R. P. Webster, R. Dalgliesh and R. Cubitt, *Langmuir*, 2009, **25**, 4093-4103.
63. E. Dickinson, D. S. Horne and R. M. Richardson, *Food Hydrocolloids*, 1993, **7**, 497-505.
64. S. Petrash, A. Liebmann-Vinson, M. D. Foster, L. M. Lander, W. J. Brittain and C. F. Majkrzak, *Biotechnology Progress*, 1997, **13**, 635-639.
65. J. R. Lu, T. J. Su, P. N. Thirtle, R. K. Thomas, A. R. Rennie and R. Cubitt, *Journal of Colloid and Interface Science*, 1998, **206**, 212-223.
66. R. J. Marsh, R. A. L. Jones, M. Sferrazza and J. Penfold, *Journal of Colloid and Interface Science*, 1999, **218**, 347-349.
67. www.ill.fr, Accessed 2018.
68. J. Webster, S. Holt and R. Dalgliesh, *Physica B: Condensed Matter*, 2006, **385-386**, 1164-1166.
69. A. V. Hughes, *RasCal. Sourceforge.* , Downloaded from: <http://sourceforge.net/projects/rscl/>. (2016) 2013.

Chapter 3: Experimental

3.1	Introduction	65
3.2	Materials	65
	3.2.1 Fingerprint Deposition	65
	3.2.2 Substrates	66
	3.2.3 Reagents	67
3.3	Instrumentation	70
	3.3.1 Imaging	70
	3.3.2 Compositional Analysis	71
	3.3.3 Surface and Interfacial Analysis	71
	3.3.4 Spectroscopy	71
	3.3.5 Neutron Reflectivity	72
3.4	Procedures	73
	3.4.1 Environmental Conditions	73
	3.4.2 Growth and Dynamics of Silver for Fingerprint Visualisation	73
	3.4.3 Split Prints	75
	3.4.4 Spot Tests	76
	3.4.5 Physical Developer Procedure	77
	3.4.6 Superglue Fuming	79
	3.4.7 Preparation of Quartz Blocks for Neutron Reflectivity	80
	3.4.8 Fingerprint Grading	81
3.5	References	81

3.1 Introduction

In this section, experimental procedures will be outlined including the methods of fingerprint deposition, substrates and environmental conditions studied, preparation of working solutions and corresponding fingerprint development processes. In addition to this, instrumentation parameters are detailed.

3.2 Materials

3.2.1 Fingerprint Deposition

One donor was used for all fingerprint samples (unless specified). For each type of sweat residue, the deposition routine was followed as described in the following sections. Fingerprint samples were deposited with light pressure onto the substrate, avoiding rolling the finger, to prevent any ridge detail becoming smudged.

3.2.1.1 Natural Fingerprints

Natural fingerprints were acquired by the donor washing their hands in warm, soapy water at least 30 minutes prior to deposition. During the time before deposition they were asked to continue with daily tasks normally. A minimum time of 30 minutes allows for 'natural' fingerprint residue to collect on the fingertips.

3.2.1.2 Sebaceous Fingerprints

Sebaceous fingerprints should consist only of the water insoluble components of fingerprint residue. To achieve sebaceous fingerprint deposits, the donor was asked to wash their hands in warm, soapy water prior to rubbing their fingers across the nose region (and behind the ears). These areas are recommended to transfer only sebaceous residue as the forehead can contain some eccrine material.¹ They were then told to rub the fingertips together to distribute the sweat before depositing their fingerprint onto the substrate.

3.2.1.3 Eccrine Fingerprints

Eccrine fingerprints are composed of water soluble components and the sweat residue is only secreted from the fingertips. Eccrine fingerprints were acquired by the donor washing their hands in warm, soapy water before wearing a nitrile glove for 15 minutes. This encourages the production of sweat from the fingertips without contamination. The donor was asked to deposit their fingerprint immediately after taking off the nitrile glove.

3.2.2 Substrates

Standard white copy paper (80 gsm) was used for all studies (in chapter 4, 5 and 6). Alternative substrates, which were studied in chapter 6, included both leather and suede surfaces. Leather and suede samples are outlined with corresponding swatches in table 3.1.

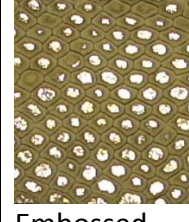
Suede	 Purple	 Nubuck	 Brown		
Leather	 Navy Matte	 White Faux	 Black Faux	 Embossed	 Patent

Table 3.1 - Leather and suede swatches - Purple suede, Nubuck suede, brown suede, navy matte leather, embossed leather and patent leather were all bovine sources (University of Northampton). White and black faux leather were sourced from an external supplier

3.2.3 Reagents

3.2.3.1 Preparation of the Maleic Acid Stock Solution

12.5 g maleic acid was dissolved in 500 ml deionized water with continuous stirring until all solid had dissolved, forming a clear, colourless solution. This solution was stored in the dark at room temperature.

3.2.3.2 Preparation of the Redox Stock Solution

Table 3.2 lists the chemicals and corresponding amounts required to make 450 ml redox solution. The chemicals were added in the order listed to 450 ml deionized water with continuous stirring. Each chemical was only added once the previous reagent had fully dissolved. Upon completion of addition of chemicals, the solution was stirred for a further 10 minutes to ensure thorough mixing. The resulting brown/orange, brown/green solution was stored in a dark container away from direct sunlight.

Chemical	Grade	Quantity/450 mL	Concentration/M
Iron (III) nitrate nonahydrate	Analytical	15 g	0.0825
Ammonium iron (II) sulfate hexahydrate	Analytical	40 g	0.2267
Citric acid, anhydrous	Analytical	10 g	0.1157

Table 3.2 - Chemicals for the redox solution

3.2.3.3 Preparation of the Detergent Solution

The original formulation for the detergent solution in PD has to be replaced due to the European banning of Synperonic N.² A detergent solution (2.8 g/0.0014 M n-dodecylamine acetate (DDAA), 2.8 g/0.0049 M Synperonic N in 1L DI water) was supplied by CAST. This detergent solution was used for all studies other than the specified alternative formulation experiments.

The reformulated detergent solutions were all prepared in 1L deionised water according to table 3.3. DGME is decaethylene glycol mono-dodecyl ether.

Detergent/1L	DDAA	Non-ionic surfactant	Conditions
DDAA/Tween20	2.8 g/0.0114 M	2.8 g/0.0023 M	
DDAA/Brij C10	1.5 g/0.0061 M 2.8 g/0.0114 M	1.5 g/0.0021 M 2.8 g/0.0041 M	Heat to at least 30°C
DDAA/DGME	1.5 g/0.0061 M 2.8 g/0.0114 M	1.5 g/0.0023 M 2.8 g/0.0046 M	

Table 3.3 - Detergent system formulations

3.2.3.4 Preparation of the Silver Nitrate Solution

Provided the silver nitrate solution is stored correctly, the shelf life is approximately 12 months. It must be stored in a dark container away from direct sunlight at room temperature due to the photosensitivity of the silver. For the purpose of latent fingerprint enhancement in a forensic case, it is advisable to use a fresh solution of silver nitrate in order to achieve the highest development. For each use of the PD working solution, a fresh silver nitrate solution was added in all experiments.

5 g of silver nitrate was added to 25 ml deionized water and stirred continuously until all solid had dissolved forming a 1.187 M solution.

3.2.3.5 Preparation of the Working Solution

The working solution was formulated from the three solutions and added in the order listed in table 3.4. Depending on the amount of samples to be developed, the exact quantities were adjusted accordingly. 495 ml was found to be sufficient to fill the processing trays and to allow the samples to float freely with minimal contact with the vessel.

Solution	Volume
Redox stock solution	450 ml
Detergent solution	20 ml
Silver nitrate solution	25 ml

Table 3.4 - Volumes for the working solution

Several working solutions were prepared throughout this thesis, to explore the efficacy of the alternative non-ionic surfactant components – Tween 20, DGME and Brij C10. The amount added to formulate the detergent solution is shown in table 3.3. The working solutions were prepared according to table 3.4 but the detergent systems varied as listed in table 3.5.

Each formulation was given a code (table 3.5) where PD corresponds to physical developer and F is the formulation number. The next letter corresponds to the surfactant used and 1 or 2 represents the lower and higher concentrations respectively. For example, PDF3B1 refers to physical developer formulation 3 where 1.5 g of Brij C10 has been added to the detergent system.

Working Solution	Detergent System	Code
Formulation 1 (current)	DDAA/Synperonic N (2.8g:2.8g)	PDF1S
Formulation 2	DDAA/Tween 20 (2.8g:2.8g)	PDF2T
Formulation 3	DDAA/Brij C10 (1.5g:1.5g)	PDF3B1
Formulation 4	DDAA/Brij C10 (2.8g:2.8g)	PDF4B2
Formulation 5	DDAA/DGME (1.5g:1.5g)	PDF5D1
Formulation 6	DDAA/DGME (2.8g:2.8g)	PDF6D2

Table 3.5 - Working solution formulations with various detergent systems

3.3 Instrumentation

3.3.1 Imaging

3.3.1.1 Photography

A DCS-5 imaging system (Foster and Freeman) was used to photograph and enhance the images of developed fingerprints. This uses the Nikon D810, 36 MP camera. The Polytec ring light and goosenecks were used as the lighting source. Samples treated with Cyanobloom/Basic Yellow 40 were viewed using the Crimelite Mark 2 light source excited at 460 nm wavelength with a GG495 viewing filter.

3.3.1.2 Optical Microscope

A Meiji Techno MT1700 Trinocular optical microscope was used to visualise secondary and tertiary level detail for developed fingerprints. In order to take a video of the PD process, a custom stage was developed and the process was recorded under 20x magnification.

3.3.1.3 Optical Profiler

A Zeta 20 Optical Profiler with 0.5 x Coupler was used to visualise fingerprint ridges under 5x magnification. Particle diameters were measured under 50x magnification using the built-in Zeta software.

3.3.1.4 Scanning Electron Microscope

The Philips XL30 Environmental Scanning Electron Microscope (ESEM) was used to visualise silver particle deposition.

3.3.2 Compositional Analysis

3.3.2.1 Energy Dispersive X-Ray Analysis

Compositional analysis of the PD treated fingerprints was acquired using the Philips XL30 ESEM coupled with the Oxford Inca Energy dispersive X-ray analysis system.

3.3.3 Surface and Interfacial Analysis

3.3.3.1 Atomic Force Microscope

The Veeco Digital Instruments Dimension 3100 Scanning Probe Microscope, operated with Nanoscope version 6.13rl software, was used. Veeco tips were used for all measurements, calibrated with a silicon wafer reference for each use. Tapping mode was the only mode used. Scan size ranged from 1-150 μm^3 .

3.3.3.2 Dynamic Light Scattering

The Malvern Zetasizer Nano S dynamic light scattering system (ISIS, Didcot, UK and University of Leicester) was used to acquire the particle distribution size of the silver particles in the working PD solution. Data analysis was performed using Malvern software.

3.3.4 Spectroscopy

3.3.4.1 Raman Spectroscopy

The Horiba Jobin Yvon Lab Ram HR spectrograph, operated with LabSpec 5 software, was used. The laser wavelength was calibrated using a silicon wafer to 532.1 nm with 300 μm hole, 100 μm slit and 1200 grating parameter settings were used for all measurements.

Bare silver surfaces were viewed and analysed using 50x objective lens and 10x for solutions on the surface. Data acquisition times were 10 s exposure times for 2 repeats over a range of 100-4000 cm^{-1} .

3.3.5 Neutron Reflectivity

3.3.5.1 Sputter Coater

The EMS300 R sputter coater was used to coat the silanised quartz blocks with silver. (3x silver targets, 57 mm diameter, 0.1 mm thickness) The coating parameters were constant for each block at 60 mA current for 500 s.

3.3.5.2 Neutron Reflectometer

Neutron reflectivity measurements were performed on INTER³ and SURF at ISIS, Rutherford Appleton Laboratory (Harwell Campus, Didcot, UK).

The wavelength range of the neutrons at ISIS is 1.5-15 Å. Static NR measurements were performed *ex situ*, for direct beam measurements (in air, through quartz) and *in situ* in H₂O and D₂O. The use of these contrasts allows the full characterisation of the surfaces and ensures maximum contrast between the hydrogenated surfactant in deuterated solvent and vice versa. A HPLC pump was connected through valves to the block to allow for the automated transfer and exchange of solvents.

INTER is capable of giving a higher flux whilst still maintaining a high signal to noise ratio and probing the lower Q_z range compared to SURF. Therefore measurements were recorded at different incident angles to cover the desired Q_z range, $0.009 < Q_z/\text{Å}^{-1} < 0.2$. (0.5° and 2.3° on INTER and at 0.25°, 0.35°, 0.65° and 1.5° on SURF).

The difference in flux also affects the data acquisition times which were subsequently longer for measurements on SURF. On INTER, data acquisition times

were ca. 45 mins for static measurements and 1.5 hr on SURF. In both cases the momentum transfer resolution ($\Delta Q/Q$) was 3-5%.

3.4 Procedures

3.4.1 Environmental Conditions

The laboratory temperature was 17 – 23 °C.

3.4.1.1 Ambient

Samples were placed into a plastic box and stored in the laboratory cupboard for a specified time of ageing (1, 14 or 28 days).

3.4.1.2 Immersion in Water

Tap water was used for all immersion samples. The samples were immersed into a plastic box containing the water for a specified time of ageing (1, 3 or 6 days).

3.4.1.3 Heated in the Oven

PD is often the last method for detection of fingerprints on porous surfaces, after ninhydrin or DFO treatment (unless the sample has previously been wetted, in which case only PD will be used). The ninhydrin and DFO process both include heating the sample. To emulate these conditions, samples were placed in an oven at 100 °C for at least 20 minutes prior to development via PD.

3.4.2 Growth and Dynamics of Silver for Fingerprint Visualisation

3.4.2.1 Interrupted Development

In order to investigate the growth of silver on the surface, a study was conducted to develop a fingerprint for a period of time from 30 seconds to 15 minutes. 15 minutes was chosen as the maximum time based on previous development times

for other samples and to avoid the risk of background development hindering the spatially selective deposition.

The donor used a different finger to deposit a natural mark in the designated area. 16 fingerprints were deposited in total. The donor was kept the same in order to ensure a similar composition of sweat. Once 10 marks were deposited, the donor was asked to wash their hands and continue their tasks as normal for 30 minutes until the remaining 6 marks could be deposited. This was to avoid any depleted levels of sweat being deposited by using the same finger for more than one mark. The same fingerprint on a substrate could not be used due to repeated immersions damaging the paper and practicality issues with using the microscopes to analyse the samples. This interrupted study with the one donor was repeated 3 times to provide an estimate of reproducibility.

Tween 20, Brij C10 and decaethylene glycol mono-dodecyl ether (DGME) have been undergoing trials within CAST as the new replacement for Synperonic N. Initial studies revealed that the Tween 20 working solution was more effective when it had been aged for 2 weeks. This is when the fingerprint development time became similar to that of the DDAA/Synperonic N system. After ageing the working solution for 2 days, the development times were up to an hour.

The working solution was prepared with DDAA/Tween 20 detergent (as described in section 3.2.3.5) and aged for 2 days and 2 weeks. The growth of silver on the surface was investigated as described above in this section.

For the 2 day old solution, 16 fingerprint samples were studied using development times from 1 minute to 60 minutes (1, 2, 3, 4, and 5 minutes followed by 5 minute intervals to 60 minutes). For the 2 week old solution as well as the Brij C10 and DGME working solutions, 16 fingerprint samples were studied with development times from 30 seconds to 15 minutes.

3.4.2.2 Dynamics of Image Development

The possibility of visualising the PD process in real time was explored by capturing the development using an optical microscope. A small section of white copy paper, with a 1 day old fingerprint, was inserted into the custom built stage and parameters were set to allow for the microscope to record the image development. The working PD solution was added to the paper via a pipette and the development was captured.

As PD is an immersion process, there is limited control to keep the paper in a fixed place. Preliminary testing was conducted by gluing an O-ring to a glass microscope slide and cutting the piece of paper to fit in the middle of the O-ring (as shown in figure 3.1 a). The working solution was introduced to the paper and the microscope settings were adjusted to tune the focus and light balance to ensure the particle deposition could be seen through the liquid. Once these parameters were optimised, a custom stage was designed (figure 3.1 b).

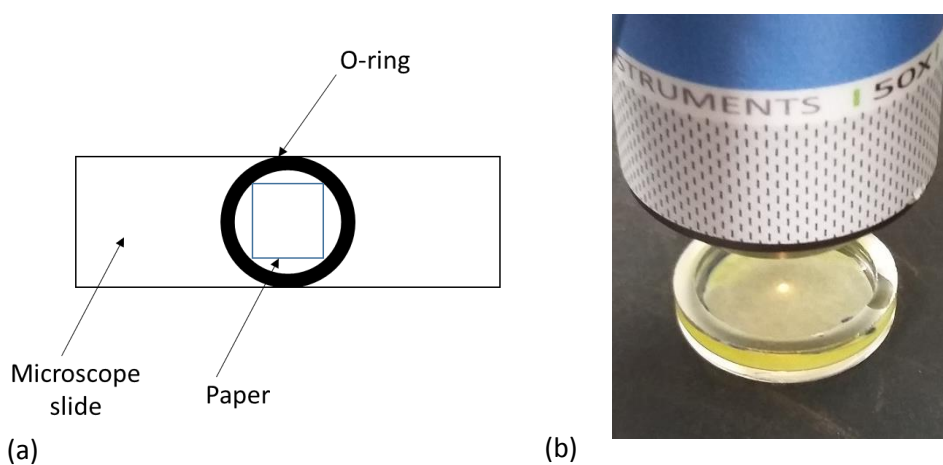


Figure 3.1 - (a) Preliminary design for recording the continuous development via PD (b) custom stage design

3.4.3 Split Prints

In order to directly compare two procedures, split prints were deposited to ensure each half of the fingerprint is similar in sweat residue.¹ Two methods of split printing were studied: a direct split into two halves for comparison of different

environmental conditions and a fingerprint split into four quarters to examine the growth of silver at different times for the same fingerprint.

3.4.4 Spot Tests

3.4.4.1 Individual Components

The components selected were chosen according to their abundance in fingerprint residue in both sebaceous and eccrine sweat that make up fingerprint residue.⁴⁻⁸ A concentration range (1-100 mM) was tested to observe the sensitivity. 20 μ L of each solution was deposited onto a grid (as shown in figure 3.2). For the eccrine components, water was used as the solvent. The sebaceous components were dissolved in dichloromethane as this resulted in the good solubility of material and volatility of solvent. A control spot of pure solvent was used in each case. The spots were aged for one day under ambient conditions and one day immersion in water.

	50 mM	10 mM	1 mM
Squalene	●	●	●
Cholesterol	●	●	●
Palmitic acid	●	●	●
Oleic acid	●	●	●

	100 mM	10 mM	1 mM
Serine	●	●	●
Glycine	●	●	●
Sodium chloride	●	●	●
Lactic acid	●	●	●

Figure 3.2 - Grids used for testing individual sebaceous (top) and eccrine (bottom) components with PD

3.4.4.2 A Mixture of Sebaceous and Eccrine Components

A mixture of the components was tested by depositing the sebaceous component first and the eccrine second and vice versa. 10 μ l of 100 mM eccrine solution was used and 10 μ l of 50 mM sebaceous components were used. These

concentrations were chosen as a result of the individual component spot tests as discussed in chapter 4 section 4.2.2.1.

3.4.4.3 Emulsions

Artificial sweat solutions were prepared to reflect fingerprint residue that would be deposited onto objects.^{4, 9, 10} Eccrine solutions were mixed with sebaceous solutions as described in table 3.6. Concentrations were chosen to reflect a natural fingerprint and the solvents were chosen based on whether the aqueous and organic material emulsified. Squalene in isopropyl alcohol (IPA) did not emulsify when mixed with the aqueous solutions so was the only sebaceous component dissolved in ethanol.

Component (Solvent)	Concentration
Serine (Water)	10 mM
Glycine (Water)	10 mM
Lactic acid (Water)	100 mM
Sodium Chloride (Water)	100 mM
Squalene (EtOH)	1 mM/10 mM
Cholesterol (IPA)	1 mM/10 mM
Palmitic acid (IPA)	1 mM/10 mM
Oleic acid (IPA)	1 mM/10 mM

Table 3.6 - Eccrine and sebaceous components with their corresponding solvent and concentration

3.4.5 Physical Developer Procedure

All glassware used throughout the physical developer process was meticulously cleaned and scratch free because any impurities will act as sites for silver particle nucleation which could render any fingerprints developed unsuccessful for identification purposes. Pyrex® dishes were used as vessels for the physical developer process. These were cleaned by washing with tap water and a mild detergent without any abrasive scrubbing followed by thoroughly rinsing three times under running water. Paper towels were used to dry the dishes.

Three types of immersion make up the physical developer process and in each dish, enough of the solutions were used to ensure the sample would be fully immersed. The efficacy of the PD working solution was first determined using a spot of AuCl_3 . If the spot darkened, the solution was deemed suitable for use.

The first dish contained the maleic acid prewash treatment. This step was included in order to neutralise the commonly used CaCO_3 alkaline filler added to many types of paper. The paper substrates were submerged for 10 minutes or until any bubbles had stopped forming. Once this step was complete the sample was then transferred to the second dish containing the working solution. To transfer the samples, nonserrated plastic photographic tongs were used to avoid adding any creases in the paper. A control sample was added to the maleic acid solution before the samples were processed to test the efficacy. This was a small piece of white copy paper without a deposited fingerprint. If this control sample darkened when added to the PD working solution, the maleic acid pre-wash solution was re-made.

Immersion times in the physical developer solution were dependent on the size of the paper, the age of the solution and the amount of samples which were to be developed. For the majority of the samples, fingerprints began to develop after ca. 5 minutes and the paper substrates were taken out of the solution after 15 minutes. This was evident from visual examination. Some samples took longer but none were left to develop for longer than 30 minutes because the background staining was too high and contrast between the background and the fingerprint was greatly weakened.

The final step was to wash the substrate in three dishes containing water to completely remove any of the PD solution and finally washing the sample under running water for 5 minutes. The substrates were dried on a paper towel at room temperature and any fingerprints were photographed once dry. A diagram of the procedure can be viewed in figure 3.3.

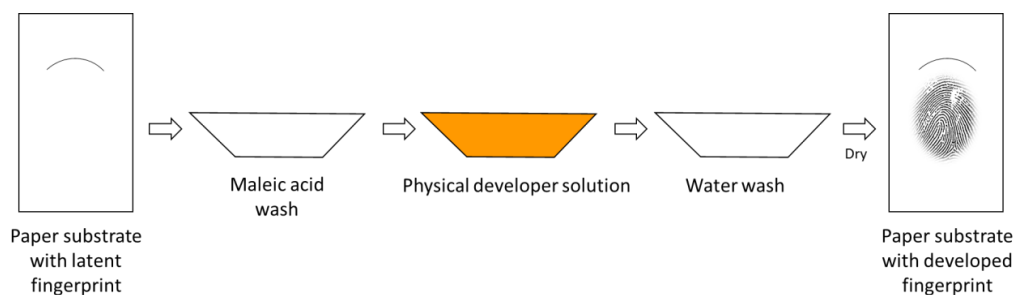


Figure 3.3 - Physical developer procedure

If any of the solutions became discoloured (in terms of the water washes) or had too much debris, they were discarded. White sediment was sometimes visible in the working solution but this had no effect on the development. If this sediment was silver/grey, then the solution was discarded because the silver had precipitated. To minimise the probability of this happening and to avoid high background staining, the development process was carried out away from direct sunlight and where possible in dim lighting.

3.4.6 Superglue Fuming

The MVC 1000 (Foster and Freeman) superglue cabinet was used for all fuming. Cyanobloom and Polycyano UV (Foster and Freeman) superglues were used. The structure of ethyl-2-cyanoacrylate (the superglue chemical reagent) is shown in figure 3.4. Polycyano UV produced by Foster and Freeman is a powder reagent consisting of polymerised ethyl-2-cyanoacrylate and dimethylamino benzaldehyde (DMAB) – a fluorescent staining dye also shown in figure 3.4. Polycyano UV is a one-step superglue method such that the developed fingerprints will fluoresce without the additional step of using a fluorescent dye as a secondary process. Cyanobloom treated samples were then immersed in Basic Yellow 40 solution and left to dry overnight.

For Cyanobloom, the cabinet was set to 80% humidity and 120 °C and was run on the AUTO cycle for 30 minutes. Polycyano UV follows the same method but the temperature was set to 230 °C.

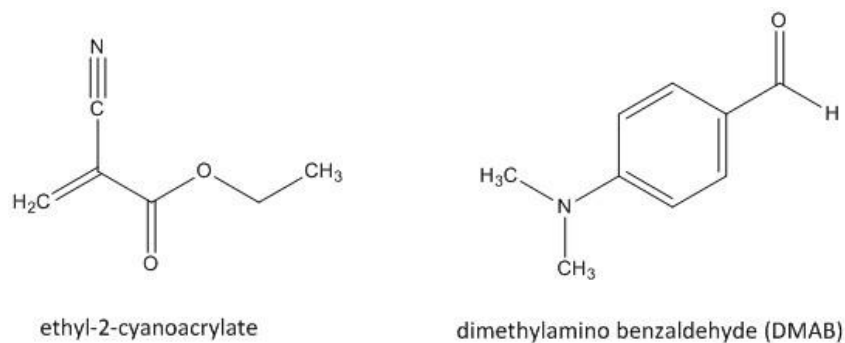


Figure 3.4 - Chemical structures of ethyl-2-cyanoacrylate and dimethylamino benzaldehyde (DMAB)

3.4.7 Preparation of Quartz Blocks for Neutron Reflectivity

Single crystal quartz blocks (80 x 50 mm) were silanised in order to acquire a silane layer on the surface of the blocks. The sulphur groups point outwards providing a surface for the silver to adhere to (see figure 3.5).

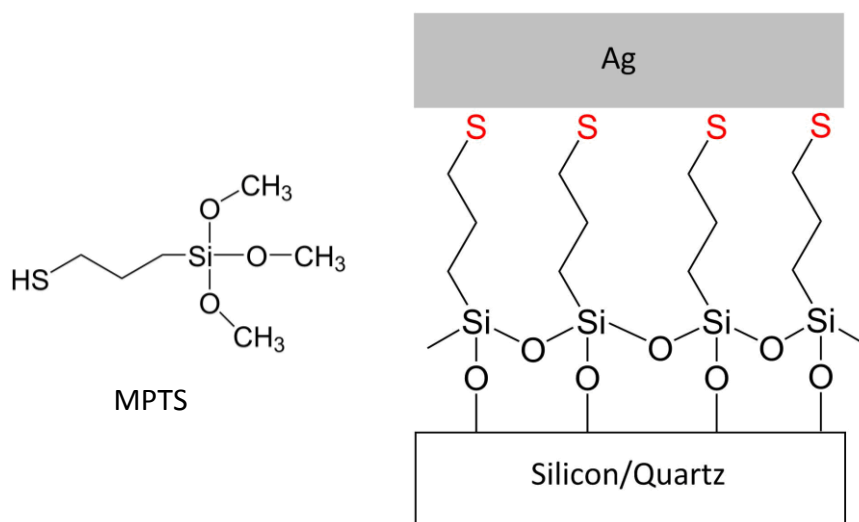


Figure 3.5 - Silanisation of quartz blocks

The blocks were cleaned in aqua regia overnight and rinsed with ultra-pure water before washing in soapy, ultra-pure water for 10 min. Then, they were sonicated in ultra-pure water for 10 min followed by sonication in isopropyl alcohol (IPA) for a further 10 min and dried with compressed air.

The silane bath was prepared with IPA (400 ml), ultra-pure water (12 ml) and (3-mercaptopropyl)-trimethoxysilane (MPTS) (12 ml) for one block (quantities adjusted for more than one block). The blocks were refluxed in this solution for 20 min and once cool, rinsed and sonicated in IPA for 10 min and finally dried with compressed air. The reflux procedure was repeated twice more and the blocks are sputter coated soon after. One block was coated at a time to ensure uniform thickness. Once coated with silver, the quartz blocks were stored under nitrogen.

3.4.8 Fingerprint Grading

Developed fingerprints were graded according to the 0-4 Bandey Scale shown in table 3.7.¹ This scale is subjective and is a visual assessment based on the amount of the fingerprint that has been developed. A numerical grade of 3 or 4 deems the fingerprint to be suitable for identification. One person graded all fingerprints to ensure continuity across the samples.

Grade	Comments
0	No evidence of a mark
1	Weak development; evidence of contact but no ridge detail
2	Limited development; about 1/3 of ridge detail is present but probably cannot be used for identification purposes
3	Strong development; between 1/3 and 2/3 of ridge details; identifiable finger mark
4	Very strong development; full ridge details; identifiable finger mark

Table 3.7 - Bandey grading system

3.5 References

1. V. G. Sears, S. M. Bleay, H. L. Bandey and V. J. Bowman, *Science & Justice*, 2012, **52**, 145-160.
2. *Directive 2003/53/EC of The European Parliament and of The Council*, Council Directive 76/769/EEC, 2003.

3. J. Webster, S. Holt and R. Dalgliesh, *Physica B: Condensed Matter*, 2006, **385-386**, 1164-1166.
4. A. Girod, R. Ramotowski and C. Weyermann, *Forensic Science International*, 2012, **223**, 10-24.
5. A. Girod and C. Weyermann, *Forensic Science International*, 2014, **238**, 68-82.
6. R. S. Croxton, M. G. Baron, D. Butler, T. Kent and V. G. Sears, *Forensic Science International*, 2010, **199**, 93-102.
7. M. Picardo, M. Ottaviani, E. Camera and A. Mastrofrancesco, *Dermato-Endocrinology*, 2009, **1**, 68-71.
8. H. Mark and C. R. Harding, *Int J Cosmet Sci*, 2013, **35**, 163-168.
9. L. Schwarz, *Journal of Forensic Sciences*, 2009, **54**, 1323-1326.
10. S. Hong, I. Hong, A. Han, J. Y. Seo and J. Namgung, *Forensic Science International*, 2015, **257**, 403-408.

Chapter 4:

Understanding the Fundamentals of the Physical Developer Process

4.1	Introduction	84
4.2	Results	84
	4.2.1 Development of Marks Derived from Different Sweat Types	84
	4.2.2 Spot tests	91
	4.2.3 Growth and Dynamics of Silver for Fingerprint Visualisation	102
	4.2.4 Compositional Analysis of the Developed Fingerprints	124
4.3	Conclusions	127
4.4	References	128

4.1 Introduction

Physical developer (PD) is a widely accepted technique for the development of latent fingerprints on porous surfaces.¹⁻⁷ The working solution has been developed and adapted to improve the quality of the developed marks, although the underlying chemistry of PD is still poorly understood.⁸⁻¹¹ In addition to this, a crucial component – the non-ionic surfactant Synperonic N – has been banned due to environmental toxicity. The fundamental chemistry of the PD process must first be explored in order to successfully reformulate the component solutions. This chapter explores the nucleation, growth and dynamics as well as the spatially selective deposition of silver particles from solution onto the surface. The current detergent system¹² of Synperonic N and n-dodecylamine acetate (DDAA) has been used throughout the experiments in this chapter.

Fingerprint residue is a complex mixture of eccrine and sebaceous sweat along with contaminants such as food and cosmetic residue. Whilst the majority of this residue is water (ca. 95-99%), most fingerprint detection methods target the remaining water soluble or water insoluble components. The components in the fingerprint that PD targets are not fully understood. In this chapter, the mechanism of PD will also be explored.

4.2 Results

4.2.1 Development of Marks Derived from Different Sweat Types

4.2.1.1 Full Fingerprints

Natural, eccrine and sebaceous fingerprints were deposited on white copy paper substrates and aged for 1, 14 and 28 days. It was expected that the eccrine marks would not show a positive reaction, i.e. silver deposition along the ridges, because eccrine components are water soluble. All solutions in the PD process are aqueous and the first immersion bath containing maleic acid is likely to dissolve any water soluble content. Figures 4.1-4.3, respectively, show examples of the three types

of mark developed via PDF1S after ageing for 1, 14 and 28 days under ambient conditions. See chapter 3, section 3.4.5 for the methodology and table 3.5 for the meaning of the code.

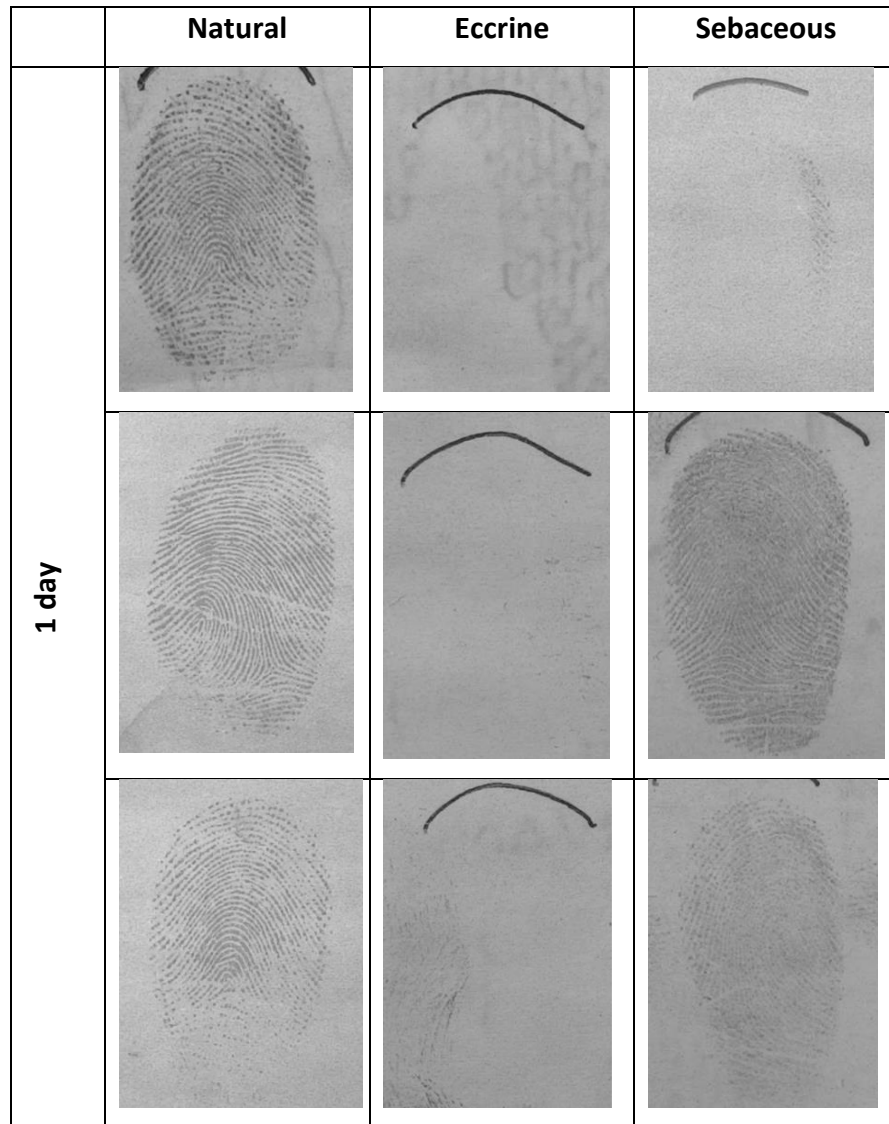


Figure 4.1 - Natural, eccrine and sebaceous fingerprints deposited on white copy paper and aged under ambient conditions for 1 day and then developed using PDF1S. The columns represent replicates for each type of mark

As figure 4.1 shows, the eccrine marks did not result in any visible fingerprint detail or indicate that a mark had been deposited. This was not an unusual result due to the solubility of eccrine content and 1 day marks are reasonably fresh, not allowing the residue content to age. The sebaceous marks showed a varied degree of development but in the majority of cases, visible fingerprint detail was evident where

silver deposition at the level of spatial resolution seen by eye, was continuous along the fingerprint ridges. All of the natural marks were developed but, in comparison to the sebaceous marks, the deposition along the ridges appears 'dotted'. In conjunction with the eccrine only marks, this result is not unexpected as natural fingerprint residue is a complex combination of both water soluble and insoluble components. Therefore, the dotted appearance suggests that the silver is targeting the sebaceous content but does not conclusively prove this fact or determine the specific components for preferable development.

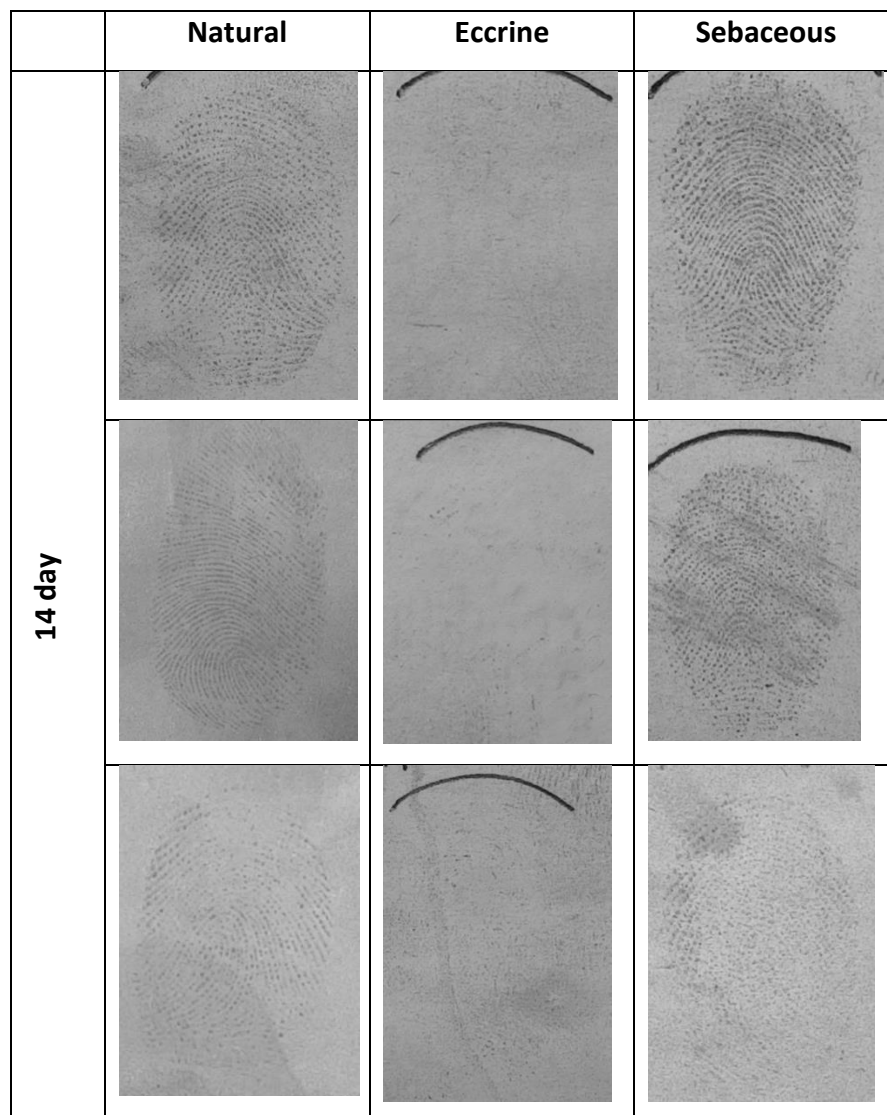


Figure 4.2 - Natural, eccrine and sebaceous fingerprints deposited on white copy paper and aged under ambient conditions for 14 days and then developed via PDF1S. The columns represent replicates for each type of mark

In comparison to the 1 day old marks, the clarity of the 14 day old developed fingerprints (natural and sebaceous) was poorer but the ridge features visible were still prominent. The silver deposition along the ridges of the sebaceous marks was less consistent suggesting that some sebaceous material had been removed through ageing. However, the quality of both the natural and sebaceous fingerprints were similar, still suggesting PD targets sebaceous material.

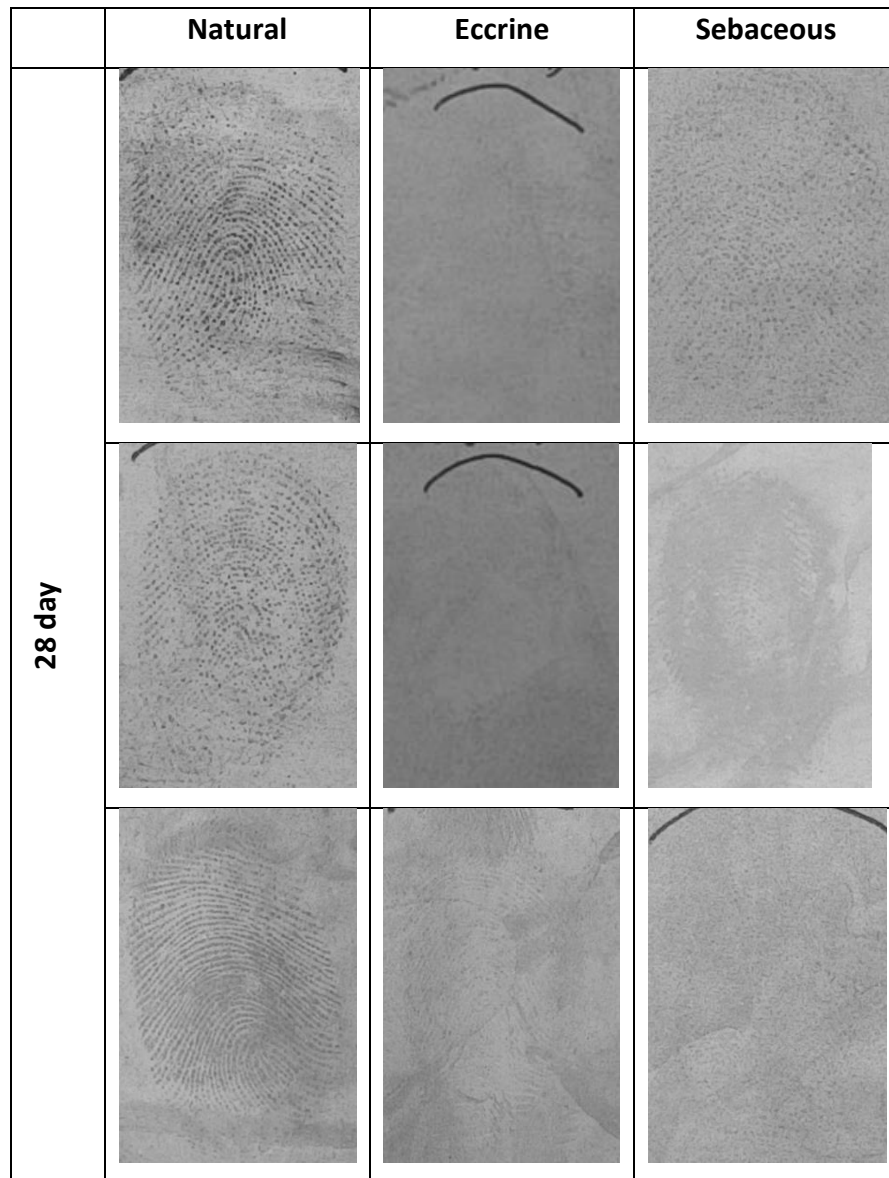


Figure 4.3 - Natural, eccrine and sebaceous fingerprints deposited on white copy paper and aged under ambient conditions for 28 days then developed via PDF1S. The columns represent replicates for each type of mark

As figure 4.3 shows, at 28 days, the quality of development of the sebaceous fingerprints diminished but the natural marks showed high contrast and strong silver deposition. In contrast to the 1 and 14 day old eccrine marks, at 28 days, there was some evidence that a fingerprint had been deposited but no visible ridge detail. This result indicates that sebaceous material cannot be the sole contributor to the development of natural fingerprints with PD. PD is also known to be more effective for aged fingerprints^{1, 13, 14}, as this result confirms, which could suggest that as the fingerprint ages some eccrine material could become trapped by the sebaceous material. However the full prints do not confirm the specific nature of the compound(s) that PD is targeting.

4.2.1.2 Split Prints

4.2.1.2.1 Effect of heat

PD is often used as the last method in a porous substrate sequence, unless the paper has been wetted in which case it is the method of choice. Typical methods prior to PD involve the application of heat.

Split prints for each type of sweat were studied where one side (left) was developed with only PD and the right side was developed with PD after the paper had been heated to 100 °C for 20 minutes. These split prints were also aged for 1, 14 and 28 days.

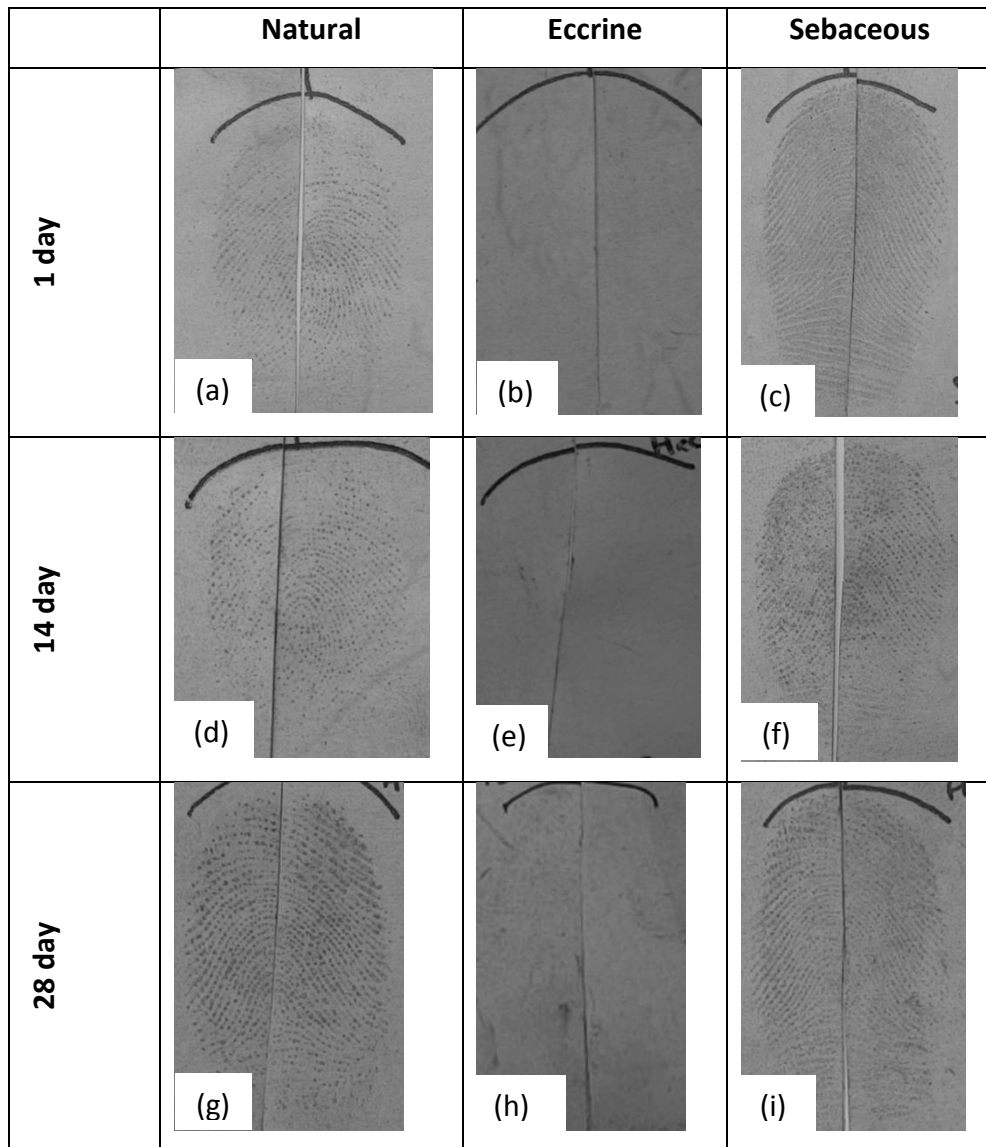


Figure 4.4 - Split prints of natural, eccrine and sebaceous fingerprints deposited on white copy paper and aged for 1 (a-c), 14 (d-f) and 28 (g-i) days under ambient conditions and then developed via PDF15. The left side of the prints were aged under ambient conditions and the right side of the prints were heated to 100 °C for 20 minutes prior to development

As figure 4.4 shows, the application of heat to the paper surface did not affect the resulting developed fingerprints for either of the ageing times or sweat types. This suggests that the elevated temperature does not aid in higher quality developed fingerprints but neither does it hinder the resulting development when using PD. These results also agree with the full print results observed in section 4.2.1.1.

4.2.1.2.2 Effect of wetting

PD is still the only technique used, in the UK, for porous surfaces which have been wetted either through immersion or being subjected to wet weather conditions. To observe any effects wetted conditions could have on the resulting developed fingerprints, split prints were prepared for all sweat types.

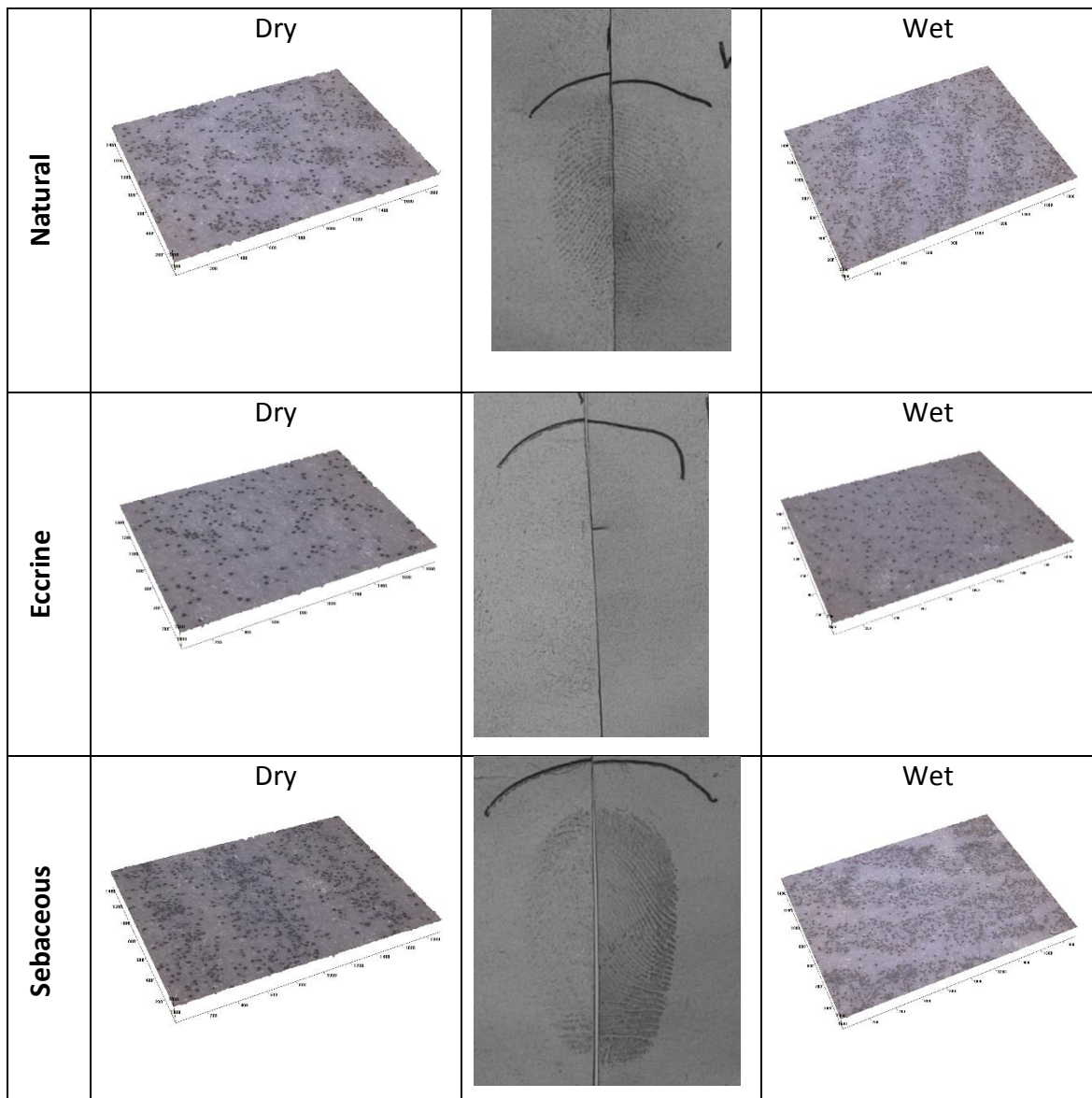


Figure 4.5 - Natural, eccrine and sebaceous split prints deposited on white copy paper and aged for 1 day under ambient (left) and wetted (right) conditions and then developed via PDF1S with the corresponding 3D microscopy image (5x). Tick marks every 200 μm

Examples of such marks (shown in figure 4.5) indicate that, similarly to the effect of heating the substrates, the effect of wetting did not improve or reduce the quality of the developed fingerprints for either sweat type. Though the wetted sebaceous mark appears darker, the overall quality of the ridge detail present was comparable to the mark stored under ambient conditions. In addition to this, the wetted natural fingerprint was comparable to the natural fingerprint stored under ambient conditions. This could indicate that PD preferably targets any water soluble content present. However the degree of silver deposition is no different between the conditions of storing the fingerprints in a dry or wet environment. Furthermore, as these fingerprints were deposited by the same donor, the overall composition of the fingerprint sweat residue would be similar.

The microscopy images shown in figure 4.5 further stress that there is no difference in the silver deposits between the marks stored under dry or wet conditions. The eccrine marks only reveal scattered background silver deposition, whereas the natural and sebaceous marks show spatially selective deposition of silver. The importance of this will be further discussed in section 4.2.3.

4.2.2 Spot Tests

The results from the development of the different types of sweat indicated that the deposition of silver for natural marks has a dotted appearance and the quality of development is increased as the fingerprints are aged. The 1 day old sebaceous marks show continuous silver deposition but this becomes more dotted as the fingerprint is aged, suggesting degradation of some sebaceous material. In order to gain further insight to the specific targets for PD, spot tests were studied to separate the sebaceous and eccrine components.

4.2.2.1 Individual Components

As previously mentioned, PD is typically used at the end of a sequence for porous items after ninhydrin and DFO, which target amino acids in fingerprint residue.

In conjunction with PD being an aqueous based immersion technique and the only development method current recommended for wetted porous items, it is a reasonable hypothesis that PD is targeting water insoluble material. It has also been shown that PD will produce more useable marks after processing with IND.¹⁵ The development of the different types of sweat in section 4.2.1 indicate that eccrine marks alone will not develop via PD but this does not conclusively state that sebaceous material is solely responsible. To test this hypothesis, spot tests were completed for the most abundant sebaceous and eccrine components commonly detected in fingerprint residue.¹⁶⁻²² The samples were aged for one day under ambient conditions prior to development using PDF1S.

Figure 4.6 shows the results for the individual eccrine components after development with PD (Three repeats were tested and results were consistent throughout – see appendix).



Figure 4.6 – PDF1S treatment applied to individual eccrine components spot test, which were deposited on white copy paper and aged for 1 day under ambient conditions - Set 1. The left hand column shows the type of eccrine component and the rows show variations in the concentration

The spot test in figure 4.6 shows that none of the eccrine components have caused any silver deposition. This is not an unexpected result, as previously mentioned in section 4.2.1.1. The first immersion into the maleic acid solution is likely to dissolve

any water soluble content, which is a crucial step in the process because of the risk of high background staining.



Figure 4.7 – PDF1S treatment applied to individual sebaceous components spot test, which were deposited on white copy paper and aged for 1 day under ambient conditions - Set 1. The left hand column shows the type of sebaceous component and the rows show the variation in concentration

On the other hand, figure 4.7 shows the sebaceous spot test results. Figure 4.7 clearly shows that only squalene and cholesterol have resulted in a positive reaction i.e. silver deposition. The decreasing concentrations of cholesterol have all reacted positively but only the highest concentration of squalene shows silver deposition. This result reflects previous work done in this area but their results were consistent.³ Figures 4.8 and 4.9 shows set 2 and 3 for the individual sebaceous spot tests.

(2)

Sebacous	50 _{mM}	10 _{mM}	1 _{mM}	CONTROL (αM)
Squalene				
Cholesterol				
Palmitic Acid				
Oleic Acid				

Figure 4.8 – PDF1S treatment applied to individual sebaceous components spot test, which were deposited on white copy paper and aged for 1 day under ambient conditions - Set 2. The left column shows the type of sebaceous components and the rows show the variation in concentration

Sebacous	50 _{mM}	10 _{mM}	1 _{mM}	
Squalene				
Cholesterol				
Palmitic acid				
Oleic acid				

Figure 4.9 – PDF1S treatment applied to individual sebaceous components spot test, which were deposited on white copy paper and aged for 1 day under ambient conditions - Set 3. The left column shows the type of sebaceous component and the rows show the variation in concentration.

The second set shown in figure 4.8 shows that as well as squalene showing some positive reaction, 50 mM palmitic acid has clear silver deposition. In addition, set 3 in figure 4.9 depicts silver deposition for squalene at all concentrations as well as

cholesterol. Though the results were not as consistent for the sebaceous material, squalene and cholesterol were the main components which resulted in silver deposition in this experiment. Palmitic acid only resulted in one positive reaction for the highest concentration 50 mM, which is not representative of natural fingerprint residue.

The positive reaction observed in these spot tests is further observed in the microscopy analysis. Figure 4.10 shows the optical image, magnified at 50 x, for the positive 50 mM squalene spot test alongside the negative 100 mM serine spot test.

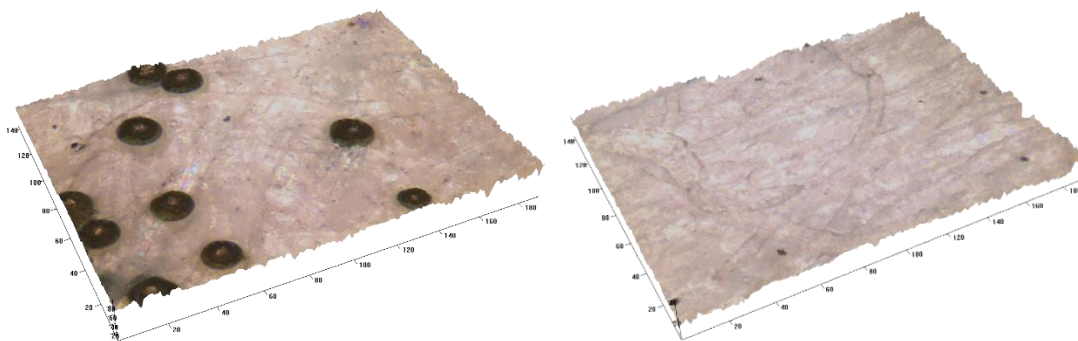


Figure 4.10 – 3D microscopy image (50x) of squalene 50 mM (left) and serine 100 mM (right) – Tick marks every 20 μm

The average Ag particulate diameter range observed for the squalene spot test was 13-20 μm . The eccrine marks did result in some silver particles, as seen in figure 4.10, with an average diameter range of 1-4 μm . However, the sebaceous components showed an accumulation of silver deposition, whereas the silver deposition for the eccrine components was largely dispersed. These spot tests were developed for 15 minutes and as the average particle diameter did not exceed 4 μm in this time, it can be concluded that the eccrine silver deposition is a result of background staining.

The individual component paper samples were immersed in water for 1 day prior to development to test the hypothesis that eccrine components would be washed away. Figure 4.11 shows the result for the wetted eccrine and sebaceous spot tests.



Figure 4.11 – PDF1S treatment applied to (a) individual eccrine component (set 1) and (b) sebaceous component (set 2) samples deposited on white copy paper and aged for 1 day under wetted conditions. The left hand columns of both images show the type of component and the rows show the variation in concentration

Figure 4.11 shows that the eccrine component samples did not show any silver deposition, supporting the assumption that this content is dissolved in the aqueous media. This was consistent across all three replicates (see appendix – set 2 is missing for the eccrine samples due to degradation of the paper when removed from the water wash). In addition to this, the sebaceous spot tests did not result in a positive reaction as seen for the analogous ambient tests and this was consistent for all three sets also (see appendix). It appears that the exposure to water has altered the surface such that the sebaceous content has been removed.

The results do suggest that sebaceous content can trigger silver deposition but does not conclude that squalene and cholesterol are the only triggers; they did not result in silver deposition after exposure to water. Natural fingerprint residue is a complex mixture of both eccrine and sebaceous material and it is possible that some eccrine components could become trapped by the sebaceous material, particularly for the older fingermarks.

4.2.2.2 Mixture of Eccrine and Sebaceous Components

In order to observe whether or not the presence of eccrine material changes the way PD develops specific targets, each sebaceous component was combined with

each eccrine component by deposition of one on top of the other and vice versa. Figure 4.12 depicts the result when the sebaceous component was deposited first and eccrine second and vice versa, aged for 1 day under ambient conditions.

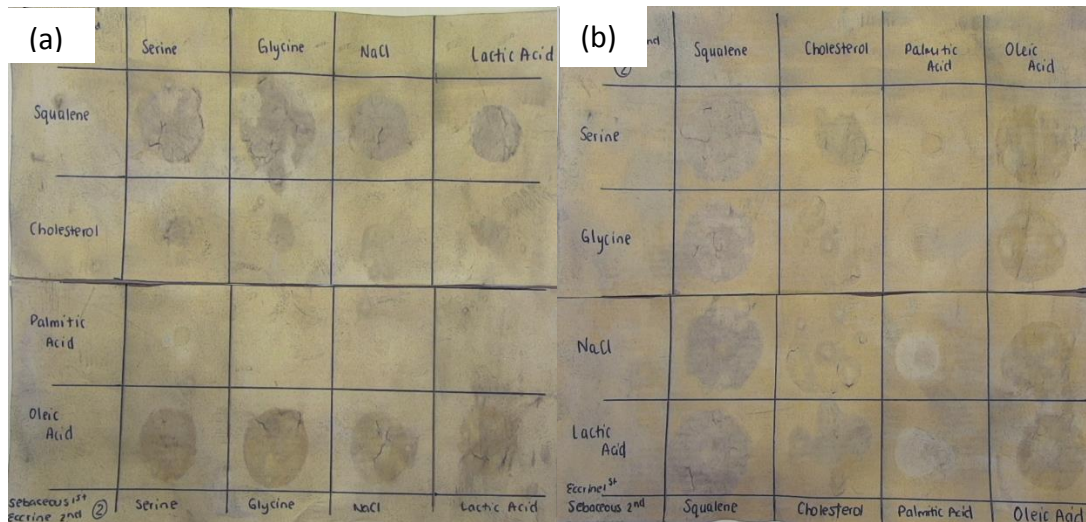


Figure 4.12 – PDF1S treatment applied to mixture of sebaceous and eccrine component deposited on white copy paper and aged for 1 day under ambient conditions: (a) sebaceous component deposited first, followed by eccrine component (set 2) and (b) eccrine component deposited first, followed by sebaceous component (set 2)

In comparison to the individual components spot tests, the combination of oleic acid with all four eccrine components has resulted in a positive reaction. In addition to this, the results for squalene mixed with the eccrine components depicts much darker spots consistent throughout all three sets (see appendix). It is indicated that having a mixture of both water soluble and insoluble material is preferential to PD to result in darker marks with clear contrast (see section 4.2.1). Furthermore, the theory that sebaceous material traps eccrine material is strengthened here.

The results from these spot tests do indicate the deposition of silver for fingerprints is enhanced when both eccrine and sebaceous content is present. However, this form of depositing the components is not reflective of 'real' fingerprint residue.

4.2.2.3 Emulsions

To formulate a more realistic 'spot' of fingerprint residue, each individual sebaceous component was combined with each individual eccrine component to create an artificial sweat solution. Table 4.1 shows the composition and concentration used for each artificial sweat solution. Isopropyl alcohol (IPA) was chosen for the sebaceous components in order to dissolve the components as well as the high miscibility with water. In the preliminary tests, squalene did not remain dissolved in the IPA when added to water, visible via an oily layer above the solution. Therefore, ethanol (EtOH) was used for squalene emulsions.

Component (Solvent)	Concentration
Serine (Water)	10 mM
Glycine (Water)	10 mM
Lactic acid (Water)	100 mM
Sodium Chloride (Water)	100 mM
Squalene (EtOH)	1 mM/10 mM
Cholesterol (IPA)	1 mM/10 mM
Palmitic acid (IPA)	1 mM/10 mM
Oleic acid (IPA)	1 mM/10 mM

Table 4.1 - Eccrine and sebaceous components with their corresponding solvent and concentration

Figure 4.13 shows the results of the 1 day old emulsion spot test. The only combination to show a positive result was palmitic acid with lactic acid. This observation was consistent with all three tests with a similar level of dark colouration. Figure 4.13 also shows the microscopy image for the palmitic acid/lactic acid spot which further emphasises the positive results.

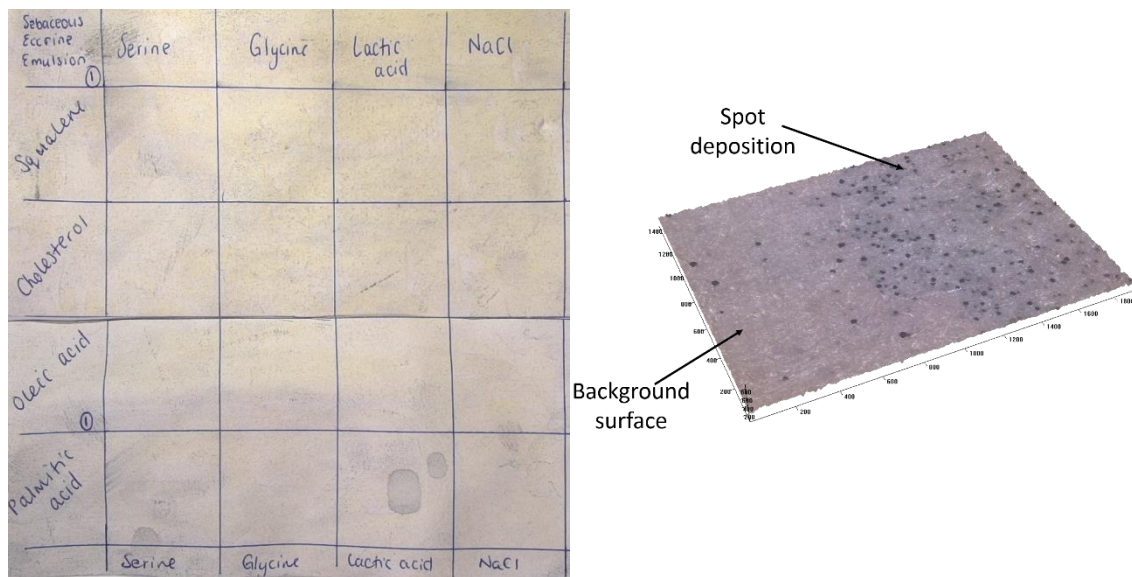


Figure 4.13 – PDF1S treatment applied to emulsion spot test deposited on white copy paper and aged for 1 day under ambient conditions with 5x 3D microscopy image of palmitic acid/lactic acid (Tick marks every 200 μm)

Although only one combination showed a positive result, it does further prove that both sebaceous and eccrine content have to be present for PD to result in high quality developed fingerprints.

PD is known to be effective on aged marks¹²; therefore the emulsion spot test samples were aged for 7, 14 and 28 days and then treated with PD. However, as figure 4.14 shows, none of the spot tests were deemed to show a positive reaction which was observed across all repeats tested.

7 days					14 days				
7 days Emulsion ①	Serine	Glycine	Lactic acid	NaCl	① Emulsion	Serine	Glycine	Lactic	NaCl
Squalene					Squalene				
Cholesterol					Cholesterol				
Palmitic lactic acid acid					Palmitic acid				
Oleic acid					Oleic acid				
28 days									
Emulsion ②	Serine	Glycine	Lactic	NaCl					
Squalene									
Cholesterol									
Palmitic acid									
Oleic acid									

Figure 4.14 – PDF1S treatment applied to emulsion spot tests deposited on white copy paper and aged for 7, 14 and 28 days

The lack of any obvious silver deposition could possibly be due to a low concentration of the component used, however 1 mM is still relatively high given that a fingerprint contains < 10 µg of material.²³ For example, for the palmitic acid spot tests, 20 µl would contain ca. 5 mg of material. In addition to this, it could be that PD does not target a specific class of sebaceous or eccrine compound in the same way that ninhydrin targets amino acids for example.

The lower concentrations of the sebaceous components were chosen to reflect a natural fingerprint but in order to test whether silver would deposit on the emulsion

spots, the sebaceous components concentration was increased to 10 mM. This would increase the amount of material available from 2×10^{-5} mol to 2×10^{-4} mol. Figure 4.15 shows the results of the higher concentration emulsion spot tests which were aged for 1, 7, 14 and 28 days prior to PD treatment.

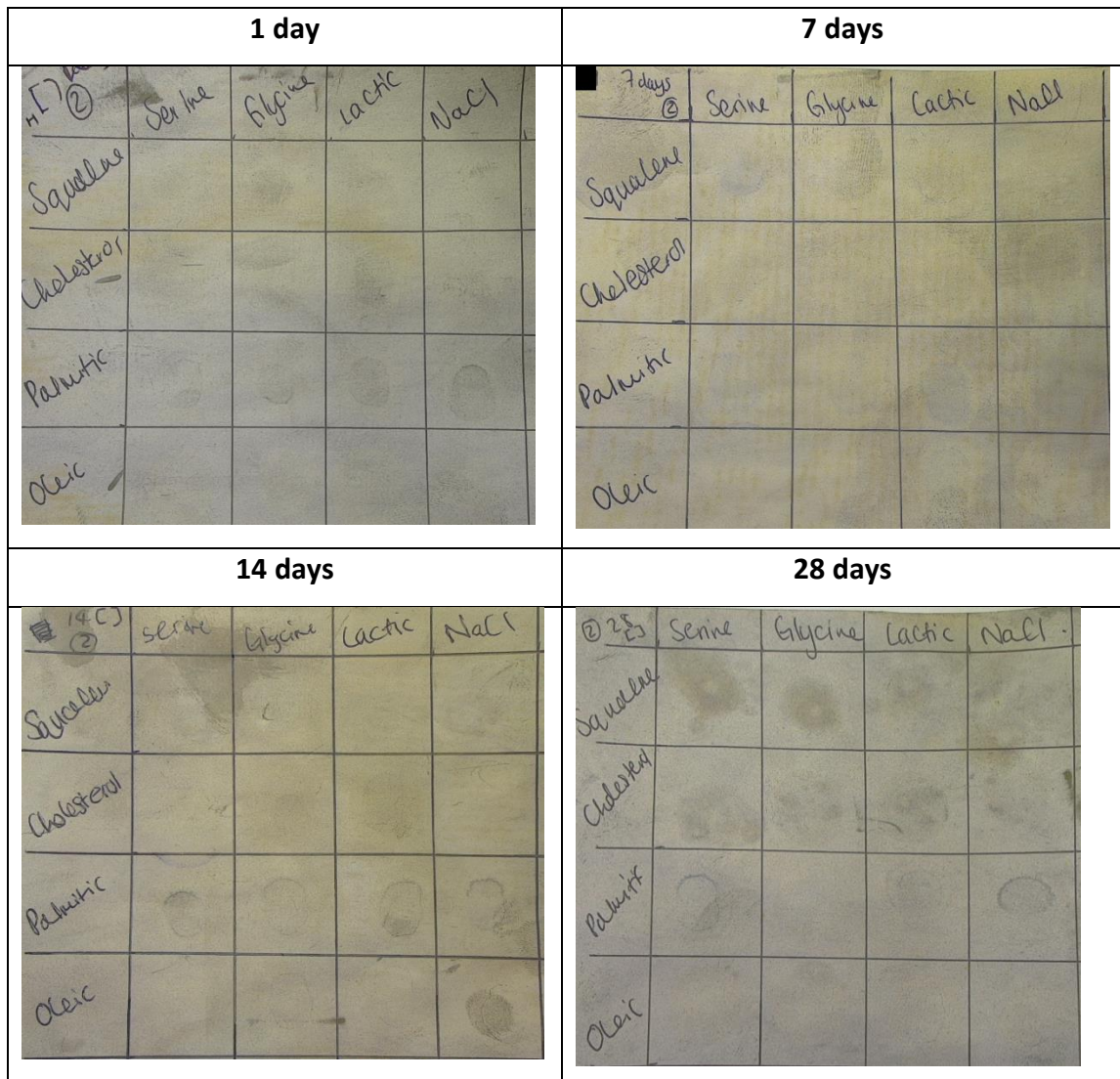


Figure 4.15 – PDF1S treatment applied to emulsion spot tests with 10 mM of sebaceous content deposited on white copy paper and aged for 1, 7, 14 and 28 days

In this case, there is clear silver deposition particularly for the palmitic acid combinations. Palmitic acid is a saturated long chain fatty acid which could potentially trap the smaller amino acid or salt molecules as the residue ages. In comparison to the 1 day old emulsion spot test of lower concentration, 1 mM (figure 4.13), the palmitic acid-lactic acid developed spot is not as dark and is very faint at 28 days. However,

there is positive reaction observed for the squalene-serine and glycine spots which was not observed previously with the shorter ageing periods and lower concentrations. This suggests that during the ageing process, squalene may degrade to a more stable, resilient component such that development with PD is more effective.

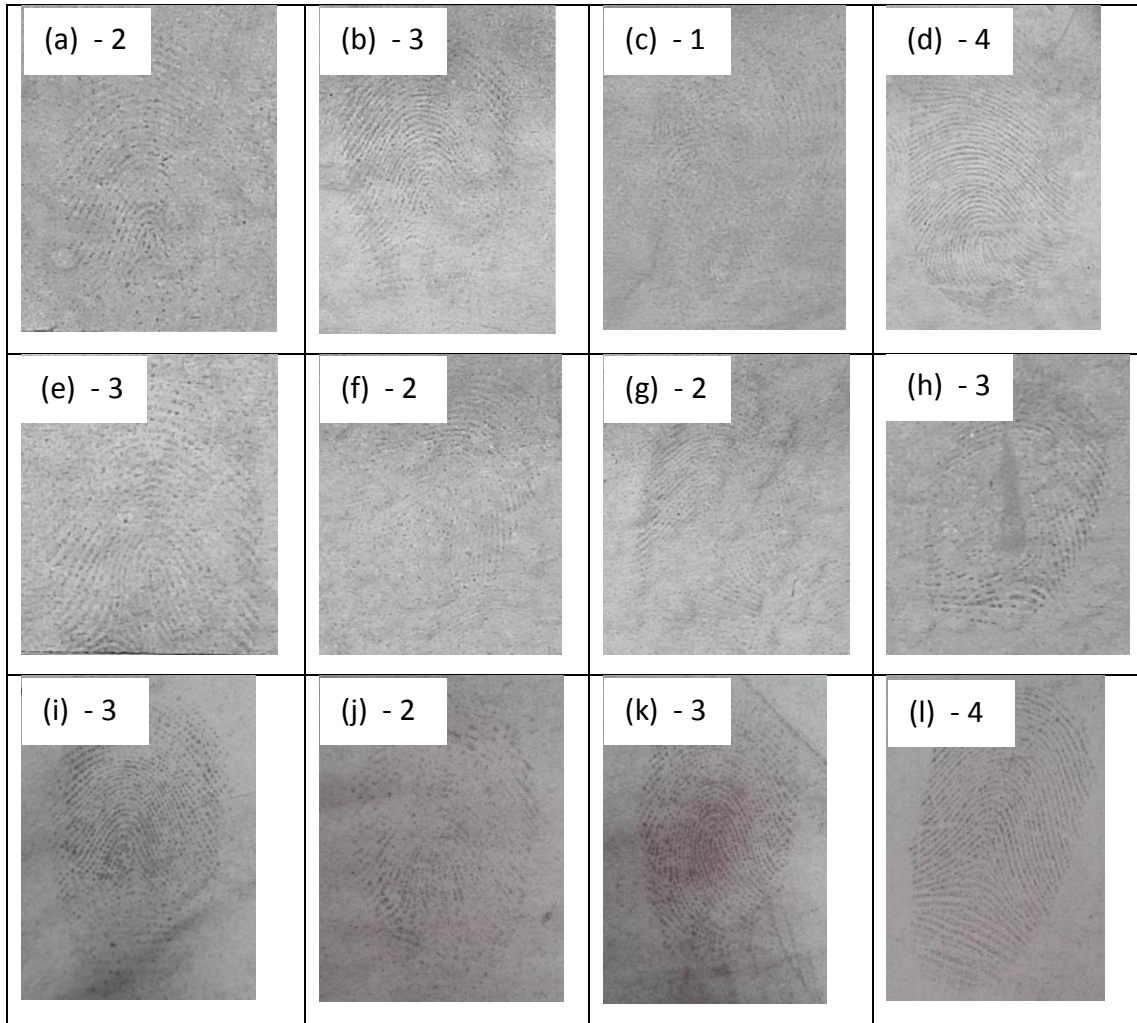
The inconsistency observed across the emulsion tests does not allow to conclusively state that PD target any specific class of compound. However, the results do indicate that any eccrine material does have to be present in order for PD to work effectively and that sebaceous components are not the only deposition triggers.

4.2.3 Growth and Dynamics of Silver Deposition for Fingerprint Visualisation

The quality of fingerprints developed using PD has been widely documented at a macroscopic level in terms of ridge detail, contrast and clarity. Whilst this is highly useful for practitioners to obtain the ‘best’ fingermarks they can for use in casework, it does not aid the understanding of the chemistry behind the PD process. In contrast to previous research into PD at a macroscopic level, i.e. what is visible to the naked eye, this work begins to understand PD on a microscopic level.

4.2.3.1 Macroscopic to Microscopic Analysis

The following image (figure 4.16) depicts fingerprints developed via PDF1S (table 3.5, chapter 3) on white copy paper, aged under ambient conditions for 1 day, accompanied by a pie chart representing the developed fingerprint grades. The fingerprints have been graded according to the Bandey Scale.²⁴ PD is an established method but the scale has been used here to indicate the high variation in the level of ridge detail that is visible such that the fingerprints would be used for identification purposes.



Quality of mark

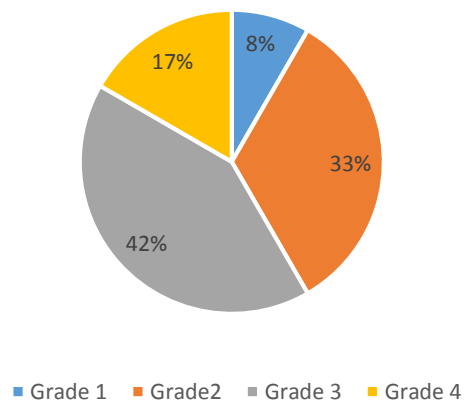


Figure 4.16 - 1 day old fingerprints deposited on white copy paper and aged under ambient conditions then developed with PDF1S with the associated Bandey grades

It is evident that there is variation in the development of the marks in terms of ridge detail, contrast and the extent of the fingerprint developed. These marks are similar to the literature and the information in the CAST fingerprint visualisation manual.¹² The pie chart was added in order to display the variation in quality of development for fingerprints deposited by one donor. The majority of the marks were given a grade of 3 which would be suitable for identification and only one of the marks was graded 1. A third of the marks were given a grade of 2 meaning there is ridge detail but not enough for identification purposes. There could be variation in the amount of sweat on each finger or the pressure of deposition. However, these possibilities were lowered by using the same donor who followed the same procedure and time window of deposition. Although 75% of the developed marks fall into the 2-3 grade band, there is large difference between a mark suitable for identification or not, especially for serious casework.

In addition to the quality of developed marks, the spatial selectivity of silver to the fingerprint residue is observed. Microscopy analysis was utilised to further examine the developed fingerprints from primary and secondary level to the morphology of the deposited silver particles, to determine any variation microscopically. Figure 4.17 depicts the view of the deposited silver particles from the full view of a developed mark to the magnified microscopy image.

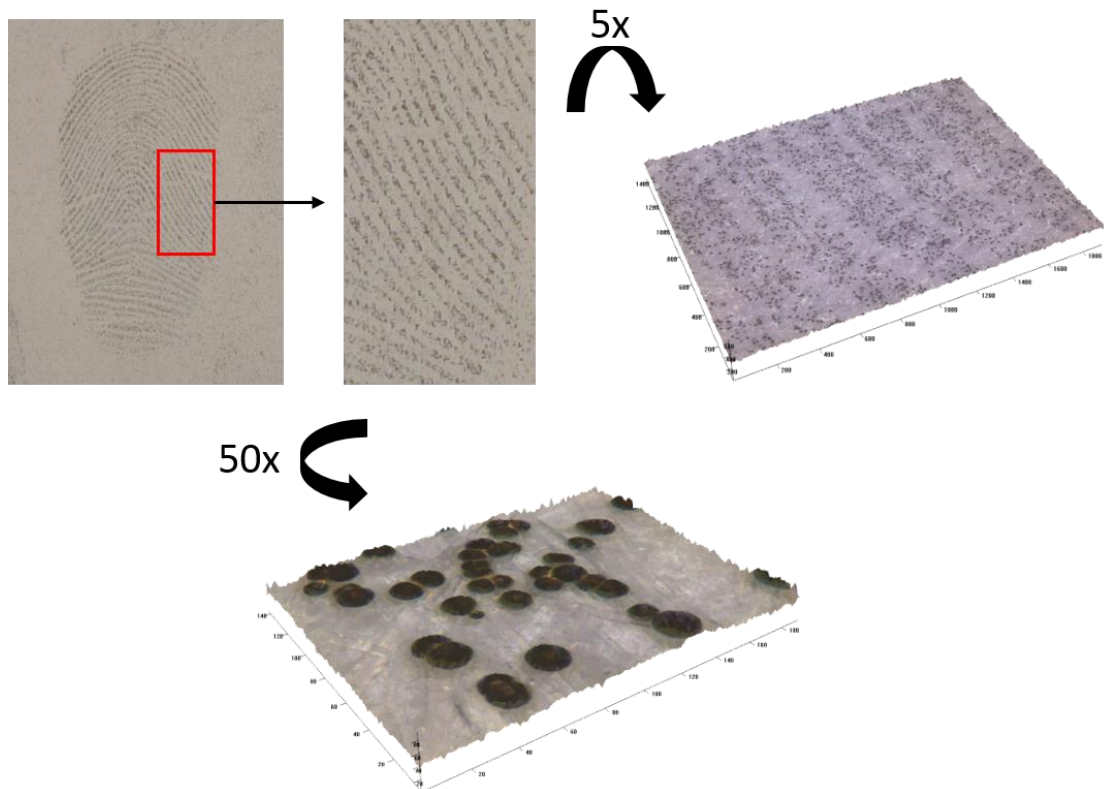


Figure 4.17 - Macroscopic to microscopic view of a fingerprint developed via PDF1S. 5x image (Tick marks every 200 μm), 50x image (Tick marks every 20 μm)

The mark in figure 4.17 produced silver deposits of 14-20 μm in diameter. This is smaller than the eye can resolve, so the developed fingerprint appears to the eye as continuous silver lines against the white paper background, similar to exemplar fingerprints used for fingerprint matching. Higher magnification starts to reveal the 'dotted' appearance of the marks as if they are a pixelated image of a series of silver dots.

The microscopy image (50x) in figure 4.17 reveals these silver deposits as monodisperse, spherical particles with a narrow diameter range. The dispersed nature of the silver clusters suggests there is a preferential site of deposition within the fingerprint residue.

The size of the silver particles in solution, i.e. prior to deposition, has never been reported. It is unclear whether the silver particles grow to a specific size in solution which is then satisfactory for deposition onto the fingerprint residue, or that

the silver particles proceed to grow after the initial deposition has happened. To address this question, the size of the silver particles in the working solution was determined using dynamic light scattering. Figure 4.18 shows the graph for the average silver particle size in solution.

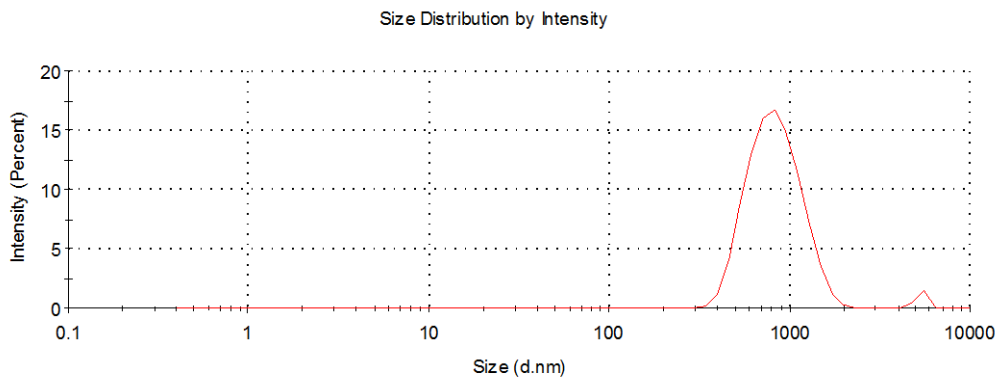


Figure 4.18 - DLS graph for particle size in the PDF1S working solution

An average particle size of 880 nm was obtained. This could apply to the silver particles alone or a micellar structure due to the surfactant components. The role of surfactant in the solution will be further explored in chapter 5 and 6.

In comparison to the silver deposits for the developed mark, there is a ca. 20x difference in the particle size of silver in solution compared to the surface. This suggests that silver growth occurs but at which point the nucleation and growth proceeds is still unclear.

4.2.3.2 Interrupted Growth

The initial analysis of the size of the silver particles, both in the working solution and on the surface, has indicated that there is a considerable growth of silver during the PD process. This generates two opposing hypotheses: (i) do the silver particles have to grow to a specific size in solution for adequate development? or (ii) do the initial silver particles deposit onto the surface thus providing nucleation sites for subsequent silver growth?

In order to begin to understand this, an interrupted growth study was carried out to measure the size of the deposited silver particles at several timescales between 30 seconds to 15 minute development times (chapter 3, section 3.4.2).

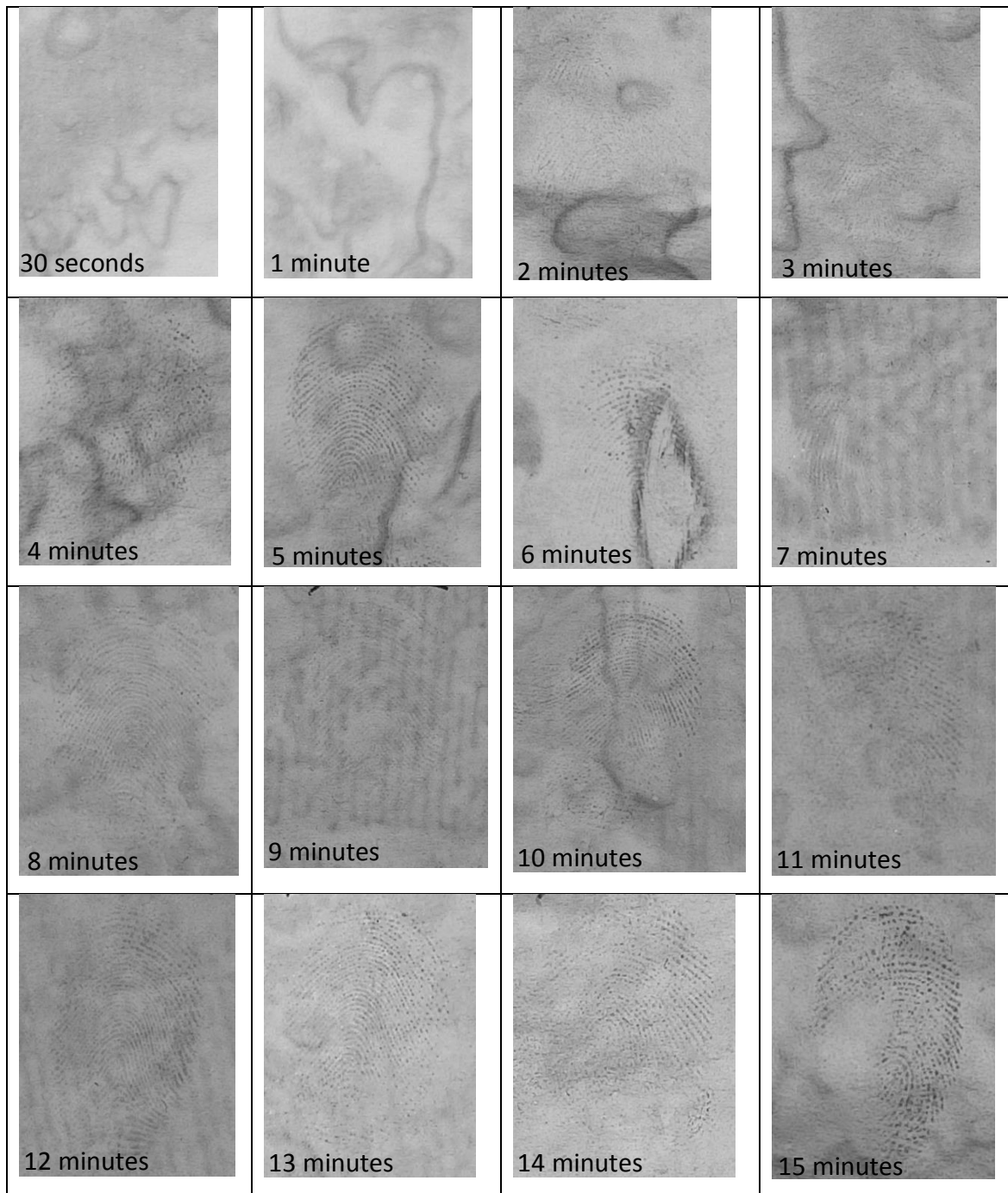


Figure 4.19 – The growth development of silver from 30 seconds to 15 minutes for fingerprints deposited on white copy paper and aged for 1 day under ambient conditions then developed via PDF1S

Figure 4.19 shows the images of the developed fingerprints which were aged for 1 day under ambient conditions. To the naked eye, some development is visible after 2 minutes and the developed image resembles a recognisable fingerprint after ca. 5 minutes. Simplistically, the developed fingerprints become clearer as time increases (with some anomalies due to the use of a new fingerprint for each time interval). If the microscopy images of these developed marks are then considered, this simplistic trend becomes much clearer. Figure 4.20 shows the corresponding microscopy image for the developed fingerprints in figure 4.19.

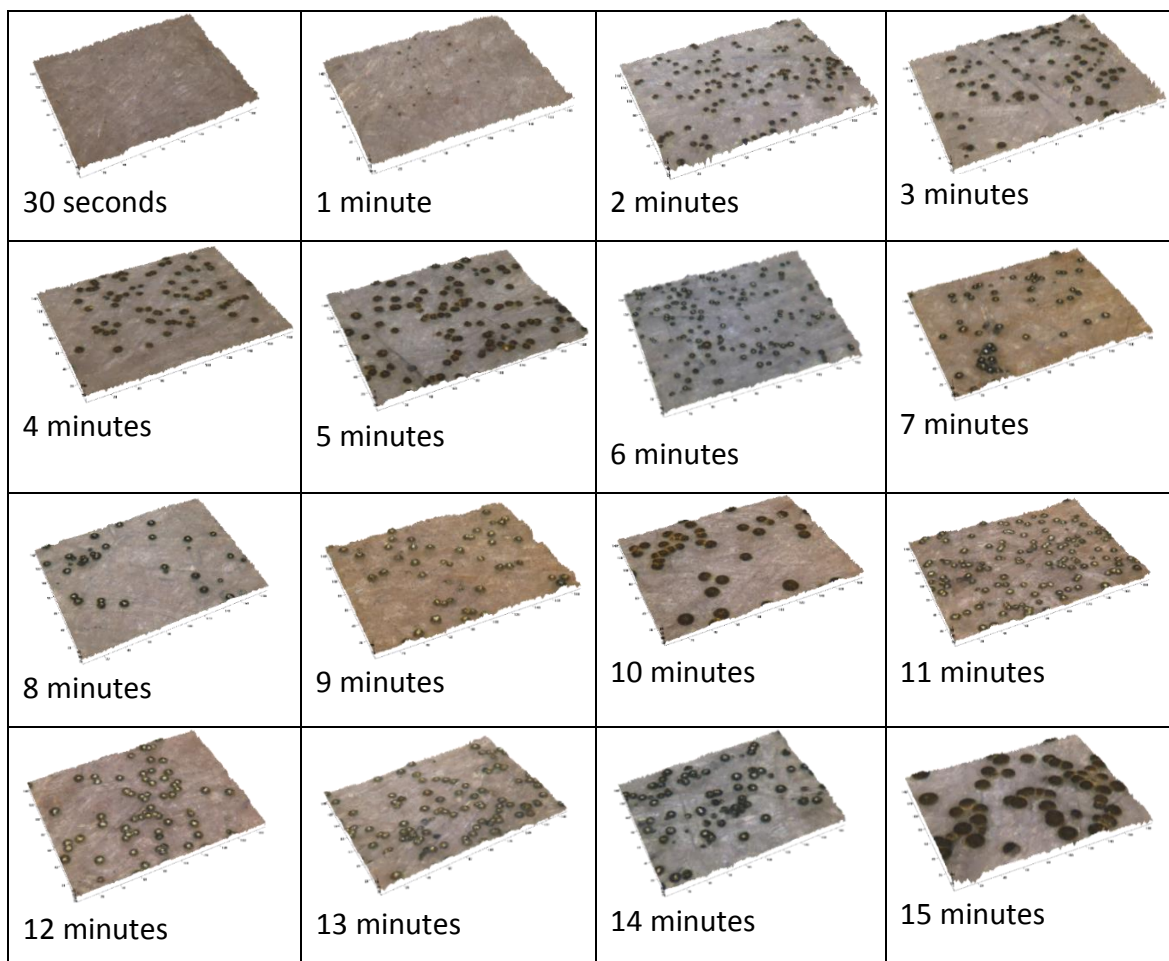


Figure 4.20 – 3D microscopy images (50x) for the growth development of 1 day old marks processed for 30 seconds to 15 minutes for the samples in figure 4.19. Tick marks every 20 μm

Figure 4.20 shows the corresponding microscopy image from each fingerprint in figure 4.19. These images are viewing a fingerprint ridge within an area of 140 μm^2 .

At 30 seconds, comparable to the developed image, there is no recognisable fingerprint ridge detail present. However some silver dots were analysed and recorded at an average diameter of 2 μm . This is roughly double the size of the silver particles in the solution (880 nm) indicating that the initial silver deposition onto the surface is relatively quick but more importantly, the high selectivity of the PD process is emphasised. In addition to this, the inherent low stability of the PD working solution is supported as silver deposition occurs within 30 seconds. After 2 minutes, microscopy reveals an increase in the density of the silver particles and an average diameter of 5 μm . This suggests the silver nucleation occurs at around 2 minutes and progressive growth is then observed throughout the remaining development period. Figure 4.21 shows the growth observed for three replicates of 1 day old sets.

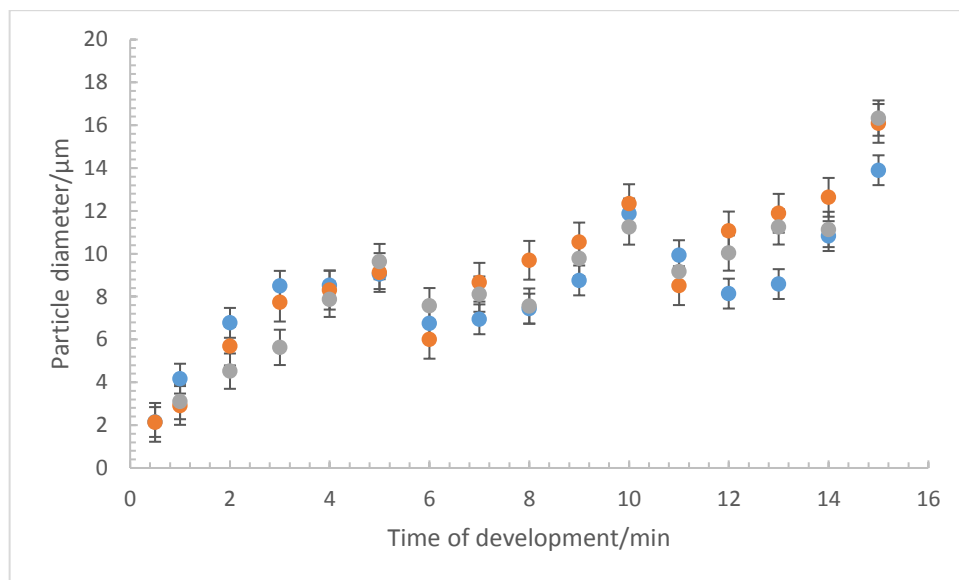


Figure 4.21 - Graph of silver particle diameter vs time of development for 3 sets of 1 day old marks aged under ambient conditions developed via PDF1S. Data from figure 4.19 and two replicates

To record the average particle diameter, the silver deposits in a microscope image of 140 μm^2 were measured. This process was repeated for all graphical representations on particle diameter vs time of development. Across the three sets studied, the general trend is the same and the particle diameter ranges do not differ significantly between the sets. The deviations observed at 6 and 10 minutes are due to

the limitation of using a separate fingerprint for each time period rather than using the same fingerprint and analysing it after each period of development.

After two minutes, there is an increase in the density as well as the diameter of the silver deposits and between 5-10 minutes the diameter increases slowly until the graph plateaus. The particle diameter after 15 minutes was $16\ \mu\text{m}$ but after 12 minutes at $11\ \mu\text{m}$, the fingerprint developed to an identifiable quality. As figure 4.19 shows, there is no difference in the quality of ridge detail between 12-15 minutes, other than contrast between the fingerprint and the background begins to reduce after 15 minutes. The microscopy analysis also reveals that the size of the silver deposits will only increase but further deposition will not occur. Therefore, it could be recommended that for a practitioner, development should be monitored as it may not be necessary to develop a mark for the full 15 minutes. This is further emphasised in figure 4.22 which shows the number of particles within the $140\ \mu\text{m}^2$ area, recorded for each time interval.

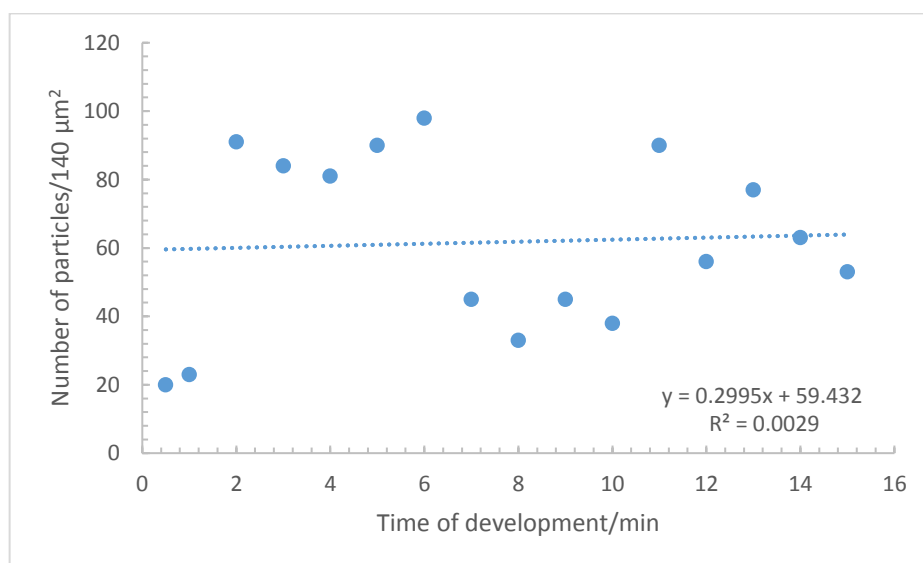


Figure 4.22 - Graph of the number of particles within $140\ \mu\text{m}^2$ area vs. time of development for 1 day old marks analysed in figure 4.19

The graph in figure 4.22 gives an average number of particles at 59 ± 13 . The initial points at 30 seconds and 1 minute are harder to view as they are smaller, therefore the values could be underestimated. In conjunction with the microscopic

analysis, it is evident the spherical silver deposits increase in size and not amount. At the point of nucleation, it appears that the deposition is then progressive as the silver in solution now has a preferential site of deposition i.e. the initial deposited silver on the surface.

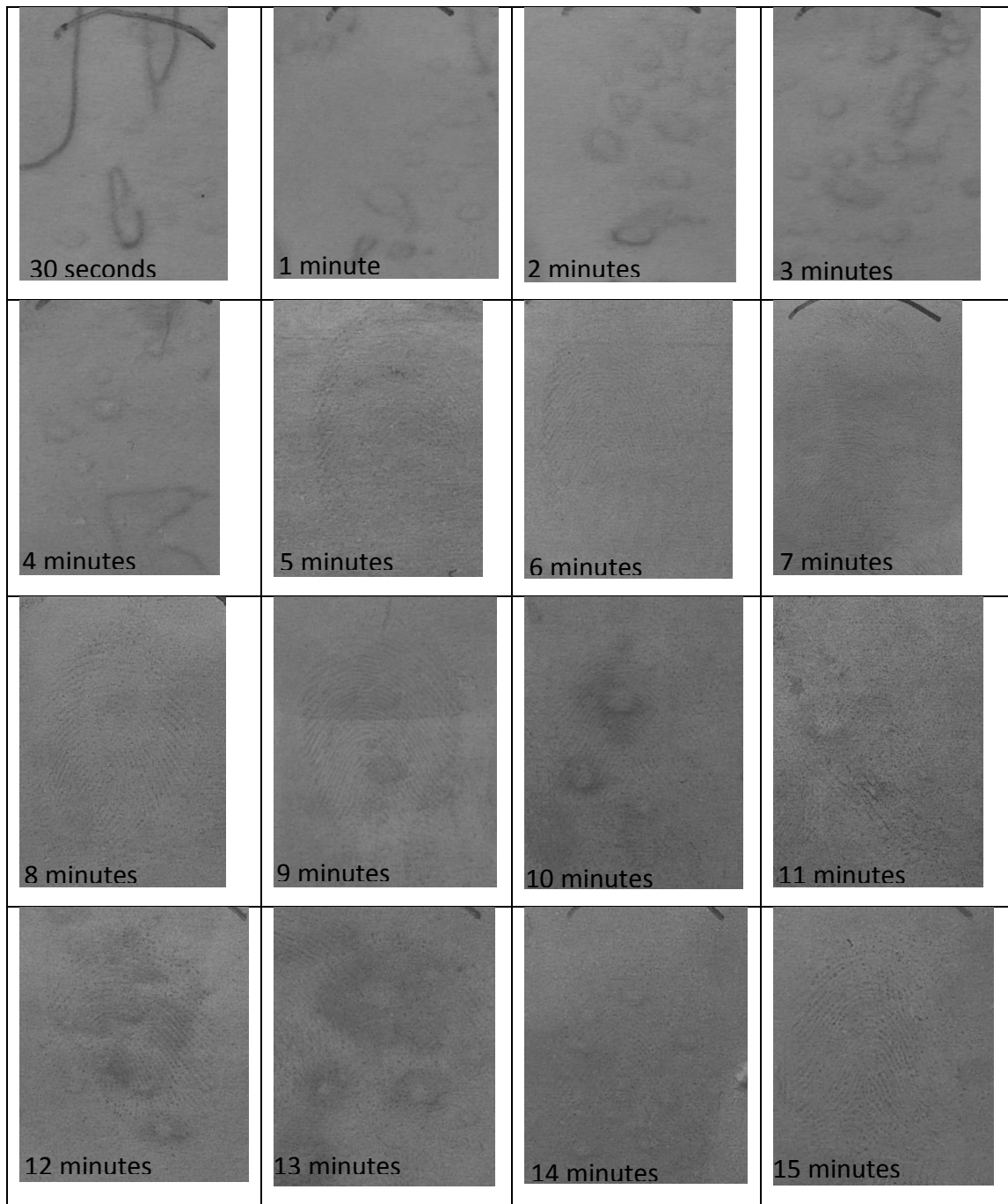


Figure 4.23 - The growth development of silver from 30 seconds to 15 minutes for fingerprints deposited on white copy paper and aged for 14 days under ambient conditions then developed via PDF1S

The growth of development was measured for aged fingerprints, to observe any variations in the trend of the growth of the deposited silver particles. Figure 4.23 shows the developed fingerprints at each time interval for 14 day old marks. The first observation, which differs to the 1 day old growth, is the higher level of background staining. The background staining reduces the contrast between the developed fingerprint and the paper surface and it is not until 5 minutes that fingerprint ridges become clear to the naked eye. After 5 minutes, there is increased silver deposition at each increasing minute. However, the dark background makes this difficult to see. Background staining is a common issue with the use of PD which is normally minimised by the maleic acid pre-wash but this result supports the discouraged use of PD in police and forensic laboratories. In comparison to the full view of a developed fingerprint, the microscopic view reveals the silver growth more clearly.

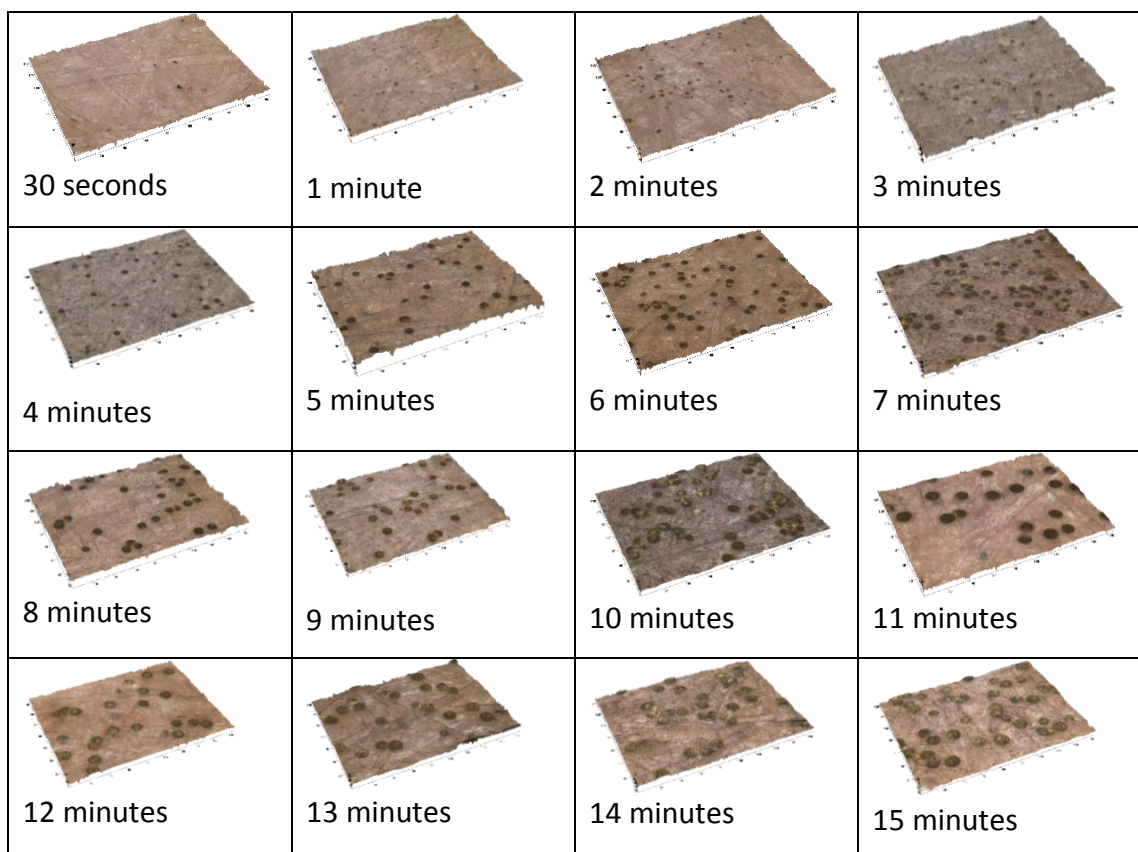


Figure 4.24 – 3D microscopy images (50x) for the growth development of 14 day old marks processed for 30 seconds to 15 minutes for the samples in figure 4.23. Tick marks every 20 μm

Figure 4.24 shows the respective microscopy image for each developed mark in figure 4.23 at each time interval. Similarly to the 1 day old growth results, the microscopy analysis reveals increased silver deposition at ca. 2 minutes (4 μm) suggesting nucleation and the diameter increases progressively till 15 minutes (15 μm). These diameters are similar to the 1 day old marks at 2 and 15 minutes respectively, suggesting that the age of the mark does not affect the resulting size of the silver deposits. Figure 4.25 shows the growth observed for the silver deposits for 3 sets of 14 day old marks.

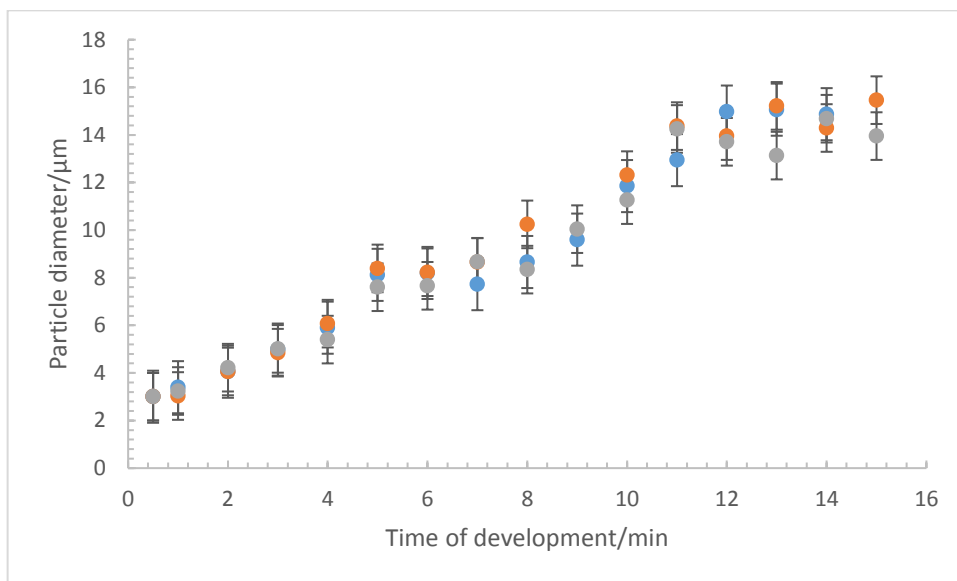


Figure 4.25 - Graph of silver particle diameter vs time of development for 3 sets of 14 day old marks aged under ambient conditions developed via PDF1S. Data from figure 4.23 and two replicates

For all three sets investigated, the diameter range is very narrow and the same general trend is observed. From 30 seconds to 4 minutes, the growth is steady and increased sharply at 5 minutes which correlates to the visibility of fingerprint ridges at 5 minutes in figure 4.23. As with the 1 day old marks, the growth is progressive and plateaus from 12-15 minutes. Figure 4.26 shows the density plot for the 14 day old marks analysed in figure 4.23.

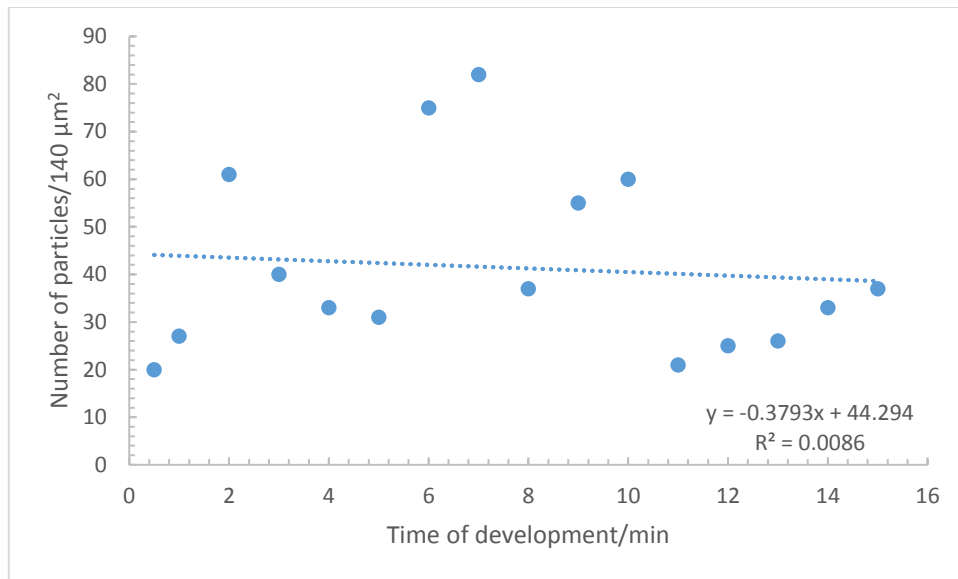


Figure 4.26 - Graph of the number of particles within 140 μm² area vs. time of development for 14 day old marks analysed in figure 4.23

An average number of particles of 44 ± 10 was recorded. Though there are extremes in the plot in figure 4.26, it is evident to see that the size of the silver deposits are increasing as opposed to the amount, similarly to the 1 day old set. The extreme values at shorter times could be due to the smaller diameter of the silver deposits which are harder to see and therefore count. At the longer times, the extremes could be due to aggregation of the silver deposits such that fewer particles are then counted separately. As previously mentioned, a separate fingerprint was developed for each period of time which limits the ability to truly see the changes of one fingerprint with time, hence the extremes in figures 4.22, 4.26 and 4.30.

The growth was investigated for 28 day old marks to complete the ageing process but also to determine any variations compared to the fresher marks as PD is said to be more effective for aged marks. Figure 4.27 shows the developed fingerprints at each time interval for 28 day old marks.

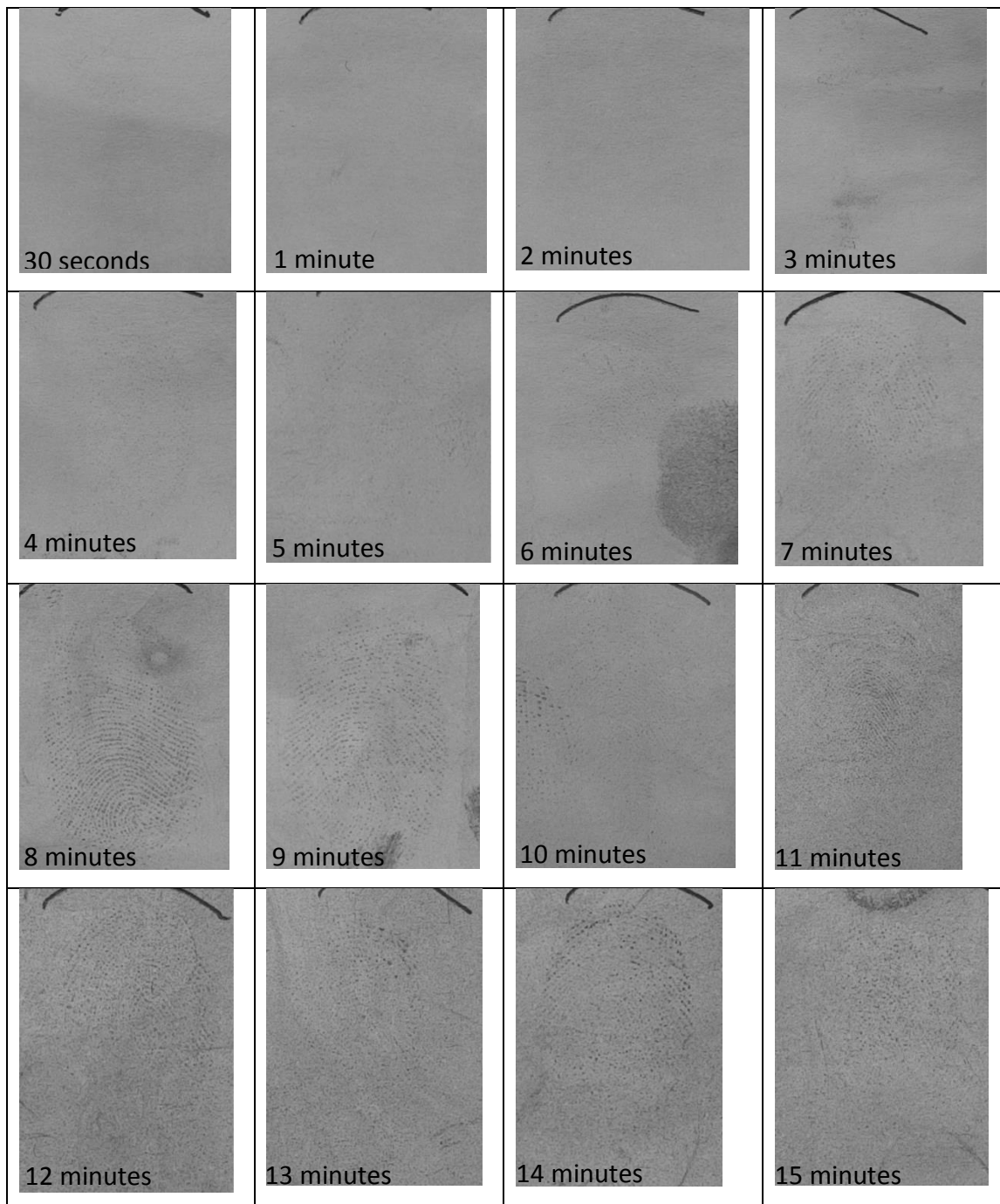


Figure 4.27 - The growth development of silver from 30 seconds to 15 minutes for fingerprints deposited on white copy paper and aged for 28 days under ambient conditions then developed via PDF1S

Similarly to the 14 day old marks, no visible fingerprint ridge detail is observed until ca. 4 minutes. The background staining is minimal compared to the 14 day old set

which shows lower clarity of the fingerprint detail. This result shows a fully developed fingerprint after 8 minutes indicating the importance of monitoring the PD development. Figure 4.28 shows the corresponding microscopy images of the developed marks in figure 4.27 at each time interval.

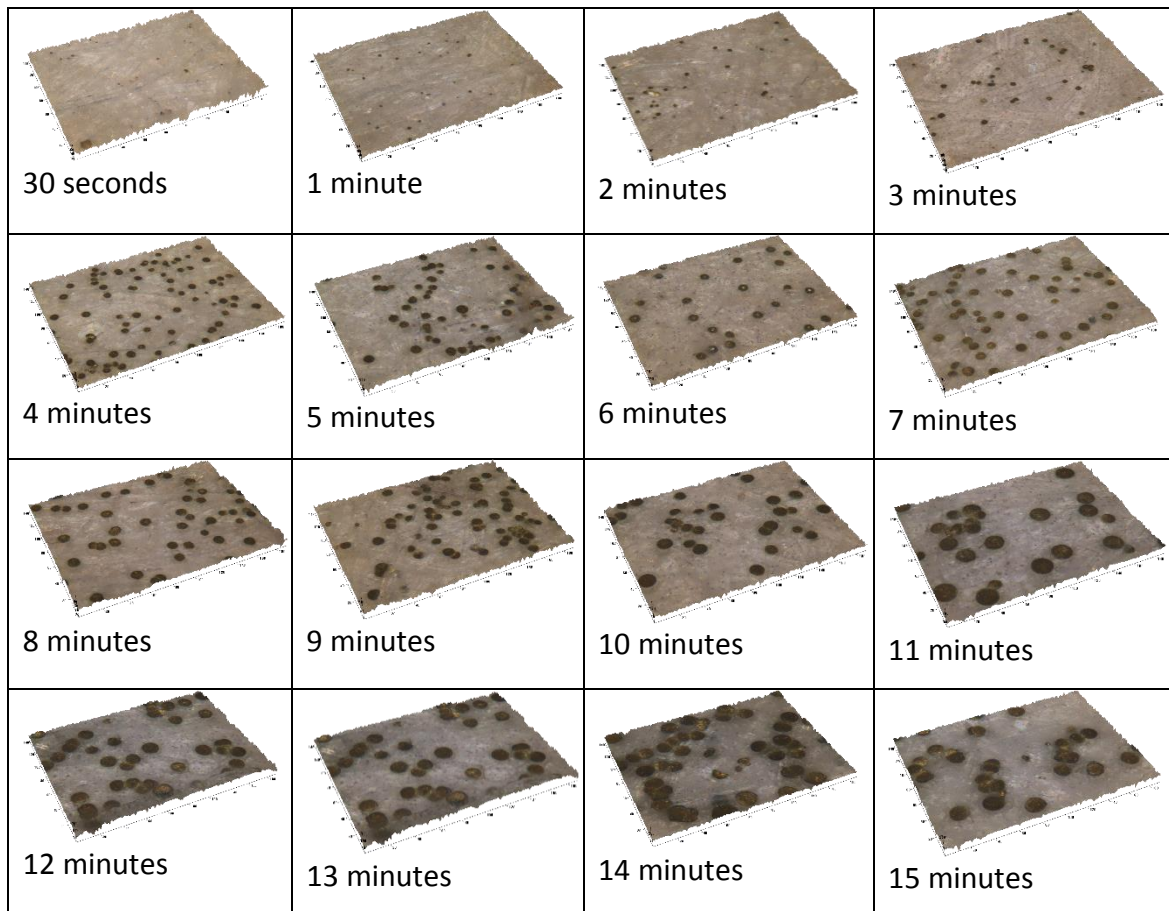


Figure 4.28 – 3D microscopy images (50x) for the growth development of 28 day old marks processed for 30 seconds to 15 minutes in figure 4.27. Tick marks every 20 μ m

Out of all the three ages tested, the 28 day old microscopy analysis depicts the general trend in the growth of the silver most effectively. It is evident that the silver deposits increase in their diameter and the monodispersed nature does not change throughout the 15 minute development time. The average particle diameter recorded at 2 minutes was 4 μ m and increased to 16 μ m after 15 minutes. This result further emphasises not only the high sensitivity of PD to recognise the fingerprint residue but also the preferential site of deposited silver for subsequent silver deposition as time progresses. Figure 4.29 shows this observation graphically.

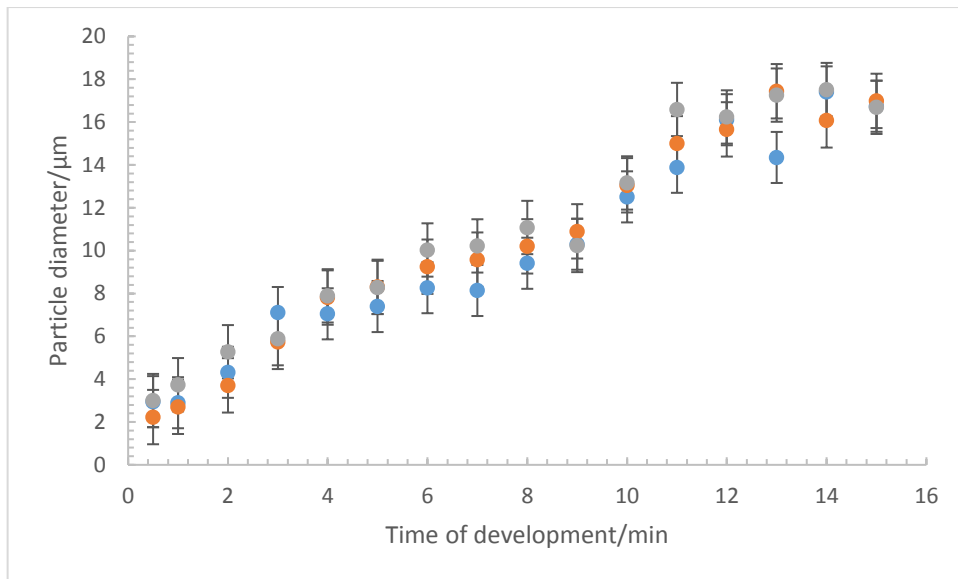


Figure 4.29 - Graph of silver particle diameter vs time of development for 3 sets of 28 day old marks aged under ambient conditions developed via PDF1S. Data from samples in figure 4.27 and two replicates

This general trend is almost identical to the 14 day old results in figure 4.25 indicating that the age of the mark does not affect the rate at which silver is deposited from the solution and the subsequent growth on the surface. This proves that the silver particles are stabilised in the solution by the surfactant components but the introduction of a sample initiates their spatially selective deposition.

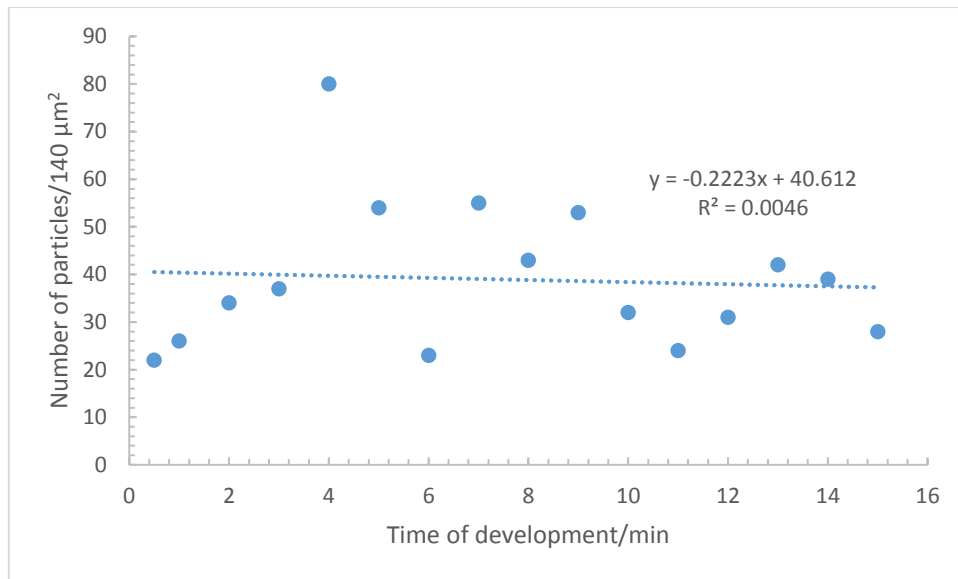


Figure 4.30 - Graph of the number of particles within 140 μm² area vs. time of development for 28 day old marks analysed in figure 4.27

Figure 4.30 represents the number of particles observed for each microscopy image at each time interval for the 28 day old marks. An average number of particles of 41 ± 8 was recorded. This is very similar to the results for the 1 day old marks (59 ± 13) and 14 day old marks (44 ± 10) highlighting the similar behaviour regardless of the age of the mark.

4.2.3.2.1 Interrupted Growth – Split Prints

The growth study in section 4.2.3.2 does indicate that the initial deposition of silver is relatively fast and progressive growth is observed throughout the development time. Figure 4.31 shows the results of 1, 14 and 28 day old developed split prints.

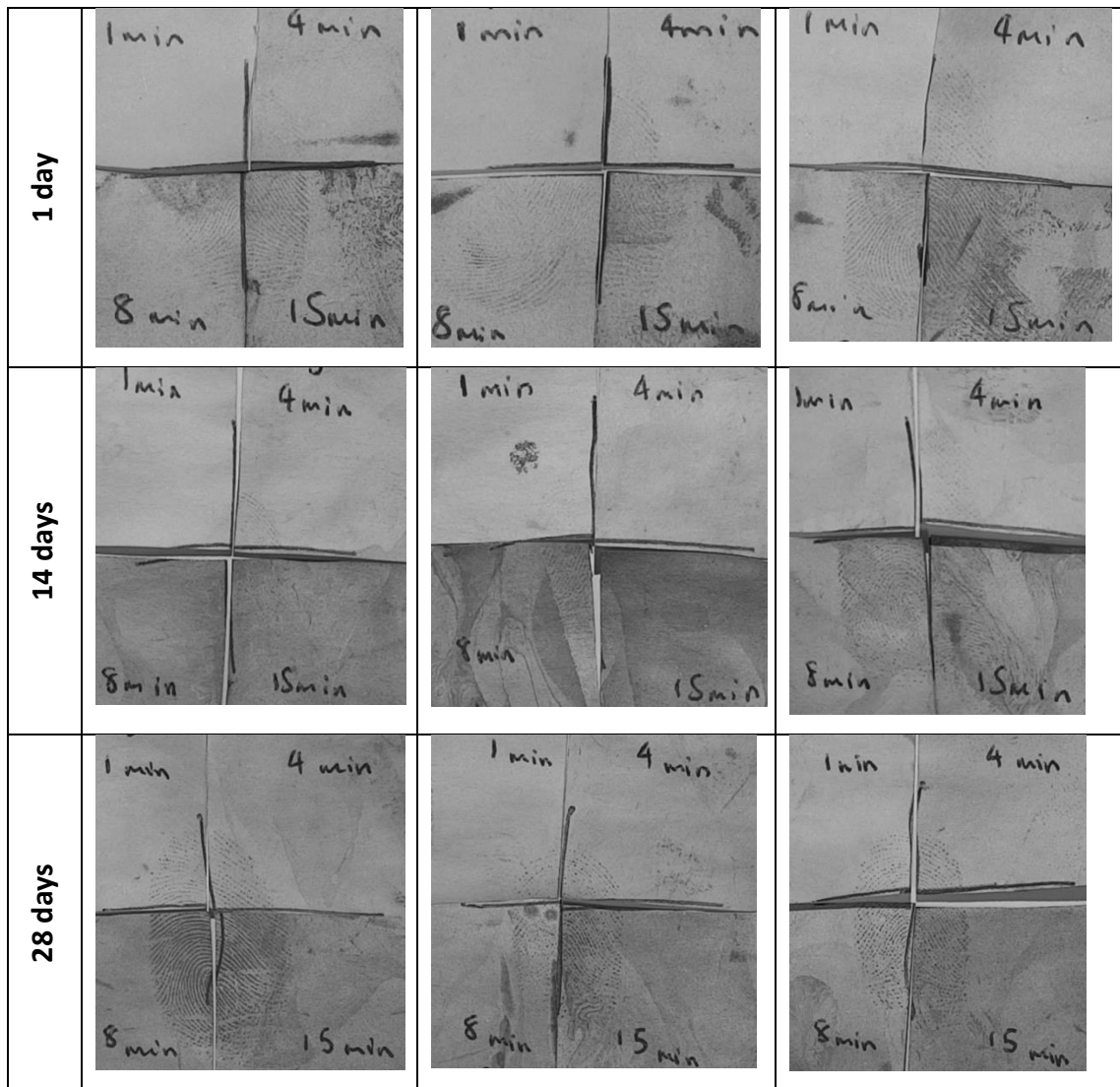


Figure 4.31 - Split prints deposited on white copy paper and aged for 1, 14 and 28 days under ambient conditions then developed via PDF1S (3 replicates for each age of mark)

The limitation to this study was having to use separate fingerprints for each stage of the development even though they were deposited by the same donor. To alleviate this limitation, split prints were studied at 1, 4, 8 and 15 minute development times as these showed the most changes in the initial growth study.

From figure 4.31, it can be seen more clearly in these results that as time progresses, the development via PD increases. At each length of time, the fingerprint is effectively 'filled in' to reveal the fingerprint ridge details. In addition to this, the effect of ageing is prevalent such that at 28 days, higher quality fingerprints are developed compared to 1 and 14 day old marks. The 14 day old marks vary in quality of

development as was observed with the 14 day old full prints in section 4.2.3.2. This could be due to the donor characteristics or simply due to the PD method itself as the microscopy results reveal that silver deposits are still growing. Therefore, the apparent lack of fingerprint detail could be a result of poor contrast.

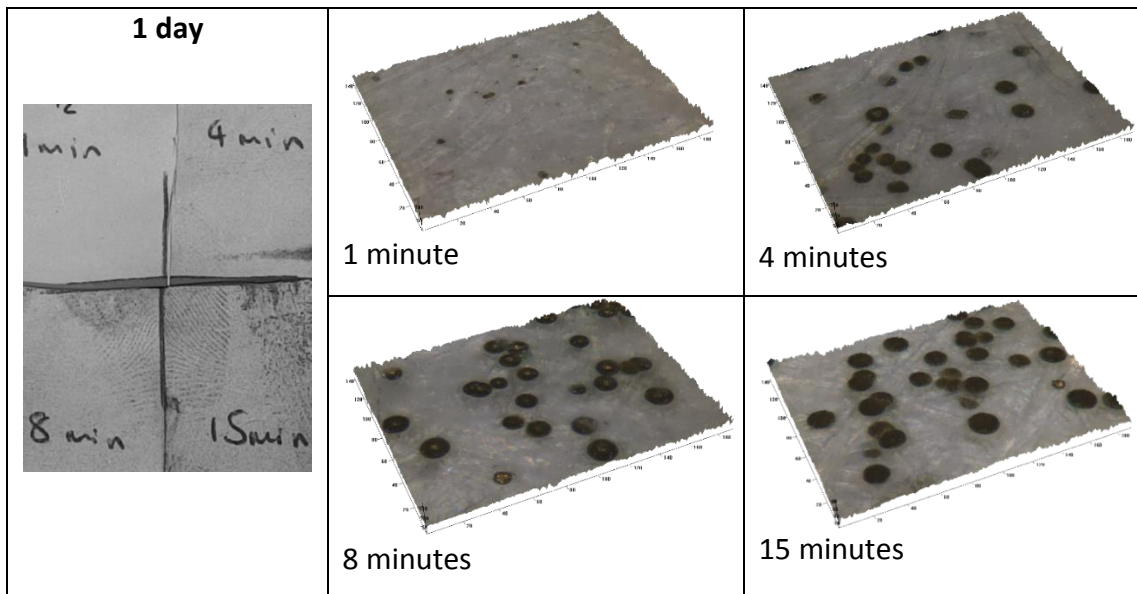


Figure 4.32 – 3D microscopy images (50x) for a sample of the growth development of a 1 day old mark processed for 1-15 minutes in figure 4.31. Tick marks every 20 μm

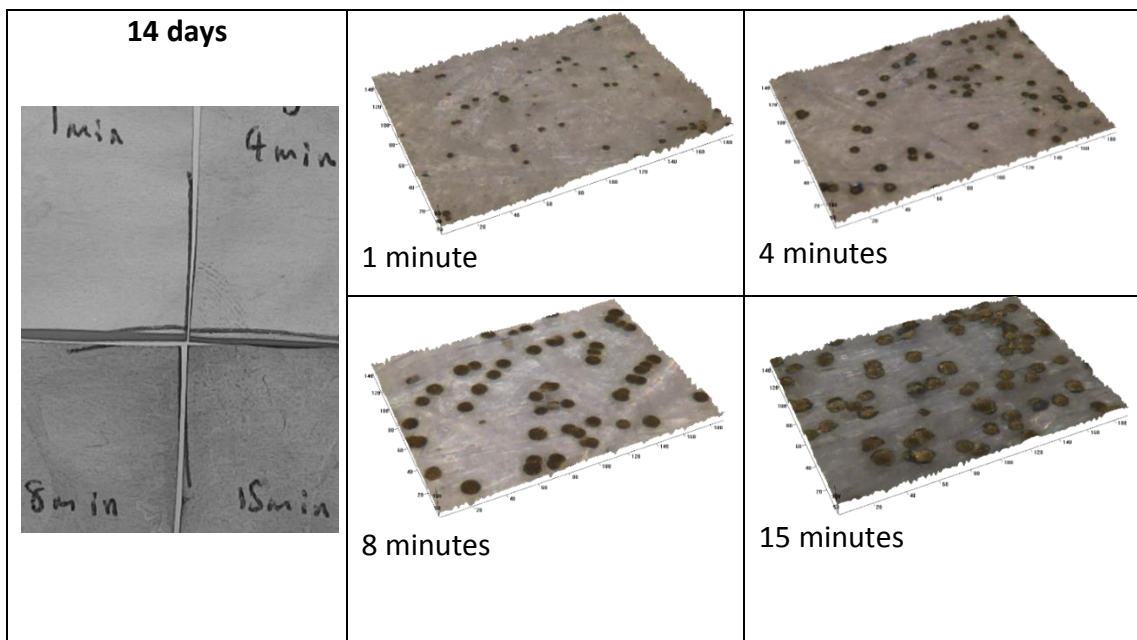


Figure 4.33 – 3D microscopy images (50x) for a sample of the growth development of a 14 day old mark processed for 1-15 minutes. Tick marks every 20 μm

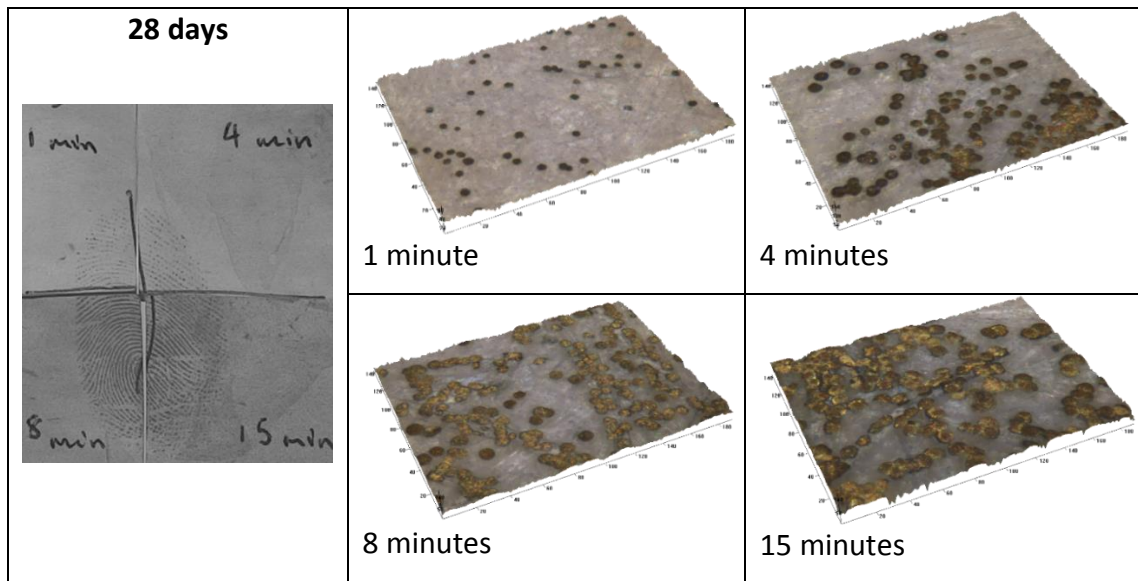


Figure 4.34 – 3D microscopy images (50x) for a sample of the growth development of a 28 day old mark processed for 1-15 minutes. Tick marks every 20 μm

Figure 4.32-4.34 shows the respective microscopy images for the split print samples analysed for each time of ageing. The progressive growth of the silver deposits is evident in the microscopy images. In contrast to the full print growth sets explored in section 4.2.3.2, there is evidence of more silver deposits, particularly after 1 minute. This could be due to the smaller area of the fingerprint initially available to the silver particles in solution for subsequent deposition. Each quadrant of the split fingerprint effectively has a higher concentration of fingerprint residue available over a smaller area resulting in more silver deposition in the same amount of time. This can be further concluded from the graph in figure 4.35 showing the particle diameter at each time interval for each age tested.

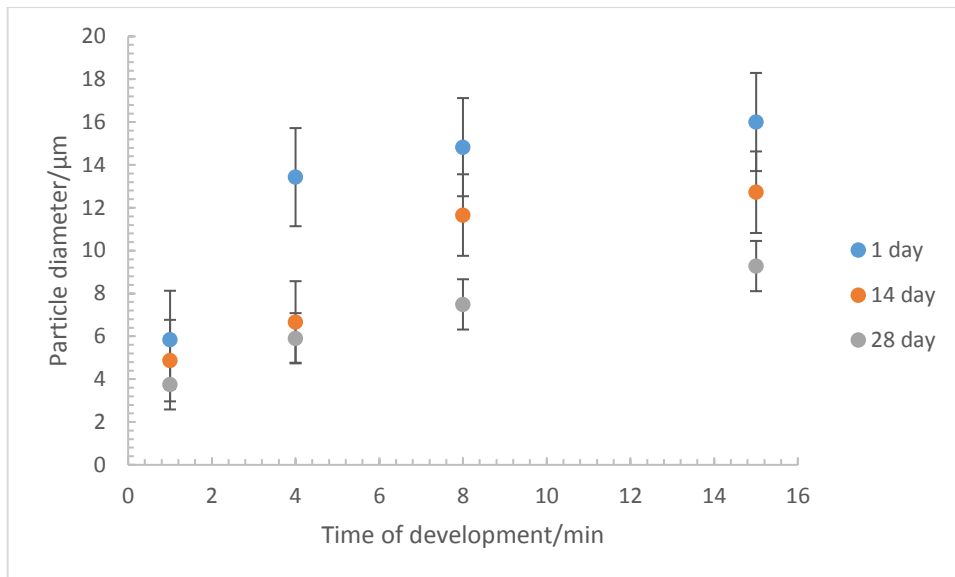


Figure 4.35 - Graph of silver particle diameter vs time of development for average of 5 sets of 1, 14 and 28 day old marks aged under ambient conditions developed via PDF1S

In comparison to the full prints, the split prints for all ages have resulted in deposited silver particles after 1 minute development of larger size. A range of 2-3 μm was observed for 1, 14 and 28 days full prints at 1 minute, whereas the split prints showed a range of 4- 6 μm after the same development time. As figure 4.35 shows, the general trend is similar to what was observed throughout section 4.2.3.2 but the increase in growth is sharper at the consecutive time intervals, particularly for the 1 day old marks. This is reflective of the smaller area initially available for silver deposition, therefore the silver deposits grow through further deposition as opposed to depositing on another area of the fingerprint residue. This can be seen clearly in the microscopy image for the 15 minute split fingerprint in figure 4.34. The monodispersed nature of the silver deposits is less evident and the silver deposits are aggregating. This can affect the clarity of the developed ridge detail as some ridges can merge together, emphasising the need to monitor the development process.

4.2.3.3 Continuous Growth

Throughout section 4.2.3, the fundamental chemistry of the silver particles from the solution to the surface was explored statically. In order to understand the dynamics of the growth further, the PD process was analysed in real-time using a

microscope (see chapter 3, section 3.4.2.2). Figure 4.36 represents some stills taken from the live video.

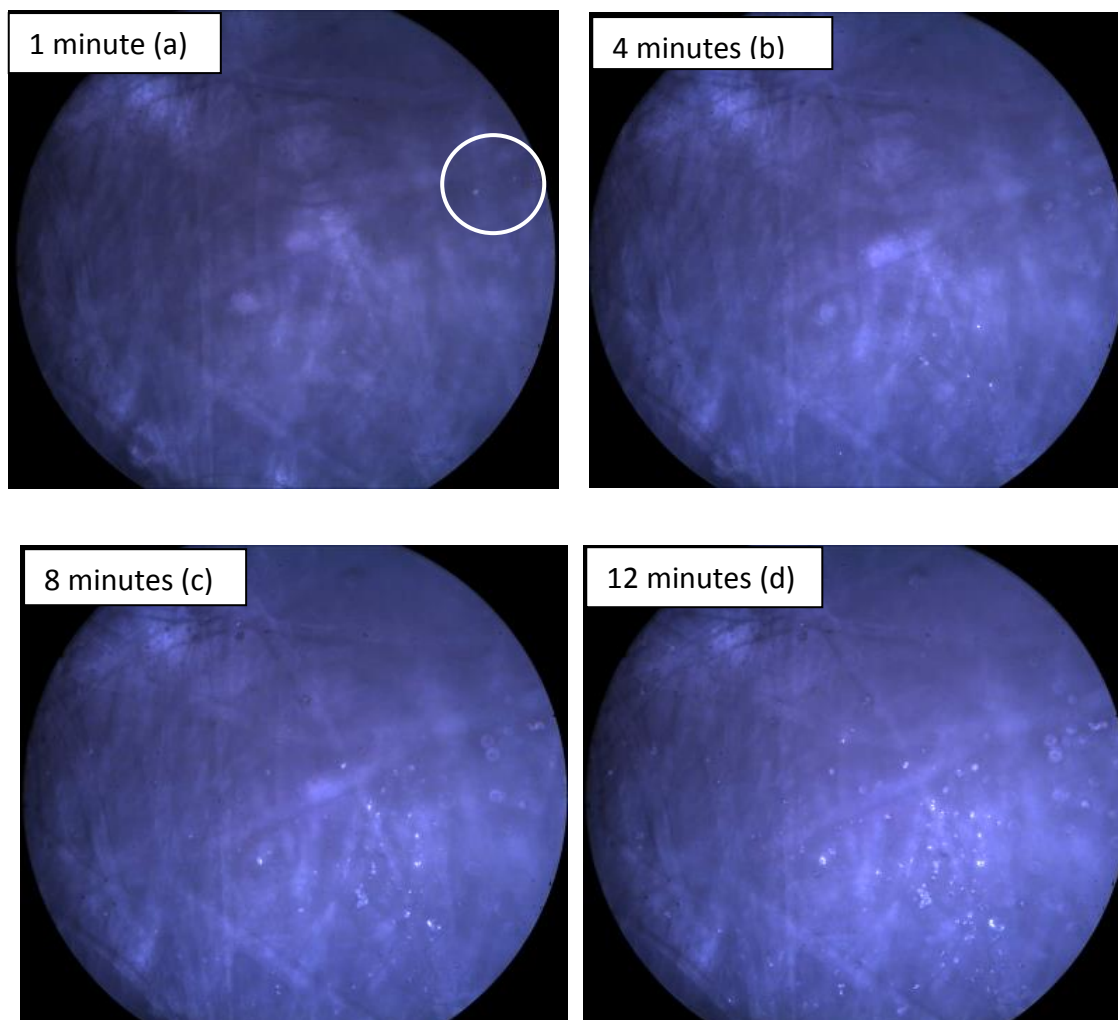


Figure 4.36 - Still images taken from the live video of the PD development process

After 1 minute (figure 4.36 a), bright particles can be seen moving through the solution and depositing on an area of the substrate. 2-3 minutes later (figure 4.36 b), there are brighter areas of silver growth showing monodispersed particles uniform in size. As time progresses, over each consecutive minute, the original areas where silver initially deposited can be seen more clearly and the brightness increases as well as the diameter (figure 4.36 c). After 12 minutes (figure 4.36 d), the resulting image reflects the static microscopy images observed in section 4.2.3.

This results further indicates the high spatial selectivity of the PD process from the visible attraction of a silver particle to the substrate. As more of those silver sites become available after the initial deposition, progressive growth follows.

4.2.4 Compositional Analysis of the Developed Fingerprints

It is a fair assumption that the deposited particles will contain silver metal but interestingly, the compositional analysis of the developed fingerprints has not been reported. Scanning electron microscope images have been published revealing the strand-like nature of the deposited silver where particle sizes of 5 μm have been reported.^{12, 14} This is considerably smaller than the particle sizes observed microscopically in sections 4.2.3.1 and 4.2.3.2. Figure 4.37 shows the compositional analysis observed for a 1 day old fingerprint aged under ambient conditions and developed over 15 minutes with PD.

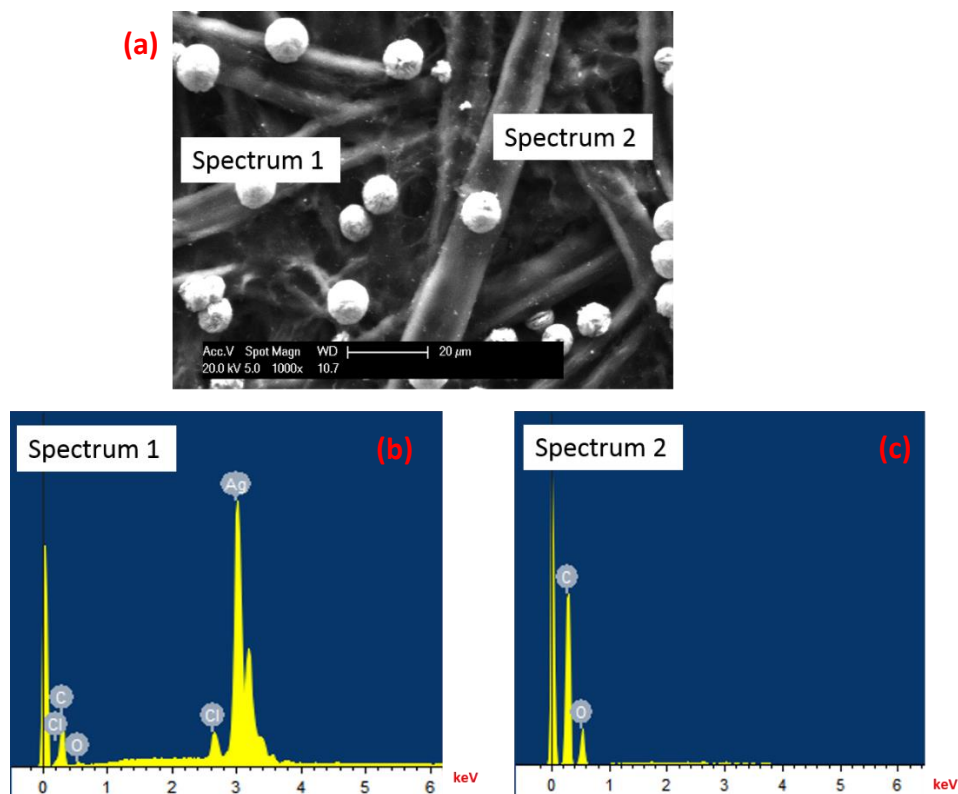


Figure 4.37 – (a) SEM image of a 1 day old fingerprint on white copy paper (figure 4.16b) aged under ambient conditions developed via PDF1S with (b) and (c) the corresponding EDX analyses in the indicated area

As expected, there is a large peak in spectrum 1 representing the presence of silver, which does not appear in spectrum 2 of the background paper. This result is not surprising. Interestingly, there is no indication of the presence of iron in either of the spectra. $\text{Fe}^{2+}/\text{Fe}^{3+}$ are paramount in the working solution to reduce the silver ions to silver particles. The compositional analysis suggests the role of the iron components is maintained within the solution and not in the deposition of silver. The iron ions are charged in the working solution so this could explain why no iron is observed in the developed fingerprint. In all of the compositional analysis conducted, an iron peak was not observed.

In spectrum 1, there are two small peaks representative of chlorine. Early theories suggested that chloride ions in the salt components of the fingerprint residue act a trigger materials, initiating silver deposition.¹⁴ This theory was later disproved from salt spot tests which PD did not react with, concluding that sodium chloride was not required for successful PD development.²⁵ However, it should be noted that these spot tests were investigated using nylon membranes as opposed to a porous paper surface. In addition, spectrum 1 resulted in a weight percentage for chlorine at only 1%. Chlorine peaks were not observed in all compositional analysis completed and only ranged from 1-3% if a peak was present. It is difficult to definitively conclude where these chloride ions originate from given that there are no chloride ions in the working solution. It is possible that chloride ions present in the eccrine residue have become trapped by the sebaceous content, hence the silver deposits in these areas.

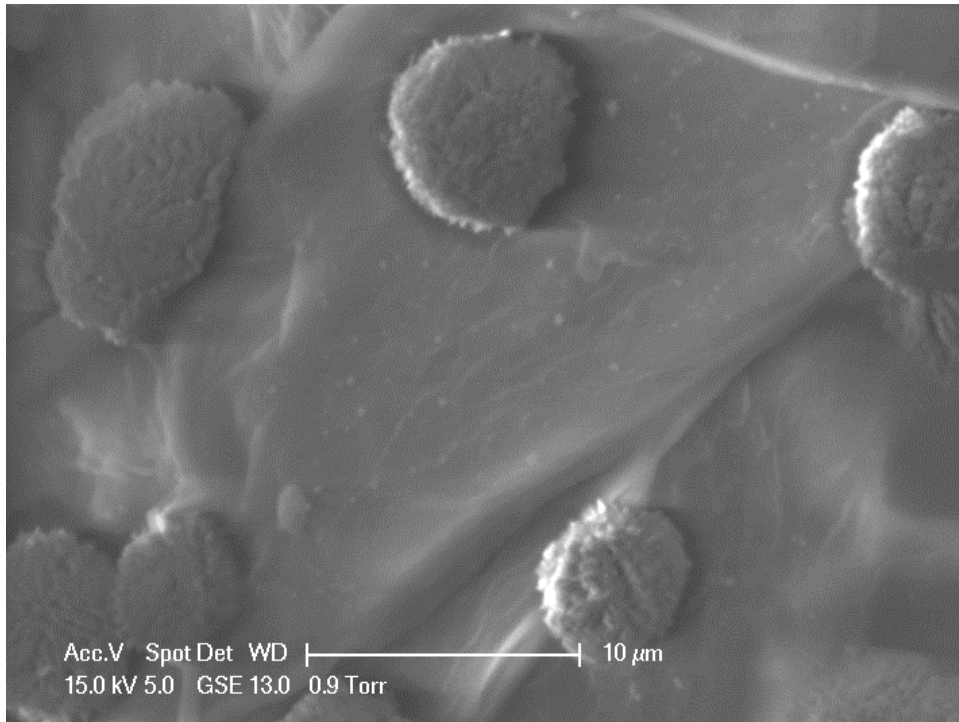


Figure 4.38 - SEM image of deposited silver particles on a 1 day old fingerprint (figure 4.16e) aged under wetted conditions developed with PDF1S

Figure 4.38 depicts the morphology of the deposited silver particles. The strand-like nature of the silver deposits is evident in figure 4.38 which further supports the conclusions thus far, that the deposited silver grows in diameter on the surface of the substrate. Figure 4.39 shows the corresponding SEM images of the developed fingerprints in figure 4.19 at 1, 5 and 15 minutes.

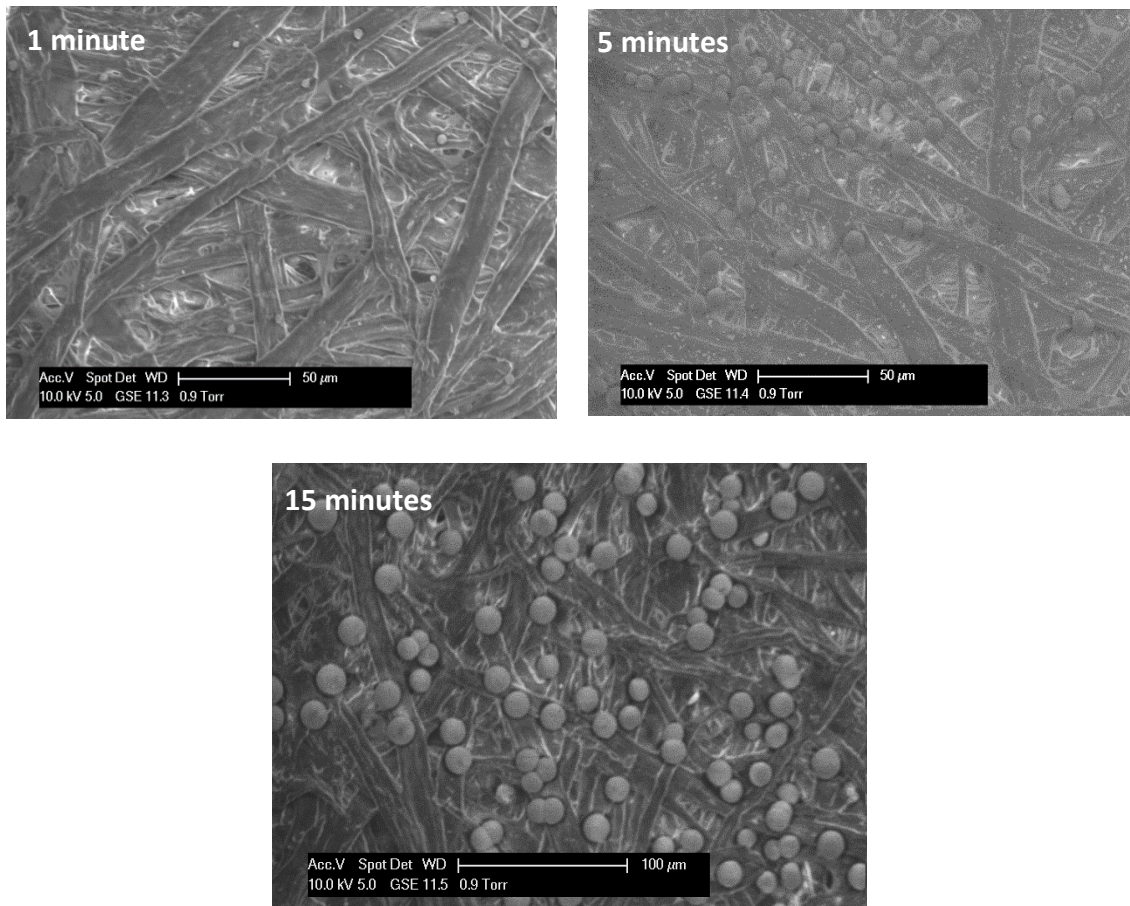


Figure 4.39 - SEM images of developed fingerprints at 1, 5 and 15 minutes for 1 day old fingerprints aged under ambient conditions developed with PDF1S

In conjunction with the microscopy analysis observed in figure 4.20, the SEM images show the growth of the silver particles at the surface. After 1 minute silver deposition is evident. In addition to this, the uniformity of the silver deposits is clearly observed in these SEM images. There is some aggregation, seen after 15 minutes, but the spherical nature of the silver particles is still maintained.

4.3 Conclusions

The exact mechanism of the PD process is complicated and unclear but it is fair to conclude that it is not only sebaceous content that PD targets, contrary to current theories. Eccrine material has to be present for PD to work effectively to give the optimum developed fingerprints possible. The ageing of fingerprint residue has an

effect on the resulting PD process such that aged marks (up to 1 month) result in high contrast and high quality developed fingerprints. The theories suggesting PD targets water-insoluble components are justified as results have shown that sebaceous material alone produces strong development. However, individual spot testing of sebaceous material was not entirely positive and stronger developments were observed for emulsions.

The average size of the silver particles in solution was determined to be 880 nm and after 30 seconds of development, this value was effectively doubled for the silver deposits. The initial deposition of silver from the solution was relatively quick, emphasising the high spatial selectivity of PD as well as the inherent instability of the working solution. It was concluded that initial nucleation of silver occurs ca. 2 minutes on the surface and progressive growth is observed thereafter. Therefore, the silver is stabilised in the solution presumably by the surfactant components and then grow on the surface to a range of 10-20 μm . This conclusion of the mechanism is depicted in figure 4.40. Compositional analysis confirms the spatially selectively silver deposition but also indicates that the iron components are only involved in the redox chemistry of the working solution.

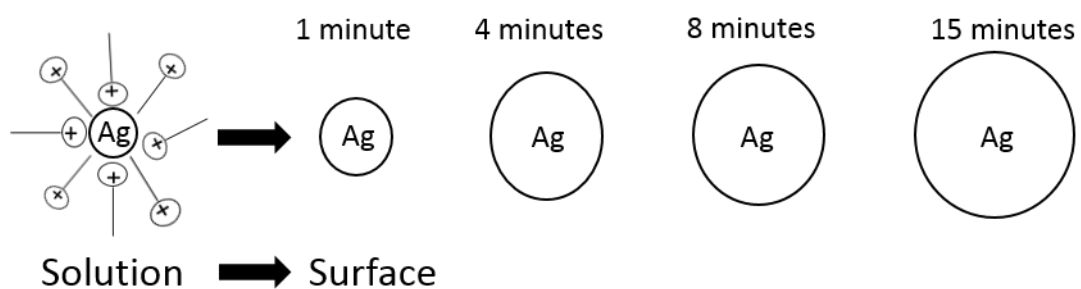


Figure 4.40 - Schematic of the size of the silver particles in solution with progressive growth of silver observed on the surface (not to scale)

4.4. References

1. G. S. Sodhi and J. Kaur, *Egyptian Journal of Forensic Sciences*, 2015, **6**, 44-47.

2. C. E. Phillips, D. O. Cole and G. W. Jones, *Journal of Forensic Identification*, 1990, **40**, 135-147.
3. M. de la Hunty, S. Moret, S. Chadwick, C. Lennard, X. Spindler and C. Roux, *Forensic Science International*, 2015, **257**, 481-487.
4. M. de la Hunty, S. Moret, S. Chadwick, C. Lennard, X. Spindler and C. Roux, *Forensic Science International*, 2015, **257**, 488-495.
5. S. A. Hardwick, *User Guide to Physical Developer - A reagent for detecting latent fingerprints*, Home Office Scientific Research and Development Branch, 1981.
6. R. Ramotowski, *Journal of Forensic Identification*, 1996, **46**, 673-677.
7. R. Ramotowski, *Lee and Gaensslen's Advances in Fingerprint Technology, Third Edition*, CRC Press Inc, GB, 2013.
8. J. D. Wilson, A. A. Cantu, G. Antonopoulos and M. J. Surrency, *Journal of Forensic Sciences*, 2007, **52**, 320-329.
9. D. Burow, *Journal of Forensic Identification*, 2003, **53**, 304-314.
10. D. Burow, D. Seifert and A. A. Cantu, *Journal of Forensic Sciences*, 2003, **48**, 1-7.
11. R. Ramotowski and A. A. Cantu, *Fingerprint Whorld*, 2001, **27**, 59-65.
12. CAST, *Home Office Centre of Applied Science and Technology Fingerprint Visualisation Manual* 1st edn., 2014.
13. R. K. Simmons, P. Deacon and K. J. Farrugia, *Journal of Forensic Identification*, 2014, **64**, 157-173.
14. A. A. Cantu, *Forensic Science Review*, 2001, **13**, 29-64.
15. M. De Puit, M. Bouwemeester, L. Koomen, J. van Wouw, M. de Gijt and C. Rodriguez, *Journal of Forensic Identification*, 2011, **61**, 166-170.
16. A. Girod, R. Ramotowski and C. Weyermann, *Forensic Science International*, 2012, **223**, 10-24.
17. A. Girod, L. Xiao, B. Reedy, C. Roux and C. Weyermann, *Forensic Science International*, 2015, **254**, 185-196.
18. L. Schwarz, *Journal of Forensic Sciences*, 2009, **54**, 1323-1326.

19. R. S. Croxton, M. G. Baron, D. Butler, T. Kent and V. G. Sears, *Forensic Science International*, 2010, **199**, 93-102.
20. M. Picardo, M. Ottaviani, E. Camera and A. Mastrofrancesco, *Dermato-Endocrinology*, 2009, **1**, 68-71.
21. H. Mark and C. R. Harding, *Int J Cosmet Sci*, 2013, **35**, 163-168.
22. S. Hong, I. Hong, A. Han, J. Y. Seo and J. Namgung, *Forensic Science International*, 2015, **257**, 403-408.
23. B. Yamashita and M. French, *The Fingerprint SourceBook - Chapter 7 Latent Print Development*, National Institute of Justice (NCJRS), 2010.
24. V. G. Sears, S. M. Bleay, H. L. Bandey and V. J. Bowman, *Science & Justice*, 2012, **52**, 145-160.
25. A. A. Cantu, *Notes on some latent fingerprint visualization techniques developed by Dr. George Saunders* U.S. Secret Service, Washington DC, 1996.

Chapter 5: Evaluation of Tween 20 Using Microscopy and Neutron Reflectivity

5.1	Introduction	132
5.2	Results	132
	5.2.1 Role of the Non-Ionic Surfactant	132
	5.2.2 Growth and Dynamics of Silver for Fingerprint Visualisation	135
	5.2.3 Neutron Reflectivity Study of Surfactant Adsorption	151
5.3	Conclusions	168
5.4	References	169

5.1 Introduction

The current formulation of PD uses the non-ionic surfactant, Synperonic-N to stabilise the colloidal silver generated and the process.¹ However, this type of reagent, a nonyl phenol, has been banned due to environmental toxicity.² The work described in chapter 4 revealed the optimum characteristics required for effective fingerprint development using the current formulation. Therefore, a suitable alternative formulation needs to be designed which produces the same, if not better, quality of fingerprint development. Since the exact role of the non-ionic surfactant is not fully understood, this must first be addressed in order to formulate an optimised PD process.

Tween 20 is the non-ionic surfactant replacement for Synperonic-N that is being used for fingerprint development in several countries worldwide including Australia, USA and Germany. The formulation for the detergent systems differs across these countries but there is agreement that the fingerprint development quality is high and the working solution is more stable. The work in this chapter will first look at the use of Tween 20 in the working solution and the effect this has on the growth and dynamics of effective silver development. In addition to this, the effect of Tween 20 on the stability of the PD working solution will be explored.

The role of both the cationic and non-ionic surfactant will be studied through the use of neutron reflectivity. This will provide a topographical and compositional perspective of the two surfactants for the interaction with a planar silver surface.

5.2 Results

5.2.1 Role of the Non-Ionic Surfactant

It is widely accepted that the cationic surfactant, dodecylamine acetate (DDAA), forms a micellar structure around the colloidal silver particles in the PD working solution.^{1, 3-5} However, the possible structural role of the non-ionic surfactant has not been considered, other than to aid the dissolution of DDAA.

5.2.1.1 Fingerprint development using only DDAA

In order to observe any effect on the quality of fingerprint development and efficiency of the PD process without the non-ionic surfactant, DDAA was used as the only surfactant in the working solution. A variation of concentrations was used to represent the current working solution concentration and several lower concentrations.

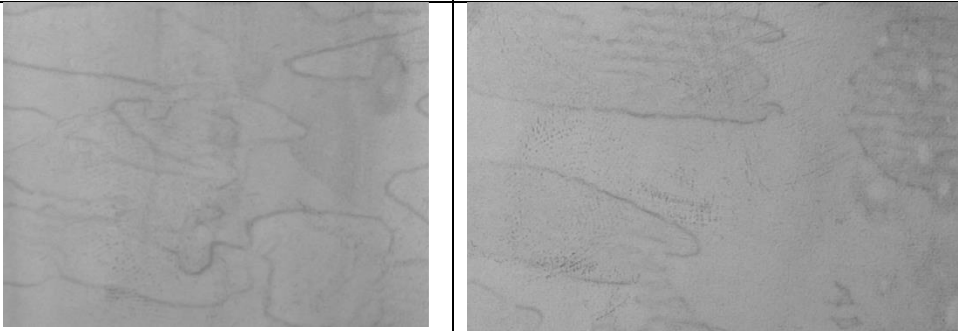
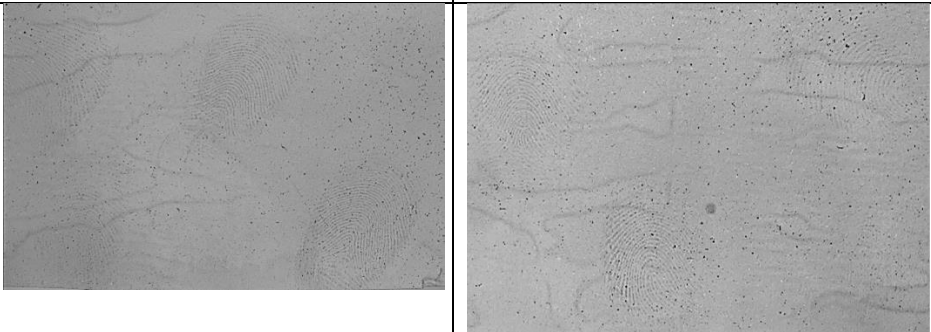
DDAA Concentration (Working solution)	
460 μM	
320 μM	
240 μM	

Figure 5.1 - 1 day old fingerprints deposited on white copy paper and aged under ambient conditions then developed with PD working solutions with only DDAA as the surfactant system (The rows are replicates for each concentration)

Figure 5.1 reveals the results of the enhancement of 1 day old fingerprints deposited on white copy paper and developed using three different concentrations of DDAA in the working solution. A DDAA concentration of 460 μM is representative of the current concentration of DDAA used in the PD working solution and 10 fingerprints out of 10 deposited by the single donor were developed. These fingerprints were considered to be of high quality in terms of the amount of fingerprint ridge detail developed, as full fingerprints were visible. However, the noticeable limiting factor is the contrast between the fingerprint and the background substrate. Silver deposition was evident as fingerprint ridges were visible within 1-2 minutes and all 10 fingerprints were fully developed after ca. 4 minutes. The background staining continued to darken throughout the rest of the development time, which was stopped after 10 minutes. Although, the fingerprints are suitably developed to a Bandey grade of 3 or 4, the contrast is quite weak and the solution did not remain stable after use. Silver precipitation was evident in the processing dish, which suggests that the addition of the non-ionic surfactant is paramount to maintaining stability of the working solution for at least 2 days.

The reduction in the concentration of the DDAA only proved further that the PD working solution is not stable with the use of only DDAA. The contrast was better for both 320 μM and 240 μM but the fingerprint development was minimal. Faint fingerprints could be observed upon magnification but as the concentration of DDAA was lowered, silver precipitated before the working solution had been fully prepared. The concentration of silver was also reduced in conjunction with the DDAA but these working solutions were rendered unusable before silver had fully dissolved.

The critical micelle concentration (CMC) would be a contributing factor to the formation of micelle structures. Goode et al. determined that the concentration of the surfactant was not the defining parameter but that it should be less than the CMC. The CMC of DDAA was determined in this thesis to be 0.52 mM, which is higher than the current working solution as well as the lower concentrations tests. Therefore, if the

concentration is less than the CMC, then the addition of the non-ionic surfactant must be undertaking a more definitive role in the stability of the colloidal silver dispersion.

5.2.2 Growth and Dynamics of Silver for Fingerprint Visualisation

The experiments conducted in chapter 4 revealed that the growth of the silver deposits on the surface was important to the resulting developed fingerprint. Thus, it is important that the potential non-ionic surfactant replacement behaves similarly to compromise between effective fingerprint development and a sufficiently stable working solution. Tween 20 has been explored as an alternative but results using this formulation within the UK have been varied in terms of the development times and stability of the working solution.⁶ It has been reported that the PD working solutions can remain stable for several months but development times can take up to 60 minutes, which can be reduced by reducing the concentration of the detergent system.⁷⁻⁹ Initial studies within CAST revealed immediate issues with stability of the reformulated PD working solution and large variations in development times. Two ages of the working solution were studied, 2 days and 2 weeks old, which resulted in inconsistent observations for both the stability of the working solution and the fingerprint development.

5.2.2.1 Tween 20 – 2 day old working solution

The growth of silver deposition was initially studied for up to 60 minutes development time due to the supposed higher stability of the new PD working solution. Figure 5.2 shows the results for 1 day old fingerprints deposited on white copy paper and developed with a 2 day old PDF2T working solution. (See chapter 3, table 3.5 for the meaning of the code).

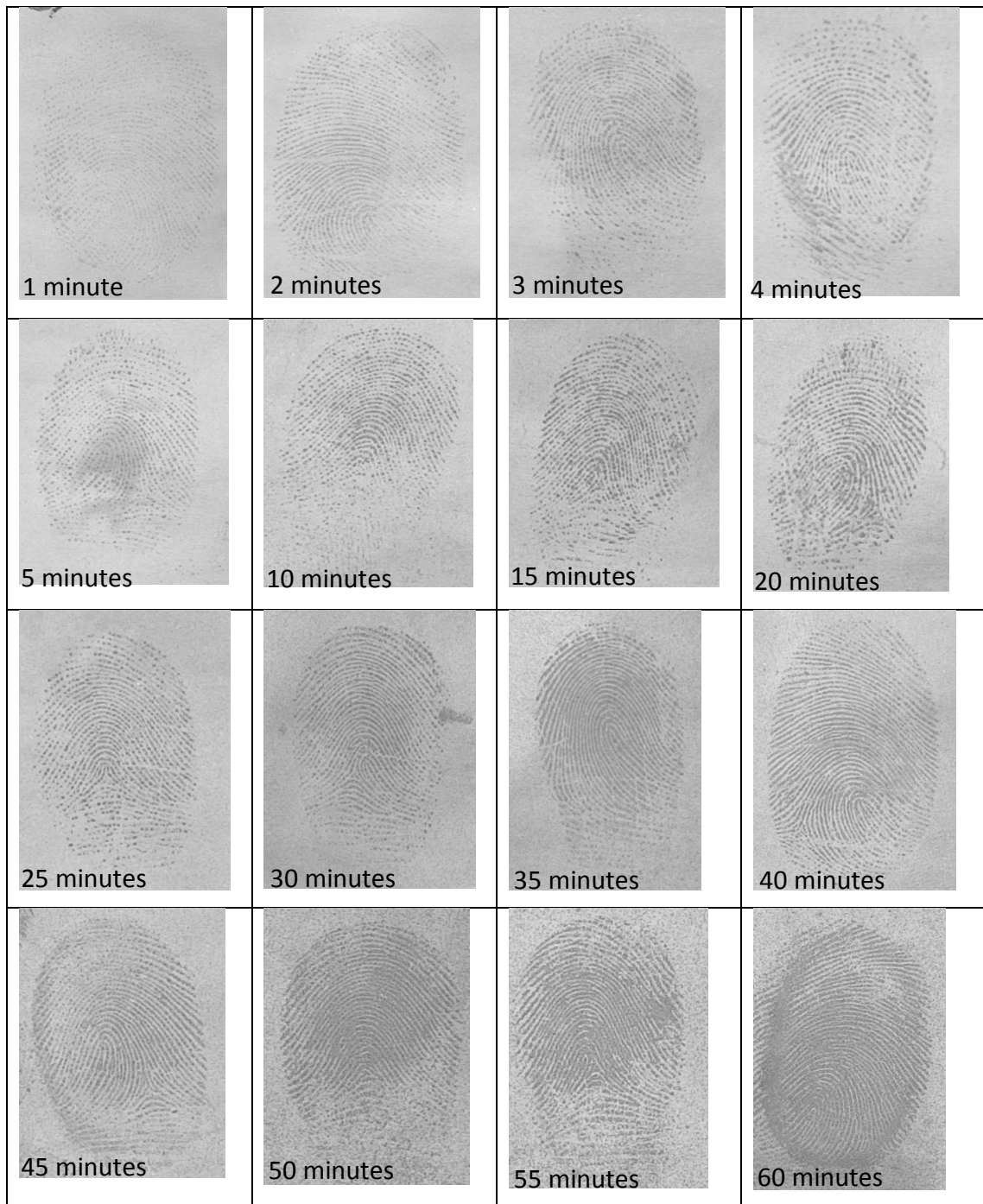


Figure 5.2 - The growth development of silver from 1 to 60 minutes for fingerprints deposited on white copy paper and aged for 1 day under ambient conditions then developed via PDF2T (2 day old solution)

From the images in figure 5.2, it is immediately evident that the fingerprints did not take very long to become visible. After 1 minute, fingerprints ridges are visible and towards the end of 15 minutes, full fingerprints are visible similar to the observations for the Synperonic-N system. From 20 to 40 minutes, the ridges appear more

continuous but the overall fingerprint quality has not improved. As development progresses, it is difficult to fully resolve the ridges. Interestingly, the contrast between the fingerprint and the background is high and does not reduce as time progresses. This is a conflicting observation with the results seen in chapter 4 given that initial silver deposition is rapid and yet it is only the fingerprint that appears to darken over 60 minutes.

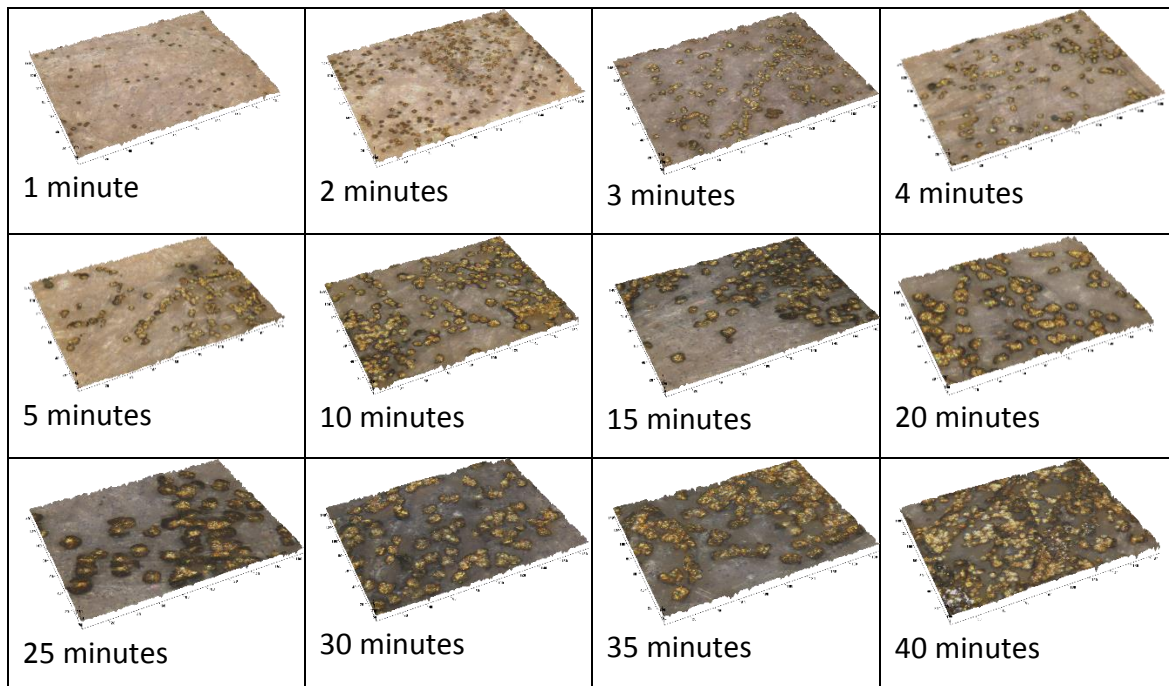


Figure 5.3 - 3D microscopy images (50x) for the growth development of 1 day old marks processed for 30 seconds to 15 minutes for the samples in figure 5.2. Tick marks every 20 µm

The growth of the silver deposits can be seen more clearly in the 3D microscopy analysis as shown in figure 5.3. The microscopy reveals that the Tween 20 PD system also results in growth of the silver on the surface similarly to the Synperonic-N system. There is some variation in the colour of the silver deposits which reflects the scattering cross section at the specific point on the surface. The diameter of the initial silver deposits ranged from 3-5 µm, which is similar to the silver particle size of the Synperonic-N system but the increase in diameter was slightly slower for the Tween 20 system. Figure 5.3 only reveals microscopy analysis up to 40 minutes as

after this time, the deposits were no longer discrete spherical particulates. This is seen more clearly in figure 5.4.

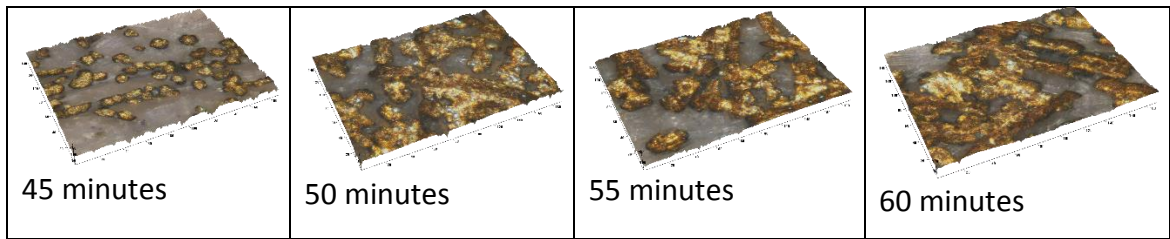


Figure 5.4 - 3D microscopy images (50x) for the growth development of 1 day old marks processed for 45 to 60 minutes for the samples in figure 5.2. Tick marks every 20 μm

As figure 5.4 shows, the silver deposits have aggregated as time progresses such that ridge detail becomes distorted. This was evident across all sets tested further indicating that the PD process must be monitored and longer development times are neither necessary nor desirable. Figure 5.5 shows the graphical representation of the growth of silver on the surface.

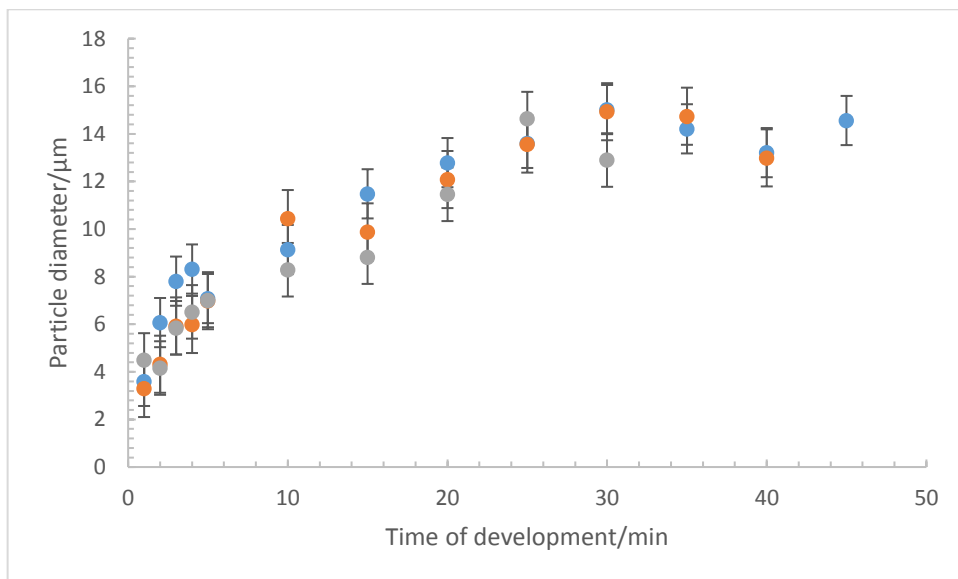


Figure 5.5 - Graph of silver particle diameter vs time of development for 3 sets of 1 day old marks aged under ambient conditions developed via PDF2T (2 day old solution). Data from figure 5.2 and two replicates

Across all of the sets tested, the silver particulate diameter range at each point of development is relatively narrow and the final diameter was between 12-15 μm .

This is very similar to the Synperonic-N system suggesting that this is the optimum size for adequate fingerprint development without obscuring any ridge features. The graph in figure 5.5 reveals some variation regarding when the growth begins to plateau but this is generally between 10-20 minutes which is an ideal time of development for a process. As both the developed images and microscopy images show, a longer development time does not improve image quality but can risk hindering the quality of the mark.

The 2 day old working solution revealed silver deposition after 1 minute (see figure 5.2), so the growth was then observed from a development time of 30 seconds to 15 minutes. Figure 5.6 shows the results for 1 day old fingerprints developed for a maximum of 15 minutes using a 2 day old working solution.

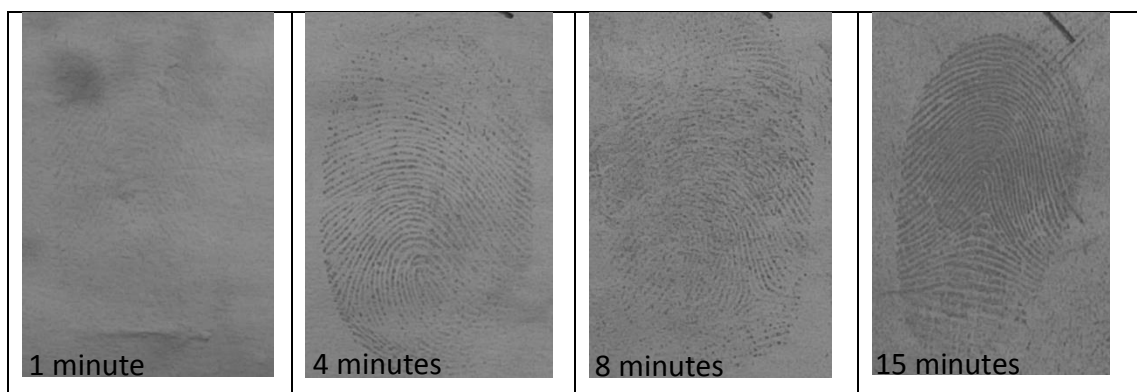


Figure 5.6 - The growth development (1-15 mins) of silver for fingerprints deposited on white copy paper and aged for 1 day under ambient conditions then developed via PDF2T (2 day old solution)

The first noticeable observation from figure 5.6 in comparison to figure 5.2 is the contrast variation. The fingerprints in figure 5.6 were only developed for a maximum of 15 minutes but the background is darker compared to figure 5.2, which suggests that the silver particles in solution are not as stable. However both of the working solutions were aged for 2 days. There is the possibility that the maleic acid pre-wash was not as successful for the images in figure 5.6. However, this is unlikely as a control sample was tested and all samples were pre-washed for at least 15 minutes and the same style of paper was used throughout. Nonetheless, fingerprints ridges are visible after 1 minute and a full fingerprint is developed after 15 minutes. The

fingerprint after 15 minutes of development appears to show continuous silver deposition as opposed to the dotted appearance.

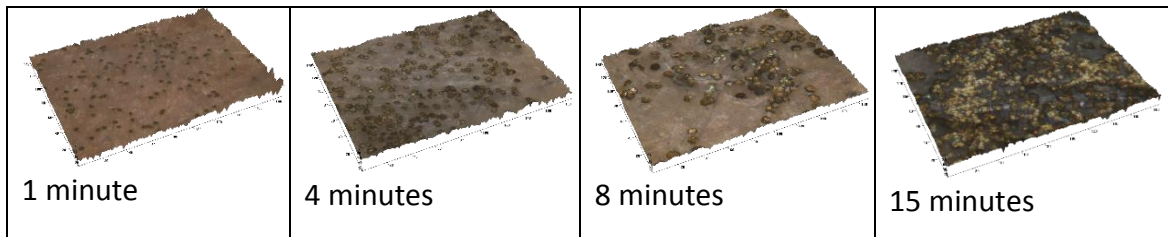


Figure 5.7 - 3D microscopy images (50x) for the growth development of 1 day old marks processed for 1 to 15 minutes for the samples in figure 5.6. Tick marks every 20 μm

This is seen also in the microscopy analysis shown in figure 5.7. Similarly to figure 5.3, the initial deposition of silver is evident after 1 minute at 4-5 μm but the final diameter is slightly smaller between 9-12 μm . In addition to this, the microscopy image at 15 minutes indicates that the silver particles are aggregating hence the continuous appearance of the ridges.

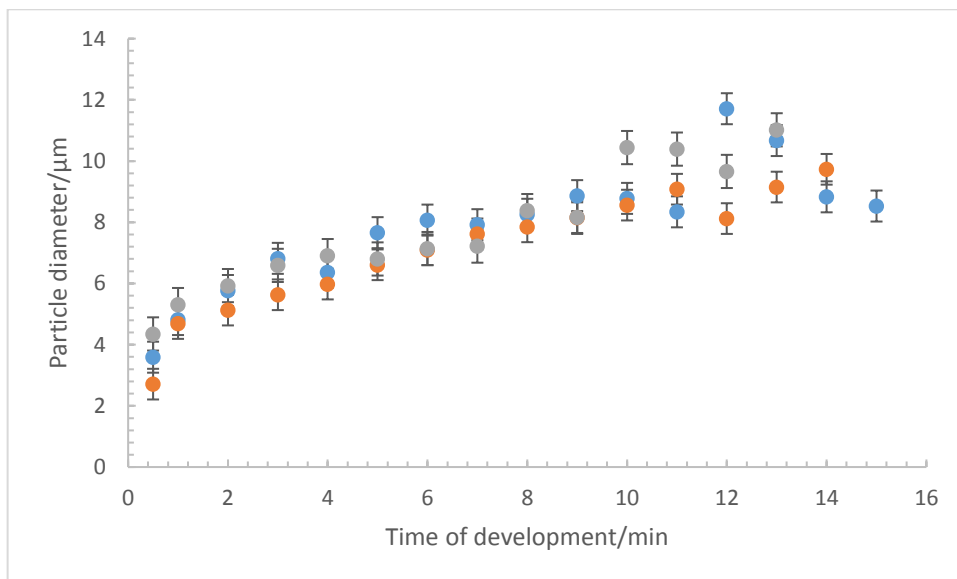


Figure 5.8 - Graph of silver particle diameter vs time of development (1-15 mins) for 3 sets of 1 day old marks aged under ambient conditions developed via PDF2T (2 day old solution). Data from figure 5.6 and two replicates

The general trend for the silver growth is shown in figure 5.8. The smaller final particle diameter seen in figure 5.8 is due to a higher amount of silver particles initially

deposited. The graph shows that the diameter range is narrow across 3 sets for each development stage apart from the latter stages between 10-14 minutes. This is due to the practical limitation of having to use separate fingerprints for each stage of the development. The progressive nature of the growth is clear in this graph showing that the silver deposits grow in small increments and particle diameter eventually plateaus after ca. 8 minutes.

All of the data in this section was obtained using a 2 day old working solution but the results vary considerably with respect to the stability of the PD working solution. Each working solution that was prepared could be used after 2 days but either only lasted for a further 2 days or silver precipitation was visible very shortly after use. This is a significantly different observation compared to the reports of several month stability.^{7, 8, 10} The variation in stability of the working solution was evident further from the split prints.

5.2.2.1.1 Split Print Development

Split prints were tested in order to eliminate the issue of using separate fingerprints but also to observe the effects of ageing the fingerprints for 14 and 28 days. Figure 5.9 shows some representative results for 1-30 minutes and 1-15 minutes development times for 1 day old marks developed with a 2 day old working solution. Each fingerprint was split into 4 to ensure a similar composition of fingerprint residue. The first samples were developed for a maximum of 30 minutes and the second samples were developed for a maximum of 15 minutes. These development times were chosen according to the results in section 5.2.2.1.

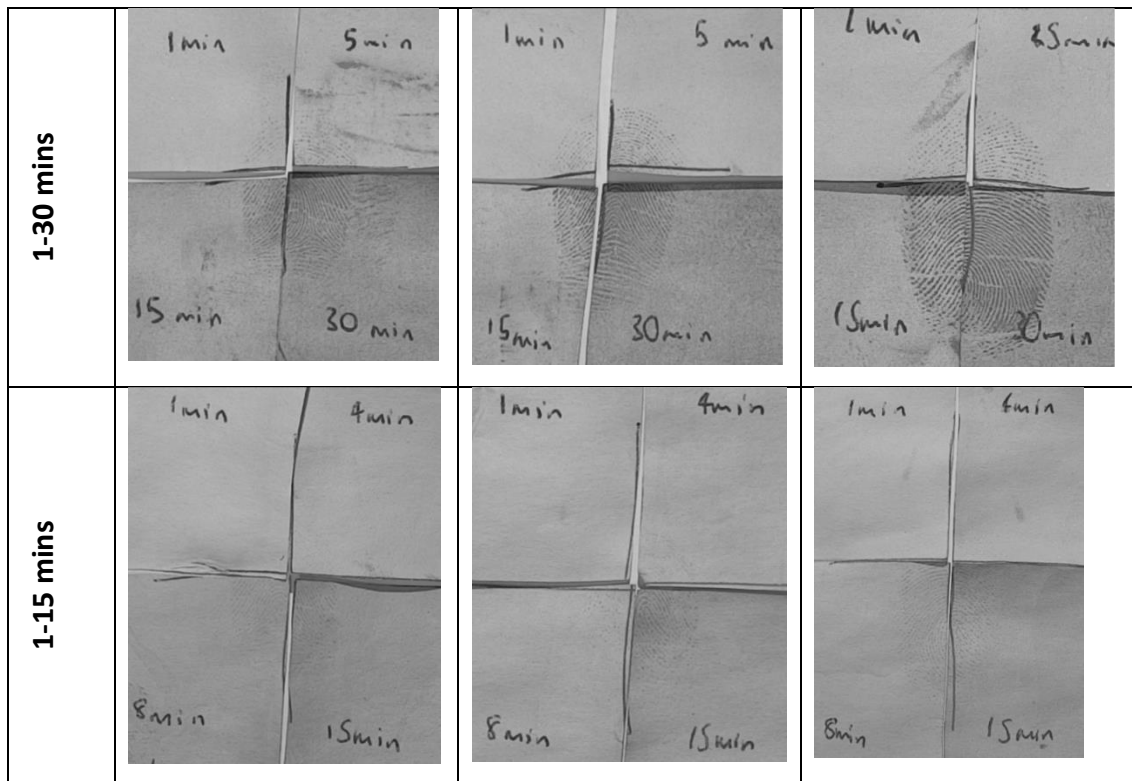


Figure 5.9 – Split prints deposited on white copy paper and aged for 1 day under ambient conditions then developed via PDF2T (2 day old solution) 3 replicates for each age of mark

In comparison to the full fingerprints developed for 15 minutes, the split prints only start to show clear signs of development for the 15 minute quadrant. The contrast between the background and the fingerprint is relatively high which is different to the observations from the full fingerprints in section 5.2.2.1. This suggests that the PD working solution in this case is more stable after 2 days and that further development would have been required. For the split prints developed for a maximum of 30 minutes, similar conclusions can be drawn to those for the full fingerprints developed for a maximum of 60 minutes. Silver deposition is evident after only 1 minute which strengthens as time progresses. There is not a significant difference between the qualities of the fingerprint at 15 minutes compared to 30 minutes other than the appearance of continuous ridges. This is shown further in the microscopy analysis depicted in figure 5.10 and 5.11.

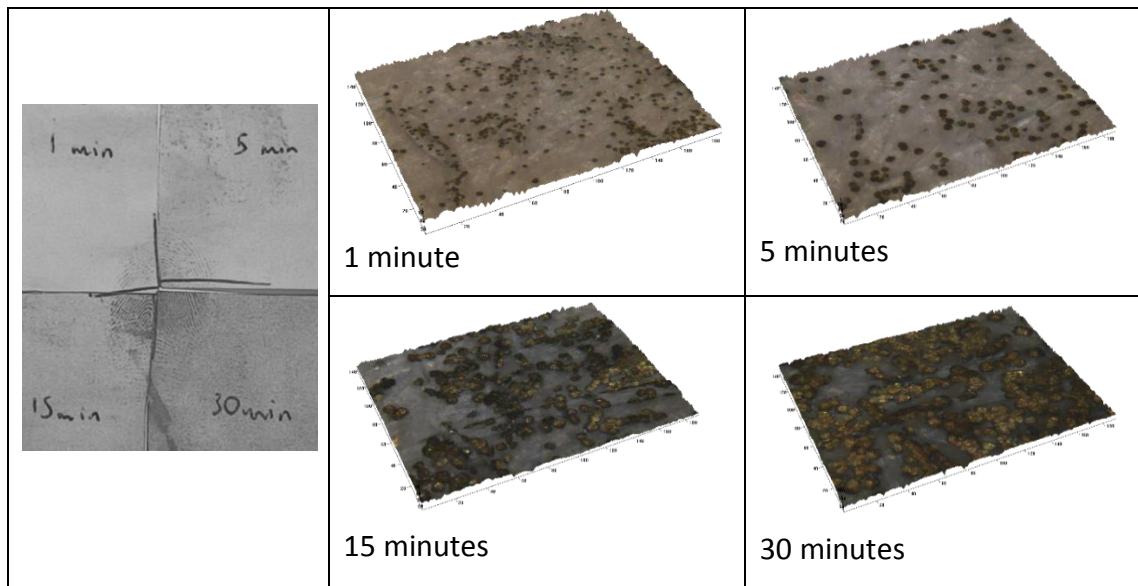


Figure 5.10 - 3D microscopy images (50x) for a sample of the growth development of a 1 day old mark processed for 1-30 minutes in figure 5.9. Tick marks every 20 μm

As figure 5.10 shows, the initial deposition of silver results in numerous silver sites for subsequent growth. Between 15 and 30 minutes, the silver particles begin to aggregate, which can become detrimental to the resulting fingerprint. In this example, the process could have been stopped after 15 minutes which is much shorter than the suggested development times indicating a variation in the stability of the working solution.

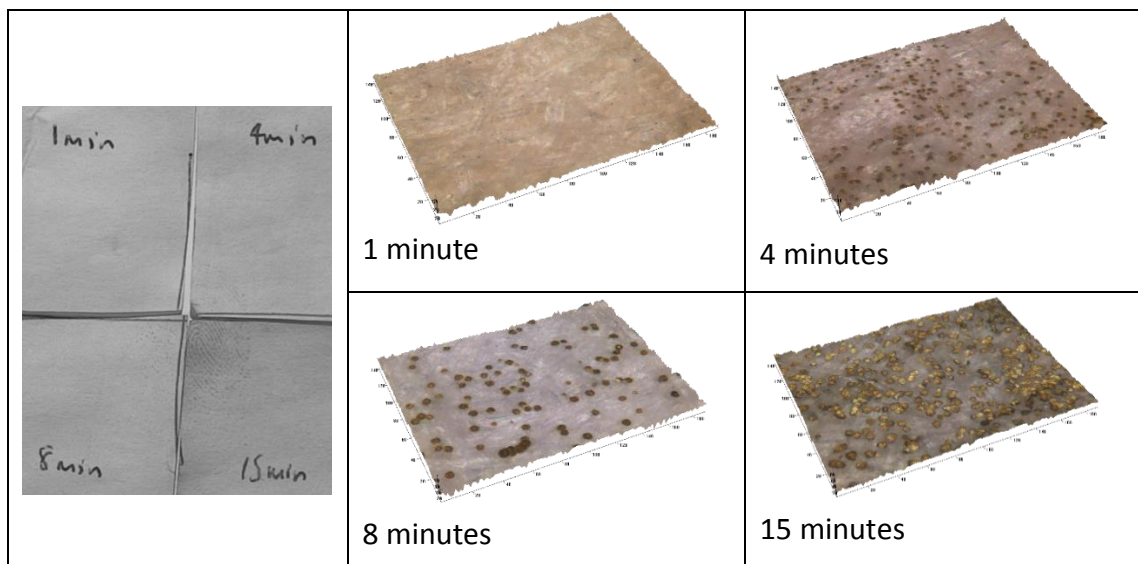


Figure 5.11 - 3D microscopy images (50x) for a sample of the growth development of 1 day old mark processed for 1-15 minutes in figure 5.9. Tick marks every 20 μm

For the split prints processed for a maximum of 15 minutes, the nucleation point for the growth of silver occurs after ca. 4 minutes and progressive growth is observed but at a slower rate. However, the microscopy image for the 15 minute quadrant reveals a high density of silver such that further development would result in aggregation of the silver deposits. The capability of being able to see early fingerprint ridges which increase in clarity is advantageous for a practitioner as it indicates the process is working. Hence, the results from the split prints developed for a maximum of 30 minutes are more desirable. Figure 5.12 represents the trend in the growth for the splits prints processed for up to 30 minutes.

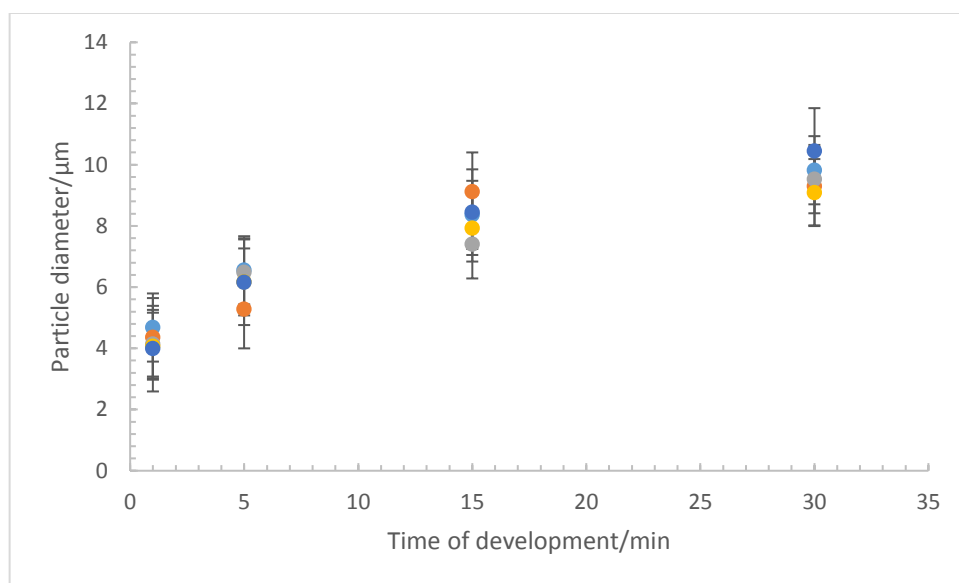


Figure 5.12 - Graph of silver particle diameter vs time of development (1-30 minutes) for the average of 5 sets of 1 day old marks aged under ambient conditions developed via PDF2T (2 day old solution)

The general trend observed in figure 5.12 is identical to the observations throughout all split prints experiments using the Synperonic-N system (other than the additional 15 minutes of development). The initial particle diameter range after 1 minute of development is very narrow, ranging from 3.9-4.6 µm. Between 15 minutes to 30 minutes the silver particle diameter increases from 7-9 µm to 9-10.4 µm. Although, the Tween 20 system behaves similarly to the Synperonic-N system in terms of fingerprint quality and silver particle growth, the nature of the working solution is unreliable with respect to the stability. This can be seen further with aged marks.

Figure 5.13 shows the split prints for 14 and 28 day old marks developed for a maximum of 15 minutes. In this situation the working solution had to be used on the day it was formulated.

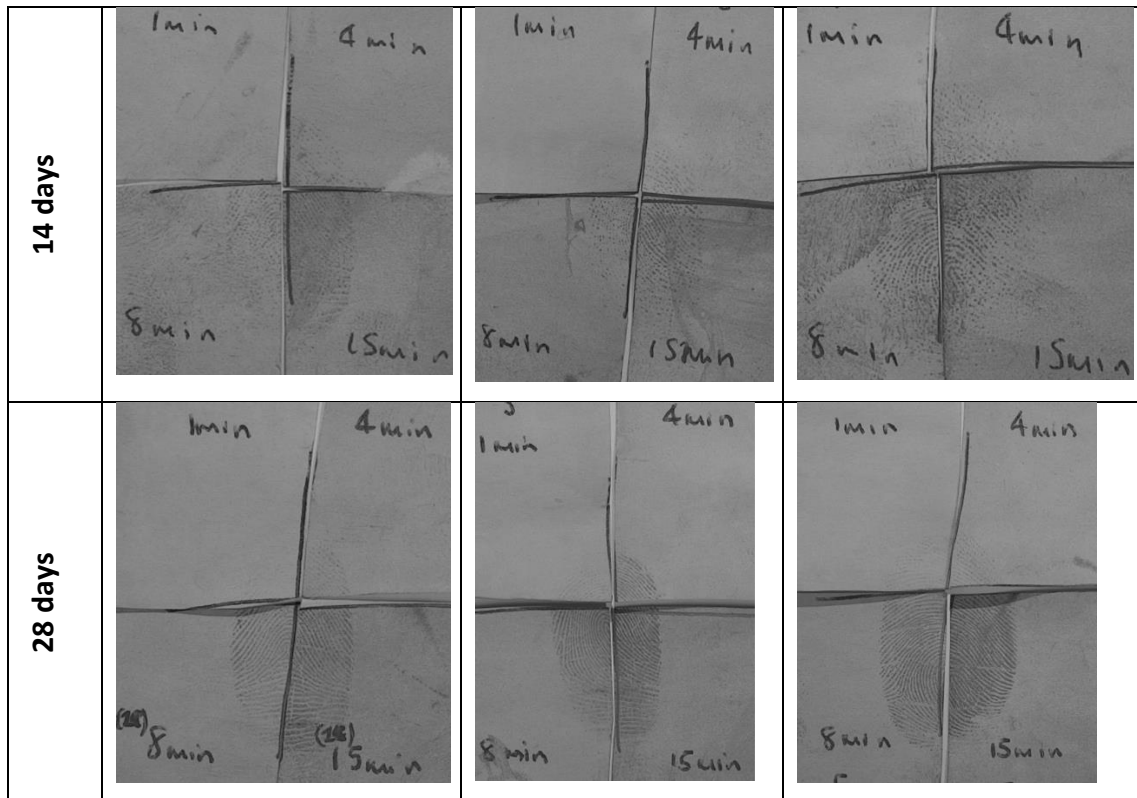


Figure 5.13 – Split prints deposited on white copy paper and aged for 14 and 28 days under ambient conditions then developed via PDF2T (3 replicates for each age of mark)

Upon the preparation of the working solution using Tween 20 in the detergent, the resulting solutions varied greatly in shelf-life. For the aged marks, a fresh solution had to be used which was prepared and used for development within 4 hours. For both ages of the deposited marks, the development gets stronger as time progresses and does not become visible until after 4 minutes. The contrast for the 28 day old marks is stronger than the 14 day old samples and the ridges appear more continuous for the 28 day marks. This would suggest that the initial deposition of silver for the 28 day old marks resulted in a greater number of silver sites for subsequent growth. However, upon microscopic examination, both ages appear to have similar nucleation points and overall deposition of silver. Figures 5.14 and 5.15 shows these microscopy results.

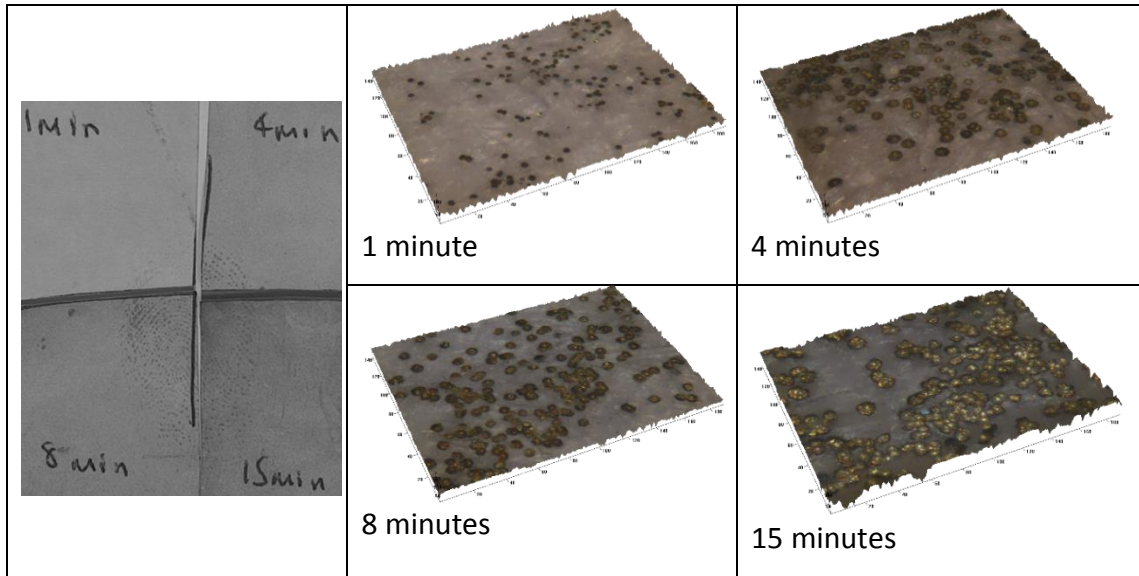


Figure 5.14 - 3D microscopy images (50x) for a sample of the growth development of 14 day old mark processed for 1-15 minutes in figure 5.13. Tick marks every 20 μm

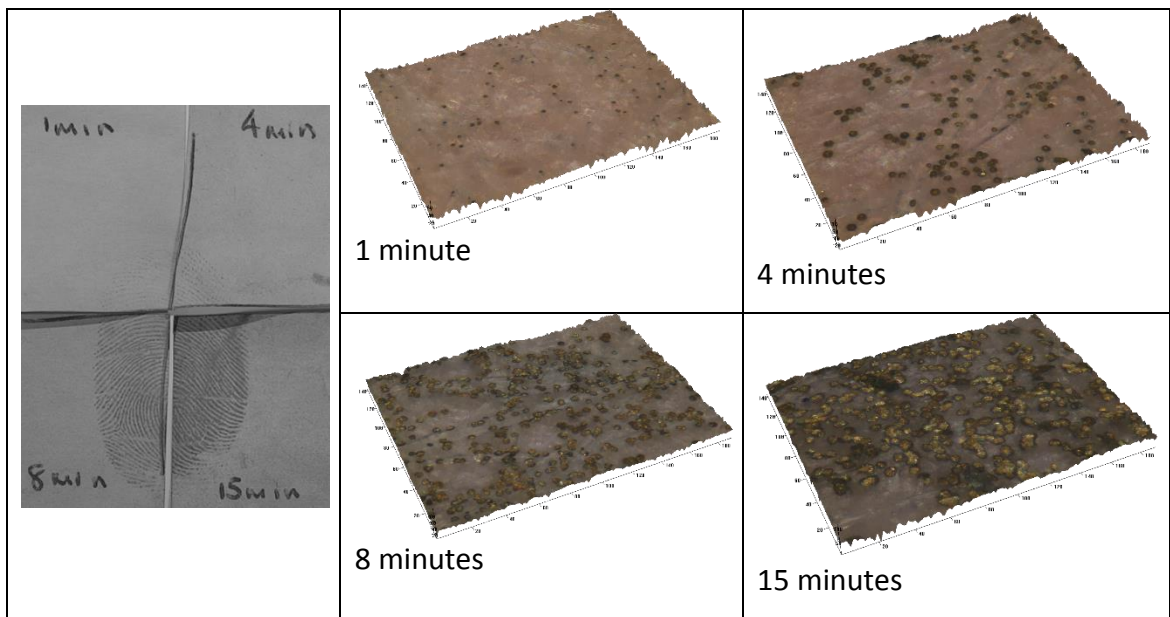


Figure 5.15 - 3D microscopy images (50x) for a sample of the growth development of a 28 day old mark processed for 1-15 minutes in figure 5.13. Tick marks every 20 μm

The results for the 14 day old marks are very similar to what was observed using the Synperonic-N system in chapter 4. The fingerprint itself is dotted in appearance and the microscopy reveals a growth in the particle diameter on the surface.

Although the fingerprint ridges are more defined in the 28 day old mark, the nucleation of silver is later than for the 14 day old marks and the resulting deposits after 15 minutes are smaller than for the 14 day old samples. This is because a greater area of the fingerprint is initially developed such that the deposition of silver is greater overall. This variation in the size of the silver deposits can be seen in figure 5.16.

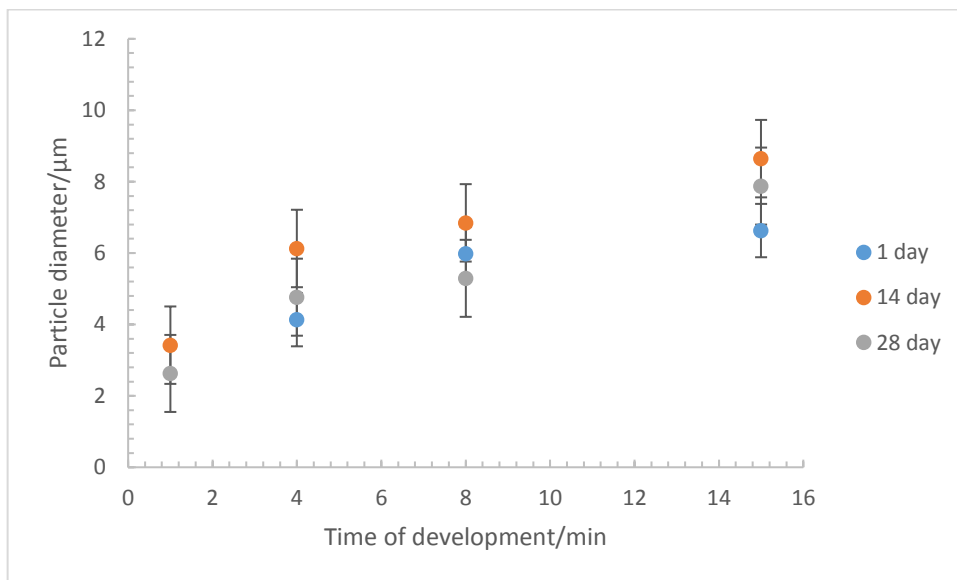


Figure 5.16 - Graph of silver particle diameter vs time of development for the average of 5 sets of 1, 14 and 28 day old marks aged under ambient conditions developed via PDF2T (Working solution age varied)

The 14 day old marks resulted in the largest silver particle diameters after the 15 minute development time at 8-9 µm compared to 6-7 µm for the 1 day old marks and 7-8 µm for the 28 day old marks. Although these ranges are not significantly different from each other, it has a greater effect on the resulting developed image. The smaller particles result in defined ridges which must be monitored to avoid overdevelopment and the larger particles produced dotted fingerprints.

5.2.2.2 Tween 20 – 2 week old working solution

The extra addition of Tween 20 has been reported to increase the shelf life of the working solution.^{8, 10} However, it was only possible to prepare a 2 week old usable working solution once.

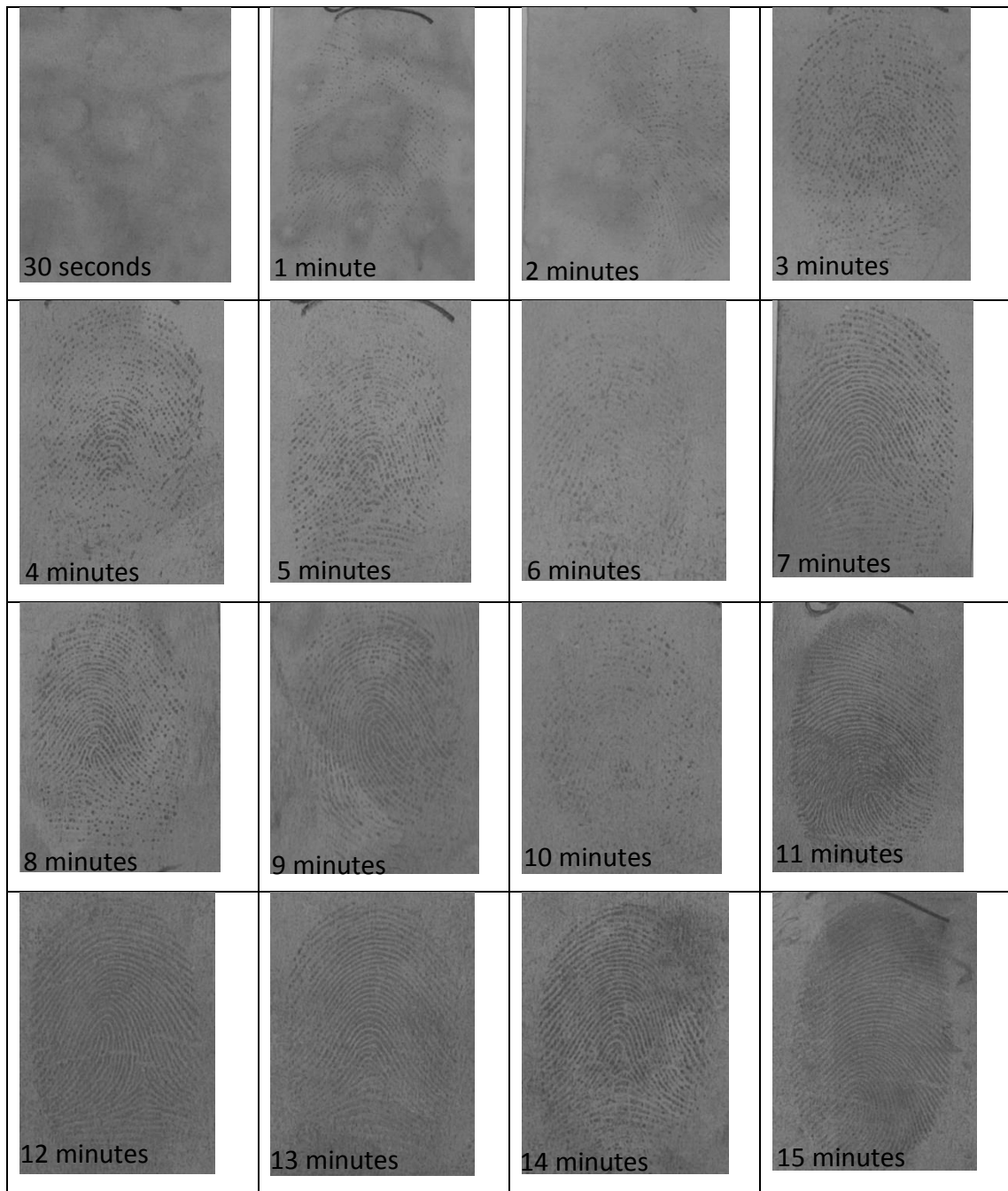


Figure 5.17 - The growth development of silver from 30 seconds to 15 minutes for fingerprints deposited on white copy paper and aged for 1 day under ambient conditions then developed via PDF2T (2 week old solution)

Figure 5.17 shows the results of developing 1 day old fingerprints developed with a 2 week old PD working solution with Tween 20. As the solution has been aged, it would be fair to assume that the development process would be quicker due to the limited stability of the colloidal silver. As figure 5.17 shows, there is visible ridge detail

present after ca. 1 minute which appears dotted until ca. 6 minutes, at which point the fingerprint gradually starts to appear as a full image. The development does result in high quality fingerprints, but the contrast is quite weak. The background deposition is high which makes the fingerprints appear fainter in colour. The colour of the resulting fingerprints is also dependent on the size of the silver particles on the surface. Figure 5.18 reveals the microscopy analysis for the set of fingerprints shown in figure 5.17.

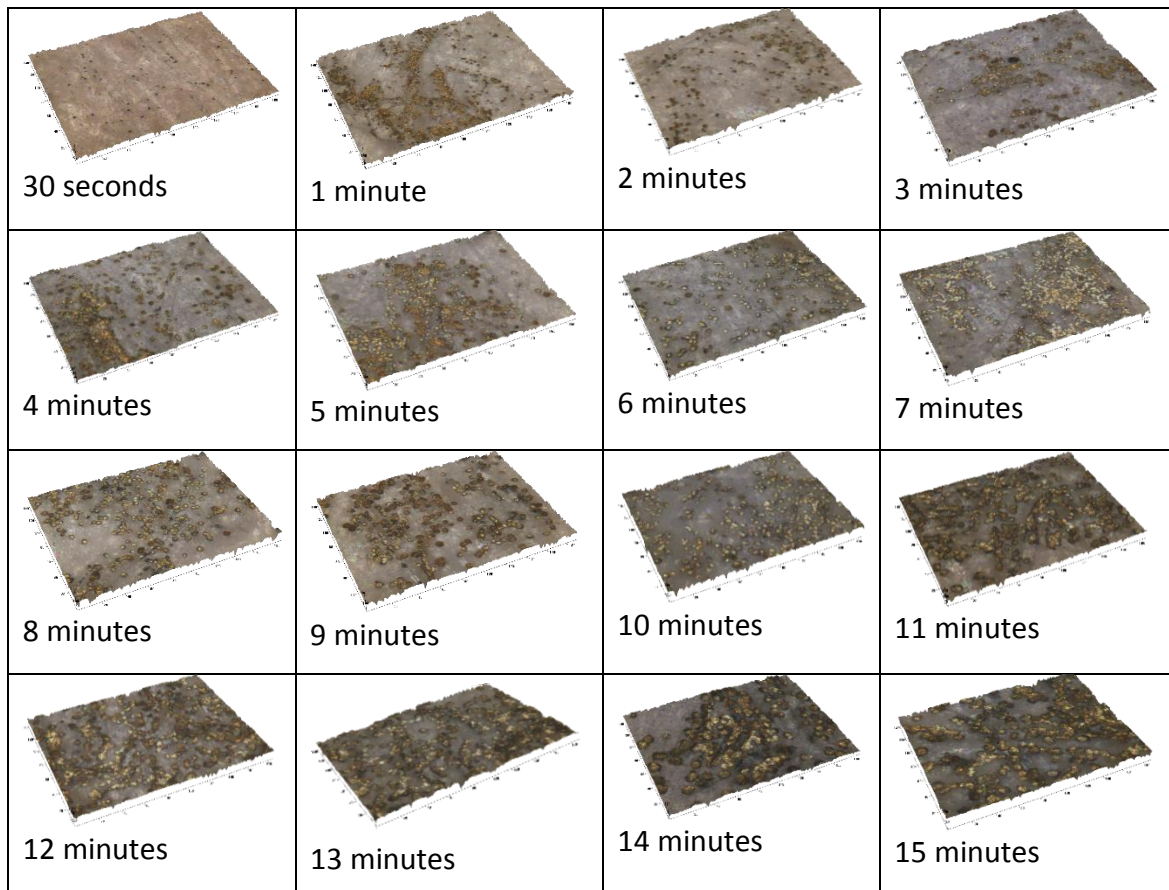


Figure 5.18 - 3D microscopy images (50x) for the growth development of 1 day marks processed for 30 seconds to 15 minutes for the samples in figure 5.17. Tick marks every 20 μm

In contrast to the fingerprints developed with a 2 day old working solution (shown in figure 5.2 and 5.3), the deposited silver particles are smaller in diameter only growing to ca. 9 μm . However, the amount of deposited silver is high initially which provides several silver sites for further growth. The aggregation of the silver deposits is evident along the ridges in the microscopy images as the monodispersed nature of the deposits lessens. The results across the 3 replicates developed with a 2 week old

solution were qualitatively similar but not consistent in terms of the diameter of the silver deposits. Figure 5.19 shows the graph for the development of the 3 replicates of 1 day old marks developed with a 2 week old solution.

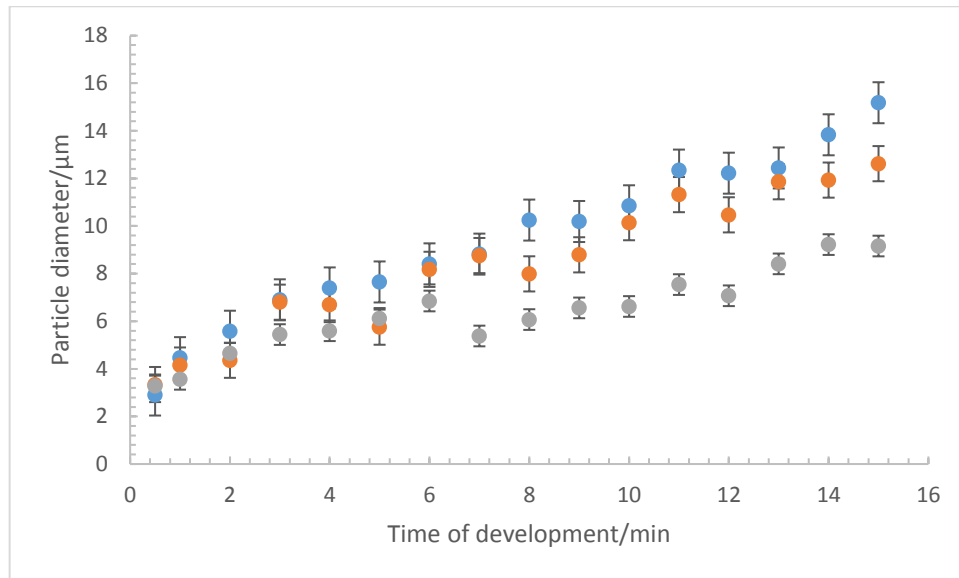


Figure 5.19 - Graph of silver particle diameter vs time of development (30 seconds-15 minutes) for 3 sets of 1 day old marks aged under ambient conditions developed via PDF2T (2 week old solution). Data from figure 5.17 and two replicates

The observed trend is the same across the 3 sets however the range between the particle diameters after ca. 7 minutes is broad. This is significantly different to the observations for the 2 day old solution but also the Synperonic-N system. The variation in the size of the deposited silver particles is due to the amount of the fingerprint that is developed. For the set shown in figure 5.17, fingerprint development gradually increased throughout the development process. The dotted appearance means that less of the total area of the fingerprint is developed, meaning that silver growth occurs on fewer sites.

The inconsistency of the results and the stability of the PD working solution with the added Tween 20 is concerning and suggests that Tween 20 is not a suitable alternative. Some fingerprints have developed effectively such that the contrast is high as well as the amount of the fingerprint developed but this result was not reproducible. The role of the non-ionic surfactant will be explored further in the

following section to understand the structural implications of the addition of Tween 20.

5.2.3 Neutron Reflectivity Study of Surfactant Adsorption

The use of neutron reflectivity can provide qualitative and quantitative information on the structure and composition of a particular layered system. In this chapter, the possible adsorption of the two types of surfactant will be considered and thus, the thickness of the layers. The qualitative determination of whether and which of the surfactants adsorb to the silver surface will aid the understanding of the structure of the silver particles in the working solution. Quantitative analysis will indicate the relative thickness, roughness and hydration parameters of the surfactants compared to the silver surface which will aid the structural understanding of the working solution further.

5.2.3.1 DDAA Adsorption

DDAA is the cationic surfactant component which is believed to be the main contributor to the stability of the silver particles in the solution by forming a staggered micelle conformation (as shown in chapter 1, section 1.4.1, figure 1.8). This presents two corresponding questions: (i) does DDAA adsorb to the silver surface and if so (ii) how thick is the adsorbed layer?

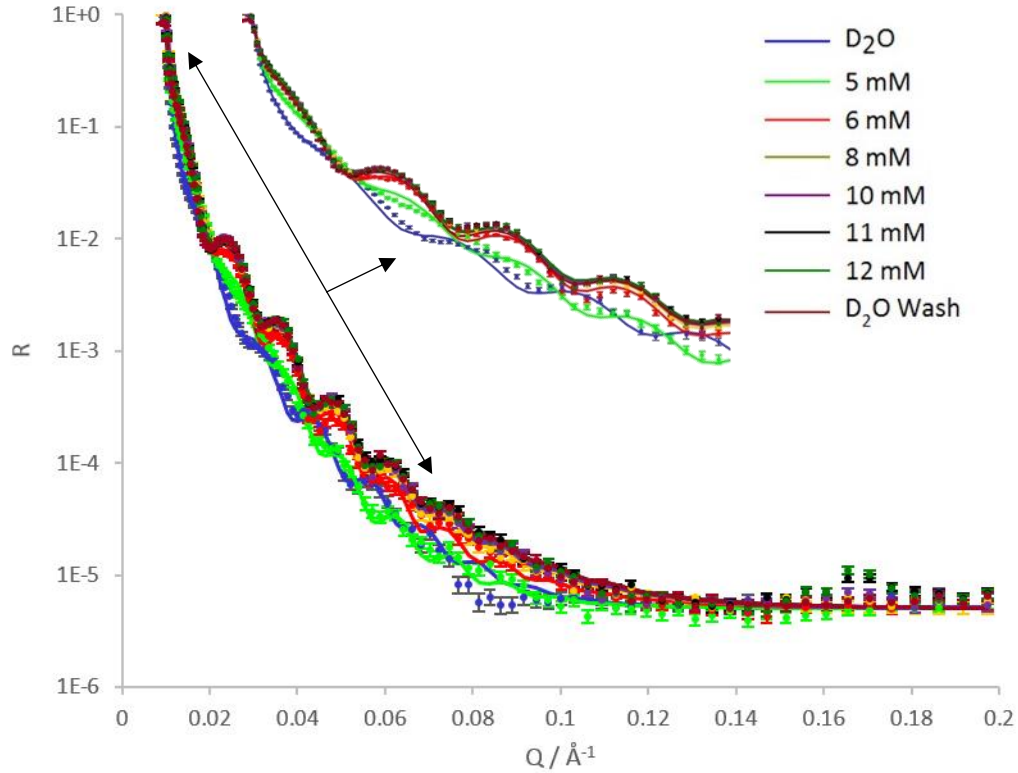


Figure 5.20 - Neutron reflectivity profiles for the adsorption of h-DDAA in D₂O with the bare silver surface in D₂O. The circles represent the measured data and the lines are the respective fits of that data, fitted using RasCal ($\chi^2 = 81.9$ for whole data set)

Figure 5.20 shows the reflectivity profiles for the adsorption of hydrated DDAA (h-DDAA) for increasing concentrations between 5-12 mM. These concentrations were chosen to be reflective of the stock detergent concentration (ca. 11 mM) to ensure data could be collected as this experiment has not been done before. The measurements were performed in D₂O to achieve maximum contrast between the h-DDAA and the deuterated solvent.

Total internal reflection is observed at $Q < 0.01 \text{ \AA}^{-1}$ where $R = 1$ by the appearance of a critical edge, Q_C . The value for Q_C can be determined using equation 5.1 where N_b is equal to the scattering length density.

$$Q_C = (16\pi\Delta N_b)^{1/2} \quad (5.1)$$

In this case, the incident electrons were transmitted through D₂O ($N_b = 6.255 \times 10^{-6} \text{ \AA}^{-2}$) and refracted through quartz ($4.182 \times 10^{-6} \text{ \AA}^{-2}$) resulting in a ΔN_b of $2.073 \times 10^{-6} \text{ \AA}^{-2}$. With this value and equation 5.1, a predicted Q_c value of 0.01 \AA^{-1} is obtained.

The blue trace corresponds to the reflectivity profile of the silver coated quartz block in D₂O. The fringes observed in the data are attributed to the respective layers in the system: binding MPTS layer and Ag. The thickness of the Ag layer can be estimated using the periodicity of a fringe in the reflectivity profile and equation 5.2.

$$d = \frac{2\pi}{\Delta Q} \quad (5.2)$$

Using the first fringe gives a ΔQ value of 0.012 \AA^{-1} and equation 5.2 produces an Ag thickness of 523 \AA which is consistent with the thickness obtained using the AFM (478 \AA). The AFM measurements were performed by scratching the Ag surface to determine the step height giving a crude estimate. The neutron reflectivity experiment gives a more accurate thickness value.

The purpose of fitting the data allows for the following parameters to be determined for each of the layers: thickness ($d / \text{ \AA}$), SLD ($N_b / \text{ \AA}^{-2} \times 10^{-6}$), roughness ($\sigma / \text{ \AA}$) and the hydration (% v/v). Along with the reflectivity profile and the fitted parameters, a scattering length density (SLD) profile is produced which is shown in figure 5.21.

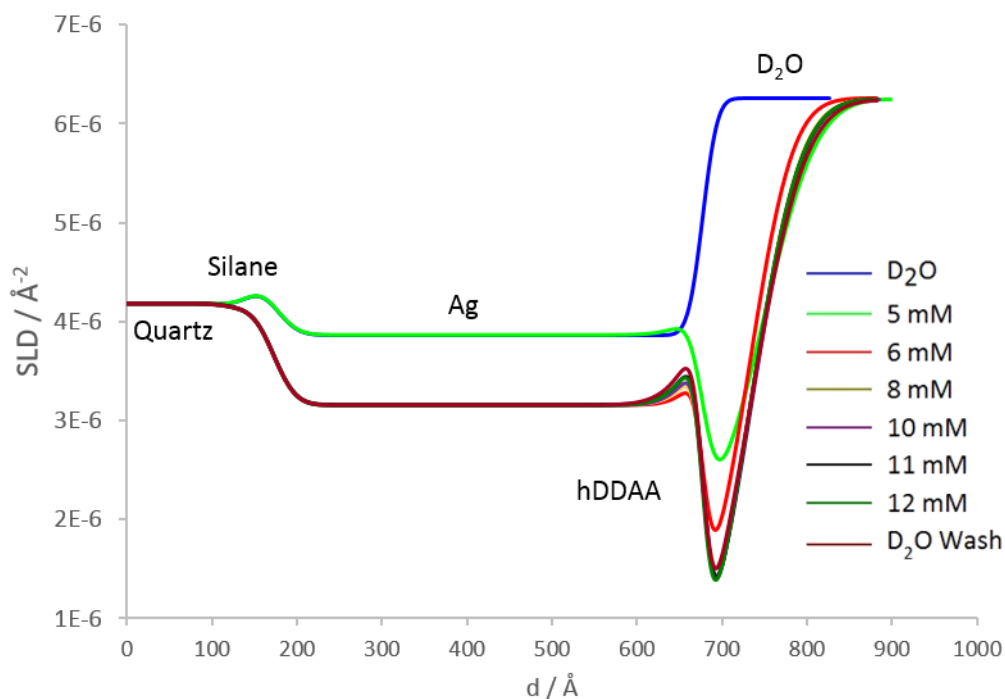


Figure 5.21 - SLD profiles for the adsorption of h-DDAA in D₂O. Data from figure 5.20 and fitted using RasCal

Table 5.1 details all the fitted parameters for the data in figure 5.20.

Layer	Thickness, d / Å	SLD, N _b / Å ⁻² x 10 ⁻⁶	Roughness, σ / Å	Hydration, % v/v
D ₂ O	Bulk	6.255	N/A	Bulk
h-DDAA 5 mM	71.3 ± 4.2	-0.039	49.2 ± 2.4	29.2 ± 2.2
h-DDAA 6 mM	54.6 ± 3.3	-0.039	39.9 ± 1.5	14.8 ± 2.2
h-DDAA 8 mM	58 ± 1.9	-0.039	44.6 ± 1.7	5.9 ± 1.9
h-DDAA 10 mM	57.3 ± 2.2	-0.039	46.1 ± 2.3	3 ± 1.9
h-DDAA 11 mM	54.7 ± 1.7	-0.039	46.9 ± 1.7	2.42E-7 ± 0.2
h-DDAA 12 mM	55.2 ± 2.7	-0.039	46.9 ± 2.6	4.07E-5 ± 1.1
h-DDAA Wash	55.3 ± 0.1	-0.039	50.8 ± 1.8	6.61E-8 ± 0.01
Ag	517.8 ± 3.9	3.80 ± 2.43E-8	13.6 ± 0.8	2.6 ± 1.1
		3.07 ± 4.34E-8	9.8 ± 0.4	
MPTS	10 ± 0.2	2.19E-6 ± 2.53E-7	23.8 ± 3.4	76.5 ± 7.1
Quartz	Bulk	4.182	19.7 ± 2.7	N/A

Table 5.1 - Fit parameters for the reflectivity profiles in figure 5.20

The SLD parameter of the h-DDAA was fixed in RasCal because the SLD of the layer takes into account levels of hydration (see equation 2.11, chapter 2). The estimated thickness of the Ag layer at 523 Å is very similar to the fitted value of 517 Å which is closer to the AFM measured thickness at 478 Å. The SLD profile in figure 5.21 and the reflectivity profile in figure 5.20 clearly show adsorption of h-DDAA on the Ag surface. With increasing concentrations from 0-8 mM, a significant change in the reflectivity profile is evident from reduced fringe spacing. After ca. 8 mM, there is no change in either the reflectivity or the SLD profile, other than the formation of a small Bragg peak at high Q in figure 5.20, suggesting that a saturation limit has been reached. The reflectivity profile is also identical after the washing of the h-DDAA indicating that the binding is irreversible.

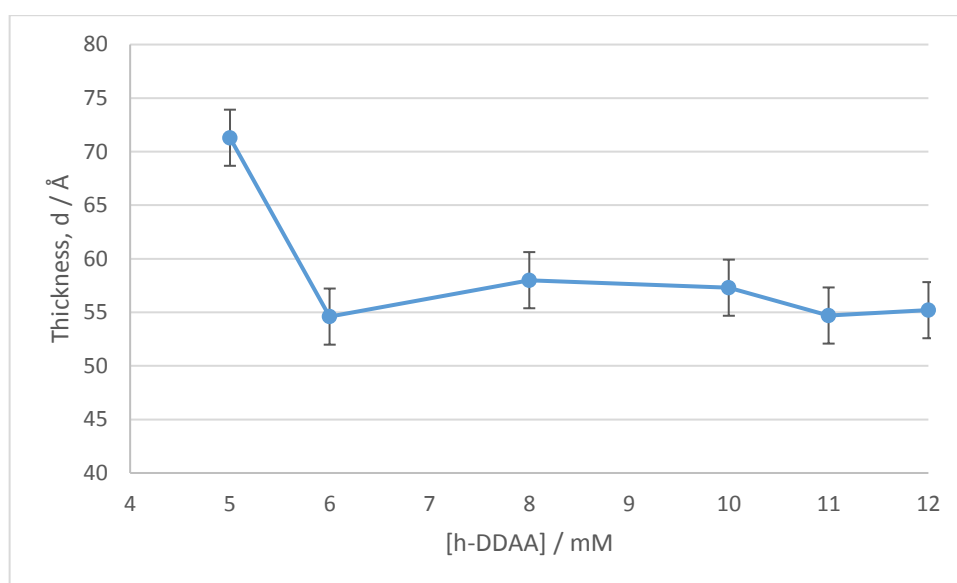


Figure 5.22 - Thickness of h-DDAA layer with increasing concentration of h-DDAA

The thickness of the h-DDAA layer does not appear to change significantly as shown in figure 5.22, with the exception of 5 mM. DDAA is a small molecule with a relatively short chain length (C=12) with an extended chain length of ca. 20 Å. Therefore, the data suggests that h-DDAA is adsorbed but as a multilayer on the planar silver surface.

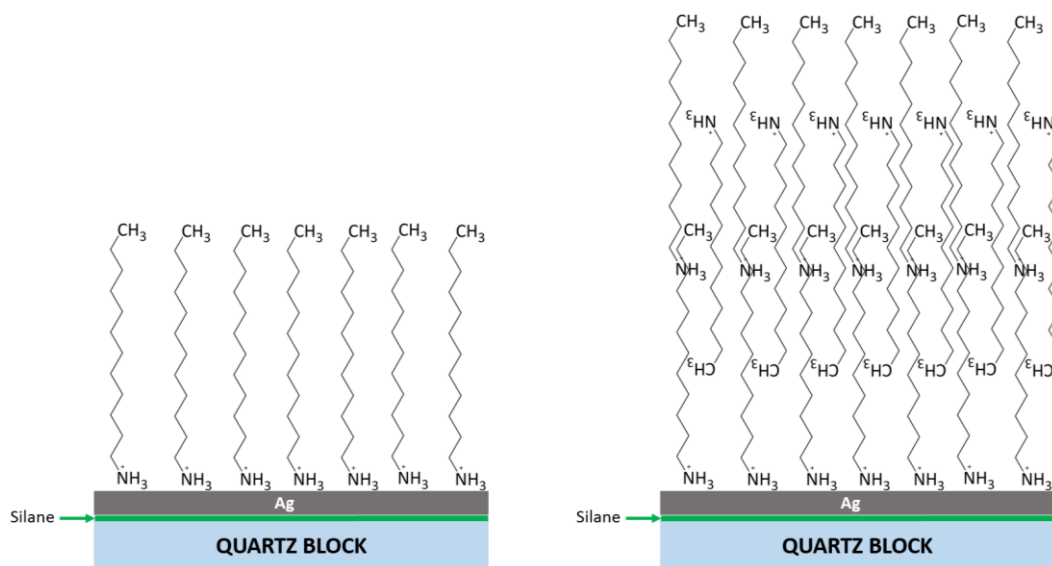


Figure 5.23 - Proposed structure of h-DDAA on the planar silver surface

The proven adsorption of h-DDAA on the Ag surface agrees with the theory that DDAA forms a micellar structure around the colloidal silver particles. The neutron reflectivity experiment was performed on a planar surface of Ag. In the solution the spherical nature of the silver particles increases the surface area allowing for more adsorption.

In table 5.1, the values for the Ag surface shown in red correspond to the Ag layer when the surfactant layer is added. The SLD and the roughness both decrease from $3.8 \times 10^{-6} \text{ \AA}^{-2}$ to $3.07 \times 10^{-6} \text{ \AA}^{-2}$ and 13.6 \AA to 9.8 \AA respectively. The Ag layer also revealed a hydration parameter of 2.6 % suggesting that it is slightly porous.

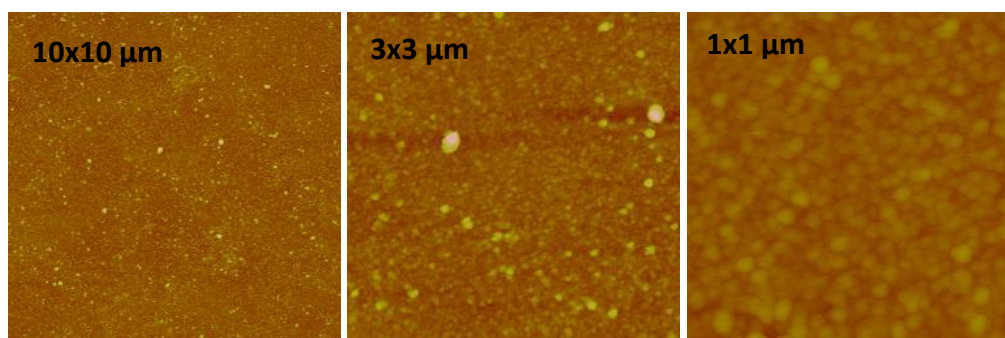


Figure 5.24 - AFM images of the Ag coating

As figure 5.24 shows, the sputtering of the Ag has produced an atomically flat coating of silver but gaps are visible which could indicate an increased porosity. As the SLD of silver is lowered upon addition of the surfactant, it is possible that the surfactant effectively fills in the gaps on the silver surface, thus lowering the SLD.

5.2.3.2 Tween 20 Adsorption

Tween 20 is being used across the world as a replacement for Synperonic-N but as the first half of this chapter shows, the results are inconsistent and the working solution is unreliable. This poses the question as to whether or not Tween 20 is aiding the stability of the silver colloidal particles in the solution or causing no effect. The second neutron reflectivity experiment focussed on the sole effect of Tween 20 on the planar silver surface. The deuteration laboratory facility at ISIS provided a hydrated and deuterated Tween 20 couple allowing for direct comparisons to be made.

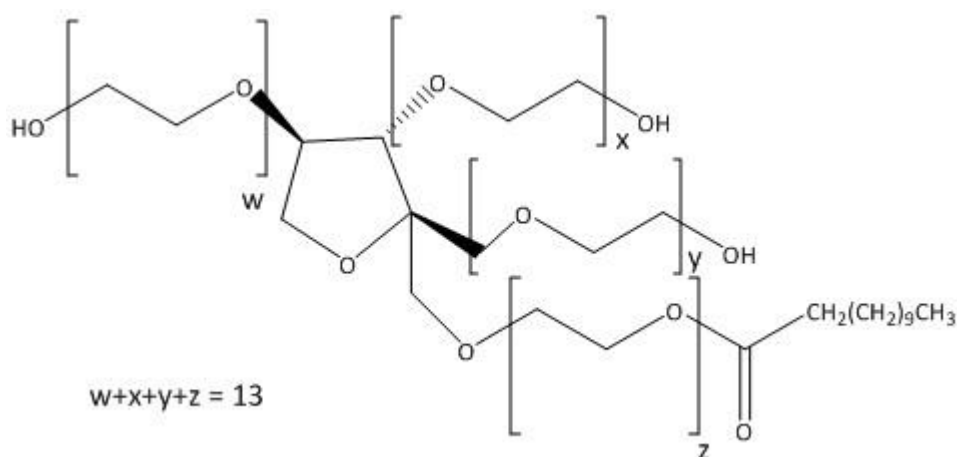


Figure 5.25 - Tween 20 (13) used in the neutron experiments

Figure 5.25 shows the structure of the Tween 20 reagent used in the neutron experiments. In this case, the number of ethoxylate groups equals 13 and it was only these groups which were deuterated in the deuterated analogue.

5.2.3.2.1 d-Tween Adsorption

The reflectivity measurements for the deuterated analogue of Tween 20 were performed in H₂O to achieve maximum contrast. Three concentrations were chosen to reflect the concentration in the stock detergent solution (ca. 2.3 mM). Similarly to the adsorption isotherm for h-DDAA, the higher concentrations were chosen to ensure data could be collected.

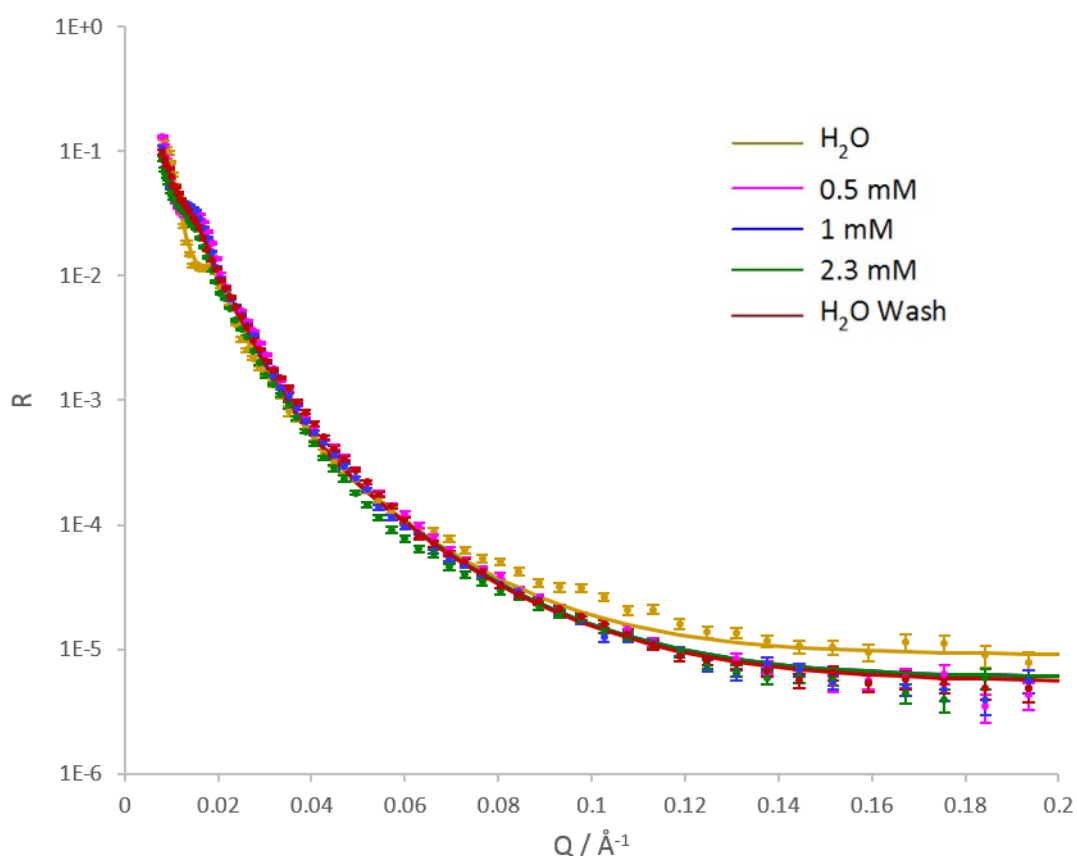


Figure 5.26 - Neutron reflectivity profiles for the adsorption of d-Tween in H₂O with the bare silver surface in H₂O. The circles represent the measured data and the lines are the respective fits of that data, fitted using RasCal ($\chi^2 = 107.3$ for whole data set)

Figure 5.26 reveals the reflectivity profiles for the characterisation of the Ag surface in H₂O and the adsorption isotherm (0.5-2.3 mM) of d-Tween followed by washing the surface. The profiles nicely demonstrate that there is no difference in reflectivity as the concentration of the surfactant increases. This is only reduced

slightly when the surface was washed with water but the wash profile is essentially identical to the profile for the three concentrations.

Unlike the reflectivity profiles in figures 5.20, there is no critical edge observed in figure 5.26. This is due to the solvent used in these experiments. H₂O has an SLD of $-0.57 \times 10^{-6} \text{ \AA}^{-2}$, which means the ΔN_b is negative.

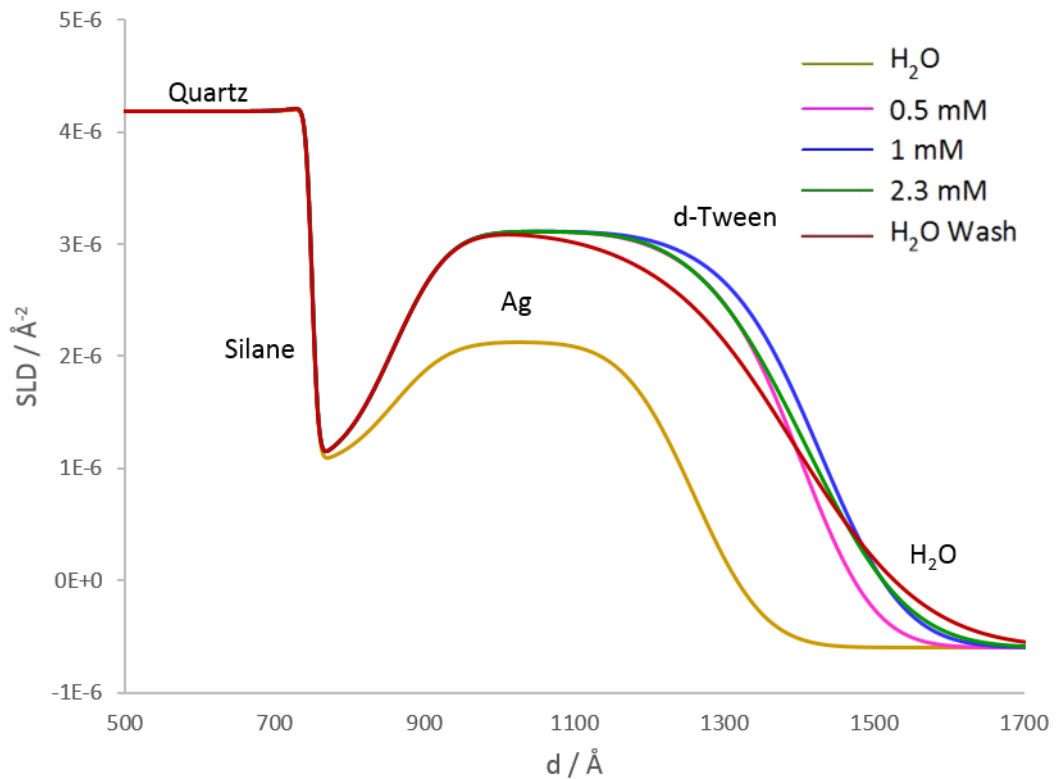


Figure 5.27 SLD profile for the adsorption of d-Tween in H₂O. Data from figure 5.26, fitted using RasCal

Figure 5.27 shows the SLD profile for the data fitted in figure 5.26. A summary of the fit parameters for the data in figure 5.26 is shown in table 5.2.

Layer	Thickness, d / Å	SLD, N _b / Å ⁻² × 10 ⁻⁶	Roughness, σ / Å	Hydration, % v/v
H ₂ O	Bulk	-0.57	N/A	Bulk
d-Tween 0.5 mM	148.2 ± 12.1	4.98	75.6 ± 19.7	43.5 ± 11.7
d-Tween 1 mM	170.9 ± 7.4	4.98	87.3 ± 4.2	39.2 ± 5.2
d-Tween 2.3 mM	153.7 ± 38.7	4.98	104.9 ± 25.6	37.4 ± 13.7
d-Tween Wash	119.9 ± 12.9	4.98	143.9 ± 20.3	28.9 ± 6.8
Ag	400.1 ± 17.1	3.00 ± 5.83E-8 4.03 ± 5.39E-8	74.4 ± 8.5	24.3 ± 6.4
MPTS	108.4 ± 7.1	1.54 ± 5.21E-8	57.7 ± 6.1	24.4 ± 4.6
Quartz	Bulk	4.182	6.8 ± 0.8	N/A

Table 5.2 Fit parameters for the reflectivity profiles in figure 5.26

Figure 5.27 depicts the SLD profile generated from the fitted parameters in table 5.2 for the data in figure 5.26. The SLD for the d-Tween surfactant layer was fixed. The smooth lines indicate rougher interfacial surfaces highlighted by the high values for the roughness of silver (74.4 Å) and d-Tween (75.6-143.9 Å). This is not unexpected given that Tween 20 is a large, complex molecule.

The surprising result from this fit is the increase in the SLD of Ag from $3.0 \times 10^{-6} \text{ Å}^{-2}$ to $4.03 \times 10^{-6} \text{ Å}^{-2}$ when the d-Tween is added. As observed with the h-DDAA experiments, the Ag surface has a degree of porosity (24.3%) meaning that the solvent can diffuse through the surface. In addition to this, both the Ag surface and d-Tween layers are quite rough. The porosity of the Ag would mean that the silver particulates allow water to pass through, which would explain the increase in the roughness. AFM results reveal a roughness of ca. 15 Å. If the roughness of the silver is increased, the d-Tween will not adsorb uniformly, thus increasing the SLD of the silver. In addition to this, once the experiment was completed and the quartz block removed from the cell, the Ag surface was beginning to delaminate. This suggests that the d-Tween and increased porosity of the Ag has caused the Ag to be removed.

5.2.3.2.2 h-Tween Adsorption

The reflectivity measurements for the hydrated analogue of Tween were performed in D₂O to achieve maximum contrast.

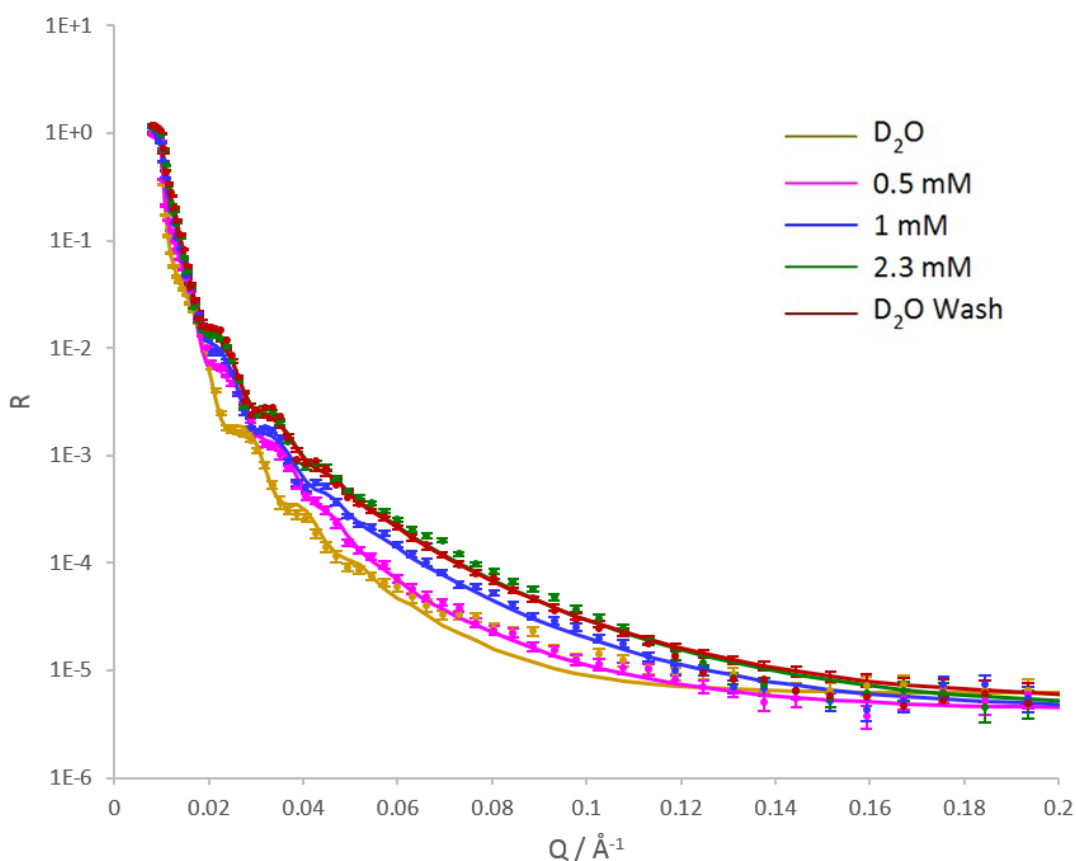


Figure 5.28 - Neutron reflectivity profiles for the adsorption of h-Tween in D₂O with the bare silver surface in D₂O. The circles represent the measured data and the lines are the respective fits of that data, fitted using RasCal ($\chi^2 = 86.4$ for whole data set)

Figure 5.28 represents the reflectivity profiles for the characterisation of the Ag surface in D₂O and the adsorption of h-Tween (0.5-2.3 mM) with the washing of the surface in D₂O. The value of Q_c can be estimated using equation 5.1 and as this experiment was performed in D₂O, the ΔN_b is equal to $2.073 \times 10^{-6} \text{ \AA}^{-2}$. This gives a predicted value of 0.01 \AA^{-1} , which corresponds to the observed value.

The reflectivity profiles indicate that there is evidence of adsorption on the Ag surface with the increased fringes shown from the yellow trace compared to the pink

trace. The profiles between the varying concentrations change slightly suggesting that the increase in concentration of h-Tween has an effect on its adsorption. The red trace highlighting the D₂O wash is practically identical to the green trace for 2.3 mM of h-Tween. This indicates that the h-Tween layer is not removed after washing. However, the SLD profile reveals an issue with the interfaces, which can be seen in figure 5.29. The Ag layer should have a defined thickness but the SLD profile shows the Ag layer smeared into the surfactant layer.

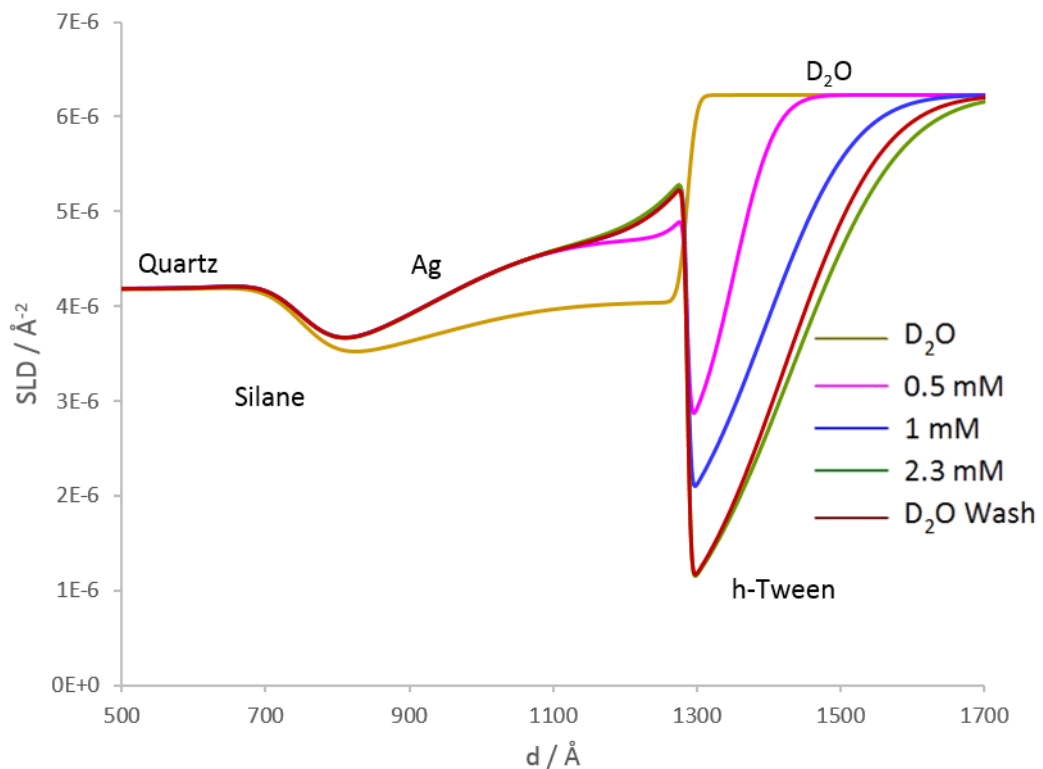


Figure 5.29 - SLD profile for the adsorption of h-Tween in D₂O. Data from figure 5.26 and fitted using RasCal

The fitted parameters for the data in figure 5.29 are summarised in table 5.3. The SLD of the h-Tween layer was fixed.

Layer	Thickness, d / Å	SLD, N _b / Å ⁻² × 10 ⁻⁶	Roughness, σ / Å	Hydration, % v/v
D ₂ O	Bulk	6.25	N/A	Bulk
h-Tween 0.5 mM	64.8 ± 4.8	0.35	45.4 ± 5.6	35.3 ± 2.3
h-Tween 1 mM	107.3 ± 19	0.35	97.9 ± 14.9	15.8 ± 2.5
h-Tween 2.3 mM	143.4 ± 30.7	0.35	119.9 ± 7.3	2.2E-10 ± 0.8
h-Tween Wash	133.9 ± 23.6	0.35	108.2 ± 8	0.9 ± 2.1
Ag	356.5 ± 8.9	3.00 ± 4.17E-8 4.00 ± 7.01E-8	10 ± 0.1 4.1 ± 1.1	32.4 ± 2.1
MPTS	180 ± 5.9	2.83 ± 2.08E-7	138.6 ± 18.7	15.1 ± 4.4
Quartz	Bulk	4.182	40.7 ± 7.7	N/A

Table 5.3 - Fit parameters for the reflectivity profiles in figure 5.28

The fitted parameters in table 5.3 confirm that washing the surface did not remove the h-Tween as the thickness only decreased from 143.4 Å to 133.9 Å. The h-Tween does adsorb onto the surface at 0.5 mM but the thickness increases by 60% from 64.8 Å to 107.3 Å for 1 mM of h-Tween. As Tween 20 is a much larger molecule compared to DDAA and structurally it has several repeating carbon and ether chains, the thickness values obtained could apply to a single layer.

The SLD profile indicates an issue with the Ag surface as the interfaces appear smeared in the profile instead of distinct quartz, silane and a silver surface. This is evident from the very high value for the quartz substrate (40.7 Å) and for the silane roughness (138.6 Å) compared to a low Ag roughness of 4.1 Å when the surfactant is added. The level of hydration on the silver layer is also higher than previously seen for h-DDAA and d-Tween adsorption at 32.4 %. Neutron reflectivity requires surfaces to be anatomically flat and homogeneous and as figure 5.29 reveals, this surface was not entirely suitable. Therefore, the surfactant adsorption in this case is unreliable.

5.2.3.3 DDAA/Tween 20 Co-Adsorption

The surfactant component of the PD working solution is added as a detergent system: DDAA and the non-ionic surfactant. Therefore, the final neutron experiment involved the co-adsorption of both DDAA and Tween 20. From section 5.2.3.1, the

reflectivity profile for h-DDAA did not change at ca. 8 mM and this was chosen as the maximum concentration (3.5-8 mM). In section 5.2.3.2, it was evident that the d-Tween reflectivity profile did not change after 0.5 mM, so this concentration was used for the d-Tween. In the co-adsorption, h-DDAA and d-Tween were chosen for contrast and the experiment was run in D₂O.

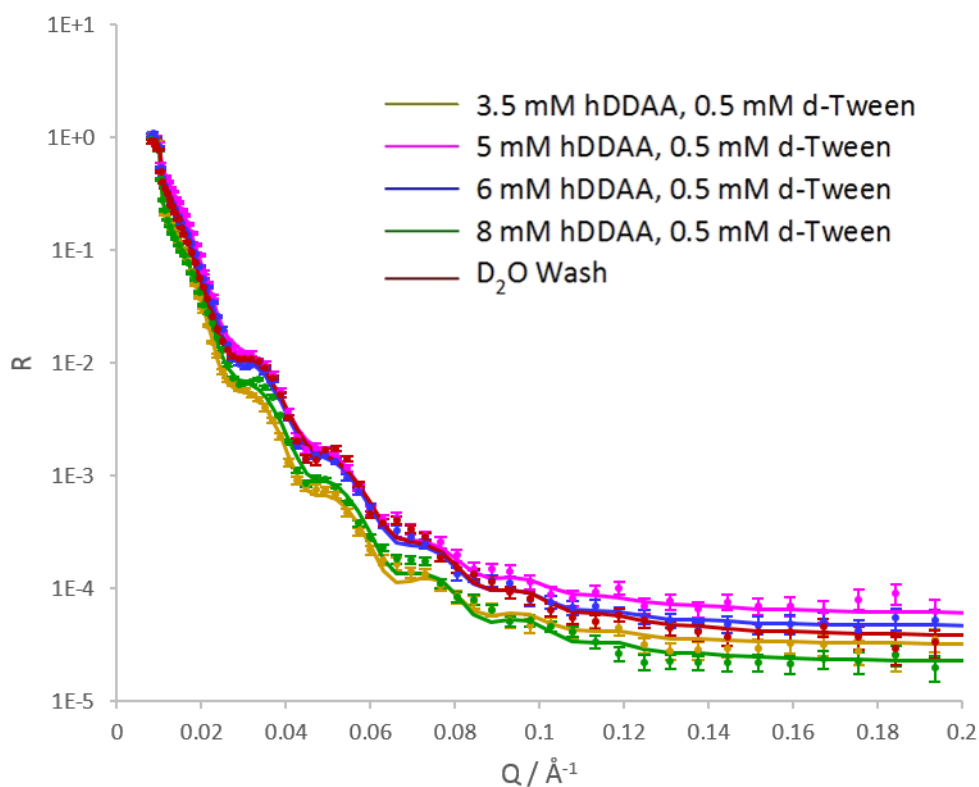


Figure 5.30 - Neutron reflectivity profiles for the adsorption of h-DDAA and d-Tween in D₂O. The circles represent the measured data and the lines are the respective fits of that data ($\chi^2 = 82.5$ for whole data set)

Figure 5.30 reveals the reflectivity profiles for the co-adsorption data. The characterisation of the Ag block in D₂O alone has not been included as the data was not usable. The critical edge for each data set had to be scaled meaning that during the experiment, the sample could have become misaligned or there could have been air in the sample. Nonetheless, the adsorption isotherm data could still be fitted.

From figure 5.30, it is evident that the hydrated surfactant, DDAA, is dominant in the adsorption comparable to the reflectivity profile observed for h-DDAA in figure

5.20. However, when the SLD profile is considered, there appears to be issues with the Ag surface, similarly to the observations for the h-Tween adsorption in figure 5.29.

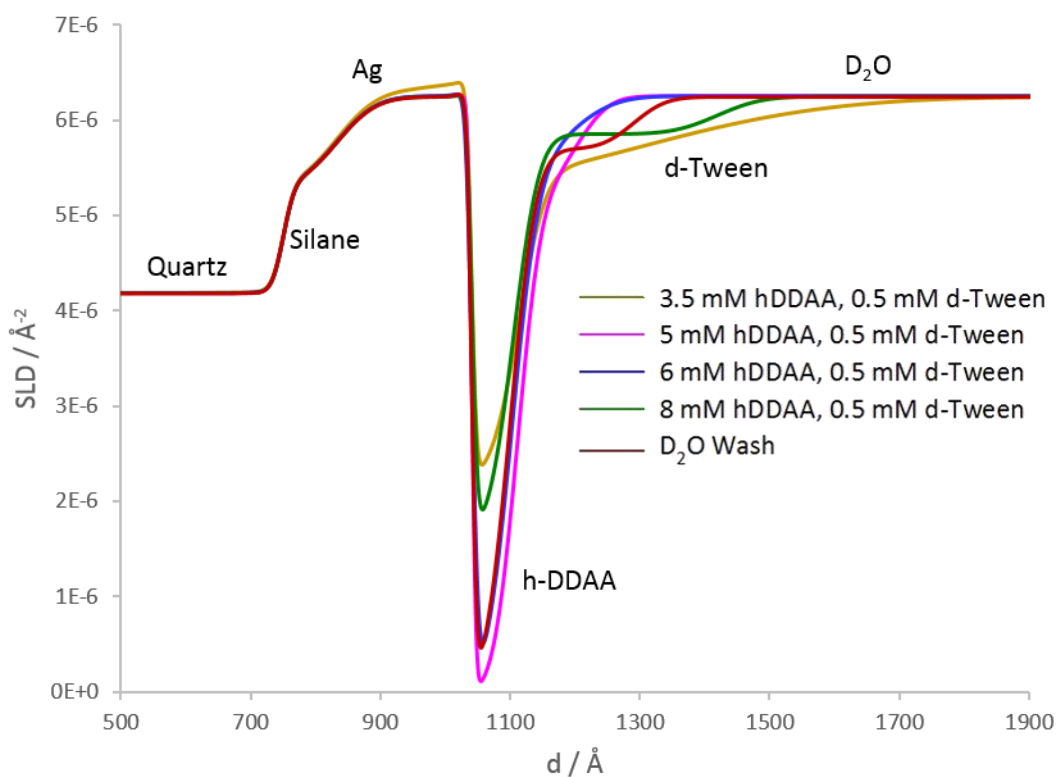


Figure 5.31 - SLD profile for the adsorption of h-DDAA and d-Tween in D_2O . Data from figure 5.30, fitted using RasCal

Figure 5.31 represents the SLD profile for the fitted data in figure 5.20 and table 5.4 summarises the fitting parameters. The SLDs for the h-DDAA and d-Tween were fixed at $-0.038 \times 10^{-6} \text{ \AA}^{-2}$ and $4.98 \times 10^{-6} \text{ \AA}^{-2}$ respectively.

Layer	Thickness, d / Å	SLD, N _b / Å ⁻² × 10 ⁻⁶	Roughness, σ / Å	Hydration, % v/v
D ₂ O	Bulk	6.25	N/A	Bulk
h-DDAA 3.5 mM	72.2 ± 1.9	-0.038	32.4 ± 2.7	33.2 ± 1.5
d-Tween	179.8 ± 12.5	4.98	241.8 ± 12.3	25.1 ± 6.1
h-DDAA 5 mM	70.2 ± 2.3	-0.038	28.9 ± 2.6	5.35E-5 ± 0.3
d-Tween	93.2 ± 14.5	4.98	38.3 ± 6.2	31.7 ± 4.4
h-DDAA 6 mM	61.1 ± 2.5	-0.038	31.9 ± 3.4	1.54E-5 ± 0.5
d-Tween	78.3 ± 20.2	4.98	59.8 ± 12.3	37.2 ± 4.4
h-DDAA 8 mM	63.8 ± 1.7	-0.038	31.3 ± 3.2	25.9 ± 1.1
d-Tween	314.7 ± 20.2	4.98	54.1 ± 9.3	72.7 ± 2.9
h-Tween Wash	59.6 ± 1.9	-0.038	31.3 ± 3.9	1.56E-4 ± 0.9
d-Tween Wash	190.5 ± 14.9	4.98	39.4 ± 5.6	62.2 ± 6.2
Ag	208.8 ± 3.7	3.18 ± 7.75E-9	6.2 ± 0.9 5.1 ± 0.2 7.7 ± 1.2 6.9 ± 1.7	100 ± 0.3
MPTS	81.9 ± 3.1	2.95 ± 9.78E-8	48.2 ± 1.4	70.7 ± 2.4
Quartz	Bulk	4.182	13.9 ± 1.2	N/A

Table 5.4 - Fit parameters for the reflectivity profiles in figure 5.26. The values for the Ag roughness in black correspond to 3.5 mM h-DDAA, red to 5 mM h-DDAA, blue to 6 mM h-DDAA and green to 8 mM h-DDAA

The value for the critical edge can be determined using equation 5.1 and the SLD of D₂O (6.247 × 10⁻⁶ Å⁻²) and quartz (4.182 × 10⁻⁶ Å⁻²). This gives a predicted Q_c value of 0.01 Å which is consistent with the observations.

The thickness parameters obtained for h-DDAA are also very consistent both between the individual values (67 ± 5 Å) and to the values recorded in table 5.1. The SLD profile is less consistent such that the adsorption does not increase with the increase in the DDAA concentration. 8 mM appears to have adsorbed less but this could be due to the addition of d-Tween 20 to the system.

Due to practical and instrument limitations, the AFM data for the block used in this neutron experiment could not be completed. However, the estimated thickness of

the Ag layer can be determined using equation 5.2 and a ΔQ value of 0.025 Å. This produces an estimated thickness of 251 Å which is 42 Å higher than the fitted value of 209 Å. The estimated thickness and fitted value are not too dissimilar but the Ag layer is noticeably thinner than the experiments for h-DDAA and Tween 20. In this experiment, only a thinner layer of Ag could be sputtered onto the quartz blocks. It has been noted that the Ag surface for the h-DDAA and Tween experiments was porous but the data from figure 5.30 has a hydration level of 100%. This is a very unreliable result as this indicates that there is no silver layer but the profiles indicate adsorption to the surface. The generated SLD profile in figure 5.31 indicates an issue with the substrate as the silane and Ag layer are not distinct, which was also observed in figure 5.29. The data suggests that there could be a layer of water on the Ag surface which would affect the surfactant adsorption.

The thickness of the h-DDAA layer is comparable to the values in section 5.2.3.1 and does not change significantly as the concentration is increased. In comparison to the d-Tween experiment in section 5.2.3.2, the thickness of the adsorbed d-Tween layer varies dramatically for the varying concentrations of DDAA. The inconsistencies observed with the d-Tween thickness and roughness values could be a result of the poorer Ag surface. The concentration of d-Tween was kept constant at 0.5 mM but the hydration parameters are also relatively high. The h-DDAA layers have very low hydration values suggesting a compact layer. This means that the h-DDAA molecules are closely packed on the Ag surface such that water molecules cannot penetrate the surfactant layer.

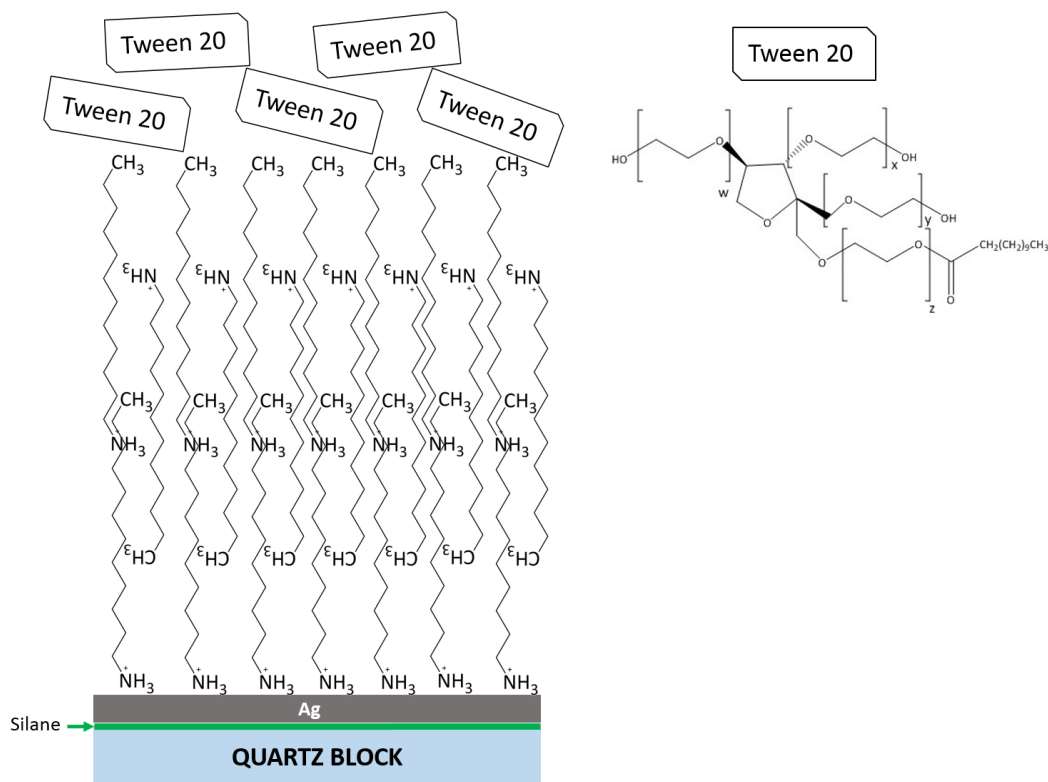


Figure 5.32 - Proposed structure of *h*-DDAA and *d*-Tween on the planar silver surface

Figure 5.32 represents the proposed structure from the co-adsorption data. The *h*-DDAA successfully competes with the *d*-Tween to adsorb onto the silver surface. The Tween 20 forms part of the remaining solvent. This theory does agree with the current theory that the cationic surfactant forms a staggered micelle around the silver particles. However, due to the unreliability of the Ag surface in the co-adsorption experiment, these measurements would need to be repeated to be able to conclusively state that *h*-DDAA competitively adsorbs against *d*-Tween.

5.3 Conclusions

The need for a replacement non-ionic surfactant is imperative to the existence of PD. Tween 20 is an environmentally benign, readily available alternative. It has been shown to successfully develop 1 to 28 day old fingerprints on white copy paper but there were significant variations with the stability of the working solution and processing times.

A 2 week old working solution with the addition Tween 20 could only be prepared once and used for fingerprint development. Every other PD working solution with Tween 20 either had to be used immediately or lasted up to 2 days. The development times also varied from a maximum of 15 minutes to a maximum of 30 minutes. The development time could be extended to an hour but this did not improve the quality of the image and in some cases reduced the clarity of ridge detail. As a replacement for Synperonic N, it will work in the same way and produce fingerprints that are of identifiable quality. However, the inconsistencies between the preparation of the working solutions and the processing times limit the reproducibility. In addition to this, a standard operating procedure could not be produced.

Neutron reflectivity measurements have enabled a greater understanding of the roles of the cationic and non-ionic surfactant components in the PD working solution. DDAA adsorbs onto a silver surface as a multilayer. The d-Tween measurements revealed adsorption onto the silver surface but the h-Tween experiment highlighted an issue with the silver surface. In the co-adsorption experiment, the same issue was observed with the preparation of the silver surface. However, DDAA adsorption was dominant. These results suggest that the proposed conformational structure of the cationic surfactant molecules surrounding the colloidal silver in the solution is highly probable. To ensure the co-adsorption measurements are reliable, the experiment would have to be repeated with a suitable silver surface.

5.4 References

1. CAST, *Home Office Centre of Applied Science and Technology Fingerprint Visualisation Manual* 1st edn., 2014.
2. *Directive 2003/53/EC of the European Parliament and of the Council, Council Directive 76/769/EEC*, 2003.
3. R. Ramotowski and A. A. Cantu, *Fingerprint Whorld*, 2001, 27, 59-65.
4. H. Jonker, A. Molenaar and C. J. Dippel, *Photographic Science and Engineering*, 1969, 13, 38-43.

5. H. Jonker, L. K. H. van Beek, C. J. Dippel, C. J. G. F. Janssen, A. Molenaar and E. J. Spiertz, *Journal of Photographic Science*, 1971, 19, 96-105.
6. V. G. Sears, *Personal Communication* 2014.
7. M. de la Hunty, *Personal Communication* 2016.
8. M. de la Hunty, S. Moret, S. Chadwick, C. Lennard, X. Spindler and C. Roux, *Forensic Science International*, 2015, 257, 481-487.
9. R. Ramotowski, *Lee and Gaensslen's Advances in Fingerprint Technology, Third Edition*, CRC Press Inc, GB, 2013.
10. M. de la Hunty, S. Moret, S. Chadwick, C. Lennard, X. Spindler and C. Roux, *Forensic Science International*, 2015, 257, 488-495.

Chapter 6: Reformulation and Optimisation of Physical Developer

6.1	Introduction	172
6.2	Results	172
6.2.1	Reformulation of the PD Working Solution with Alternative Non-Ionic Surfactants	172
6.2.2	Raman Spectroscopy of Surfactant Adsorption	204
6.2.3	Extension of PD to Alternative Porous Surfaces	211
6.3	Conclusions	218
6.4	References	219

6.1 Introduction

Physical developer is a valuable fingerprint development technique and without it, UK law enforcement will lose the capability to develop any fingerprints on wetted porous surfaces. In addition, the advantage of developing further fingerprints by using PD as the last process in the porous surface sequence will cease to be an option. Results discussed in chapter 5 have indicated the need for a non-ionic surfactant component to replace the currently used Synperonic-N. Tween 20 is being used in Australia, parts of Europe and the United States but results using this formulation in this thesis and within the UK are extremely varied in terms of efficacy, stability of solutions and the working parameters. This section critically evaluates two potential replacements – Brij C10 and decaethylene glycol mono-dodecyl ether (DGME).

In addition to evaluating the detergent systems on a macroscopic level, i.e. the quality of the developed mark, the effect of the detergents on the size of silver particulates in solution will be explored through light scattering. Raman spectroscopy will be utilised to understand the interfacial relationship between the surfactant and a silver surface.

The possibility to extend the capability of PD will be investigated through the development of fingerprints deposited on alternative surfaces, such as leather and suede. These types of surfaces are known to be particularly difficult for the retrieval of identifiable fingermarks. PD will be compared to the conventional superglue fuming method.

6.2 Results

6.2.1 Reformulation of the PD Working Solution with Alternative Non-Ionic Surfactants

The formulations including Brij C10 and DGME, were tested in house within CAST and found to work similarly to the current formulation in terms of the quality of

fingerprint development as well as development times and appearance of the working solutions. Brij C10 and DGME are similar in chemical structure differing only in carbon chain length. The structures are shown in figure 6.1.

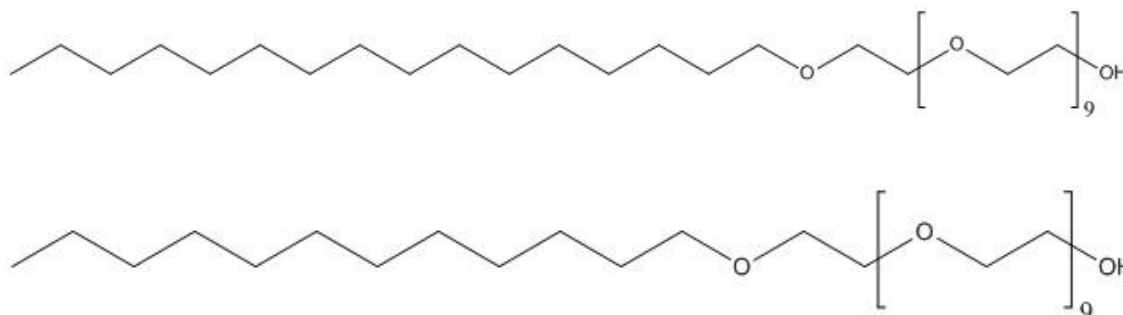


Figure 6.1 - Structure of Brij C10 (above) and DGME (below)

Unlike Tween 20 (see figure 1.11, chapter 1), Brij C10 and DGME are similar in chemical structure to Synperonic-N (see figure 1.10 chapter 1). Brij C10, DGME and Synperonic-N are all long chain hydrocarbon molecules with repeating ether functional groups, but Synperonic-N has additional methyl groups and a phenyl group in the carbon chain. The steric hindrance could aid the stability of the silver particles in the solution and the Brij C10 and DGME could effectively bend the carbon chain to wrap around the silver particle. The surfactant-silver interaction will be explored in section 6.2.2.

The results in the following section focus on a comparative study between the current Synperonic-N formulation and the two new formulations with Brij C10 and DGME, in terms of the deposition and growth of silver towards the fingerprint residue. The formulations are listed in chapter 3, section 3.2.3.5, table 3.5.

6.2.1.1 Brij C10

6.2.1.1.1 – Formulation 3 (PDF3B1)

Initial results collected by CAST indicated that using Brij C10 in the working solution was developing marks. In this thesis, Brij C10 was directly substituted for

Synperonic-N as well as reducing the concentration of the detergent used to test the effects on fingerprint development and stability of the working solution.

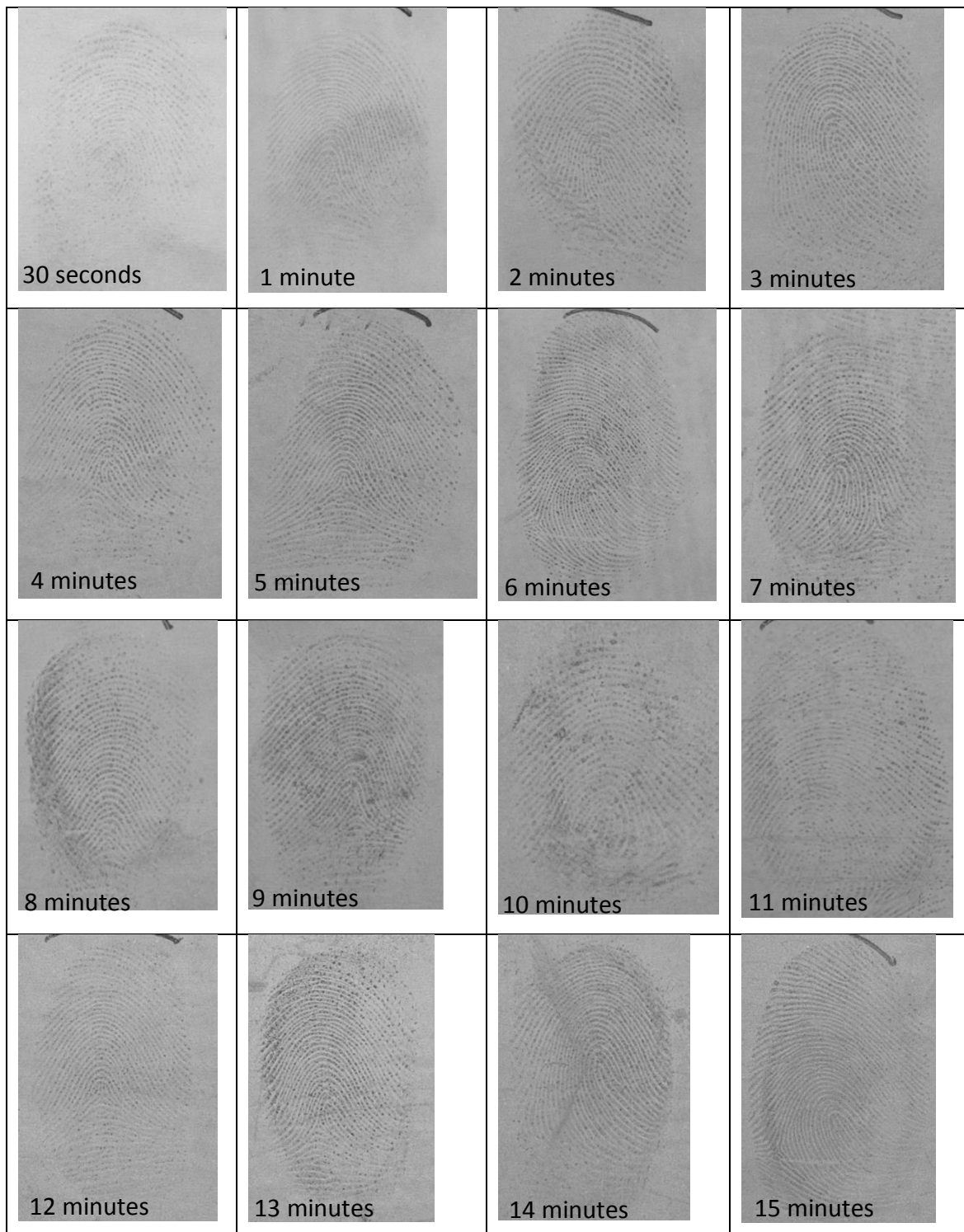


Figure 6.2 - The growth development of silver from 30 seconds to 15 minutes for fingerprints deposited on white copy paper and aged for 1 day under ambient conditions then developed via PDF3B1

Figure 6.2 shows the results of 1 day old fingerprints deposited on white copy paper and developed using formulation 3 at each time interval from 30 seconds to 15 minutes. (See chapter 3, table 3.5 for the meaning of the code). As figure 6.2 shows, the quality of the resulting developed fingerprints is very high in terms of contrast variation and clarity of ridge detail. After 1-2 minutes, a full fingerprint is visible to the naked eye and each of those fingerprints could be used for identification. The rapid development indicates the inherent instability of the silver in the working solution which was further proved by the working solution only lasting between 0-2 days. After this time, silvery deposits were visible, which is a clear sign the solution is not useable, but the working solutions would also become cloudy and green in colour (see figure 6.3).

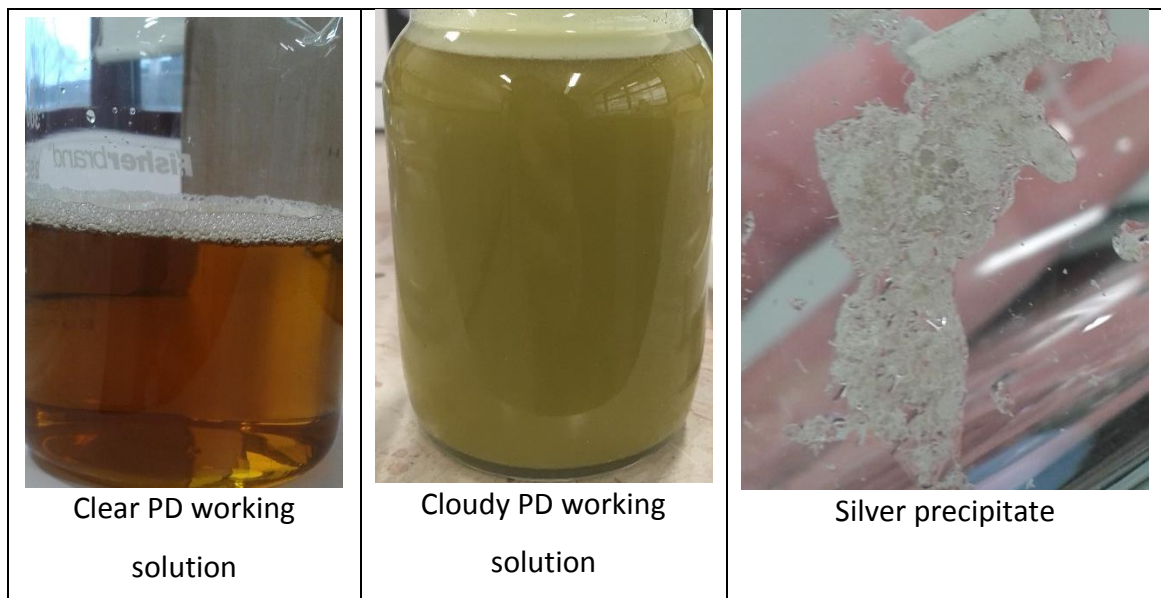


Figure 6.3 - Difference between a clear and cloudy PD working solution (0-2 days) and evidence of silver precipitation (0-2 days)

From a practitioner's perspective, shorter development times and the quality of the developed marks are desirable features. However, the variation in the shelf life of the working solution is an issue as a working solution made a day before use would become obsolete for fingerprint development. Ideally, a working solution needs to be stable, i.e. no silver deposition until use, for at least two days to allow the solution to be prepared the day before use.



Figure 6.4 - 3D microscopy images (50x) for the growth development of 1 day old marks processed for 30 seconds to 15 minutes for the samples in figure 6.2. Tick marks every 20 μm

Figure 6.4 shows the corresponding microscopy images to figure 6.2 which indicates the rapid deposition and growth of silver from the solution to the fingerprint residue. In comparison to the 1 day old fingermarks analysed in chapter 4, section 4.2.3, silver deposition is much clearer after 30 seconds in the microscopic image. However, the particle diameter was still between 2-3 μm . This suggests that, regardless of the detergent system used, the silver particles remain ca. 1 μm in the solution but the surfactant used only controls the timescale of development, not the outcome. In this case, it appears that formulation 3 is reducing the stability but this in turn increases the amount of silver deposited thus increasing the contrast of the developed fingerprint and the paper background. The general trend observed for the silver growth is the same as seen with the Synperonic-N detergent system as seen in figure 6.5.

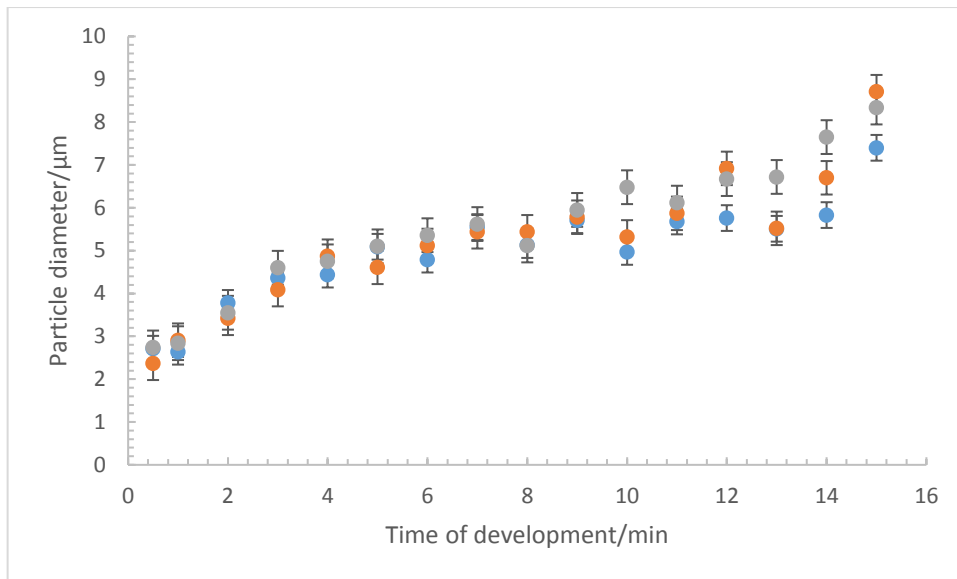


Figure 6.5 - Graph of silver particle diameter vs time of development for 3 sets of 1 day old marks aged under ambient conditions developed via PDF3B1. Data from figure 6.2 and two replicates

The only noticeable difference between the growth of silver in the presence of Brij C10 and Synperonic-N is the final diameter of the deposited silver particles (see figure 6.33 for clarification). As figure 6.5 shows, the final diameter in the presence of Brij C10 was 7-9 µm compared to 13-16 µm for the 1 day old fingerprints developed in the presence of Synperonic-N. Progressive growth is still observed with the Brij C10 system and the lower final diameter is a result of more initial sites of silver available at the beginning of the development process for subsequent silver growth. The silver particles are still monodisperse with a narrow particle size range and as the penultimate minutes of development show in figure 6.4, the silver deposits begin to aggregate as opposed to depositing in an alternative area of the fingerprint residue. This is the reason the ridges of the developed fingerprints lose the dotted appearance normally observed and the ridges can merge, distorting the unique ridge features of that print. Hence, monitoring of the PD process is required as it is not always necessary to develop for as long as 15 minutes.

6.2.1.1.2 – Formulation 4 (PDF4B2)

The following image, figure 6.6, shows the results of the silver growth for 1 day old developed fingermarks using formulation 4.

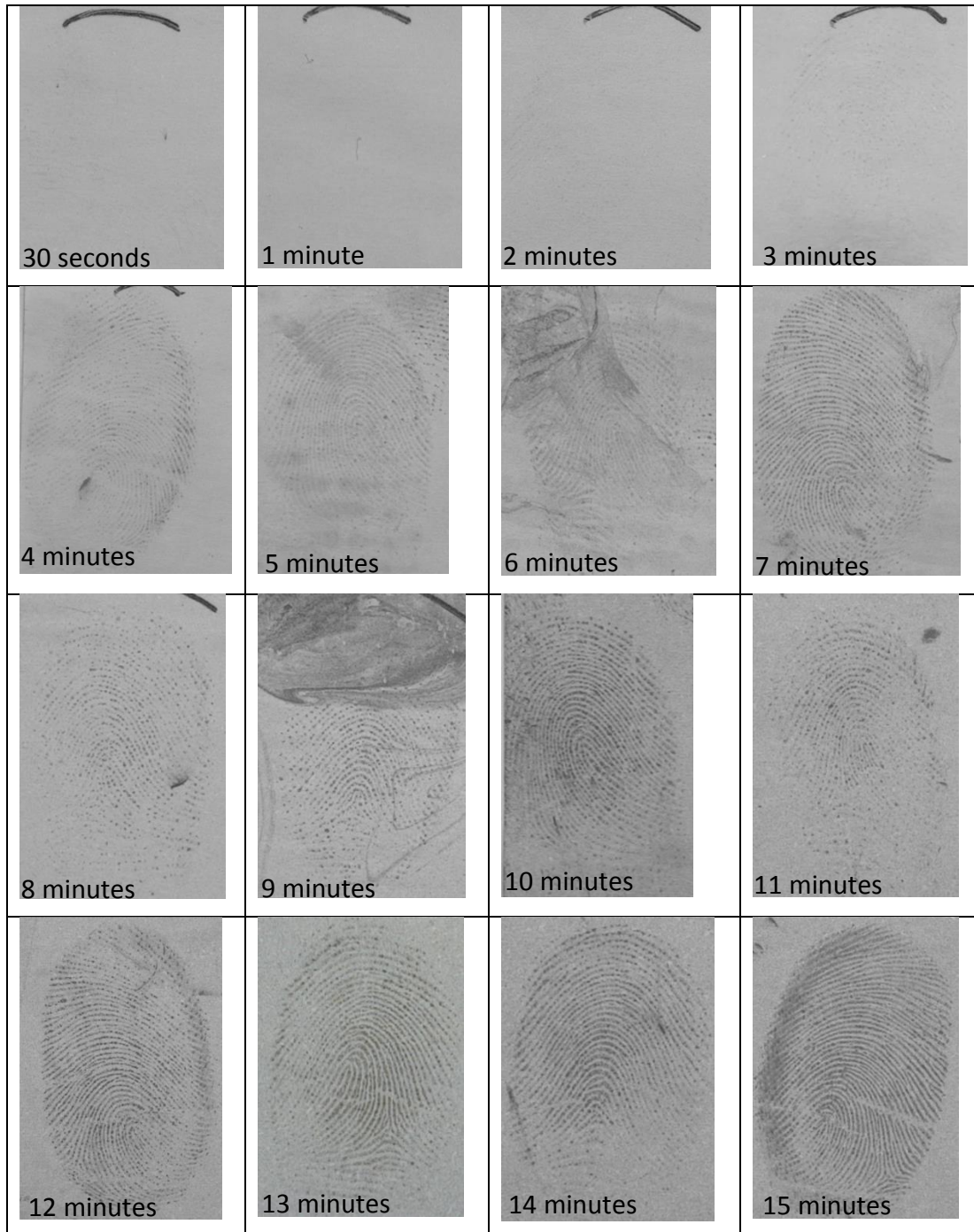


Figure 6.6 - Growth development from 30 seconds to 15 minutes for 1 day old marks deposited on white copy paper and aged for 1 day under ambient conditions then developed via PDF4B2

As figure 6.6 shows, the quality of the fingerprint development towards the latter stages of the 15 minute process is very high in terms of amount and clarity of the ridge detail. The rate of development is slower than for the results seen in figure 6.2. Fingerprint ridges are not visible until ca. 3 minutes and after 4 minutes the image resembles a fingerprint. After ca. 10 minutes, the quality of the fingerprint is neither hindered nor greatly improved with further development. The ridges do appear to become more continuous - to the naked eye – towards the end of the 15 minute development process. However, the microscopic analysis still reveals spherical and monodispersed silver deposits, which begin to aggregate as the particles grow in size and effectively get closer in proximity to each other.

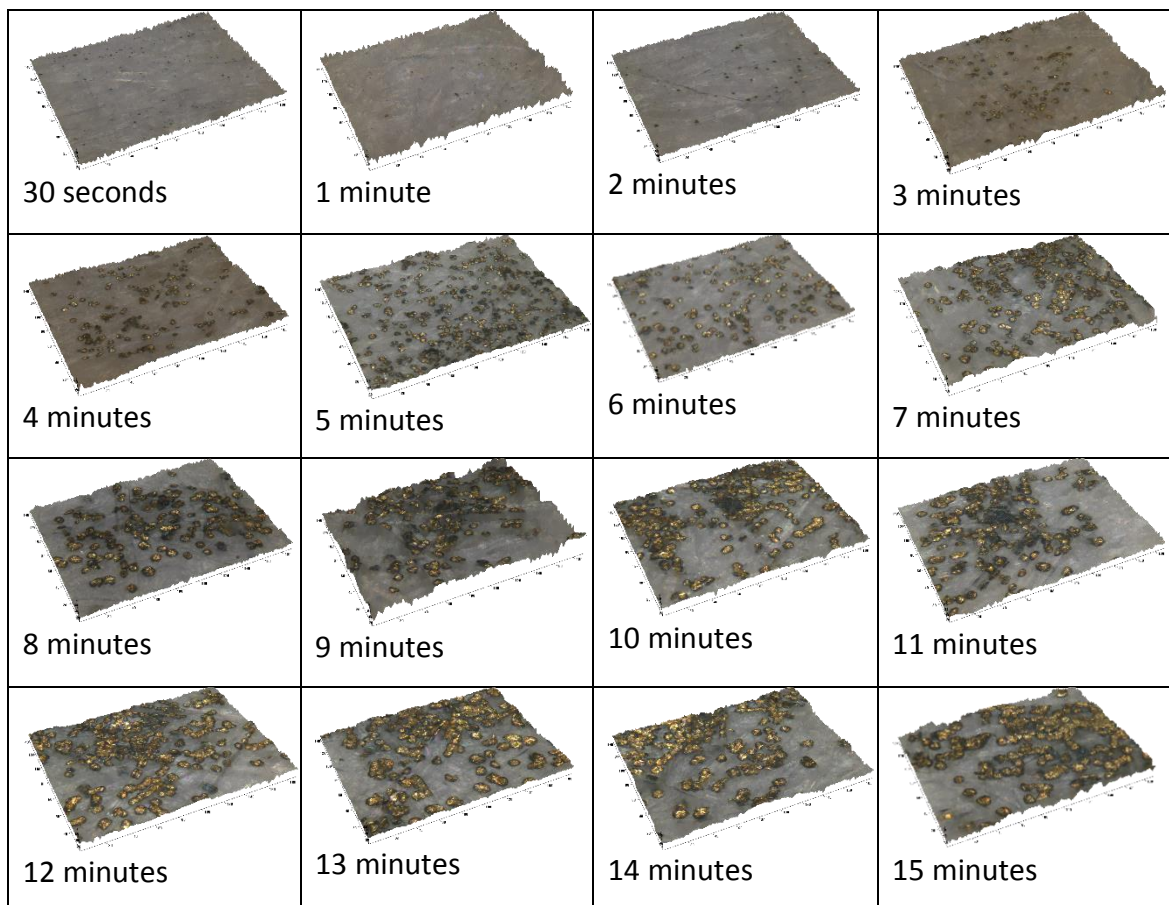


Figure 6.7 - 3D microscopy images (50x) for the growth development of 1 day old marks processed for 30 seconds to 15 minutes for the samples in figure 6.6. Tick marks every 20 μm

Figure 6.7 reveals the corresponding microscopic images to the 1 day old marks developed in figure 6.6. In comparison to figure 6.4, there is less silver deposition in the initial stages of development. There are still some silver deposits visible but there are not as many compared the results from formulation 3. This suggests that the increase in concentration of Brij C10 results in greater stabilisation. It could be that the increased amount of Brij C10 offers further steric hindrance to the silver particles and the cationic surfactant, DDAA. After ca. 3 minutes, nucleation of silver is evident and progressive growth is observed thereafter. After 10 minutes, the particle diameter is not changing sharply and the deposits can be seen aggregating. This is illustrated more clearly by the graph seen in figure 6.8.

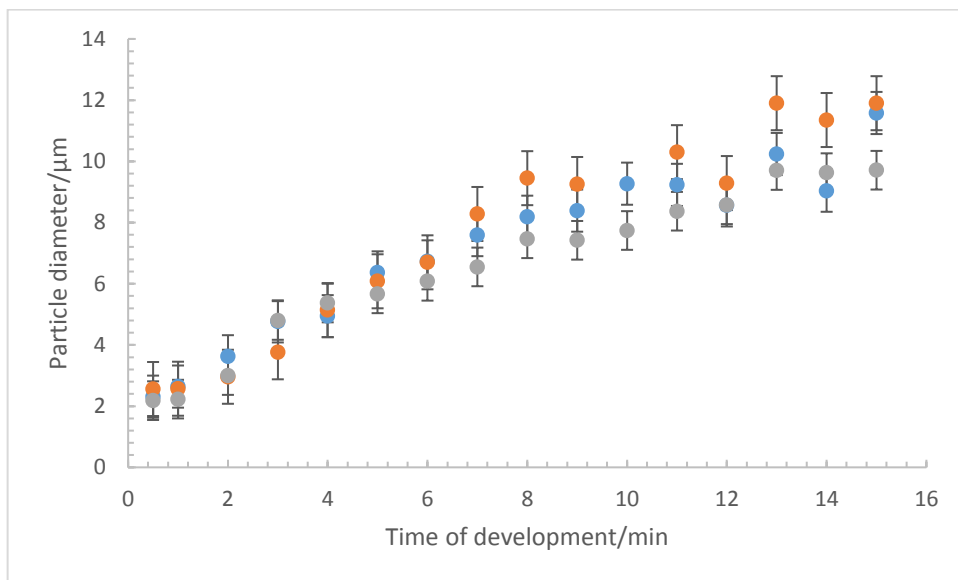


Figure 6.8 - Graph of silver particle diameter vs time of development for 3 sets of 1 day old marks aged under ambient conditions developed via PDF4B2. Data from figure 6.6 and two replicates

As seen in the growth results for the various detergent systems studied, the same trend in silver growth is observed. There is a slow increase in the particle diameter after 2 minutes (3-4 μm) up to 8 minutes (7-9 μm). The final particle diameter was recorded at 9-12 μm . This is larger than 7-9 μm seen for formulation 3 and not too dissimilar to the Synperonic-N system (13-15 μm). This is because, at the nucleation point, there are less initial silver sites for subsequent silver growth, as seen in figure 6.7.

The development time was extended to 20 minutes for a few fingerprints to observe whether the longer development time had any effects on the quality of the fingerprint as well as the nature of the silver deposits. Figure 6.9 shows three 1 day old fingerprints developed for 20 minutes and the corresponding microscopic images.

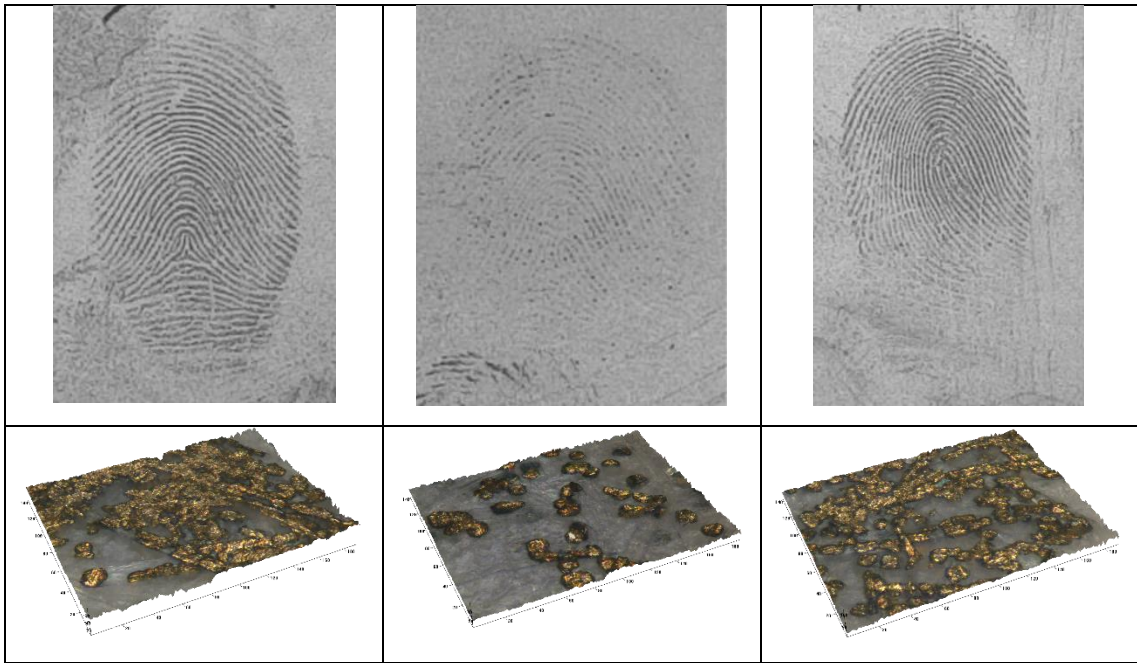


Figure 6.9 - 1 day old fingerprints deposited on white copy paper and aged under ambient conditions then developed after 20 minutes using PDF4B2 with corresponding microscopy data. Tick marks every 20 μm

The developed images reveal fingerprints of high quality aside from the second mark. The microscopic images correlate to the darker fingerprint ridges as the silver deposits appear to aggregate. However, the background staining also becomes darker and the ridges can become distorted losing the identifying features. The diameter for the second mark was 10-12 μm indicating that the silver deposits still grow on the surface with a narrow particle diameter range.

6.2.1.1.3 Split Print Development Using Formulation 4 (PDF4B2)

In order to begin to understand if the age of the mark is a factor for the development with the new detergent systems, split prints were studied which could be

aged up to 28 days. (This was not done with formulation 3 as the working solution was too unstable).

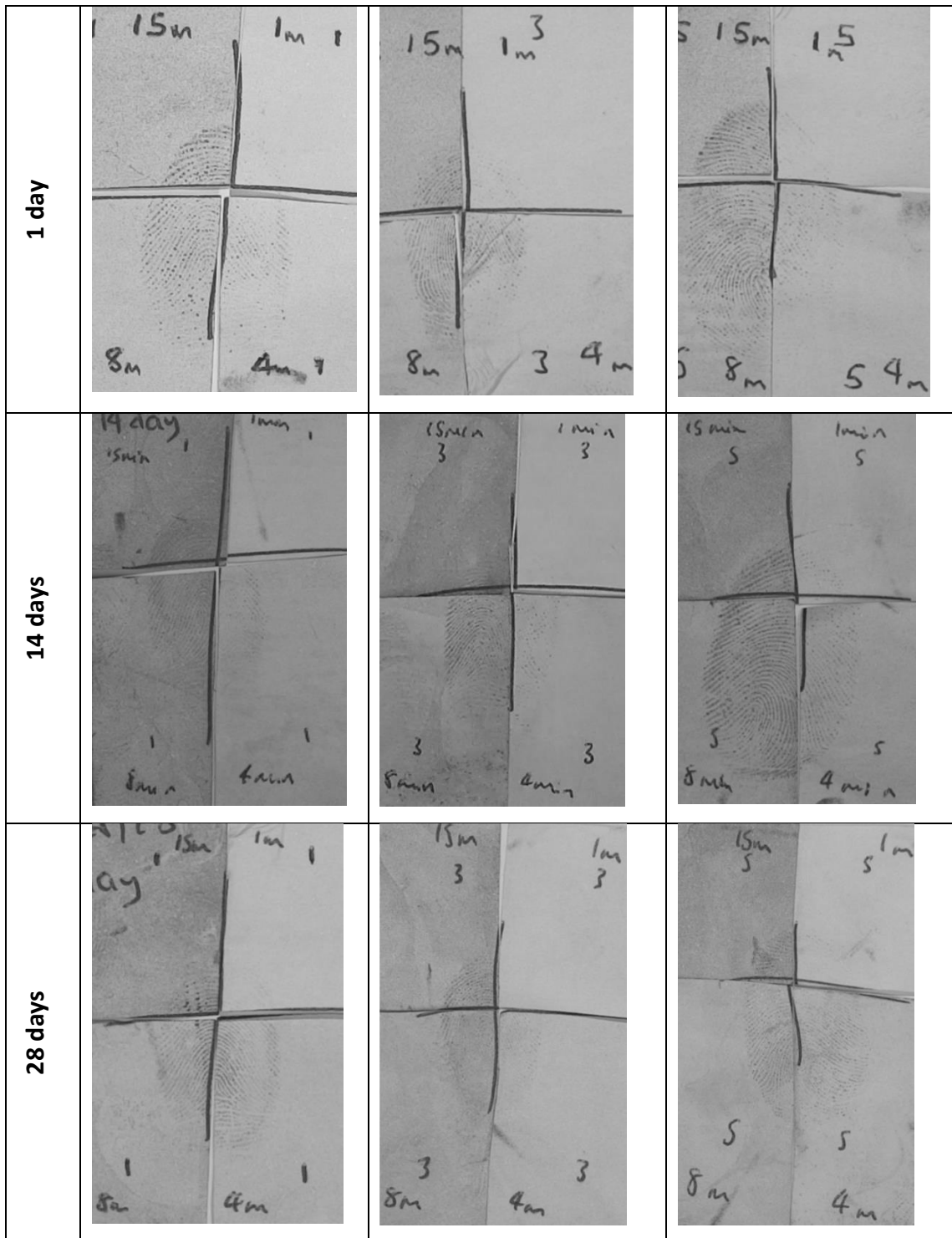


Figure 6.10 - Split prints deposited on white copy paper and aged for 1, 14 and 28 days under ambient conditions then developed via PDF4B2. 'm' refers to minutes. (3 replicates for each age of mark)

Figure 6.10 shows examples of 1, 14 and 28 day old split prints developed using 2.8 g Brij C10, formulation 4, in the detergent solution. Ageing the mark does not appear to greatly affect the resulting developed fingerprint in terms of quality of development. In comparison to the full fingerprints studied in section 6.1.1.1.2, the 15 minute quadrants are less developed in terms of contrast and ridge detail. This is a surprising result given that splitting the full fingerprint reduces the amount of fingerprint residue initially exposed for silver deposition. In this case, formulation 4 appears to be more stable than formulation 3.

The split prints do reveal the higher stability of the silver in the working solution as visible fingerprint detail is not clear until after 4 minutes. The older fingermarks show much fainter silver deposition, which is not ideal given that fingerprints from a scene are likely to be older than 1 day. This is due to the size of the silver deposits – the larger the particles are and the higher the amount, the darker the resulting developed ridges are. This is clear in the microscopy analysis as shown in figures 6.11-6.13 and the comparison graph in figure 6.14.

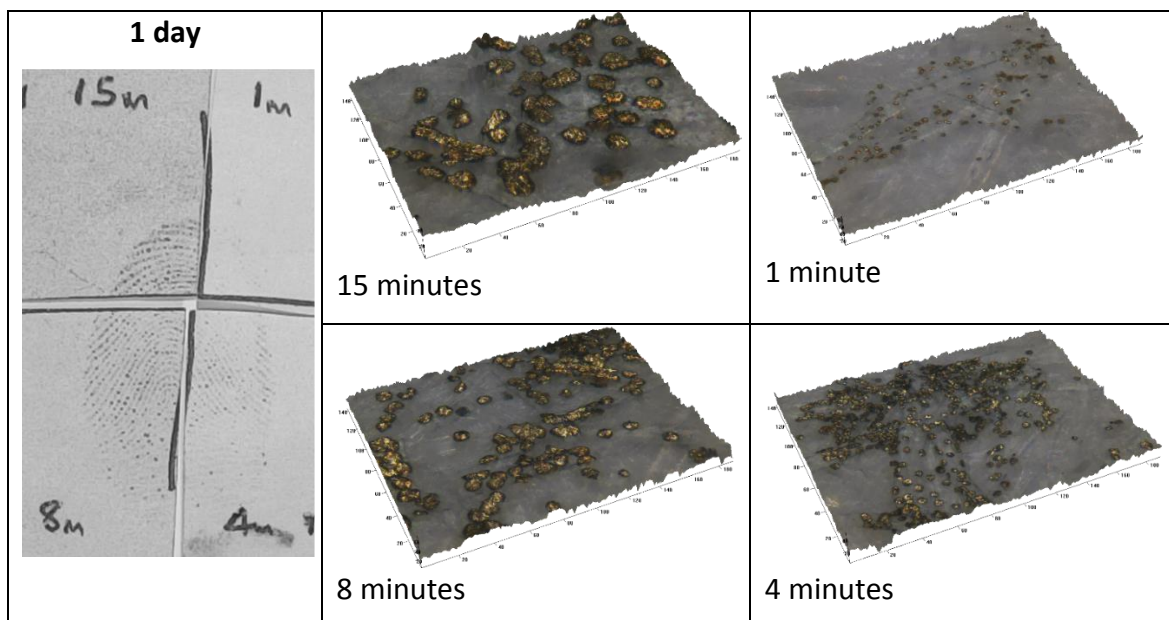


Figure 6.11 – 3D microscopy images (50x) for the growth development of a 1 day old mark processed for 1-15 minutes using PDF4B2. Tick marks every 20 μm

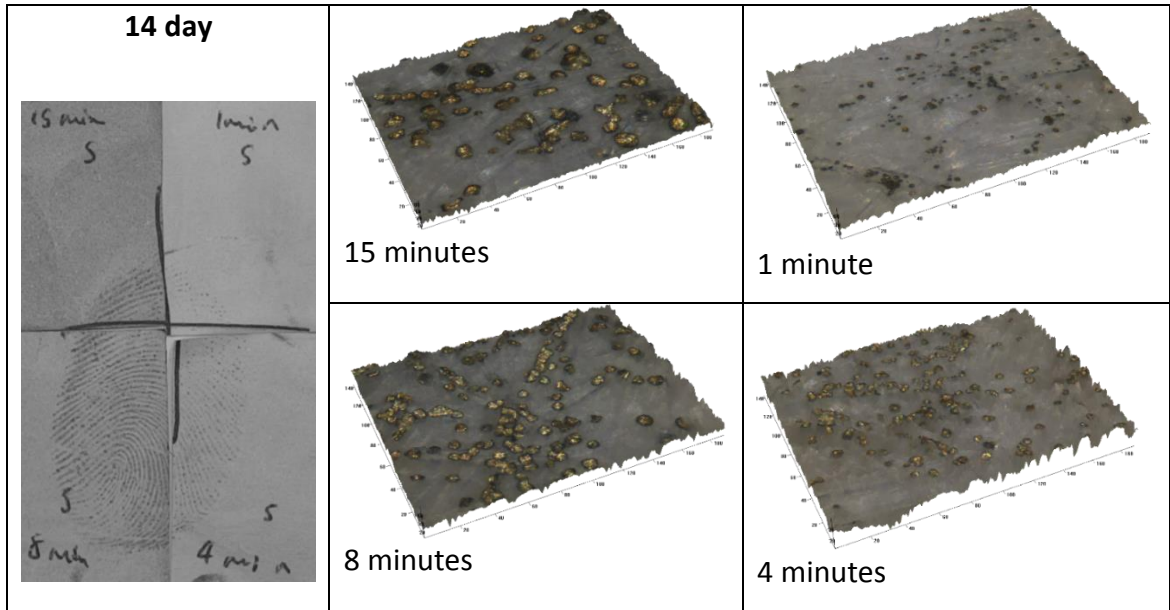


Figure 6.12 – 3D microscopic images (50x) for the growth development of a 14 day old mark processed for 1-15 minutes using PDF4B2. Tick marks every 20 μm

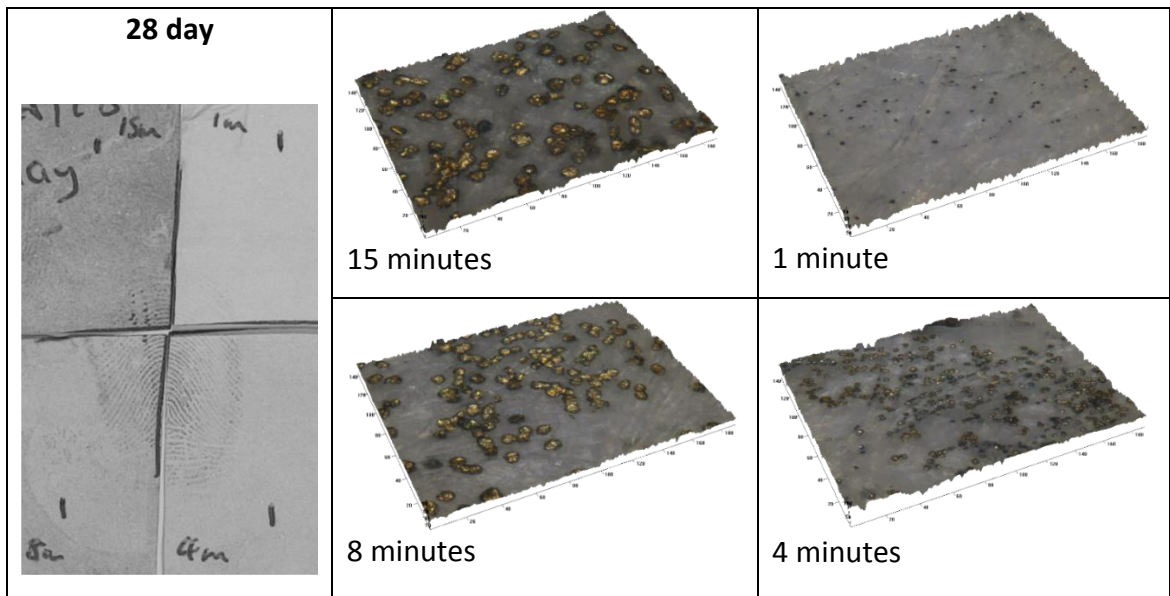


Figure 6.13 – 3D microscopy images (50x) for the growth development of a 28 day old mark processed for 1-15 minutes using PDF4B2. Tick marks every 20 μm

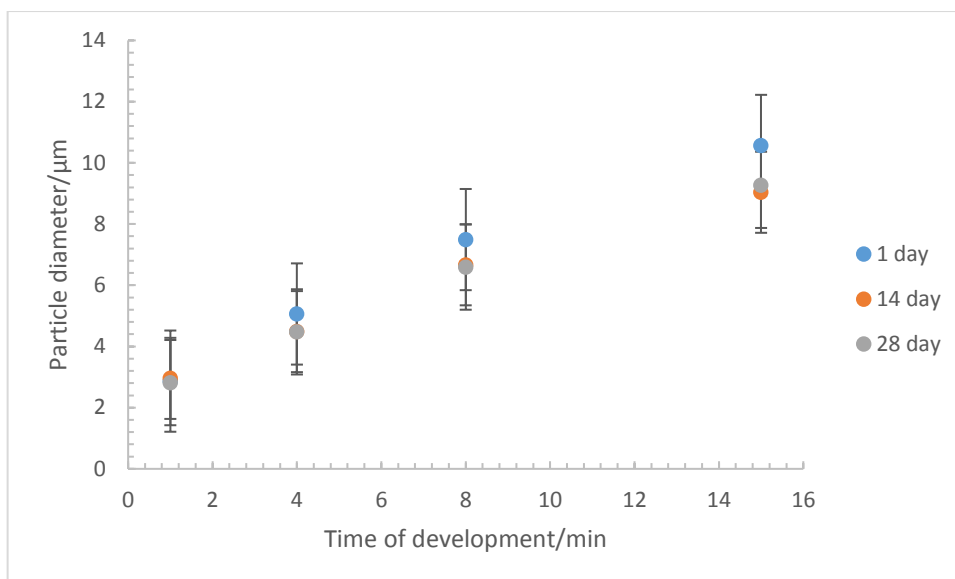


Figure 6.14 - Graph of silver particle diameter vs time of development for average of 5 sets of 1, 14 and 28 day old marks aged under ambient conditions developed via PDF4B2

Although the general trend in the growth of the silver deposits is the same as observed throughout this thesis, the ageing of the mark has affected the size of the deposits. Though this difference is not extensive in microscopic terms, the developed image is affected by fainter marks.

6.2.1.2 DGME

The nucleation and growth of silver was also explored for 0.0023 M DGME and directly substituting DGME for Synperonic-N. The one practical advantage that DGME has over Brij C10 is the preparation of the detergent solution. Brij C10 is a hard, waxy substance and heat has to be applied to allow for complete dissolution. This is a factor that will dissuade practitioners from using it compared to DGME which can be dissolved at room temperature.

6.2.1.2.1 – Formulation 5 (PDF5D1)

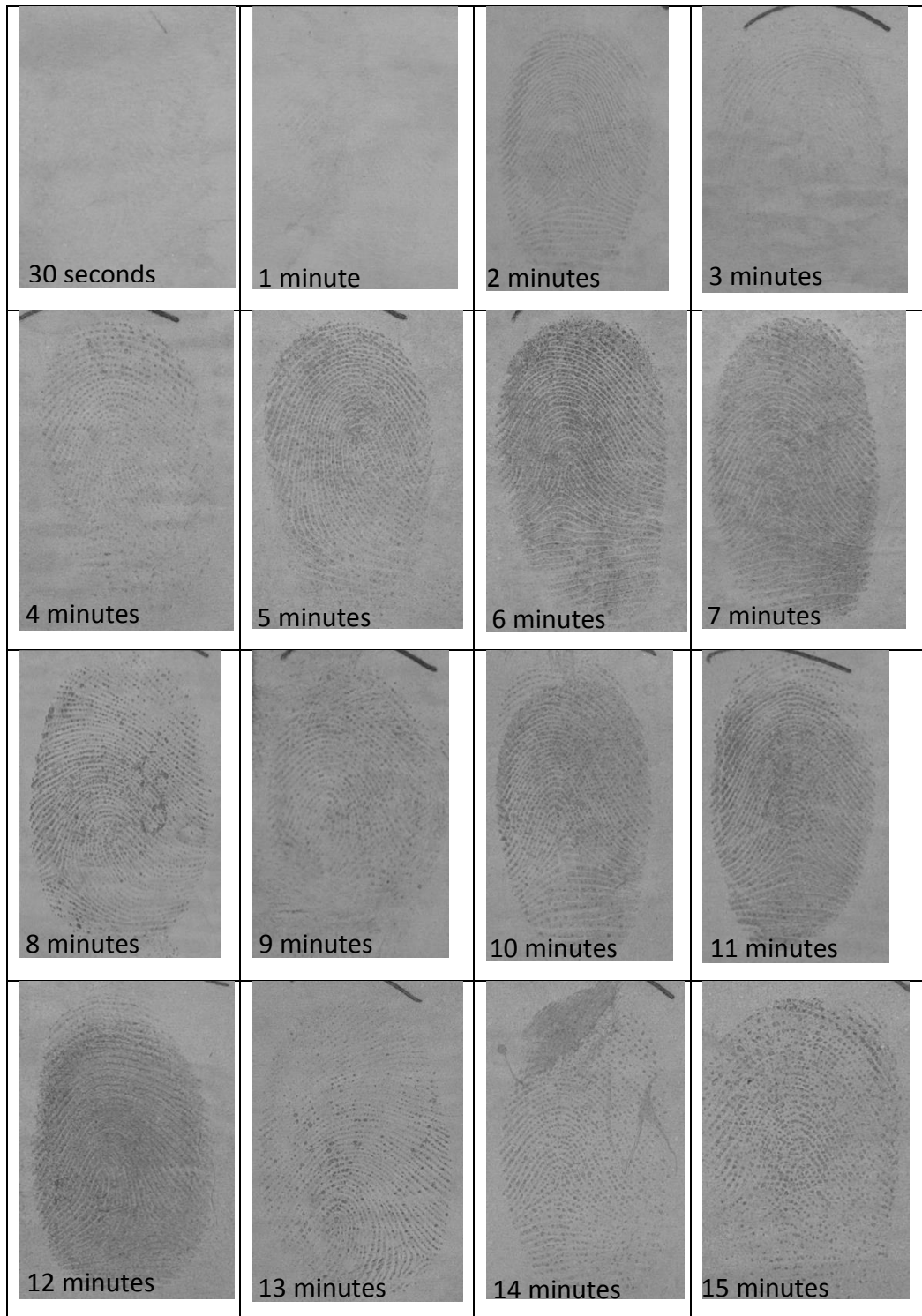


Figure 6.15 - The growth development of silver from 30 seconds to 15 minutes for fingerprints deposited on white copy paper and aged for 1 day under ambient conditions then developed via PDF5D1

Figure 6.15 shows the results of developing 1 day old marks using formulation 5 for time intervals between 30 seconds to 15 minutes. The developed fingerprints show high contrast between the ridges and the background as well as the typical 'dotted' appearance of the fingerprint. After 2 minutes, a full fingerprint is visible and some very faint ridges are visible after 1 minute, in comparison to formulation 3 where deposition was obvious after 30 seconds. This suggests that DGME is acting as slightly stronger stabiliser compared Brij C10. In addition to this, the working solution lasted between 5-7 days after use, further indicating a more stable colloidal dispersion. Though the fingerprints treated for 14 and 15 minutes appear less developed than the fingerprints at 6 and 7 minutes for example, the growth of the silver deposits follows the same trend observed throughout. Figure 6.16 shows the corresponding microscopy images to figure 6.15.

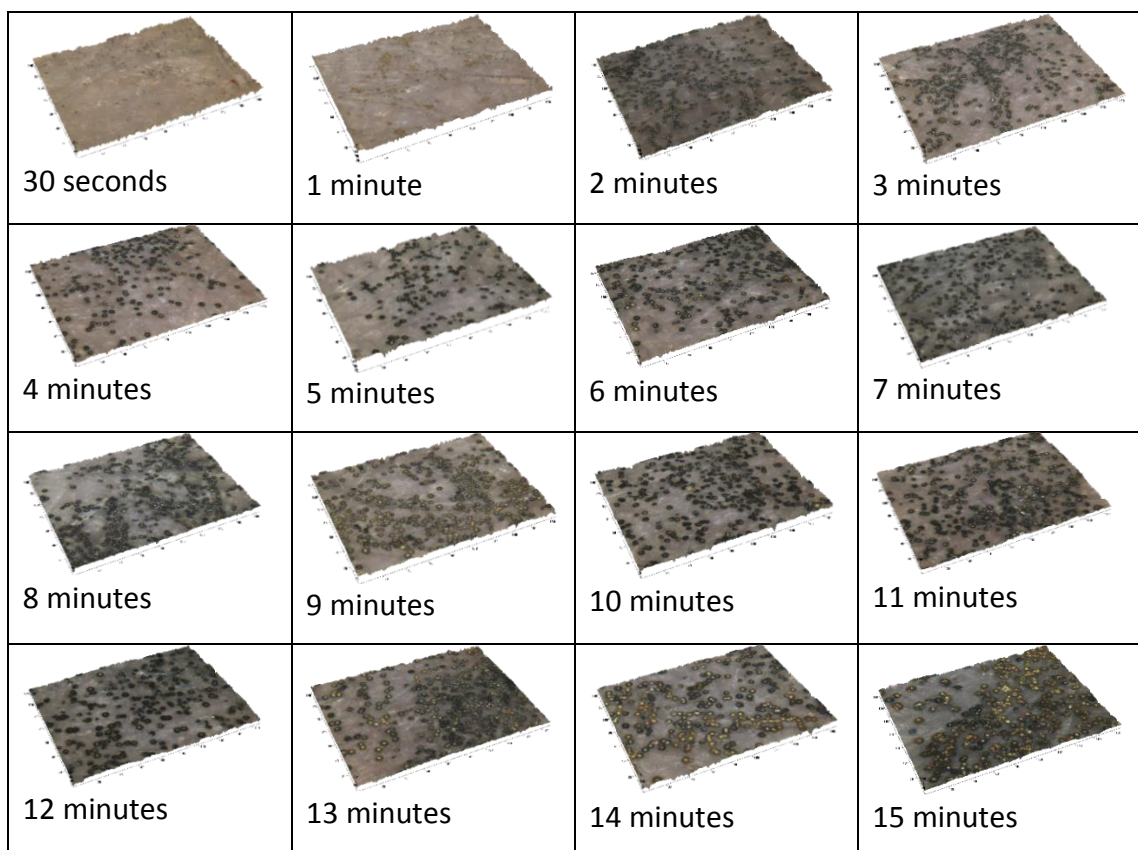


Figure 6.16 - 3D microscopy images (50x) for the growth development of 1 day old marks processed for 30 seconds to 15 minutes for the samples in figure 6.15. Tick marks every 20 µm

It is evident that the point of nucleation of the silver occurs after ca. 2 minutes as the density of silver deposits increases significantly. The deposits themselves are still monodisperse but are in closer proximity compared to those seen using Synperonic-N. This suggests that the silver is able to access more components of the fingerprint residue initially such that progressive growth occurs thereafter on more silver sites. The final diameter range was recorded at 7-9 μm which is still narrow but also smaller than observed with Synperonic-N. This is a reflection of the greater number of silver sites available at the beginning of the development process and indicates a level of stability in the working solution that encourages both shorter development times and high quality development.

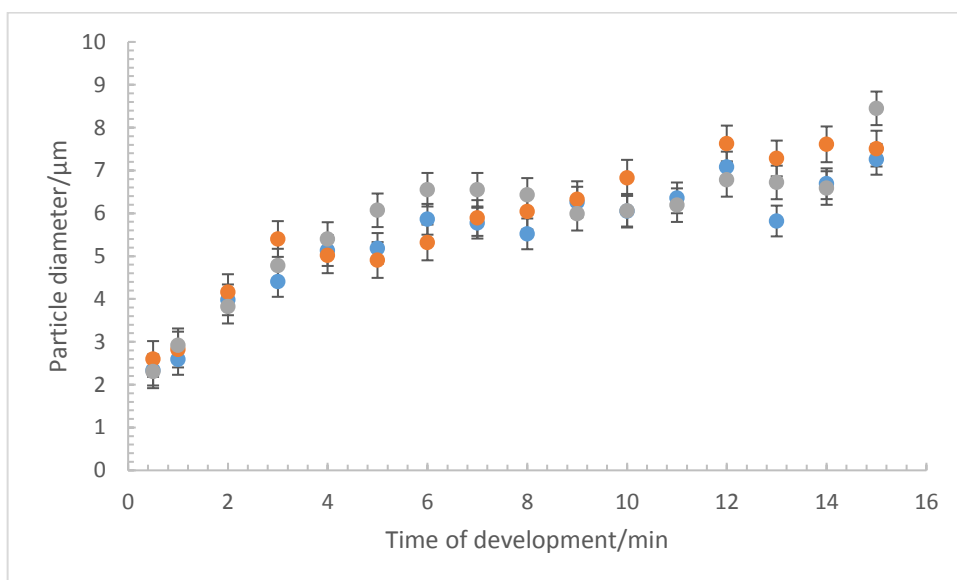


Figure 6.17 - Graph of silver particle diameter vs time of development for 3 sets of 1 day old marks aged under ambient conditions developed via PDF5D1

Figure 6.17 reveals the graph for the 1 day old growth development for the 1.5 g of DGME used in the detergent solution. The graph clearly indicates a point of nucleation as the particle diameter increases from ca. 2 to 4 μm from 1 to 2 minutes. After this, the trend slowly begins to plateau from ca. 6 to 12 minutes. Similarly to the Brij C10 2.8 g system, fingerprints were developed for 20 minutes to observe any increases in the silver growth as well fingerprint quality. Figure 6.18 shows examples of, 1 day old fingerprints developed using formulation 5.

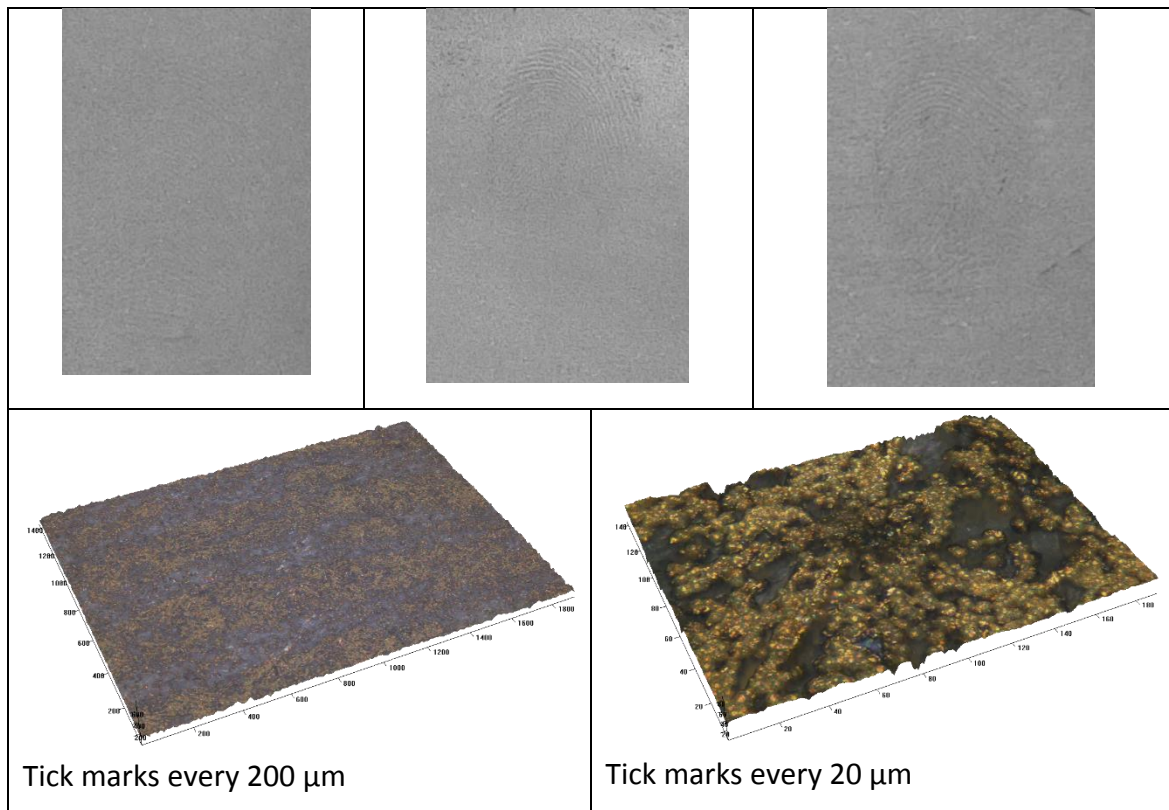


Figure 6.18 – Fingerprints deposited on white copy paper and aged for 1 day under ambient conditions then developed after 20 minutes using PDF5D1 with corresponding microscopy images 5x (left) and 50x (right) for the second fingerprint

Figure 6.18 shows examples of, 1 day old fingerprints developed using formulation 5. Figure 6.18 shows that the extended length of development has been detrimental to the quality of the fingerprint such that all ridges have been obscured and the deposited silver on the ridges has lost all contrast with the background. This is evident in the microscopic images as the silver deposits have completely aggregated and become yellow in colour indicating larger scattering cross sections. These results indicate that a 15 minute cut-off should be followed but PD should be monitored as fingerprints may be sufficiently developed before 15 minutes.

6.2.1.2.2 Split Print Development Using Formulation 5 (PDF5D1)

Split prints were examined to identify any possible effects of ageing. Figure 6.19 shows 1, 14 and 28 day old split prints developed with PD using formulation 5.

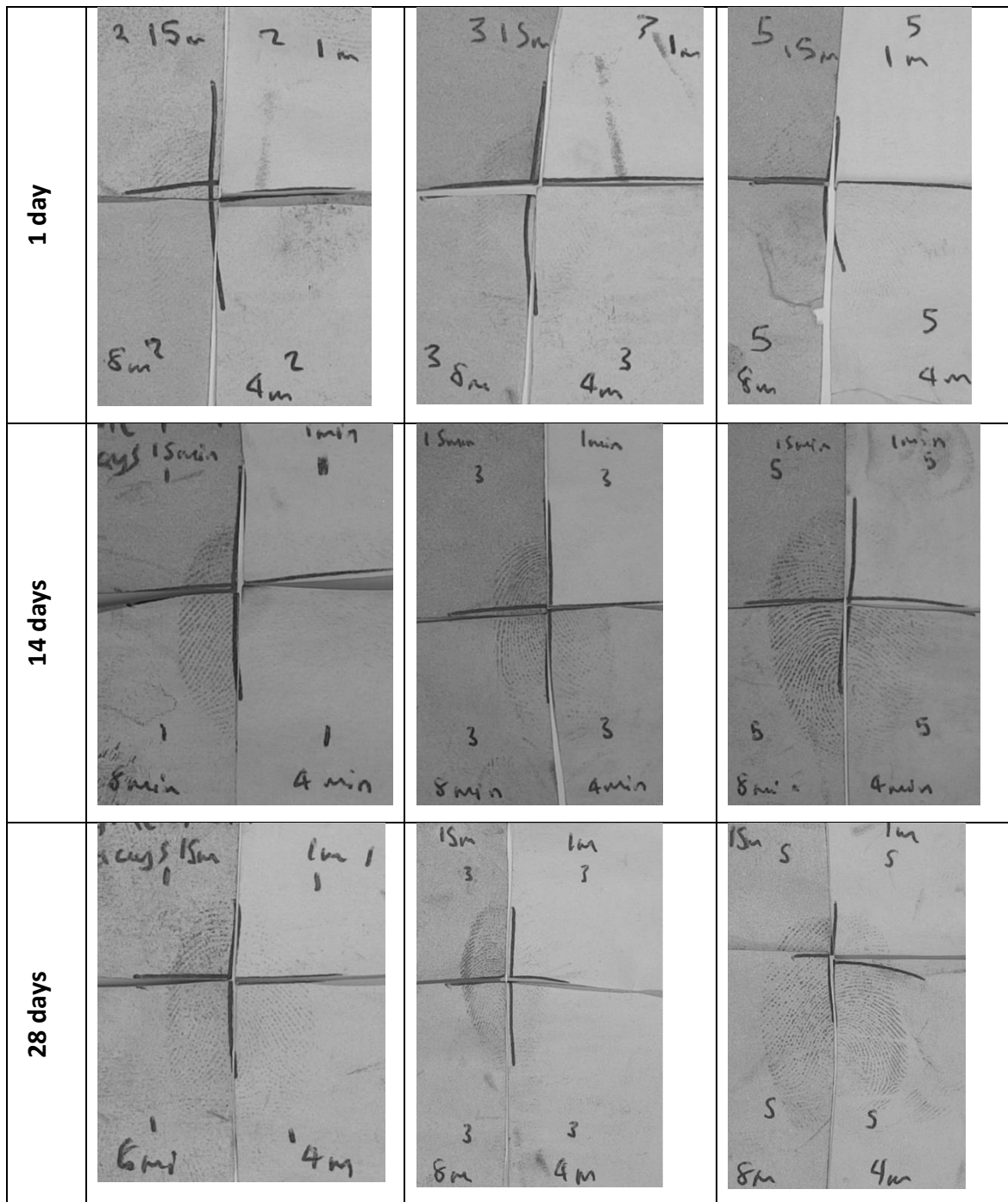


Figure 6.19 - Split prints deposited on white copy paper and aged for 1, 14 and 28 days under ambient conditions then developed via PDF5D1 (3 replicates for each age of mark)

The split print images show that ageing of the mark has not been detrimental to the development but rather that older marks show increased development at each time interval. In comparison to the 1 day old full prints studied in figure 6.15, the split prints resulted in fainter marks. However, the development does increase from 1 to 15

minutes. This is not a negative result given that fingerprints at a crime scene may be much older than 1 day and the 15 minute quadrants of 14 and 28 day old prints show strong development with visible, clear ridge detail.

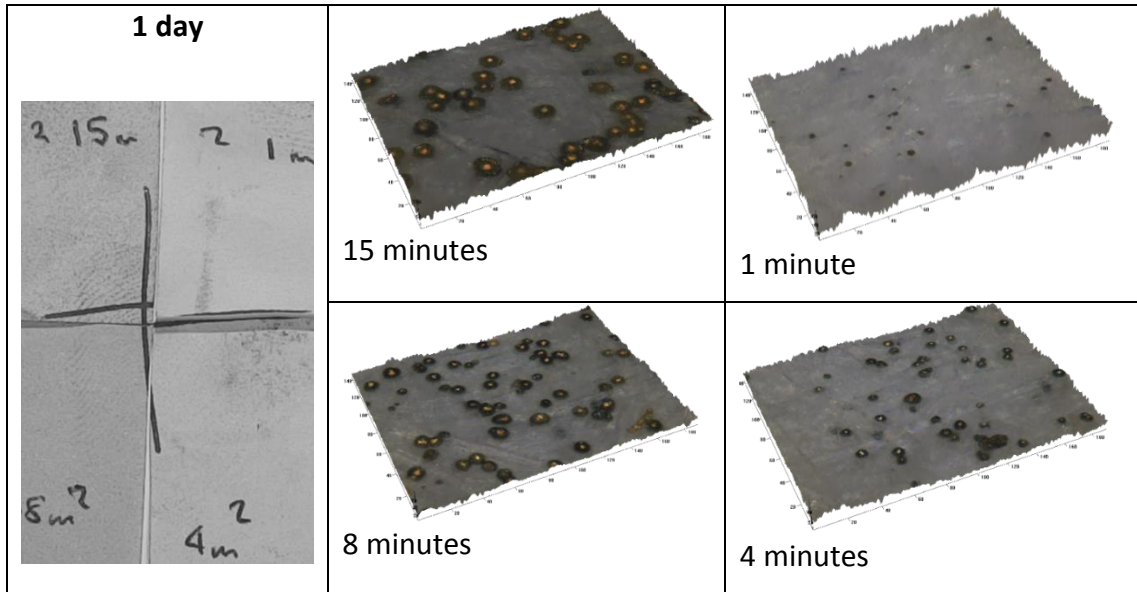


Figure 6.20 – 3D microscopy images (50x) for the growth development of a 1 day old mark processed for 1-15 minutes. Tick marks every 20 μm ('m' refers to minutes)

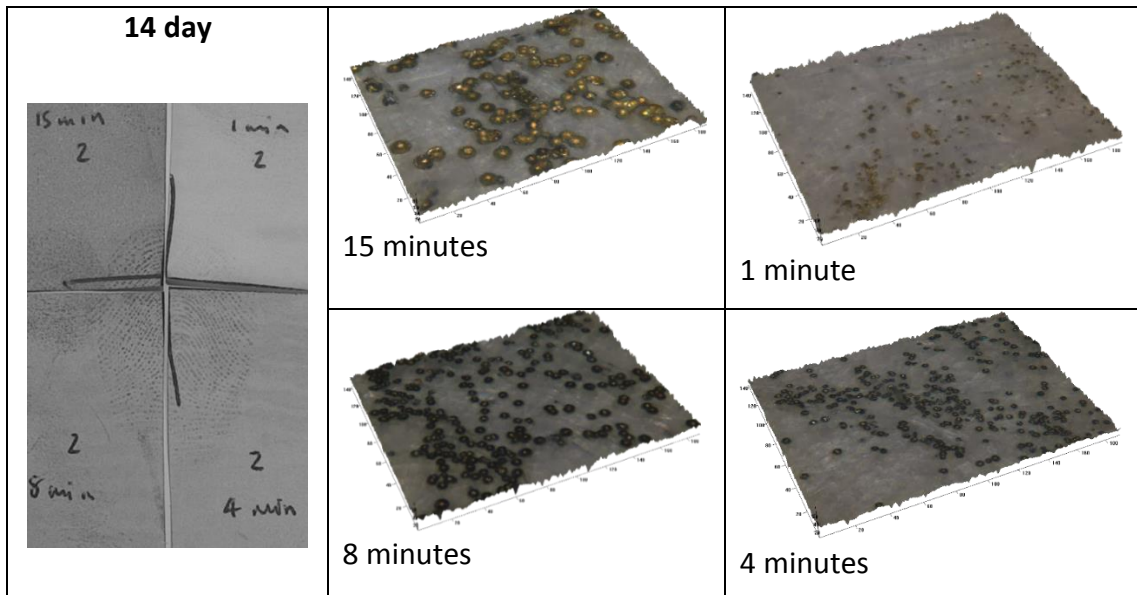


Figure 6.21 – 3D microscopy images (50x) for the growth development of a 28 day old mark processed for 1-15 minutes. Tick marks every 20 μm

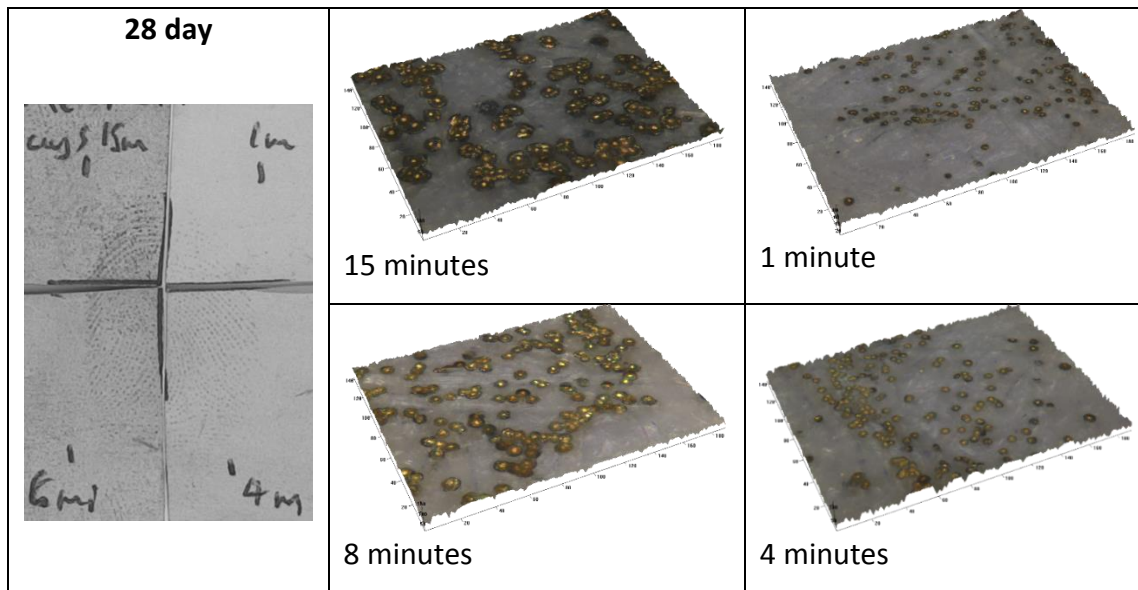


Figure 6.22 – 3D microscopy images (50x) for the growth development of a 28 day old mark processed for 1-15 minutes. Tick marks every 20 μm ('m' refers to minutes)

The split prints do reveal the progressive growth of silver which is more clearly seen in the microscopy images of figures 6.20-6.22. The deposited silver particles increase in diameter as time progresses and if more of the fingerprint is visibly developed, the density of silver deposits also increases (see figure 6.20). The silver deposits are spherical and monodisperse throughout all times and ages of the mark. The silver particle diameter is smaller overall, similarly to the 1 day old full prints in figure 6.15.

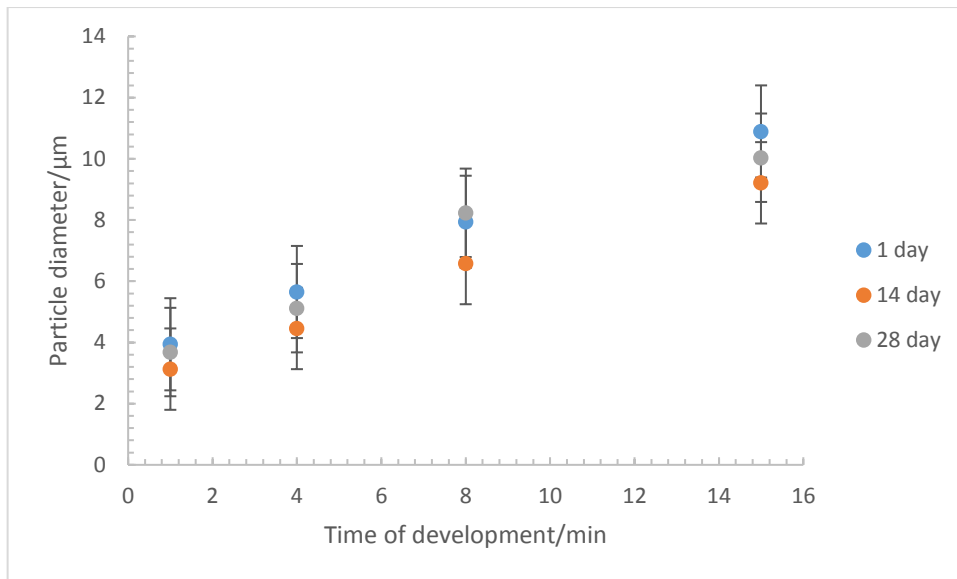


Figure 6.23 - Graph of silver particle diameter vs time of development for average of 5 sets of marks aged under ambient conditions for 1, 14 and 28 days then developed via PDF5D1

Figure 6.23 shows the graph of the silver particle diameter for 1, 14 and 28 day old split prints developed using formulation 5. The overall trend of silver particle growth is similar to all growth studies observed in this thesis but compared to Synperonic-N, the final particle diameter is smaller – 9-11 µm. In conjunction with the 1 day old marks discussed in section 6.2.1.2.1, the smaller diameter is a result of an increased amount of silver initially deposited, thus providing more deposition sites for subsequent silver growth.

6.2.1.2.3 – Formulation 6 (PDF6D2)

In this section, DGME was directly substituted for DDAA. Figure 6.24 shows the 1 day old fingerprints developed using formulation 6.

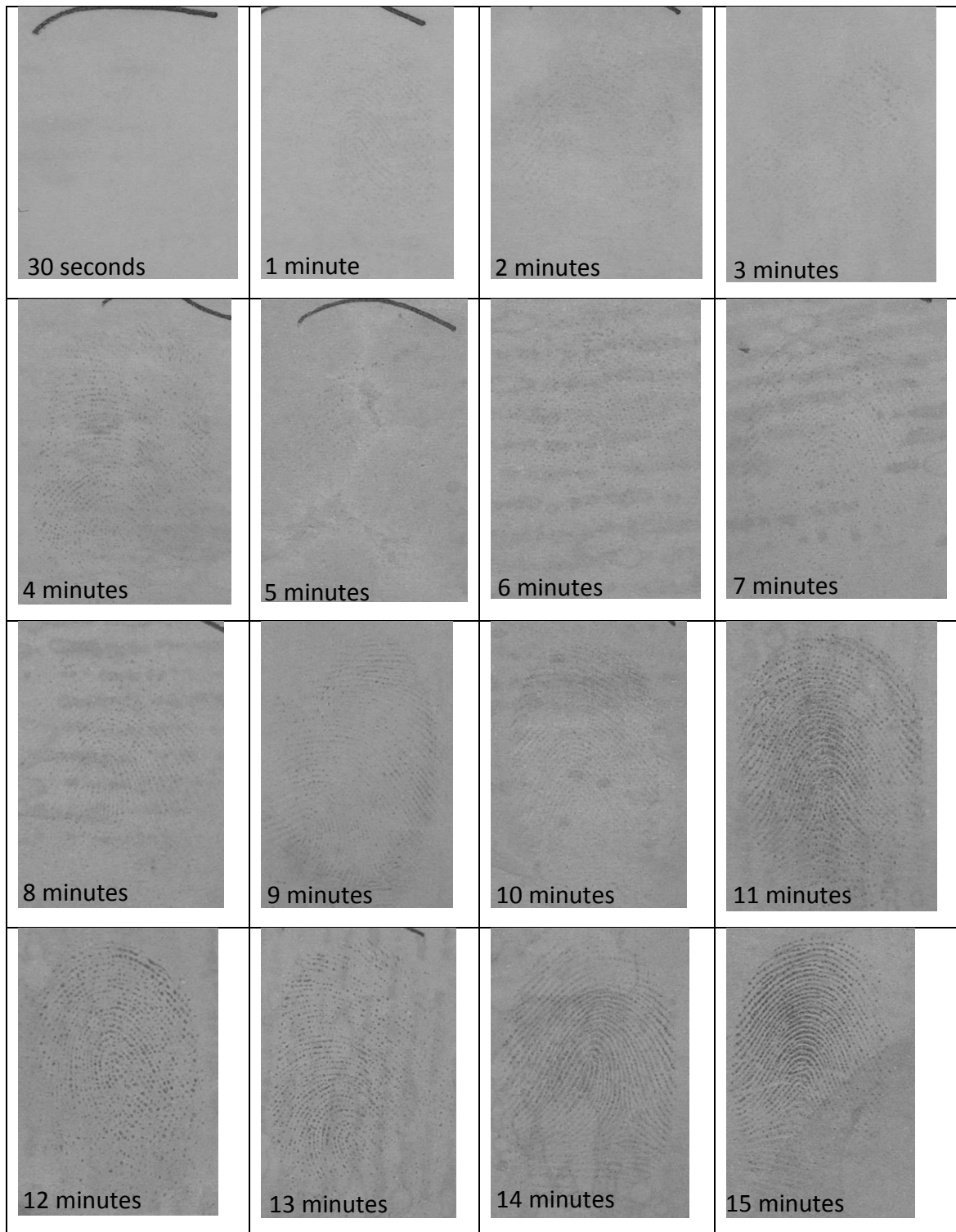


Figure 6.24 - The growth development of silver from 30 seconds to 15 minutes for fingerprints deposited on white copy paper and aged for 1 day under ambient conditions then developed via PDF6D2

From figure 6.24, it is evident that fingerprints have been developed from ca. 11-15 minutes, however none of those marks has fully developed. They are dotted in

appearance, which is characteristic of PD, but several areas show no development at all. In addition to this, the contrast is lower for these marks compared to the marks treated using formulation 5. Even though there is slight development visible between 1- 8 minutes, the fingerprint visibility does not improve until ca. 9 minutes. After this point the quality of fingerprint development does not appear to change. Furthermore, the point of nucleation for the silver deposits appears to be much later than observed for formulations 3, 4 and 5. This indicates that the colloidal silver dispersion is more stable in formulation 6. In addition to this, the selectivity of silver deposition is hindered as background deposition is stronger.

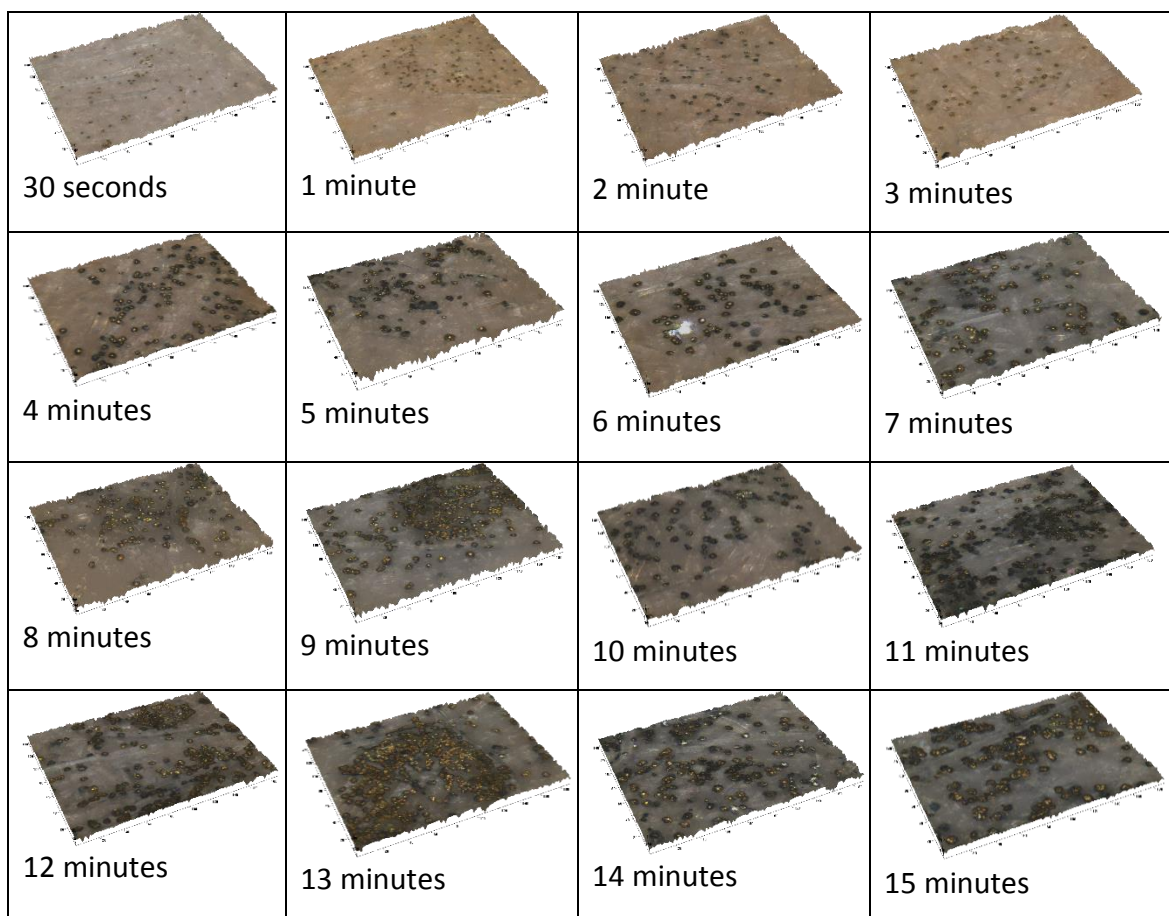


Figure 6.25 - 3D microscopy images (50x) for the growth development of 1 day old marks processed for 30 seconds to 15 minutes for the samples in figure 6.24. Tick marks every 20 μm

Figure 6.25 shows the corresponding microscopic analysis for the marks in figure 6.24. The developed images in figure 6.24 appear to show faint ridges after ca. 2 minutes until ca. 8 minutes. The microscopic images in figure 6.25 show silver deposition after 30 seconds and the particle diameter increases steadily thereafter. Therefore, silver deposition does still occur but the deposits are visibly smaller, which reflects the faint appearance of the developed images.

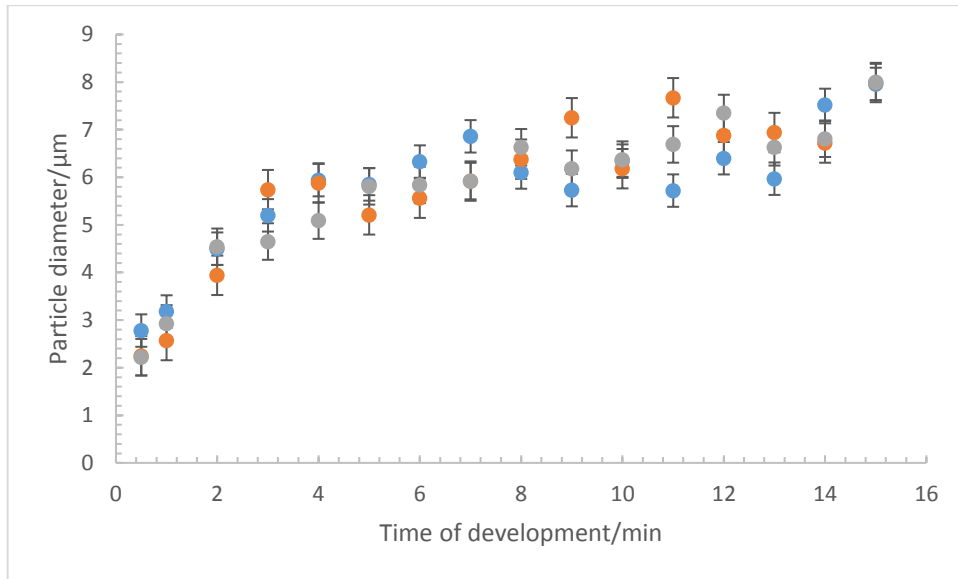


Figure 6.26 - Graph of silver particle diameter vs time of development for 3 sets of 1 day old marks aged under ambient conditions developed via PDF6D2. Data from figure 6.24 and two replicates

Figure 6.26 shows the trend in silver particle growth over the 15 minute development period. After ca. 1 minute, the particle diameter increases sharply, followed by progressive growth which appears to plateau after ca. 10 minutes. The final particle diameter is 8-9 μm , which is similar to formulation 5 but fingerprint quality is reduced in terms of ridge contrast detail. As this working solution appeared to be more stable, fingerprints were developed for 20 minutes to observe whether more time was required to achieve higher quality fingerprints.

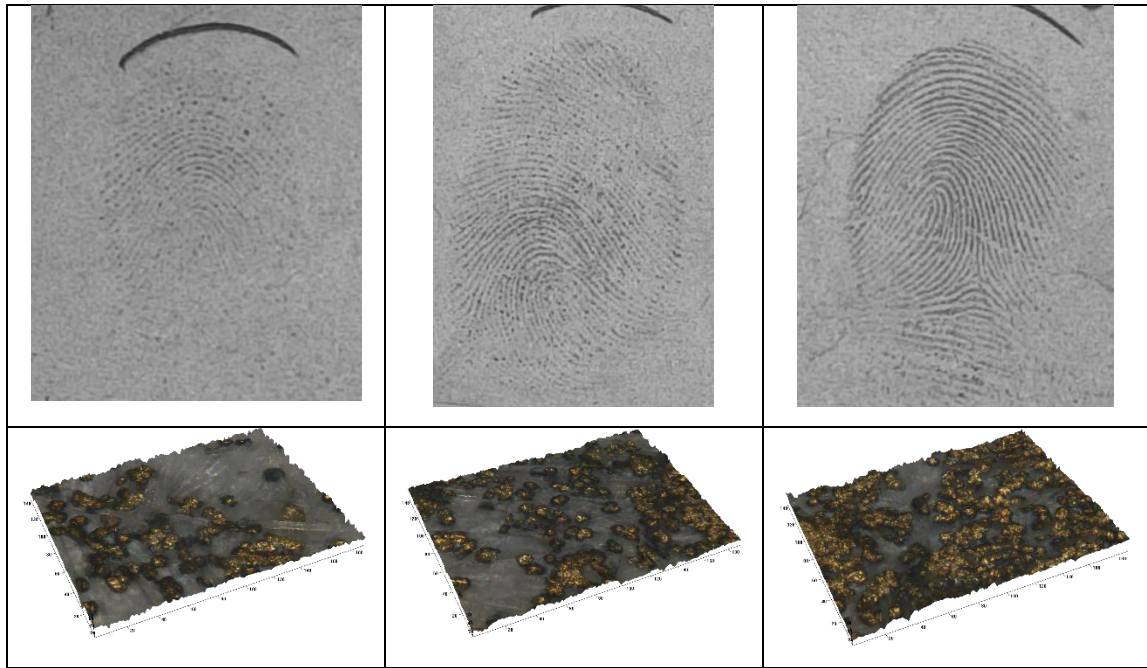


Figure 6.27 – Fingerprints deposited on white copy paper and aged for 1 day under ambient conditions then developed after 20 minutes via PDF6D2 with corresponding microscopy images (50x – Tick marks every 20 μm)

Figure 6.27 shows examples of 1 day old fingerprints developed for 20 minutes using formulation 6. For the third fingerprint shown in figure 6.27, the quality has appeared to improve as the ridges have increased in contrast and more of the fingerprint has been developed. However, as the corresponding microscopic image shows, the silver particles have aggregated. Any further aggregation risks losing crucial fingerprint ridge detail. The remaining fingerprints resulted in particle diameters of 8-10 μm which is not much larger than after 15 minutes. Development times longer than 15 minutes are discouraged and the analysis of the marks developed using formulation 6 suggests the working solution is too stable.

6.2.1.2.4 Split Print Development Using Formulation 6 (PDF6D2)

Split prints were studied to observe the growth of silver using the formulation 6 system as well as the effect of fingerprint development for aged marks. Figure 6.28 shows the results for 1, 14 and 28 day old split prints developed using formulation 6.

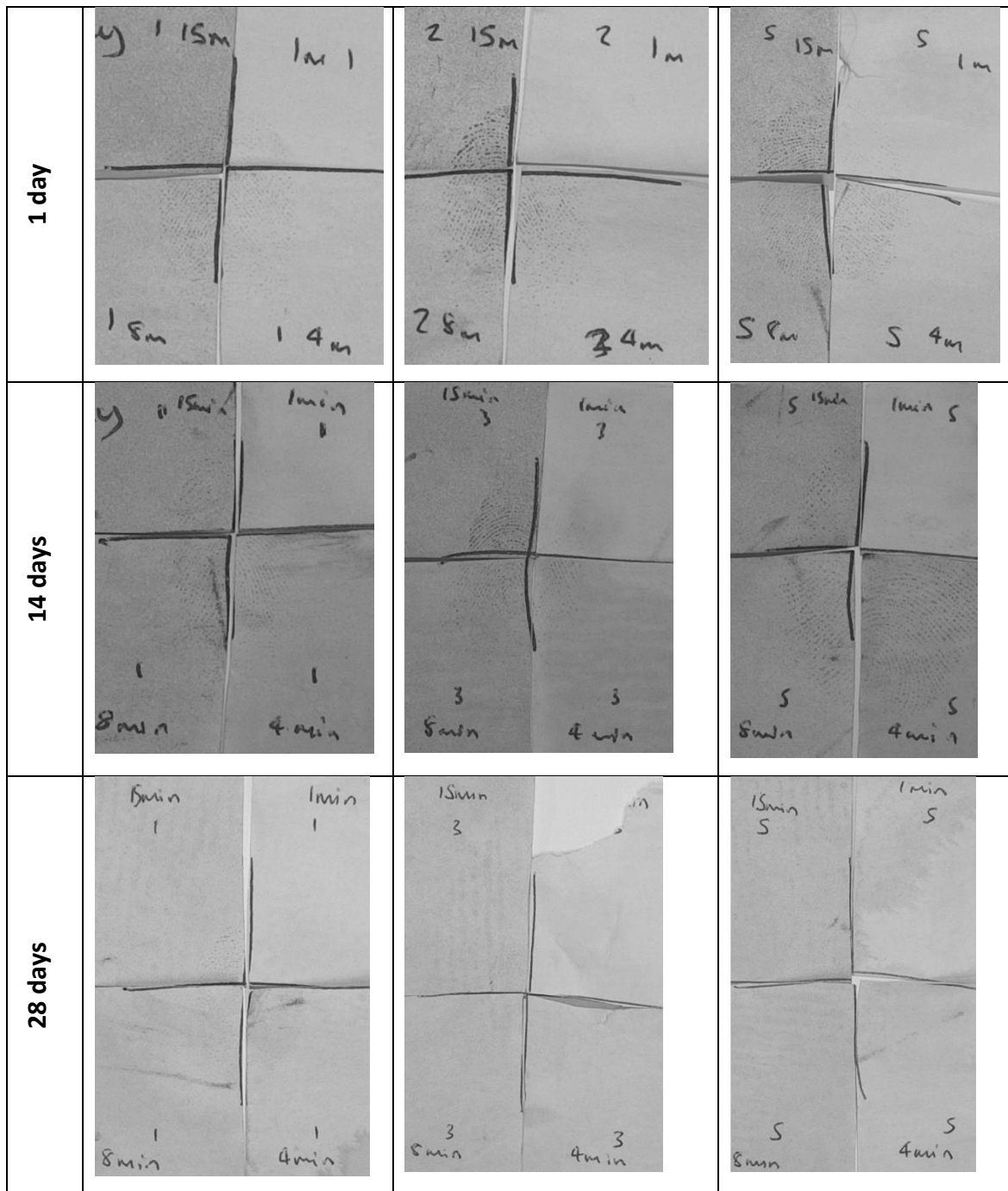


Figure 6.28 - Split prints deposited on white copy paper and aged for 1, 14 and 28 days under ambient conditions then developed via PDF6D2 (3 replicates for each age of mark)

As figure 6.28 shows, fingerprint development has not been successful for 14 or 28 day old marks. 2 day old working solutions were used after testing positive with the gold spot tests (chapter 3, section 3.4.5) but there was no development. Fresh solutions were used for the images in figure 6.28 but these still resulted in limited or

no development for the 14 and 28 day old marks. This result is surprising given that PD is generally more effective for aged marks. The 14 day old marks have shown some development which increases clockwise by quadrant but the background deposition is high, lowering the contrast. These split prints further suggest that formulation 6 is too stable for spontaneous deposition.

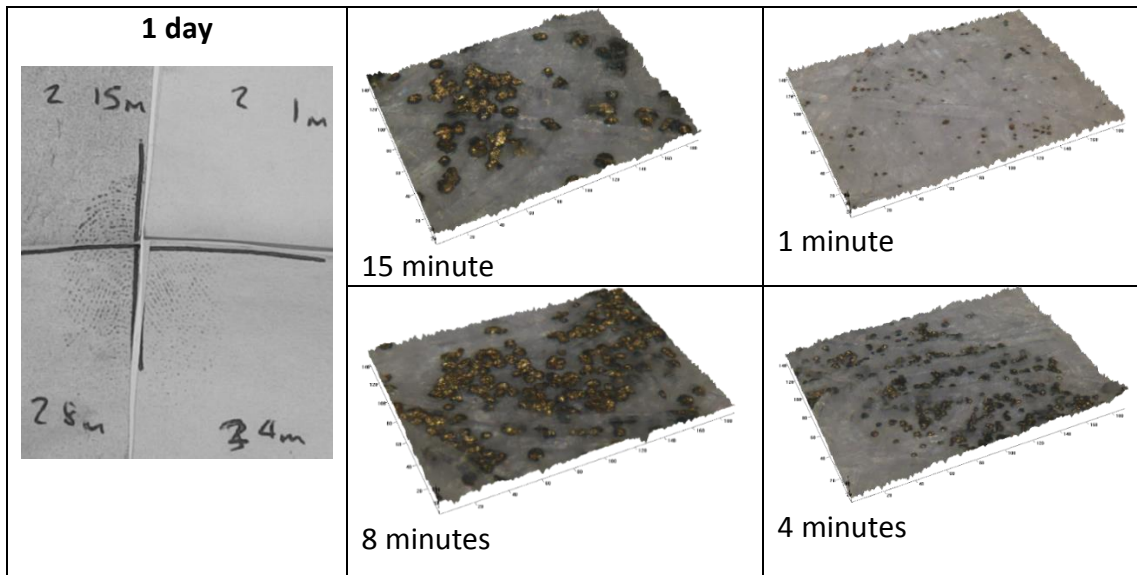


Figure 6.29 – 3D microscopy images (50x) for the growth development of a 1 day old mark processed for 1-15 minutes. Tick marks every 20 μm ('m' refers to minutes)

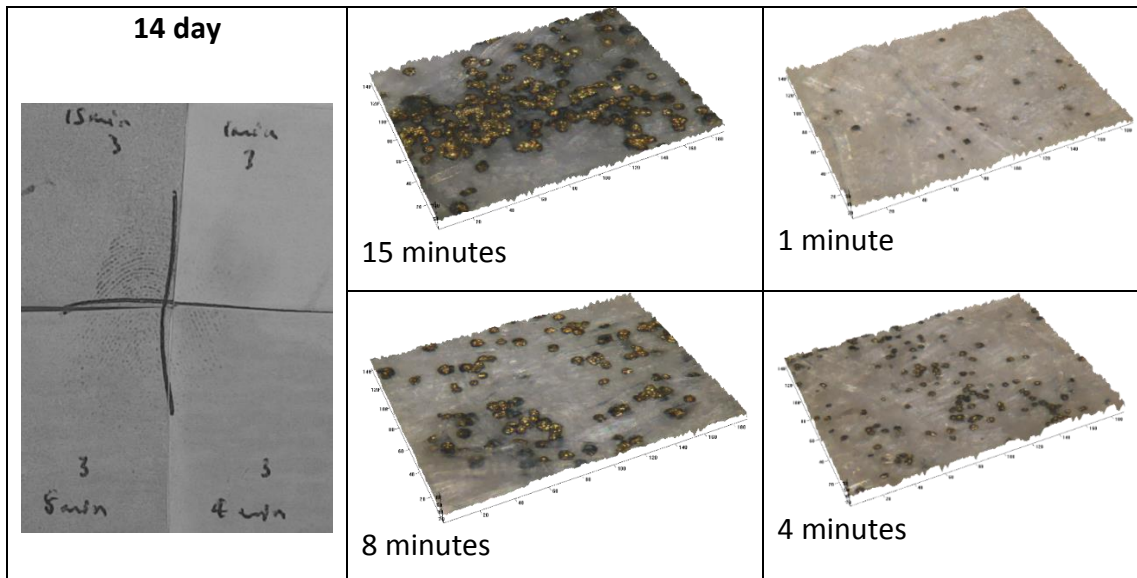


Figure 6.30 – 3D microscopy images (50x) for the growth development of a 14 day old mark processed for 1-15 minutes. Tick marks every 20 μm

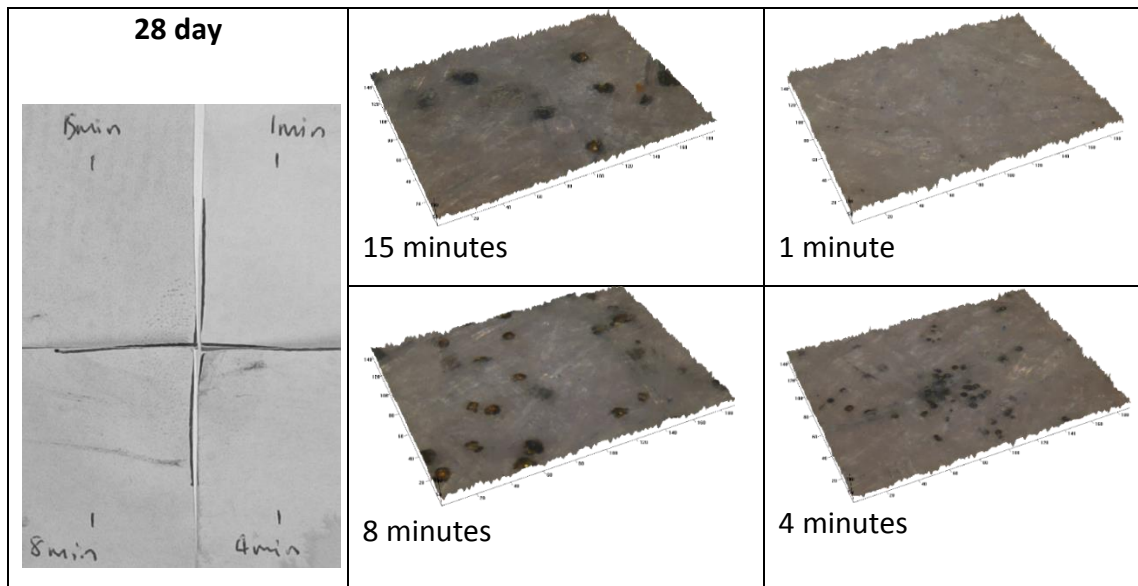


Figure 6.31 – 3D microscopy images (50x) for the growth development of a 28 day old mark processed for 1-15 minutes. Tick marks every 20 μm

Figures 6.29-6.31 show the microscopy images of selected split prints for 1, 14 and 28 day aged marks. As figure 6.31 shows, silver deposition is sparse compared to 1 and 14 day old marks. The silver growth still follows the same trend but there is not enough silver deposition to warrant a visible fingerprint.

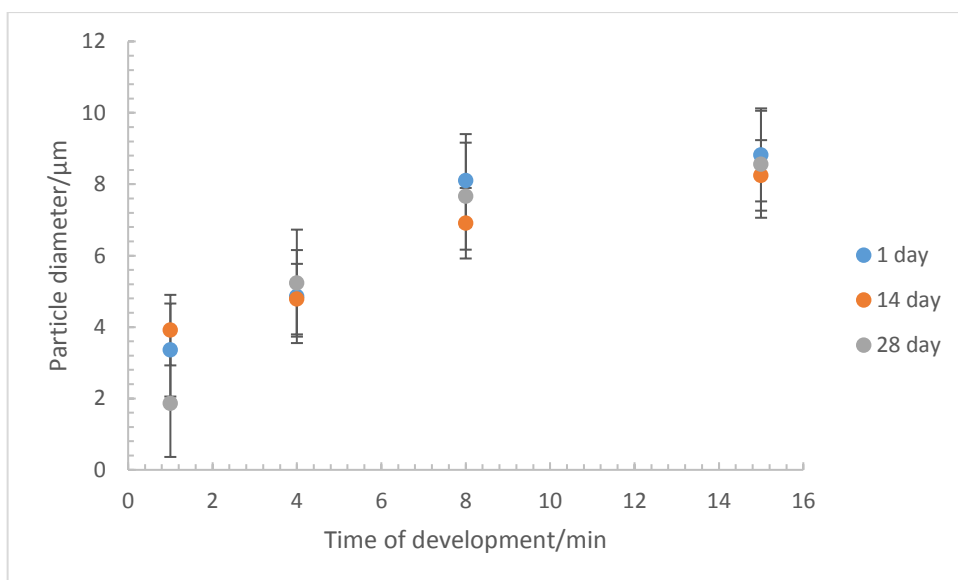


Figure 6.32 - Graph of silver particle diameter vs time of development for average of 5 sets of 1, 14 and 28 day old marks aged under ambient conditions developed via PDF6D2

Figure 6.32 shows the growth trend for the 1, 14 and 28 day old split prints. The graph clearly shows similarity in particle diameter between the different ages and the same trend in the growth of the silver deposits. This indicates that DGME is a suitable alternative as it behaves similarly to Synperonic-N but the concentrations need to be adjusted to achieve a balance between stability and fingerprint development.

6.2.1.3 Growth of Silver from the Solution onto the Surface

The studies in section 6.2.1 related to the growth and dynamics of the PD process have revealed that the silver particles grow progressively on the surface, regardless of the detergent system used. DLS measurements in chapter 4, section 4.2.3, revealed silver particle sizes of ca. 880 nm in the PD working solution, which grow up to 20 µm on the surface. After 30 seconds of development, deposited silver particles ranged from 2-3 µm; therefore one can assume that the 880 nm refers to the silver particles themselves. However, the question arises as to whether the chosen surfactant affects the size of the silver particulates in the solution. The size of the surfactant particles individually and the particles sizes in the detergent systems, as well as the particle sizes in the various PD working solutions were determined with DLS. The results are summarised in table 6.1-6.3.

Surfactant	Synperonic-N	DDAA	Tween 20	DGME	Brij C10
Particle Size (nm)	15	200-300	8	7	90-300

Table 6.1 - DLS results of surfactant particle sizes

Detergent System	Synperonic-N-DDAA	Tween 20-DDAA	DGME-DDAA 1.5/2.8g	Brij C10-DDAA
Particle Size (nm)	100-250	N/A due to cloudy solution	180-190/ 170-200	200-250

Table 6.2 - DLS results of particle sizes in the detergent systems

PD working solution	Synperonic-N-DDAA	Tween 20-DDAA	DGME-DDAA 1.5g/2.8g	Brij C10-DDAA
Particle Size (nm)	700-800	300-500	300-500/ 400-600	300-500

Table 6.3 - DLS results of particle sizes in the PD working solutions

As table 6.2 reveals, the Tween 20-DDAA detergent system was not suitable for DLS measurements because the solution was too cloudy. This in turn causes the PD working solution to become cloudy rendering it unusable. Each sample was run 5 times to achieve the diameter ranges in the tables. The 300-500 nm diameter size was measured using a PD working solution with Tween 20 and DDAA, which was made immediately prior to the DLS measurement. The Brij C10 solution resulted in a broad diameter size of 90-300 nm because Brij C10 has low solubility. This means that the particles in solution would be polydisperse. The variation in diameter narrowed for the Brij C10-DDAA detergent system to 200-250 nm which increased to 300-500 nm in the PD working solution.

All the other detergent systems in the PD working solutions resulted in a particle diameter which was smaller than the original Synperonic-N formulation at 700-800 nm. This could be due to the Tween 20 and DGME micelle sizes being smaller than Synperonic N as table 6.3 reveals. (Brij C10 results are unreliable due to low solubility). The DDAA micelles are larger than all non-ionic surfactants at 200-300 nm but the detergent systems have a smaller diameter than the DDAA alone. This could suggest that the addition of the non-ionic surfactant component is to aid the solubility of the DDAA, rather than contributing to the structure of the micelle.

The particle diameters in the PD working solutions do not appear to affect the subsequent growth of silver on the surface as each growth study revealed a similar particle diameter after 30 seconds. Progressive growth of silver was observed thereafter for all detergent systems. The interaction between the silver and each surfactant was studied using Raman spectroscopy which will be discussed in section 6.2.2.

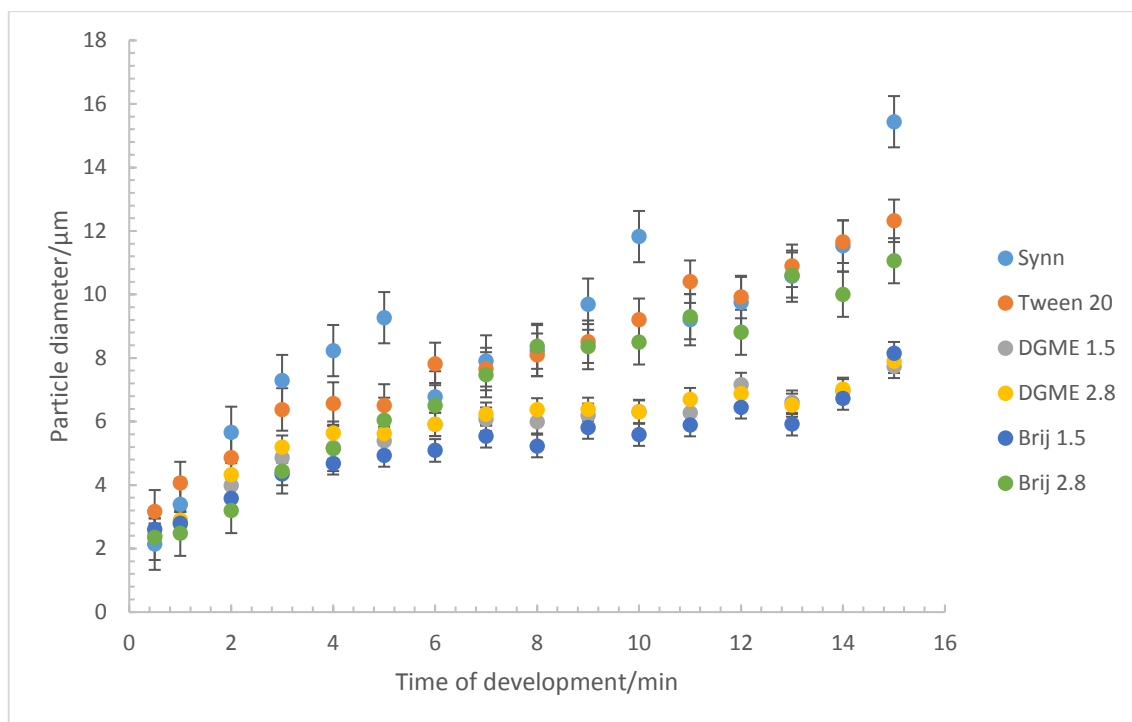


Figure 6.33 - Graph of the silver particle diameter vs time of development for the average of 3 sets for 1 day old fingerprints aged under ambient conditions and then developed with varying detergent systems of PD shown in the graph legend

Figure 6.33 shows an average for the growth of silver on the surface for 1 day old marks which have been developed using the different detergent systems in the working solution. As figure 6.33 shows, the trend in the silver growth is the same regardless of the detergent system used. After 30 seconds, the deposited silver resulted in a particle diameter of 2-3 µm which effectively doubled to 3-6 µm after ca. 2 minutes. After a progressive growth from 2-8 minutes, the diameter does not increase sharply and appears to plateau.

The noticeable difference between the detergent systems is the diameter of the deposited silver. The Synperonic-N system results in the largest particles at each point of development. From the experimental results concerning the growth of the silver on the surface in conjunction with the microscopic analysis, if a larger area of the fingerprint is developed initially, the particle diameter will be lower. This is due to the silver site being preferable to another area of the fingerprint residue. Therefore, the sizes of the particles in the solution do not affect the initial stages of the silver growth.

6.2.2 Raman Spectroscopy of Surfactant Adsorption

In order to observe the interfacial interactions between the surfactant molecules and the silver, Raman spectroscopy was utilised. Silver was sputter coated onto a glass slide, representing a planar silver surface, and a drop of each surfactant and detergent system was added.

The first point to note are the peaks observed in the silver spectrum, predominantly at 973 cm^{-1} , 1013 cm^{-1} , 1347 cm^{-1} and 1588 cm^{-1} . These peaks could be due to an impurity on the silver surface. Similar values have been recorded for doped and bare silver nanoparticles^{1, 2} as well as silver electrodes in various electrolyte solutions.³ In addition to this, it is probable that the two peaks observed at 973 cm^{-1} and 1013 cm^{-1} could refer to a Ag-O peak.⁴ As the silver was sputter coated and then transported in the open atmosphere to the Raman instrument, the silver surface could oxidise.

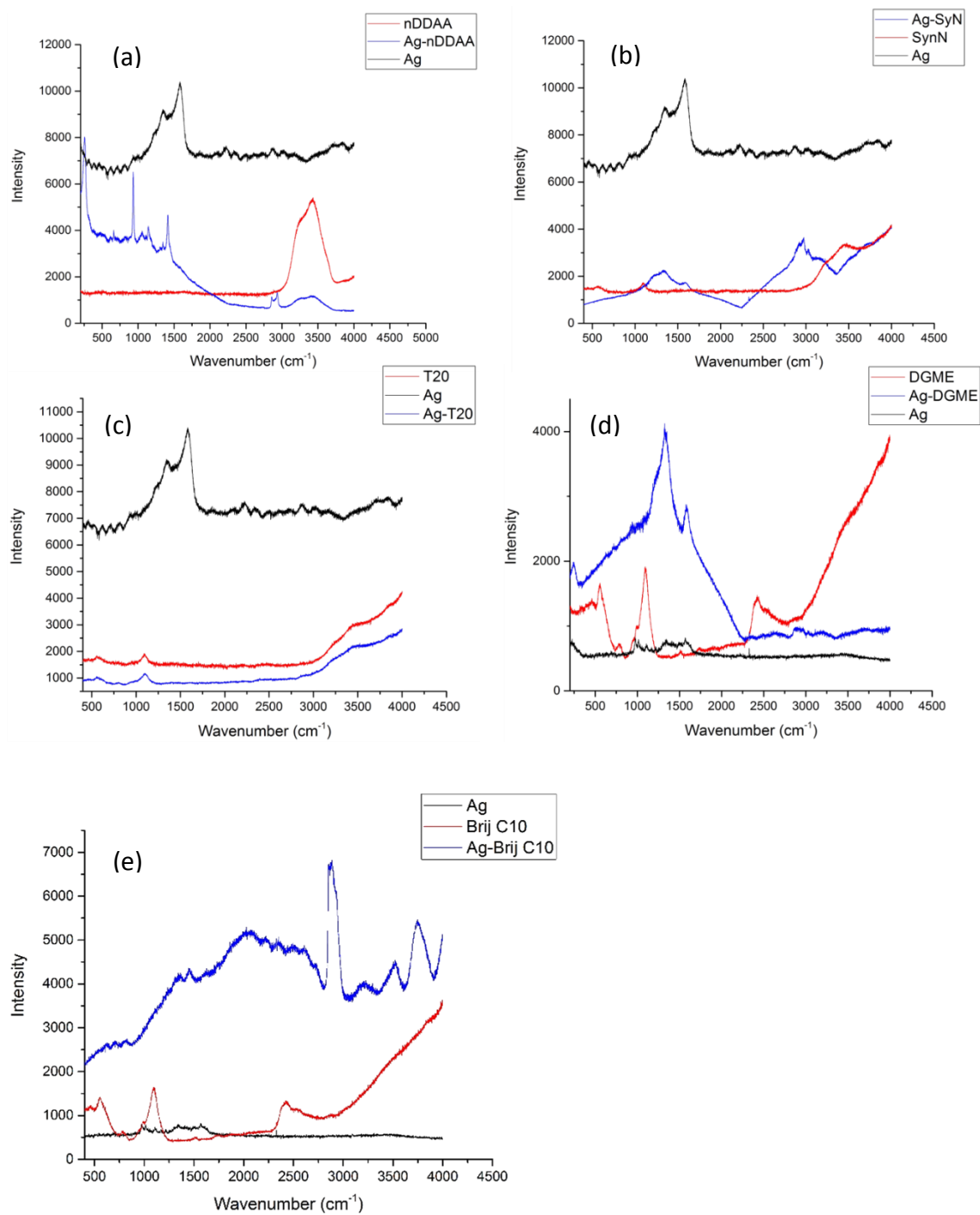


Figure 6.34 - Raman spectra of the silver surface, surfactant component and silver-surfactant interaction for (a) DDAA (b) Synperonic-N (c) Tween 20 (d) DGME and (e) Brij C10

The two peaks in the Tween 20 spectrum at 562 cm⁻¹ and 1091 cm⁻¹ have shifted to 549 cm⁻¹ and 1095 cm⁻¹ suggesting an element of some physical adsorption. However, the intensity does not change significantly. This data corroborates with the

neutron reflectivity experiments in chapter 5, section 5.2.2, which suggests the Tween 20 is in solution but not interacting with the silver surfaces.

The remaining non-ionic surfactants show differences in the Raman spectra of the individual surfactant spectrum compared to the Ag-surfactant spectrum. Firstly, considering Synperonic-N, the two peaks observed in the silver spectrum have shifted to 1329 cm^{-1} and 1594 cm^{-1} but the intensity is not very high. This suggests that the silver surface has enhanced the vibrations observed within the surfactant. For both the DGME and Brij C10 systems, the intensity of the spectrum increases significantly when the surfactant is added to the silver surface.

The spectrum for DDAA reveals a large peak at 3422 cm^{-1} which is likely to be representative of the amine group (N-H) in DDAA. This peak is shifted slightly (3410 cm^{-1}) when DDAA is added to the silver surface, suggesting adsorption. There is an additional peak at 255 cm^{-1} . This peak could be attributed to a Ag-O or Ag-N bond.⁴ It also appears in the Ag-DGME spectrum and since DGME does not have any nitrogen atoms, it cannot be assigned conclusively as a Ag-N peak.

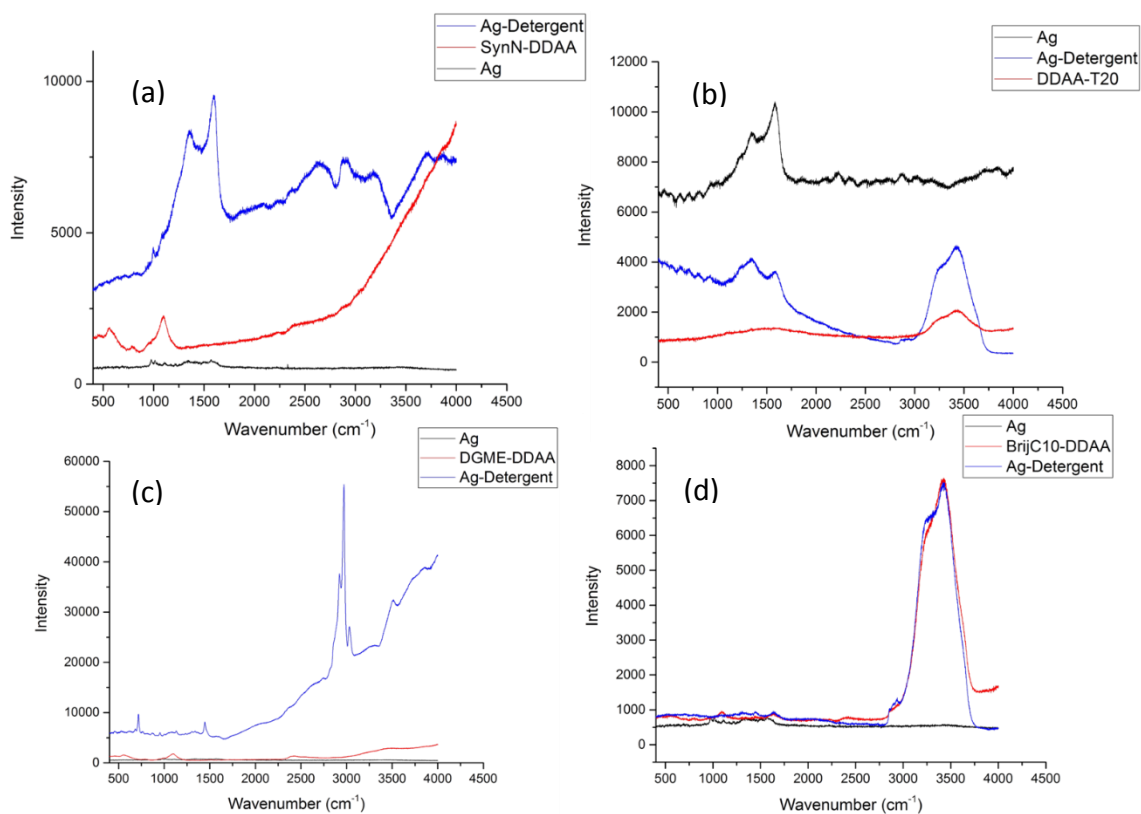


Figure 6.35 - Raman spectra of the silver surface, detergent system and silver-detergent interaction for (a) DDAA-Synperonic-N (b) DDAA-Tween 20 (c) DDAA-DGME and (d) DDAA-Brij C10

The spectrum for the Synperonic-N-DDAA interaction with the Ag surface shows a significant increase in the intensity. The peaks observed in the silver spectrum have been shifted slightly (1347 cm^{-1} to 1329 cm^{-1} and 1588 cm^{-1} to 1594 cm^{-1}) but also increased in intensity. This suggests that the Ag surface is enhancing the vibrations of the surfactant.

In the spectrum for the Tween 20-DDAA system on the Ag surface, the broad peak most likely corresponding to of the N-H in DDAA, has shifted from 3430 cm^{-1} to 3412 cm^{-1} . There is also an increase in the intensity of this peak. The addition of Tween 20 in the detergent has not resulted in any additional peaks suggesting that there is DDAA adsorption but no effect from Tween 20.

For the DGME-DDAA detergent on the silver surface, there is a significant increase in the intensity suggesting surface enhancement but there are also additional

peaks, which are not present in the DGME-DDAA spectrum. The presence of the additional peaks does suggest physical adsorption but the characteristic amine peaks from DDAA are not visible. Therefore it is difficult to fully assign the peaks.

The last spectrum for the Brij C10-DDAA detergent on the silver surface is almost identical to the Brij C10-DDAA spectrum. The broad peaks at 3252 cm^{-1} and 3421 cm^{-1} do shift to 3241 cm^{-1} and 3405 cm^{-1} suggesting some adsorption but given the similarity to the DDAA spectrum in figure 6.34a, it is likely this adsorption is dominated by the DDAA.

The accepted theory states that the cationic surfactant forms a staggered micelle around the negatively charged silver particles. From the Raman spectra and the various growth studies discussed in section 6.2.1 and chapter 4, section 4.2.3 and chapter 5, sections 5.2.1 and 5.2.2, it is clear that DDAA is responsible for stabilising the silver particulates. The addition of the non-ionic surfactant affects the stability of the working solution but with varied results concerning both the stability and the quality of fingerprint development. The following structures have been proposed for the silver-surfactant conformations in the working solution.

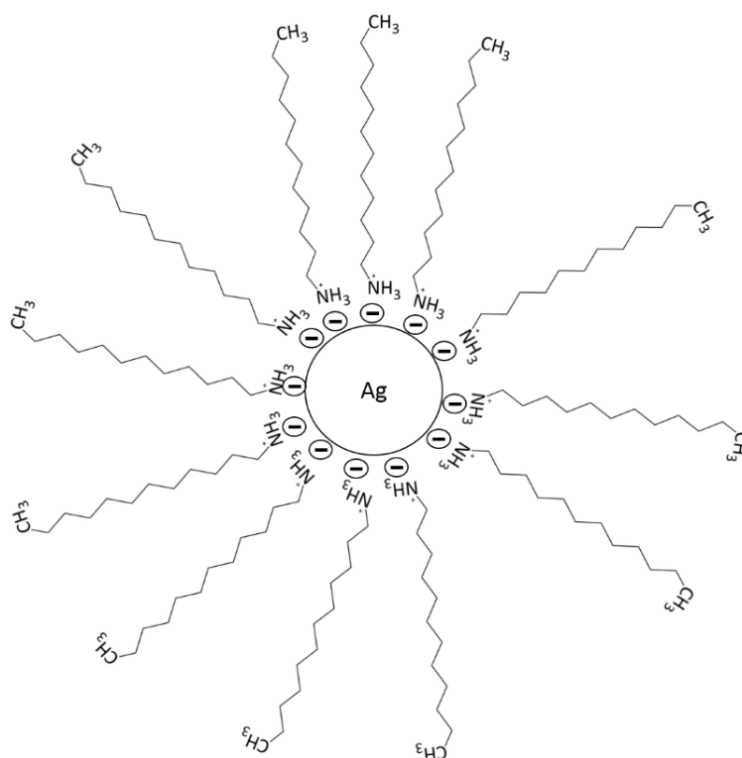


Figure 6.36 – Schematic of the structural conformation of DDAA and the silver particulate (not to scale)

Figure 6.36 represents the structure of the silver particulates and DDAA in the working solution. The pH of the PD working solution is ca. 2-3 and the pK_a of the DDAA amine groups is ca. 10. Therefore, it is likely that the positively charged amine group adsorbs to the negatively charged silver particle. The negative charge on the silver colloid could be due to the adsorption of citrate ions in the solution.⁵ In chapter 5, section 5.2.1, the neutron reflectivity experiments that DDAA competed successfully with Tween 20 such that Tween 20 was not adsorbed onto the silver surface. The Raman spectra in this section also agree with this and therefore Tween 20 is purely a component of the solution as shown in chapter 5, section 5.2.3.2 figure 5.32.

DGME and Brij C10 working solution formulations produced developed fingerprints that were reproducible and the Raman spectra indicate a degree of adsorption.

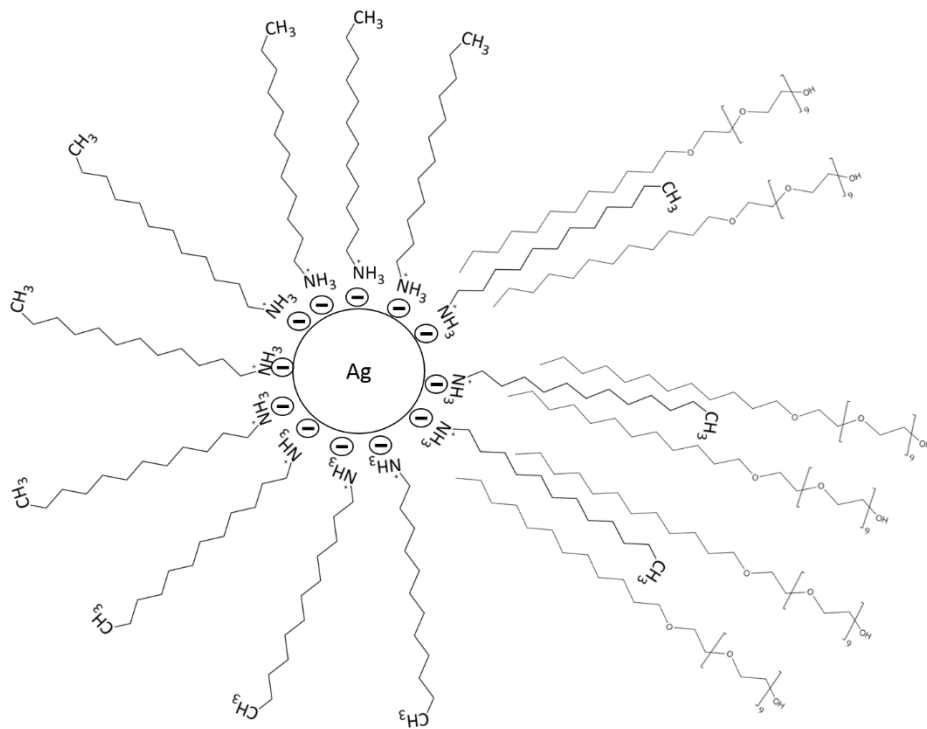


Figure 6.37 – Schematic of the structural conformation of DGME and the silver particulate (not to scale)

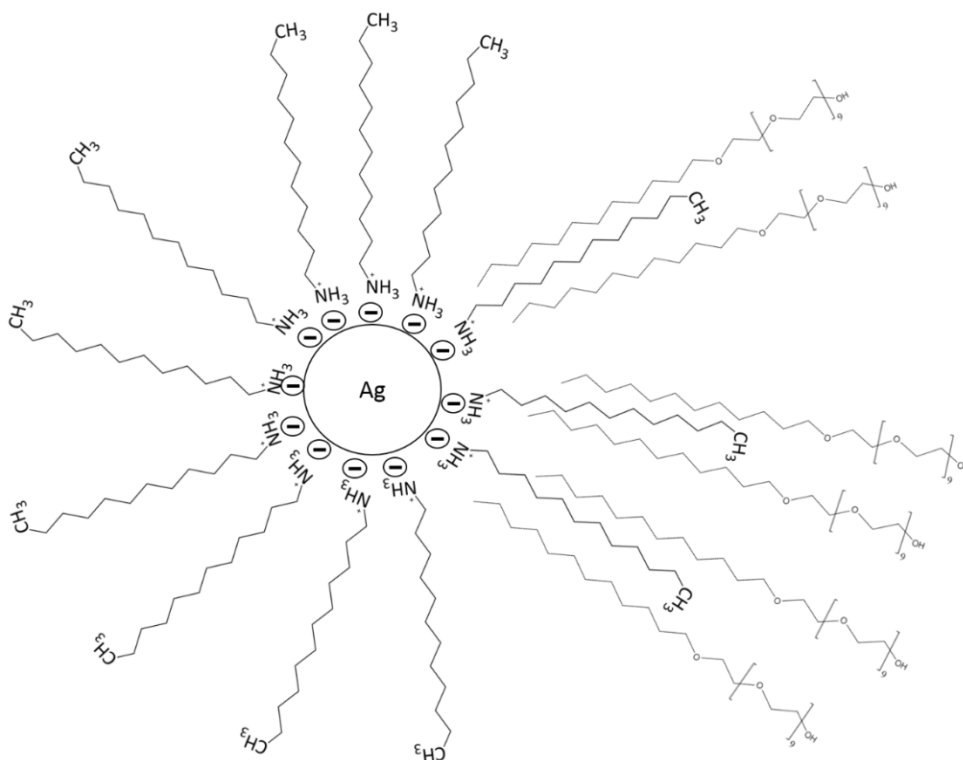


Figure 6.38 – Schematic of the structural conformation of Brij C10 and the silver particulate (not to scale)

As figures 6.37 and 6.38 show, the DGME and Brij C10 molecules do not interact with the silver particulate directly but can aid the overall stability of the silver particles sterically.

6.2.3 Extension of PD to Alternative Porous Surfaces

6.2.3.1 PD vs Superglue Fuming on Leather and Suede Surfaces

The wider capability of PD was explored by developing fingerprints on various leather and suede surfaces (see chapter 3, section 3.2.2). Leather and suedes are semi-porous with the extent of the porosity being dependent on the finish of the substrate. For example, patent leather tends to be non-porous as it is finished with a patent film. Leather and suede surfaces are notoriously difficult surfaces to achieve any fingerprint development.⁶ Superglue fuming is often the best method of choice and has been shown to be effective for impression development on various fabric surfaces.⁷⁻¹¹ PD is a technique specified for porous surfaces and was compared to the conventional superglue fuming method.

Fingerprints were deposited and aged 1 day and 7 days by a known poor and good donor onto the substrates.



Figure 6.39 - Leather and suede (bovine sources) surfaces that showed no fingerprint development with PDF1S or superglue fuming

There were several substrates that did not result in any development with either technique: black faux leather, white faux leather, embossed leather, purple suede, Nubuck and brown suede. An example of each case is shown in figure 6.39. The black faux leather was discoloured when using PD, as was Nubuck suede, but no visible fingerprint detail was observed. The only surface where both PD and superglue fuming developed fingerprint ridges was on patent leather, which is the least porous leather surface. Figure 6.40 shows the results of 1 day old marks on patent leather developed with PD.

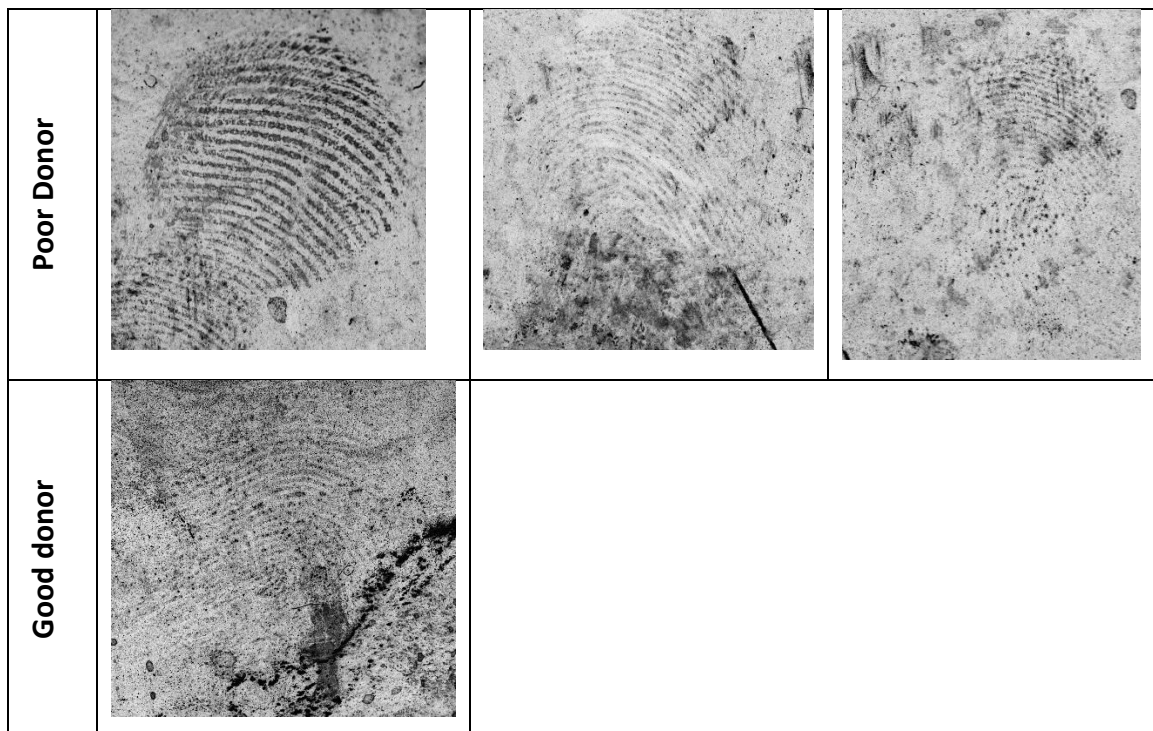


Figure 6.40 – Fingerprints deposited on patent leather and aged for 1 day under ambient conditions then developed using PDF1S

Interestingly, the notionally poor donor marks resulted in stronger development than those deposited by the good donor. The fingerprint ridge details are clearer for the poor donor but nonetheless, fingerprints have been developed on a relatively non-porous surface using PD.

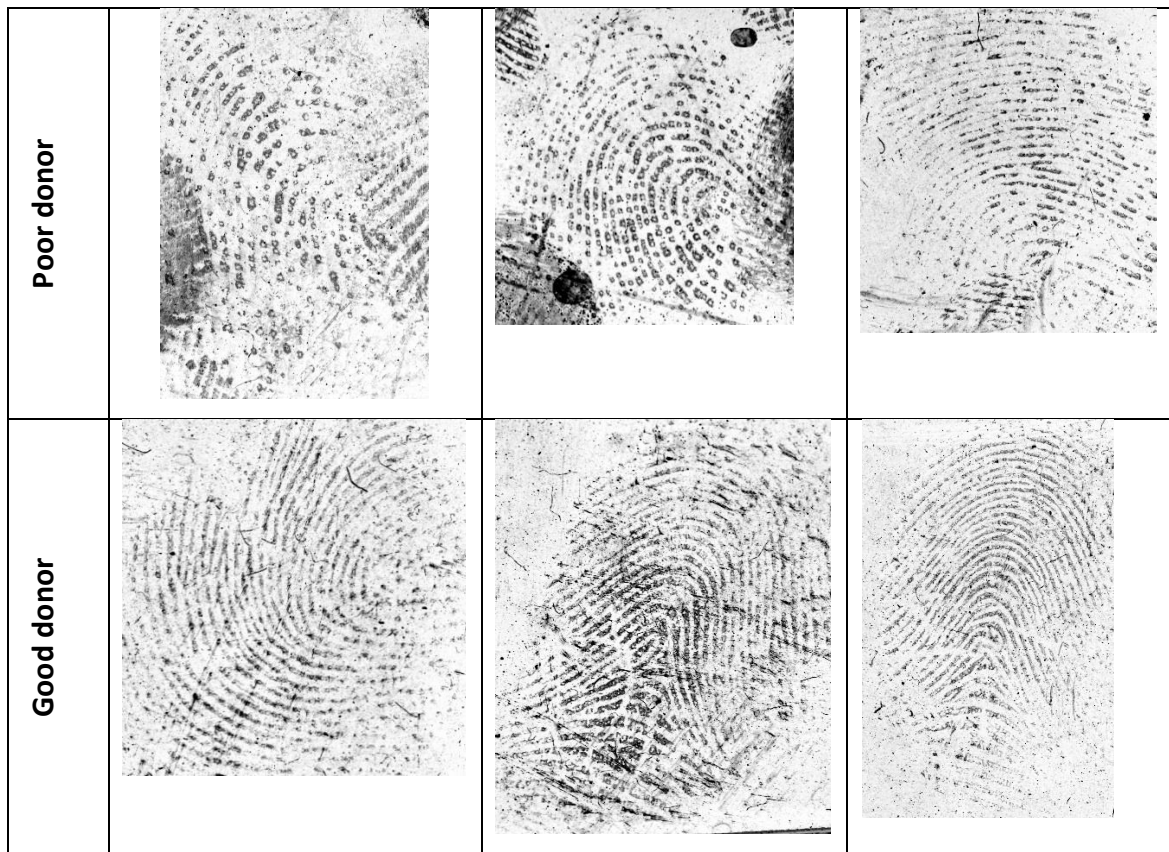


Figure 6.41 – Fingerprints deposited on patent leather and aged for 1 day under ambient conditions then developed on patent leather using superglue fuming (chapter 3, section 3.4.6) – 3 replicates

Figure 6.41 shows the 1 day old marks developed with superglue fuming. Both donors have resulted in high quality fingerprint development with clear ridge details and high contrast. (The colour has been inverted to allow visualisation of the marks). For these fresher marks, superglue fuming has been more effective compared to PD but this is not unexpected, given PD is more effective for aged marks.

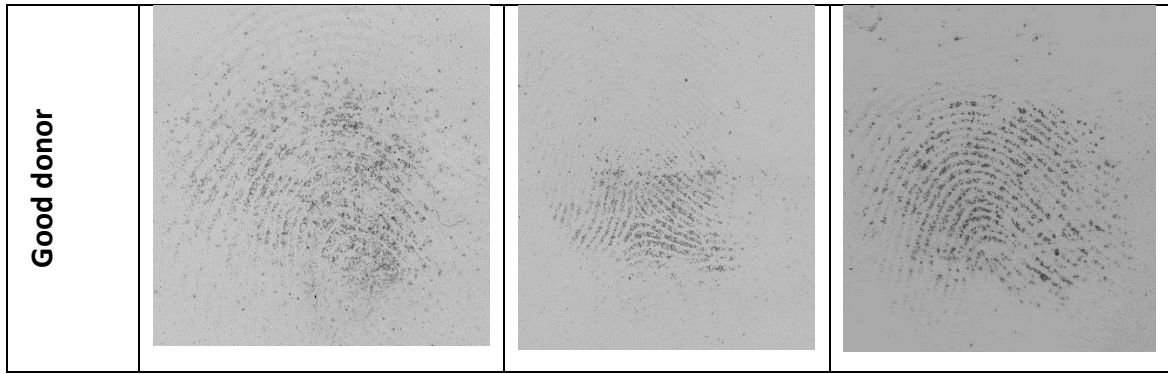


Figure 6.42 – Fingerprints deposited on patent leather and aged for 7 days under ambient conditions then developed using PDF1S

Figure 6.42 shows the results for 7 day old marks on patent leather using PD. For the aged marks, PD was only successful for the good donor and even in this case only partial marks were developed. However, this is a promising result for the capability of PD introducing a new alternative technique that could be used on patent leather surfaces.

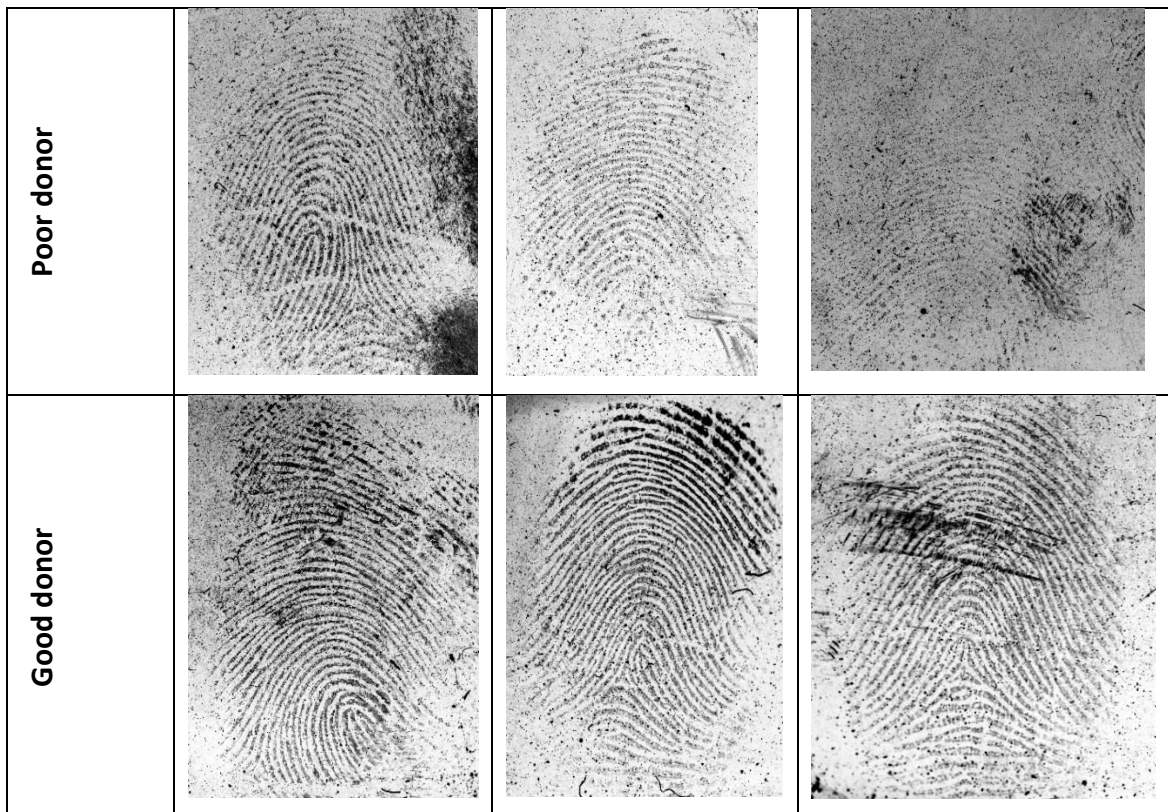


Figure 6.43 – Fingerprints deposited on patent leather and aged for 7 days under ambient conditions then developed using superglue fuming

Figure 6.43 shows the 7 day old marks developed with superglue fuming. In comparison to the PD developed marks, superglue fuming has resulted in fingerprints with high ridge detail and contrast for both the poorer and good donor marks. Even though these results are only positive for the patent leather surface, it does indicate that both superglue fuming and PD are options for fingerprint development on patent leathers.

6.2.3.2 Microscopic Analysis of Leather Surfaces

Patent leather has a non-porous finish and the successful development was a positive, yet surprising result. The deposition of silver was analysed using optical profilometry. Figure 6.44 shows an example of developed fingerprint ridge detail on patent leather.

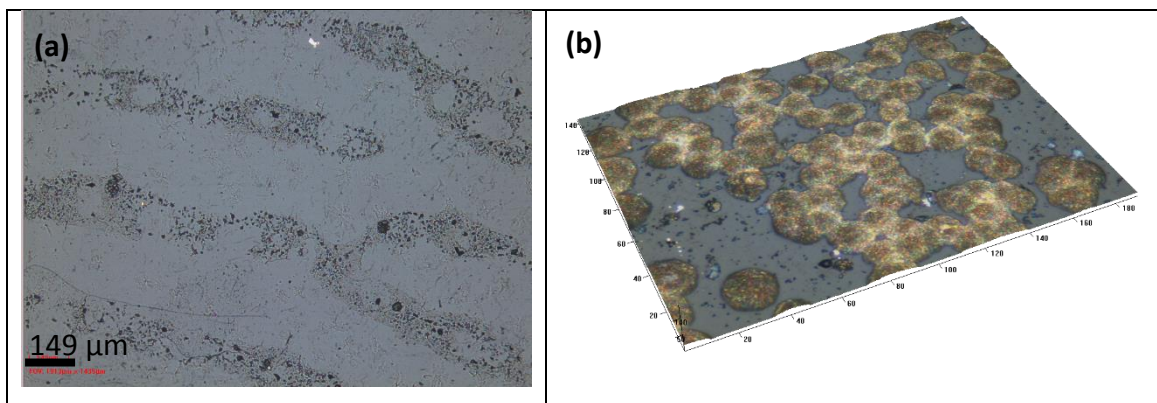


Figure 6.44 – Microscopy analysis of fingerprint ridge detail for a 1 day old mark on patent leather developed using PDF1S – (a) 2D image and (b) 3D image (50x) - tick marks every 20 µm

The microscopy image in figure 6.44a clearly shows a ridge ending and bifurcation of high contrast and clarity. In addition to this, sweat pores are visible indicating that silver has not deposited in these eccrine dominant areas. This could be a factor of the non-porous nature of the patent finish and sebaceous content would adhere stronger than eccrine components. Figure 6.44b reveals spherical silver particles, as observed on paper surfaces, with a particle diameter range of 10-20 µm. In comparison to superglue fuming, PD also developed marks on navy matte and white faux leather.

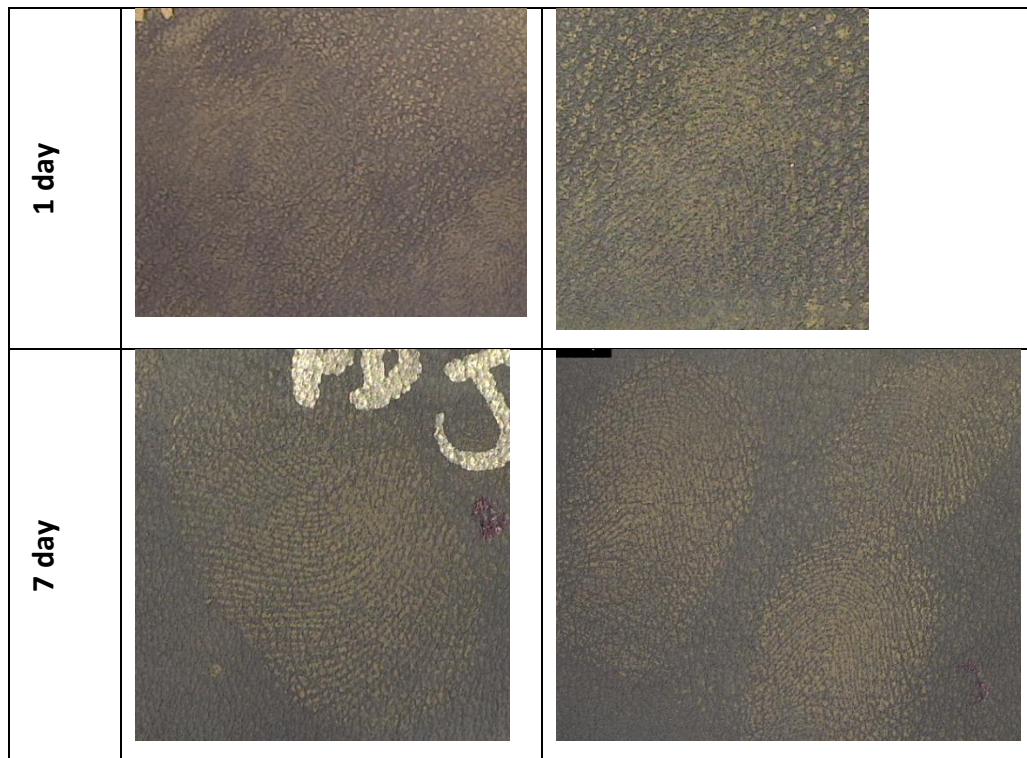


Figure 6.45 – Fingerprints deposited on navy matte leather and aged for 1 and 7 days under ambient conditions on then developed using PDF1S

Figure 6.45 shows 1 and 7 day old marks on navy matte leather developed using PD. It should be noted that only the good donor marks were developed. The 1 day old marks are not as clear as the 7 day old marks but visible fingerprint ridge detail is present. The 7 day old marks have developed full prints with definitive contrast between the fingerprint and the background. This suggests that a high level of sweat residue is required on these more difficult surfaces in order for PD to be successful.

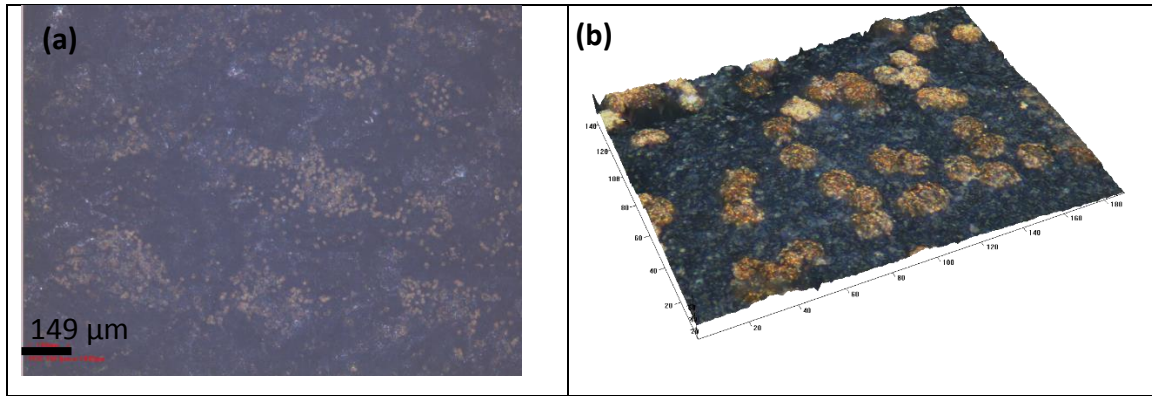


Figure 6.46 – Microscopy analysis of a fingerprint ridge for a 7 day old mark on navy matte leather developed using PDF1S – (a) 2D image (b) 3D image (50x) - tick marks every 20 μm

Figure 6.46 shows an example of the microscopy analysis of marks developed on navy matte leather. The microscopy images indicate that the fingerprints have only partially developed along the individual ridges with denser areas. This could be reflective of the sebaceous content having a stronger capability of remaining on the surface. The particle diameter ranged from 10-20 μm similarly to the patent leather.

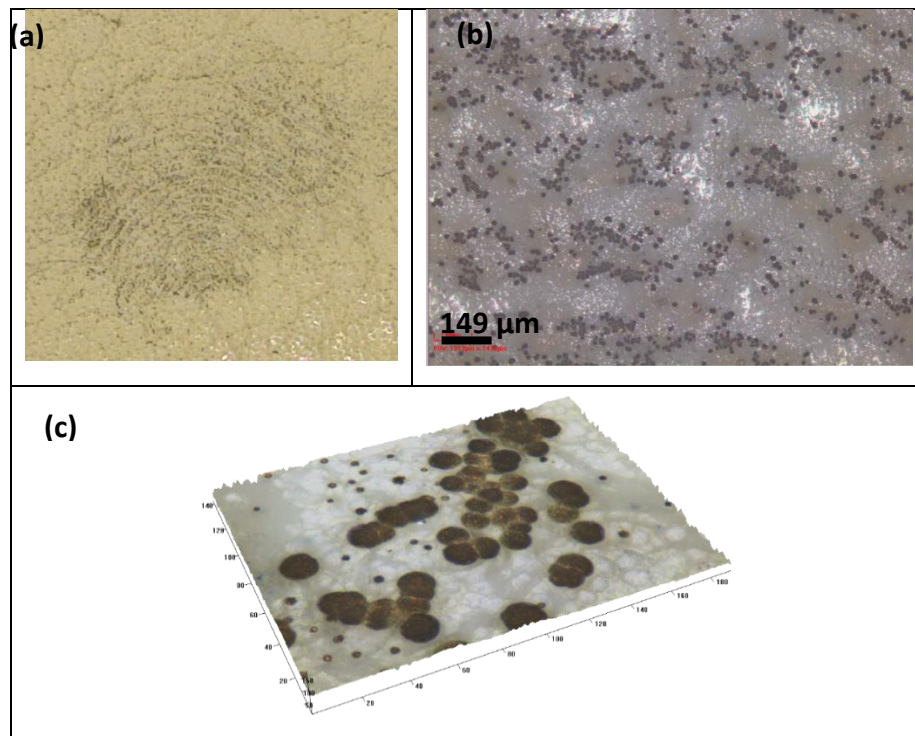


Figure 6.47 – (a) Fingerprint deposited on white faux leather and aged for 7 days under ambient conditions developed using PDF1S (b) 2D image (c) 3D image (50x) - tick marks every 20 μm

Figure 6.27 shows a mark developed on white faux leather. The developed mark is partial but the silver deposition is evident in the microscopic analysis as spherical particles with a narrow particle diameter range (10-20 μm). It is worth mentioning that the white faux leather had to be treated in maleic acid prior to PD development. This was to remove any artificial fillers used to dye the leather white similar to the calcium carbonate filler used in paper. This did not need to be done for the other leather or suede surfaces.

The results on the three leather surfaces, patent, navy matte and white faux, are positive and extend the possibility of using PD on surfaces other than paper. Similar results for characteristics of the silver deposits on paper surfaces was observed on these leather surfaces, such that the deposited particles are spherical, monodisperse and reach a particle diameter of ca. 20 μm .

6.3 Conclusions

Two non-ionic surfactants, Brij C10 and DGME, were used to reformulate the PD working solution. The growth of the silver deposits was measured over a 15 minute development period and the results indicated that both Brij C10 and DGME formulations behaved similarly to the current Synperonic-N system. This was observed through the identical trend in the silver deposit growth on the surface. Various formulations were explored and each one resulted in developed fingerprints with very good ridge detail. There were some discrepancies in the stability of the working solutions such that formulation 5 was determined to be the most suitable reformulation. Since this work has been completed, results from CAST have indicated that a formulation of 1.25 g/0.0019M DGME and 1.5 g/0.0061M DDAA was the most effective, which corroborates with the results in this chapter.

Though it is difficult to fully assign the various peaks produced in the Raman spectra of the various detergents and the silver surface, it can be concluded that DDAA does adsorb on the silver surface. This result is consistent with the neutron reflectivity experiments described in chapter 5. In addition to this, Tween 20 does not appear to

adsorb onto the silver surface but DGME and Brij C10 reveal additional peaks in the Ag-detergent spectra. Alongside the reproducible results from the silver growth on the paper surface, this indicates that DGME and Brij C10 are suitable alternatives for a consistently stable PD working solution.

The capability of PD has been extended to leather surfaces – white faux, navy matte and patent leather. Superglue fuming was more effective on the patent leather than PD but fingerprints were still developed using PD. In addition to this, PD was the only technique that developed marks on the white faux and navy matte leather. Microscopic analysis revealed that silver was not deposited in the eccrine rich areas and the silver particle diameter was comparable to the observations on paper surfaces.

6.4 References

1. G. Naja, P. Bouvrette, S. Hrapovic and J. H. Luong, *The Analyst*, 2007, **132**, 679-686.
2. M. Muniz-Miranda and G. Sbrana, *Journal of Molecular Structure*, 2001, **565-566**, 159-163.
3. A. J. McQuillan, P. J. Hendra and M. Fleischmann, *Journal of Electroanalytical Chemistry*, 1975, **65**, 933-944.
4. I. Martina, R. Wiesinger, D. Jembrih-Simburger and M. Schreiner, *e-Preservation Science*, 2012, **9**.
5. A. A. Cantu, *Forensic Science Review*, 2001, **13**, 29-64.
6. R. P. Downham, S. Kelly and V. G. Sears, *Feasibility studies for fingermark visualization on leather and artificial leather*, 2015.
7. C. Fairley, S. M. Bleay, V. G. Sears and N. NicDaeid, *Forensic Science International*, 2012, **217**, 5-18.
8. J. Fraser, P. Deacon, S. Bleay and D. H. Bremner, *Science & Justice*, 2014, **54**, 133-140.
9. S. Knighting, J. Fraser, K. Sturrock, P. Deacon, S. Bleay and D. H. Bremner, *Science & Justice*, 2013, **53**, 309-314.

10. E. Sonnex, M. J. Almond and J. W. Bond, *Journal of Forensic Sciences*, 2016, **61**, 1100-1106.
11. K. J. Farrugia, H. Bandey, L. Dawson and N. N. Daeid, *Journal of Forensic Sciences*, 2013, **58**, 1472-1485.

Chapter 7:

Conclusions and Future Work

7.1	Conclusions	222
7.2	Future Work	226
7.3	References	227

7.1 Conclusions

The overarching theme of this thesis has been to understand the fundamental chemistry of the physical developer process with the secondary aim of a new generation formula. The underlying principles regarding the mechanism of silver deposition were explored macroscopically (full fingerprint) and microscopically (fingerprint ridges). In addition to this, the role of the two surfactant components in the working solution was studied using the technique of neutron reflectivity, which has not been used to explore this before. The latter work conducted for this thesis focused on the reformulation of the working solution. This was accomplished macroscopically, i.e. the efficacy of the development of fingerprints and spectroscopically. Finally, the capability of PD was extended to alternative porous surfaces.

Natural and groomed (sebaceous and eccrine) fingerprints were deposited and aged for 1, 14 and 28 days prior to development with PD. The eccrine fingerprints across all ages studied did not result in silver deposition most likely due to the water soluble content dissolving, when the paper is treated in the maleic acid prewash. The groomed sebaceous fingerprints did result in developed fingerprints with high contrast and defined ridge detail but this was not observed for the older fingermarks. With the increase in the age of the fingermark, the resulting developed fingerprints lacked clarity. However, the natural developed fingerprints showed defined ridge details and high contrast even when the fingermark was aged for 28 days. This was a clear indication that both sebaceous and eccrine material have to be present for PD to work effectively for both fresh and aged marks.

PD is often used as the last method for a porous surface, unless the substrate has previously been wetted. DFO and ninhydrin, the primary porous surface development methods, involve exposing the substrate to heat. Therefore, the effect of heat and wetting was explored using split prints. It was concluded that neither heating nor wetting the surface prior to development with PD significantly increased or reduced the resulting developed fingerprint quality.

The development of different sweat types revealed that PD development is more effective when both eccrine and sebaceous content is present in the fingerprint residue. To understand the mechanism of PD further, spot tests were utilised to explore any specific targets for silver deposition. The eccrine material did not result in a positive reaction, i.e. silver deposition, only squalene, cholesterol and palmitic acid revealed some silver deposition. However, these results were not consistent for the replicates. When the eccrine and sebaceous contents were deposited onto the paper as a mixture, much darker silver deposition was observed for both the squalene and oleic acid combinations with all eccrine components. This result was another clear indication that both sebaceous and eccrine content have to be present for PD to work optimally. In order to evaluate realistic fingerprint residue, emulsion spot tests were studied. The results were not entirely comparable to the mixture of components as only palmitic acid-eccrine material combinations showed strong silver deposition. Squalene with serine and glycine showed some silver deposition for aged spots. Therefore, the exact class of compounds or trigger materials cannot be definitively identified but for PD to be as effective as possible both sebaceous and eccrine material must be present.

PD has been studied macroscopically i.e. the visualisation of a fingerprint but the microscopic analysis was explored in this thesis regarding the behaviour of the silver particles in the working solution as well as the deposited silver particulates on the surface.

For the first time, the size of the particles in the working solution was defined for both the current formulation and the reformulated working solutions. The Synperonic-N formulation revealed the largest silver particle diameter at 700-800 nm, whereas the reformulated solutions had a smaller silver particle diameter at 300-600 nm. However, the size of the particles in the solution did not have a significant effect on the initial size of the deposited silver particulates within the 30 seconds-2 minute timeframe of development.

By studying the size of the silver deposits from 30 seconds to 15 minutes, it was concluded that the initial deposition of silver is relatively fast as the silver deposits had a diameter range of 2-4 μm after 30 seconds of development. Microscopic analysis revealed a nucleation point after ca. 2 minutes and progressive growth is observed until a plateau is reached from ca. 10 minutes. The silver deposits are spherical and monodisperse. This trend in the growth of the silver deposits on the surface was the same and observed for all formulations studied. The only noticeable difference was the final diameter value of the silver deposits after 15 minutes. The silver particle diameter varied from ca. 8-15 μm , with the Synperonic-N formulation showing the largest silver deposits and the DGME formulations showing the smallest. From the macroscopic and microscopic analysis of each of the developed fingerprints at each time interval, it was concluded that the resulting diameter of the silver particulates is dependent on the initial deposition of silver. If there is a larger area of the fingerprint developed initially, this provides a greater number of silver sites for subsequent silver growth. Therefore, the final silver deposits are smaller in their diameter. This result was also confirmed through the use of split prints and ageing of the fingerprints.

Compositional analysis of the silver deposits revealed the expected result of Ag for the particulates and no Ag peak on the background paper fibres. However, the interesting result concluded that no iron is present in the silver deposits. This means that although a crucial component of the redox reaction in the working solution, iron is not involved in the deposition of silver on the surface.

A new generation formula was accomplished after observing the growth of the silver particulates and the interaction of the surfactant with a planar silver surface. The trend in the growth of the silver was the same regardless of the detergent system used; therefore the quality of the resulting developed fingerprints had to be considered. The PD working solution with Tween 20 was unpredictable in terms of the stability and efficacy of development. In comparison to other countries where Tween 20 is being used and producing stable solutions of up to a month, only one solution was made and remained stable for only two weeks in this thesis. In addition to this, the

development times varied from a maximum of 15 minutes to a maximum of 45 minutes. The developed fingerprints did show defined ridge detail but the contrast was weak for some samples. Due to the inconsistency in the stability of the PD working solutions prepared with Tween 20 and the undesirable processing times, Tween 20 was deemed to be an unsuitable replacement.

Neutron reflectivity experiments confirmed that DDAA is most likely adsorbing onto a planar silver surface in the presence of Tween 20. The adsorption of DDAA and Tween 20 was measured using a planar silver surface for DDAA and Tween 20 alone, followed by a competitive adsorption. The DDAA forms a multilayer on the surface which confirms that DDAA could form a micellar structure around the silver particles in the colloidal dispersion. This fundamental result was explored for the first time since Jonker et al. proposed the staggered conformation of DDAA around the silver particles.^{1,2} However, the cationic surfactant, DDAA, cannot stabilise the working solution alone as revealed from development of fingerprints for various concentrations of DDAA in the working solution. The silver precipitates either immediately after use or before the working solution is completely prepared.

In addition to this, Raman spectroscopy revealed that the non-ionic surfactant does have an effect on the silver surface. This was observed for both DGME and Brij C10, with DGME showing the most significant peak changes when the detergent was introduced to the silver surface. Taking into the account the results from the Raman spectroscopy and the growth of silver on the surface, it was concluded that DGME and Brij C10 aid the stability of the working solution.

Formulation 5 (0.0023 M DGME, 0.0061 M DDAA detergent system) was determined to be the most suitable reformulation. The processing times were up to 15 minutes but with careful monitoring of the PD process, fingerprints could be removed after ca. 10 minutes. Results were reproducible across the replicates studied. The initial development was fast and full fingerprints could be visualised after only 2 minutes. The ridge detail was clearly defined in all fingerprints and split prints studied with a high contrast between the print and the background. In addition to this, the

working solution remained stable for 5-7 days even after repeated use, which was reproducible.

Finally, the capability of PD was extended to alternative porous surfaces – leathers and suedes. PD was successful and both partial and full fingerprints were developed on patent, white faux and navy matte leathers. Microscopic analysis revealed that the silver deposits were spherical, monodisperse and had a particle diameter range of 10-20 μm , similarly to PD on paper. In addition to this, microscopy was able to show that silver did not deposit in the eccrine rich pore areas of the fingerprint. PD was compared to superglue fuming which was more effective on patent leather, but only PD developed fingermarks on white faux and navy matte leather. These results extend the application of PD but also offers an alternative method for these leather surfaces.

7.2 Future Work

The PD working solution was successfully reformulated using DGME as the replacement non-ionic surfactant. Since this work has been completed and in collaboration with CAST, a detergent solution containing 1.25 g/0.0019 M of DGME and 1.5 g/0.0061 M of DDAA has been deemed as the most suitable replacement.

This thesis evaluated the new formulation with respect to the stability of the working solution, the quality of fingerprint development, the growth of silver on the surface and the interfacial interaction of the surfactant and silver surface. However, only one donor was used for fingerprint deposition and one type of paper – 80 gsm white copy paper. In order to fully evaluate the new formulation, the sensitivity of the technique must be explored. This would include the use of multiple donors as well as various paper types and age of the mark. In addition, the substrates would need to be exposed to different environmental conditions, particularly wetted conditions. PD is the only technique currently capable of fingerprint development on wetted porous surfaces in the UK, so this must be possible with the new formulation. As well as other paper types, it would be beneficial to explore the use of the new formulation for

fingerprint recovery on the leather surfaces that were successful in chapter 6 but also the potential to recover fingerprints from more leather or suede surfaces.

The neutron reflectivity experiments were novel in this area and indicated that DDAA does adsorb to the surface. It would be useful to repeat the experiments using DGME in order to fully characterise the new formulation. The NR measurements were completed using a planar silver surface. Small angle neutron scattering (SANS) is another neutron scattering technique that can determine the structure of a system on the scale of 1 – 100 nm.³ SANS offers the experimental advantage that a solution can be used. From the knowledge gained from the NR measurements in chapter 5 and DLS measurements in chapter 6, a system could be carefully formulated for the SANS application. The physical properties such as radius, shape, interfacial interactions and nature of the micelles (aggregated or homologous) could be determined.³ This technique could provide an insight into the exact structure of the colloidal silver dispersion. It has already been utilised to explore the micelle conformations of Tween and other surfactants in the presence of various additives.⁴⁻⁷

7.3 References

1. H. Jonker, A. Molenaar and C. J. Dippel, *Photographic Science and Engineering*, 1969, **13**, 38-43.
2. H. Jonker, L. K. H. van Beek, C. J. Dippel, C. J. G. F. Janssen, A. Molenaar and E. J. Spiertz, *Journal of Photographic Science*, 1971, **19**, 96-105.
3. M. Ceretti, F. Cousin, W. Paulus, M. H. Mathon and C. Ritter, *EPJ Web of Conferences*, 2015, **104**, 01004.
4. R. K. Mahajan, J. Chawla, M. S. Bakshi, G. Kaur, V. K. Aswal and P. S. Goyal, *Colloid and Polymer Science*, 2004, **283**, 164-168.
5. J. Penfold and R. K. Thomas, *Current Opinion in Colloid & Interface Science*, 2014, **19**, 198-206.
6. R. K. Mahajan, J. Chawla, K. K. Vohra and V. K. Aswal, *Journal of Applied Polymer Science*, 2010, **117**, 3038-3046.

7. R. R. Hegde, S. Kumar, V. K. Aswal, A. Verma, S. S. Bhattacharya and A. Ghosh, *Journal of Dispersion Science and Technology*, 2014, **35**, 783-788.

Appendix

A. Spot Tests

230

A. Spot Tests

A.1 Individual Components

②

Eccrine	100 _{mM}	10 _{mM}	1 _{mM}	CONTROL (H ₂ O)
Serine				
Glycine				
Sodium Chloride				
Lactic Acid				

Figure 1 - PD treatment applied to individual eccrine components spot test, 1 day old aged under ambient conditions - Set 2

Eccrine	100 _{mM}	10 _{mM}	1 _{mM}	CONTROL (H ₂ O)
Serine				
Glycine				
Sodium Chloride				
Lactic Acid				

Figure 2 - PD treatment applied to individual eccrine components spot test, 1 day old aged under ambient conditions - Set 3

(Wet) Ecotine ③	100 _{mM}	10 _{mM}	1 _{mM}
Serine			
Glycine			
NaCl			
Lactic acid			

Figure 3 - PD treatment applied to individual eccrine components spot test, 1 day old aged under wetted conditions - Set 3

	10 _{mM}	1 _{mM}
myralene		
Cholesterol		
Palmitic acid		
Dlec acid		

Figure 4 - PD treatment applied to individual sebaceous components spot test, 1 day old aged under wetted conditions - Set 1

Sebacous	50 μ M	10 μ M	1 μ M
Squalene			
Cholesterol			
Palmitic acid			
Oleic acid			

Figure 5 – PD treatment applied to individual sebaceous components spot test, 1 day old aged under wetted conditions - Set 3

A.2 Mixture of Eccrine and Sebaceous Components

Sebacous 1 st Eccrine 2 nd	Serine	Glycine	NaCl	Lactic Acid
Sebacous 1 st Eccrine 2 nd ③				
Squalene				
Cholesterol				
Palmitic Acid				
Oleic Acid				
Sebacous 1 st Eccrine 2 nd ②				
Squalene				
Cholesterol				
Palmitic Acid				
Oleic Acid				

Figure 6 - PD treatment applied to mixture of sebaceous and eccrine components, 1 day old aged under ambient conditions. Set 1 and set 3 where the sebaceous component has been deposited first, followed by the eccrine component

Eccrine 1 st Sebacous 2 nd	Squalene	Cholesterol	Palmitic Acid	Oleic Acid
Serine				
Glycine				
NaCl				
Lactic Acid				
Eccrine 1 st Sebacous 2 nd	Squalene	Cholesterol	Palmitic Acid	Oleic Acid

Eccrine 1 st Sebacous 2 nd	Squalene	Cholesterol	Palmitic Acid	Oleic Acid
③				
Serine				
Glycine				
NaCl				
Lactic Acid				
Eccrine 1 st Sebacous 2 nd	Squalene	Cholesterol	Palmitic Acid	Oleic Acid
④				

Figure 7 - PD treatment applied to mixture of sebaceous and eccrine components, 1 day old aged under ambient conditions. Set 1 and set 3 where the eccrine component has been deposited first, followed by the sebaceous component

A.3 Emulsions

7 day	7 days Emulsion ②	Serine	Glycine	Lactic acid	NaCl
	Squalene				
	Cholesterol				
	Palmitic acid				
	Oleic acid				
	←				

7 days ③	Serine	Glycine	Lactic acid	NaCl
Squalene				
Cholesterol				
Palmitic acid				
Oleic acid				

Figure 8 - PD treatment applied to 7 day old emulsion spot tests – set 2 and set 3

14 day	DR 14 days ② Emulsion	Serine	Glycine	Lactic	NaCl	DR 14 days ③ Emulsion	Serine	Glycine	Lactic	NaCl
	Squalene					Squalene				
	Cholesterol					Cholesterol				
	Palmitic acid					Palmitic acid				
	Oleic acid					Oleic acid				

Figure 9 - PD treatment applied to 14 day old emulsion spot tests – set 2 and set 3

28 day	DR 28 days ① Emulsion	Serine	Glycine	Lactic	NaCl	DR 28 days ② Emulsion	Serine	Glycine	Lactic	NaCl
	Squalene					Squalene				
	Cholesterol					Cholesterol				
	Palmitic acid					Palmitic acid				
	Oleic acid					Oleic acid				

Figure 10 - PD treatment applied to 28 day old emulsion spot tests – set 1 and set 2

Bibliography

A. P. Abbott, J. Griffith, S. Nandhra, C. O'Connor, S. Postlethwaite, K. S. Ryder and E. L. Smith, *Surf. Coat. Technol.*, 2008, **202**, 2033-2039.

N. E. Archer, Y. Charles, J. A. Elliott and S. Jickells, *Forensic Science International*, 2005, **154**, 224-239.

P. A. Ash, C. D. Bain and H. Matsubara, *Current Opinion in Colloid & Interface Science*, 2012, **17**, 196-204.

C. Au, H. Jackson-Smith, I. Quinones, B. J. Jones and B. Daniel, *Forensic Science International*, 2011, **204**, 13-18.

M. J. Bailey, R. Bradshaw, S. Francese, T. L. Salter, C. Costa, M. Ismail, R. P. Webb, I. Bosman, K. Wolff and M. de Puit, *The Analyst*, 2015, **140**, 6254-6259.

A. Beaudoin, *Journal of Forensic Identification*, 2004, **54**, 413-421.

A. Becue, A. Scoundrianos and S. Moret, *Forensic Science International*, 2012, **219**, 39-49.

J. Belloni, *C. R. Physique 3*, 2002, 381-390.

J. Belloni, *Radiation Physics and Chemistry*, 2003, **67**, 291-296.

A. Bentolila, J. Totre, I. Zozulia, M. Levin-Elad and A. J. Domb, *Macromolecules*, 2013, **46**, 4822-4828.

S. Berdejo, M. Rowe and J. W. Bond, *Journal of Forensic Sciences*, 2012, **57**, 509-514.

A. L. Beresford and A. R. Hillman, *Anal Chem*, 2010, **82**, 483-486.

S. Bhattacharjee, *J Control Release*, 2016, **235**, 337-351.

D. E. Bicknell and R. S. Ramotowski, *Journal of Forensic Sciences*, 2008, **53**, 1108-1116.

K. Braasch, M. de la Hunty, J. Deppe, X. Spindler, A. A. Cantu, P. Maynard, C. Lennard and C. Roux, *Forensic Science International*, 2013, **230**, 74-80.

R. Bradshaw, R. Wolstenholme, L. S. Ferguson, C. Sammon, K. Mader, E. Claude, R. D. Blackledge, M. R. Clench and S. Francese, *The Analyst*, 2013, **138**, 2546-2557.

S. K. Bramble, *Journal of Forensic Sciences*, 1995, **40**, 969-975.

R. M. Brown and A. R. Hillman, *Physical Chemistry Chemical Physics: PCCP*, 2012, **14**, 8653-8661.

G. S. Bumbrah, *Egyptian Journal of Forensic Sciences*, 2016, **6**, 328-332.

G. S. Bumbrah and R. M. Sharma, *Egyptian Journal of Forensic Sciences*, 2016, **6**, 209-215.

D. Burow, D. Seifert and A. A. Cantu, *Journal of Forensic Sciences*, 2003, **48**, 1-7.

D. Burow, *Journal of Forensic Identification*, 2003, **53**, 304-314.

S. Cadd, M. Islam, P. Manson and S. Bleay, *Science & Justice*, 2015, **55**, 219-238.

S. J. Cadd, L. Mota, D. Werkman, M. Islam, M. Zuidberg and M. de Puit, *Anal. Methods*, 2015, **7**, 1123-1132.

A. A. Cantu, *Notes on some latent fingerprint visualization techniques developed by Dr. George Saunders* U.S. Secret Service, Washington DC, 1996.

A. A. Cantu, *Forensic Science Review*, 2001, **13**, 29-64.

A. A. Cantu, D. A. Leben and K. Wilson, *Proc. SPIE 5071, Sensors and Command, Control, Communications and Intelligence (C31) Technologies for Homeland Defense and Law Enforcement II*, 2003, **5071**, 164-167.

CAST, *Home Office Centre of Applied Science and Technology Fingerprint Visualisation Manual* 1st edn., 2014.

M. Ceretti, F. Cousin, W. Paulus, M. H. Mathon and C. Ritter, *EPJ Web of Conferences*, 2015, **104**, 01004.

S. Chadwick, L. Xiao, P. Maynard, C. Lennard, X. Spindler and C. Roux, *Australian Journal of Forensic Sciences*, 2014, **46**, 471-484.

C. Champod, C. Lennard, P. Margot and M. Stoilovic, *Fingerprints and other ridge skin impressions*, CRC Press, Boca Raton, 2004.

P. Chatterjee and S. Hazra, *RSC Adv.*, 2015, **5**, 69765-69775.

C. C. Chen, C. K. Yang, J. S. Liao and S. M. Wang, *Forensic Science International*, 2015, **257**, 314-319.

D. J. Cooke, J. R. Lu, E. Lee and R. K. Thomas, *J. Phys. Chem.*, 1996, **100**, 10298-10303. R. W. J. Croft, *Under the Microscope : A Brief History of Microscopy*, World Scientific Publishing Co Pte Ltd, Singapore, 2006.

T. L. Crowley, E. M. Lee, E. A. Simister, R. K. Thomas, J. Penfold and A. R. Rennie, *Colloids and Surfaces*, 1991, **52**, 85-106.

R. S. Croxton, M. G. Baron, D. Butler, T. Kent and V. G. Sears, *Forensic Science International*, 2010, **199**, 93-102.

P. G. Cummins, J. Penfold, R. K. Thomas, E. Simister and E. Staples, *Physica B*, 1992, **180 & 181**, 483-484.

F. Cuthbertson, *The chemistry of fingerprints* AWRE Report No. 013/69, 1965.

B. T. Cutro and J. National Institute of, *The fingerprint sourcebook - chapter 4* U.S. Department. of Justice, Office of Justice Programs, National Institute of Justice, Washington, DC, 2011.

P. Czekanski, M. Fasola and J. Allison, *Journal of Forensic Sciences*, 2006, **51**, 1323-1328.

G. Dan, X. Guoxin and L. Jianbin, *Journal of Physics D: Applied Physics*, 2014, **47**, 013001.

L. W. Davis, P. F. Kelly, R. S. King and S. M. Bleay, *Forensic Science International*, 2016, **266**, e86-92.

L. Davis and R. Fisher, *Science & Justice*, 2015, **55**, 97-102.

M. de la Hunty, S. Moret, S. Chadwick, C. Lennard, X. Spindler and C. Roux, *Forensic Science International*, 2015, **257**, 481-487.

M. de la Hunty, S. Moret, S. Chadwick, C. Lennard, X. Spindler and C. Roux, *Forensic Science International*, 2015, **257**, 488-495.

V. D'Elia, S. Materazzi, G. Iuliano and L. Niola, *Forensic Science International*, 2015, **254**, 205-214.

E. Dickinson, D. S. Horne and R. M. Richardson, *Food Hydrocolloids*, 1993, **7**, 497-505.

Directive 2003/53/EC of The European Parliament and of The Council, Council Directive 76/769/EEC, 2003.

R. P. Downham, E. R. Brewer, R. S. P. King, A. M. Luscombe and V. G. Sears, *Forensic Science International*, 2017, **275**, 30-43.

D. T. Downing and J. S. Strauss, *Journal of Investigative Dermatology*, 1974, **62**, 228-244.

R. P. Downham, S. Kelly and V. G. Sears, *Feasibility studies for fingermark visualization on leather and artificial leather*, 2015.

V. Drapel, A. Becue, C. Champod and P. Margot, *Forensic Science International*, 2009, **184**, 47-53.

- J. Eastoe and J. S. Dalton, *Advances in Colloid and Interface Science*, 2000, **85**, 103-144.
- C. Fairley, S. M. Bleay, V. G. Sears and N. NicDaeid, *Forensic Science International*, 2012, **217**, 5-18.
- K. J. Farrugia, P. Deacon and J. Fraser, *Science & Justice*, 2014, **54**, 126-132.
- K. J. Farrugia, H. Bandey, L. Dawson and N. N. Daeid, *Journal of Forensic Sciences*, 2013, **58**, 1472-1485.
- J. R. Ferraro, K. Nakamoto and C. W. Brown, *Introductory Raman Spectroscopy*, Elsevier Science, San Diego, United States 2002.
- G. Fragneto-Cusani, *Journal of Physics: Condensed Matter*, 2001, **13**, 4973-4989.
- S. Francese, R. Bradshaw and N. Denison, *The Analyst*, 2017, **142**, 2518-2546.
- J. Fraser, P. Deacon, S. Bleay and D. H. Bremner, *Science & Justice*, 2014, **54**, 133-140.
- A. Furrer, J. Mesot and T. Strassle, *Neutron Scattering in Condensed Matter Physics*, World Scientific Publishing Co. Ltd, Singapore, 2009.
- F. Galton, *Finger Prints*, Macmillan and Co., London 1892.
- A. Girod, R. Ramotowski and C. Weyermann, *Forensic Science International*, 2012, **223**, 10-24.
- A. Girod and C. Weyermann, *Forensic Science International*, 2014, **238**, 68-82.
- A. Girod, L. Xiao, B. Reedy, C. Roux and C. Weyermann, *Forensic Science International*, 2015, **254**, 185-196.
- A. Glidle, J. Cooper, A. R. Hillman, L. Bailey, A. Jackson and J. R. P. Webster, *Langmuir*, 2003, **19**, 7746-7753.
- A. Glidle, C. S. Hadyoon, N. Gadegaard, J. M. Cooper, A. R. Hillman, A. R. Wilson, K. S. Ryder, J. R. P. Webster and R. Cubitt, *Journal of Physical Chemistry B*, 2005, **109**, 14335-14343.
- A. Glidle, A. R. Hillman, K. S. Ryder, E. L. Smith, J. M. Cooper, R. Dalgliesh, R. Cubitt and T. Geue, *Electrochimica Acta*, 2009, **55**, 439-450.
- A. Glidle, J. Cooper, A. R. Hillman, L. Bailey, A. Jackson and J. R. P. Webster, *Langmuir*, 2003, **19**, 7746-7753.

A. Glidle, A. R. Hillman, K. S. Ryder, E. L. Smith, J. Cooper, N. Gadegaard, J. R. P. Webster, R. Dalgliesh and R. Cubitt, *Langmuir*, 2009, **25**, 4093-4103.

G. C. Goode, J. R. Morris and J. M. Wells, *Chemical Aspects of Fingerprint Technology* SSCD Memo. No. 510, 1976-1977.

G. C. Goode and J. R. Morris, *Latent Fingerprints: A Review of their Origin, Composition and Methods of Detection* AWRE Report no. 022/83, 1985.

R. S. Greene, D. T. Downing, P. E. Pochi and J. S. Strauss, *Journal of Investigative Dermatology*, 1970, **54**, 240-247.

G. Groeneveld, S. Kuijer and M. de Puit, *Science & Justice*, 2014, **54**, 42-48.

F. Haque, A. D. Westland, J. Milligan and F. M. Kerr, *Forensic Science International*, 1989, **41**, 73.

S. A. Hardwick, *User Guide to Physical Developer - A reagent for detecting latent fingerprints*, Home Office Scientific Research and Development Branch, 1981.

M. Harker, H. Coulson, I. Fairweather, D. Taylor and C. A. Daykin, *Metabolomics*, 2006, **2**, 105-112.

G. Haugstad, *Atomic Force Microscopy : Understanding Basic Modes and Advanced Applications*, Wiley, United States, 2012.

M. R. Hawthorne, *Fingerprints: analysis and understanding*, CRC Press, Boca Raton, 2009.

P. Hazarika and D. A. Russell, *Angewandte Chemie*, 2012, **51**, 3524-3531.

I. Hefetz, A. Cohen, Y. Cohen and A. Chaikovsky, *Journal of Forensic Sciences*, 2014, **59**, 1226-1230.

R. R. Hegde, S. Kumar, V. K. Aswal, A. Verma, S. S. Bhattacharya and A. Ghosh, *Journal of Dispersion Science and Technology*, 2014, **35**, 783-788.

S. A. Holt, P. A. Reynolds and J. W. White, *Physical Chemistry Chemical Physics*, 2000, **2**, 5667-5671.

S. Hong, I. Hong, A. Han, J. Y. Seo and J. Namgung, *Forensic Science International*, 2015, **257**, 403-408.

M. M. Houck, *Forensic Fingerprints*, Elsevier Science, San Diego, United States, 2016.
J. R. Howse, R. Steitz, M. Pannek, P. Simon, D. W. Schubert and G. H. Findenegg, *Physical Chemistry Chemical Physics*, 2001, **3**, 4044-4051.

A. V. Hughes, *RasCal*. Sourceforge., Downloaded from: <http://sourceforge.net/projects/rscl/>. (2016) 2013.

A. R. W. Jackson and J. M. Jackson, *Forensic Science*, Pearson Prentice Hall, Harlow, 2004.

R. Jelly, E. L. Patton, C. Lennard, S. W. Lewis and K. F. Lim, *Analytica chimica acta*, 2009, **652**, 128-142.

B. J. Jones, R. Downham and V. G. Sears, *Surface and Interface Analysis*, 2010, **42**, 438-442.

N. Jones, D. Mansour, M. Stoilovic, C. Lennard and C. Roux, *Forensic Science International*, 2001, **124**, 167-177.

N. Jones, M. Stoilovic, C. Lennard and C. Roux, *Forensic Science International*, 2001, **115**, 73-88.

H. Jonker, A. Molenaar and C. J. Dippel, *Photographic Science and Engineering*, 1969, **13**, 38-43.

M. M. Joullie and T. R. Thompson, *Tetrahedron*, 1991, **47**, 8791-8830.

H. Jonker, L. K. H. van Beek, C. J. Dippel, C. J. G. F. Janssen, A. Molenaar and E. J. Spiertz, *Journal of Photographic Science*, 1971, **19**, 96-105.

A. Khuu, S. Chadwick, X. Spindler, R. Lam, S. Moret and C. Roux, *Forensic Science International*, 2016, **263**, 126-131.

P. Klemarczyk, *Polymer*, 2001, **42**, 2837-2848.

S. Knighting, J. Fraser, K. Sturrock, P. Deacon, S. Bleay and D. H. Bremner, *Science & Justice*, 2013, **53**, 309-314.

M. Kreuzer, T. Kaltofen, R. Steitz, B. H. Zehnder and R. Dahint, *Review of Scientific Instruments*, 2011, **82**, 023902.

S. Krickl, D. Touraud and W. Kunz, *Industrial Crops and Products*, 2017, **103**, 169-174.

S. Kundu, D. Langevin and L. T. Lee, *Langmuir*, 2008, **24**, 12347-12353.

G. T. C. Lambourne, *Journal of the Forensic Science Society*, 1977, **17**, 95-98.

E. M. Lee, R. K. Thomas, P. G. Cummins, E. Staples, J. Penfold and A. Rennie, *Chemical Physics Letters*, 1989, **162**, 196-202.

H. C. Lee and R. E. Gaensslen, *Advances in fingerprint technology*, 2nd edn., CRC Press, Boca Raton, 2001.

L. T. Lee, E. K. Mann, O. Guiselin, D. Langevin, F. B. and J. Penfold, *Macromolecules*, 1993, **26**, 7046-7052.

L. T. Lee, *Current Opinion in Colloid & Interface Science*, 1999, **4**, 205-213.

Y. Leng, *Materials Characterization : Introduction to Microscopic and Spectroscopic Methods*, John Wiley & Sons, Incorporated, Weinheim, Germany 2013.

C. Lennard, *Australian Journal of Forensic Sciences*, 2013, **45**, 356-367.

C. Lennard, *Australian Journal of Forensic Sciences*, 2013, **46**, 293-303.

P. X. Li, C. C. Dong and R. K. Thomas, *Langmuir*, 2011, **27**, 1844-1852.

P. X. Li, Z. X. Li, H. H. Shen, R. K. Thomas, J. Penfold and J. R. Lu, *Langmuir*, 2013, **29**, 9324-9334.

J. R. Lu, E. Simister, E. Lee, R. K. Thomas, A. Rennie and J. Penfold, *Langmuir*, 1992, **8**, 1837-1844.

J. R. Lu, R. K. Thomas and J. Penfold, *Advances in Colloid and Interface Science*, 2000, **84**, 143-304.

J. R. Lu, T. J. Su, P. N. Thirtle, R. K. Thomas, A. R. Rennie and R. Cubitt, *Journal of Colloid and Interface Science*, 1998, **206**, 212-223.

R. K. Mahajan, J. Chawla, M. S. Bakshi, G. Kaur, V. K. Aswal and P. S. Goyal, *Colloid and Polymer Science*, 2004, **283**, 164-168.

R. K. Mahajan, J. Chawla, K. K. Vohra and V. K. Aswal, *Journal of Applied Polymer Science*, 2010, **117**, 3038-3046.

M. F. Mangle, X. Xu and M. de Puit, *Science & Justice*, 2015, **55**, 343-346.

P. J. Mankidy, R. Rajagopalan and H. C. Foley, *Polymer*, 2008, **49**, 2235-2242.

H. Mark and C. R. Harding, *Int J Cosmet Sci*, 2013, **35**, 163-168.

C. Marriott, R. Lee, Z. Wilkes, B. Comber, X. Spindler, C. Roux and C. Lennard, *Forensic Science International*, 2014, **236**, 30-37.

R. J. Marsh, R. A. L. Jones, M. Sferrazza and J. Penfold, *Journal of Colloid and Interface Science*, 1999, **218**, 347-349.

- I. Martina, R. Wiesinger, D. Jembrih-Simburger and M. Schreiner, *e-Preservation Science*, 2012, **9**.
- A. J. McQuillan, P. J. Hendra and M. Fleischmann, *Journal of Electroanalytical Chemistry*, 1975, **65**, 933-944.
- B. A. McSwiney, *Proceedings of the Royal Society of Medicine*, 1934, **27**, 839-848.
- C. E. Morgan, C. J. Breward, I. M. Griffiths, P. D. Howell, J. Penfold, R. K. Thomas, I. Tucker, J. T. Petkov and J. R. Webster, *Langmuir*, 2012, **28**, 17339-17348.
- K. Morishima and T. Sato, *Langmuir*, 2014, **30**, 11513-11519.
- J. R. Morris, *The Detection of Latent Fingerprints on Wet Paper Samples* SSCD Memo. No. 367, 1975.
- J. R. Morris, *Progress Sheet 8* AWRE Report, 1977-1978.
- J. R. Morris, *Progress Sheet 1* AWRE Report 1979.
- H. Moses Daluz, *Fundamentals of Fingerprint Analysis*, CRC Press, Boca Roca, United States, 2014.
- M. Muniz-Miranda and G. Sbrana, *Journal of Molecular Structure*, 2001, **565-566**, 159-163.
- G. Naja, P. Bouvrette, S. Hrapovic and J. H. Luong, *The Analyst*, 2007, **132**, 679-686.
- Neutron News*, 1992, **3**, 29-37.
- T. Nikkari, *Journal of Investigative Dermatology*, 1974, **62**, 257-267.
- G. W. Padua and Q. Wang, *Nanotechnology Research Methods for Food and Bioproducts*, Wiley, Hoboken, United States 2012.
- J. Penfold and R. K. Thomas, *J. Phys. Condens. Matter* 1990, **2**, 1369-1412.
- J. Penfold, R. K. Thomas, E. Simister, E. Lee and A. Rennie, *J. Phys. Condens. Matter*, 1990, **2**, SA411-SA416.
- J. Penfold, E. Staples, L. Thompson and I. Tucker, *Colloids and Surfaces A: Physiochem. Eng. Aspects*, 1995, **102**, 127-132.
- J. Penfold, E. J. Staples, I. Tucker, L. Thompson and R. K. Thomas, *Physica B*, 1998, **248**, 223-228.

- J. Penfold, E. J. Staples, I. Tucker, L. J. Thompson and R. K. Thomas, *International Journal of Thermophysics*, 1999, **20**, 19-34.
- J. Penfold, E. Staples and I. Tucker, *Langmuir*, 2002, **18**, 2967-2970.
- J. Penfold, L. Tucker, J. Petkov and R. K. Thomas, *Langmuir*, 2007, **23**, 8357-8364.
- J. Penfold and R. K. Thomas, *Current Opinion in Colloid & Interface Science*, 2014, **19**, 198-206.
- J. Penfold, R. K. Thomas, P. Li, J. T. Petkov, I. Tucker, A. R. Cox, N. Hedges, J. R. Webster and M. W. Skoda, *Langmuir*, 2014, **30**, 9741-9751.
- J. Penfold, R. K. Thomas, P. X. Li, J. T. Petkov, I. Tucker, J. R. Webster and A. E. Terry, *Langmuir*, 2015, **31**, 3003-3011.
- T. Perevozchikova, H. Nanda, D. P. Nesta and C. J. Roberts, *J. Pharm. Sci.*, 2015, **104**, 1946-1959.
- S. Petrash, A. Liebmann-Vinson, M. D. Foster, L. M. Lander, W. J. Brittain and C. F. Majkrzak, *Biotechnology Progress*, 1997, **13**, 635-639.
- C. E. Phillips, D. O. Cole and G. W. Jones, *Journal of Forensic Identification*, 1990, **40**, 135-147.
- M. Picardo, M. Ottaviani, E. Camera and A. Mastrofrancesco, *Dermato-Endocrinology*, 2009, **1**, 68-71.
- N. Porpiglia, S. Bleay, L. Fitzgerald and L. Barron, *Science & Justice*, 2012, **52**, 42-48.
- C. Prete, L. Galmiche, F. G. Quenum-Possy-Berry, C. Allain, N. Thiburce and T. Colard, *Forensic Science International*, 2013, **233**, 104-112.
- R. Ramotowski, *Journal of Forensic Identification*, 1996, **46**, 673-677.
- R. Ramotowski, *Journal of Forensic Identification*, 2000, **50**, 363-384.
- R. Ramotowski and A. A. Cantu, *Fingerprint Whorld*, 2001, **27**, 59-65.
- R. Ramotowski, *Lee and Gaensslen's Advances in Fingerprint Technology, Third Edition*, CRC Press Inc, GB, 2013.
- B. Richard, J. L. Lemyre and A. M. Ritcey, *Langmuir*, 2017, **33**, 4748-4757.
- R. M. Richardson, M. J. Swann, A. R. Hillman and S. J. Roser, *Faraday Discussions*, 1992, **94**, 295-306.

- A. Richmond-Aylor, S. Bell, P. Callery and K. Morris, *Journal of Forensic Sciences*, 2007, **52**, 380-382.
- S. Robinson and A. H. Robinson, *Physiological reviews*, 1954, **34**, 202-220.
- R. Saferstein, *Criminalistics: an introduction to forensic science*, Pearson Education, Upper Saddle River, N.J; Harlow, 2010.
- K. Sato, W. H. Kang, K. Saga and T. Sato, *J. American Academy of Dermatology*, 1989, **20**, 537-563.
- G. Sauzier, A. A. Frick and S. W. Lewis, *Journal of Forensic Identification*, 2013, **63**, 70-88.
- B. Schnetz and P. Margot, *Forensic Science International*, 2001, **118**, 21-28.
- J. C. Schulz, G. G. Warr, P. D. Butler and W. A. Hamilton, *Physical Review E*, 2001, **63**, 041604.
- L. Schwarz, *Journal of Forensic Sciences*, 2009, **54**, 1323-1326.
- V. G. Sears, S. M. Bleay, H. L. Bandey and V. J. Bowman, *Science & Justice*, 2012, **52**, 145-160.
- R. Shahlori, G. I. N. Waterhouse, T. A. Darwish, A. R. J. Nelson and D. J. McGillivray, *CrystEngComm*, 2017, **19**, 5716-5720.
- S. S. Shetage, M. J. Traynor, M. B. Brown, M. Raji, D. Graham-Kalio and R. P. Chilcott, *Skin research and technology : official journal of International Society for Bioengineering and the Skin*, 2014, **20**, 97-107.
- J. Siegel, *Forensic Science*, Oneworld Publications, New York, NY, United States, 2016.
- R. K. Simmons, P. Deacon and K. J. Farrugia, *Journal of Forensic Identification*, 2014, **64**, 157-173.
- J. W. Slot and H. J. Geuze, *European Journal of Cell Biology*, 1985, **38**, 87-93.
- G. S. Sodhi and J. Kaur, *Forensic Science International*, 2001, **120**, 172-176.
- G. S. Sodhi and J. Kaur, *Egyptian Journal of Forensic Sciences*, 2015, **6**, 44-47.
- E. Sonnex, M. J. Almond and J. W. Bond, *Journal of Forensic Sciences*, 2016, **61**, 1100-1106.
- G. L. Squires, *Introduction to the Theory of Thermal Neutron Scattering*, Dover Publications, New York, USA, 1997.

- E. Staples, L. Thompson and L. Tucker, *Langmuir*, 1994, **10**, 4136-4141.
- E. Staples, L. Thompson, I. Tucker, J. Hines, R. K. Thomas and J. R. Lu, *Langmuir*, 1995, **11**, 2496-2503.
- E. Stauffer, A. Becue, K. V. Singh, K. R. Thampi, C. Champod and P. Margot, *Forensic Science International*, 2007, **168**, e5-9.
- R. Steitz, P. Müller-Buschbaum, S. Schemmel, R. Cubitt and G. H. Findenegg, *Europhysics Letters (EPL)*, 2004, **67**, 962-968.
- S. V. Stevenage and C. Pitfield, *Forensic Science International*, 2016, **267**, 145-156.
- M. Stoilovic, *Forensic Science International*, 1993, **60**, 141-153.
- F. Sun, T. C. Jaspers, P. M. van Hasselt, W. E. Hennink and C. F. van Nostrum, *Pharm Res*, 2016, **33**, 2168-2179.
- T. Tani, *Photographic Sensitivity : Theory and Mechanisms*, Oxford University Press, Cary, United States, 1995.
- D. J. Taylor, R. K. Thomas and J. Penfold, *Advances in Colloid and Interface Science*, 2007, **132**, 69-110.
- N. A. Taylor and C. A. Machado-Moreira, *Extreme physiology & medicine*, 2013, **2**, 4.
- R. K. Thomas, *Annual Review of Physical Chemistry*, 2004, **55**, 391-426.
- S. Vargas, B. E. Millan-Chiu, S. M. Arvizu-Medrano, A. M. Loske and R. Rodriguez, *J Microbiol Methods*, 2017, **137**, 34-39.
- C. Wallace-Kunkel, C. Lennard, M. Stoilovic and C. Roux, *Forensic Science International*, 2007, **168**, 14-26.
- S. P. Wargacki, L. A. Lewis and M. D. Dadmun, *Journal of Forensic Sciences*, 2007, **52**, 1057-1062.
- S. P. Wargacki, L. A. Lewis and M. D. Dadmun, *Journal of Forensic Sciences*, 2008, **53**, 1138-1144.
- J. Webster, S. Holt and R. Dalgliesh, *Physica B: Condensed Matter*, 2006, **385-386**, 1164-1166.
- K. A. Weston-Ford, M. L. Moseley, L. J. Hall, N. P. Marsh, R. M. Morgan and L. P. Barron, *Science & Justice*, 2016, **56**, 1-8.

- C. Weyermann, C. Roux and C. Champod, *Journal of Forensic Sciences*, 2011, **56**, 102-108.
- K. Wilke, A. Martin, L. Terstegen and S. S. Biel, *International Journal of Cosmetic Science*, 2007, **29**, 169-179.
- D. Wilkinson, *Forensic Science International*, 2000, **109**, 87-103.
- B. T. M. Willis and C. J. Carlile, *Experimental Neutron Scattering*, Oxford Univeristy Press 2009.
- J. D. Wilson, A. A. Cantu, G. Antonopoulos and M. J. Surrency, *Journal of Forensic Sciences*, 2007, **52**, 320-329.
- H. Wolfschmidt, C. Baier, S. Gsell, M. Fischer, M. Schreck and U. Stimming, *Materials*, 2010, **3**, 4196-4213.
- M. A. Wood and T. James, *Science & Justice*, 2009, **49**, 272-276.
- J.-C. Wu, T.-L. Lin, U. S. Jeng and N. Torikai, *Physica B: Condensed Matter*, 2006, **385-386**, 838-840.
- L. Xu, C. Zhang, Y. He and B. Su, *Science China Chemistry*, 2015, **58**, 1090-1096.
- B. Yamashita and M. French, *The Fingerprint SourceBook - Chapter 7 Latent Print Development*, National Institute of Justice (NCJRS), 2010.
- R. Yang and J. Lian, *Forensic Science International*, 2014, **242**, 123-126.
- R. Zhang and P. Somasundaran, *Advances in Colloid and Interface Science*, 2006, **123-126**, 213-229.